The role of FHY3 and FAR1 in plant-microbial interaction in *Arabidopsis thaliana*

PhD thesis

Andreas Ebertz

Supervised by Dr. Paul Devlin

Royal Holloway, University of London

School of Biological Sciences

Egham

2017

Declaration of Authorship

I, Andreas Ebertz, hereby declare that this thesis and the work presented in it is entirely my own. Where I have consulted the work of others, this is always clearly stated.

07. February 2017

Abstract

The transposase-derived transcription factors FAR-RED ELONGATED HYPOCOTYL 3 (FHY3) and FAR-RED IMPAIRED RESPONSE 1 (FAR1) hold multifunctional roles in *A. thaliana*, such as in resetting the circadian clock, flowering and chloroplast division. This thesis aimed to investigate the cause of extensive leaf-lesion formation observed in *fhy3 far1* mutants, reminiscent of the programmed cell death (PCD) associated with plant defence responses.

Global gene expression analysis suggested a constitutively activated defence response in *fhy3 far1* mutants causing the mutant's leaf-lesions. However, defence marker gene expression associated with Salicylic Acid (SA)- and Jasmonic Acid (JA)/Ethylene (ET)-signalling, the two groups of signalling compounds that mediate defence response, was downregulated at the same time. Analysis of transcriptional changes upon biotic challenges suggested that this was the result of negative regulatory feedback in *fhy3 far1* mutants.

A microarray analysis of key differentially expressed genes in *fhy3 far1* mutants revealed an upregulation of the pro-PCD gene *CYSTEINE-RICH RECEPTOR-LIKE PROTEIN KINASE 13* (*CRK13*) and a downregulation of the PCD-inhibiting *METACASPASE 2* (*MC2*). The function of *CRK13* and *MC2* in PCD suggested that their misregulation in *fhy3 far1* mutants could be part of the primary reason for increased leaf-lesion formation in double mutant plants. Transcriptional analysis of responses to biotic challenges in *MC2* and *CRK13* misexpression lines, however, revealed little similarity to the responses seen in *fhy3 far1* mutants.

A constitutively activated defence response infers alterations of the associated microbiota. Initial investigations indicated that the *fhy3 far1* mutant plant's phenotypical changes of extended leaf-lesion formation will be very likely to affect the phyllosphere, which prompted a next generation sequencing investigation of the phyllospheric microbiota. Its composition showed greatly increased species richness and a more even spectrum of abundances of bacterial species in *fhy3 far1*, a pattern that is commonly associated with continuing environmental disruption. The WT phyllosphere showed a stronger domination by a few species that were associated with the production of antimicrobials. In addition, the fungal community in *fhy3 far1* mutant plants contained more pathogenic fungi in comparison to more saprotrophic fungi in WT. These findings support the suggestion that pathogen-protective properties of beneficial microbes in the phyllosphere are a community characteristic linked to microbial competition.

Table of Content

ABBREVIATIONS

5-ALA	5-Aminolevulinic Acid
AA	Amino Acid
ABA	Abscisic Acid
ABI5	*ABA INSENSITIVE 5*
ACD2	*ACCELERATED CELL DEATH 2*
ALAD	ALA Dehydratase
AP1	*APETALA1*
ARC3/5/6	*ACCUMULATION AND REPLICATION OF CHLOROPLASTS 3/5/6*
ARD1	*ACTIVATED DISEASE RESISTANCE 1*
AtbZIP10	*ARABIDOPSIS THALIANA BASIC LEUCIN ZIPPER 10*
ATCSA-1	*At COCKAYNE SYNDROME A PROTEIN-1*
Avr gene	Avirulence-gene
AXR1	*AUXIN RESISTANT 1*
BR	Biological replicate
BTH	Benzo-(1,2,3)-thiadiazole-7-carbothioic acid S-methyl ester
C	Cystein
CAT1/2/3	*CATALASE 1/2/3*
CBS	CCA1-Binding Site
CC	Coiled-Coil
CCA1	*CIRCADIAN CLOCK ASSOCIATED 1*
CERK1	*CHITIN ELICITOR RECEPTOR KINASE 1*
Cfu	Colony forming units
CO	*CONSTANS*
COI1	*CORONATINE INSENSITIVE 1*
Col-0	Columbia
COP1	*CONSTITUTIVE PHOTOMORPHOGENESIS 1*
CPR1	*CONSTITUTIVE EXPRESSOR OF PATHOGENESIS RELATED GENES 1*
CRK13	*CYSTEINE-RICH RECEPTOR-LIKE PROTEIN KINASE 13*
CRK13-Ox	*CYSTEINE-RICH RECEPTOR-LIKE PROTEIN KINASE 13* overexpressor
DAB	3,3'-Diaminobenzidine
dCAPS	derived Cleaved Amplified Polymorphic Sequences
DEX	Dexamethasone
DND1	*DEFENSE NO DEATH 1*
Dpi	Days post inoculation
EC	Evening Complex
EDS1	*ENHANCED DISEASE SUSCEPTIBILITY 1*
EE	Evening Element
EF-Tu	Elongation Factor Tu
ELF3/4	*EARLY FLOWERING 3/4*
EODFR	End of day far-red light pulse
ERF4/6	*ETHYLENE RESPONSIVE ELEMENT BINDING FACTOR 4/6*
ET	Ethylene
ETI	Effector-triggered Immunity
EtOH	Ethanol
ETS	Effector-triggered Susceptibility
FAC	Florigen Activation Complex
FAD3/7/8	*FATTY ACID DESATURASE 3/7/8*
FAR1	*FAR-RED IMPAIRED RESPONSE 1*
FB1	Fumonisin B1

FBS	FHY3-FAR1-Binding Site
FD	*FLOWERING LOCUS D*
FHL	*FAR-RED-ELONGATED HYPOCOTYL 1-LIKE*
FHY1/3	*FAR-RED-ELONGATED HYPOCOTYL 1/3*
FR/FRc	Far-red light/constant far-red light
FRS4	*FAR1-RELATED SEQUENCE 4*
FT	*FLOWERING LOCUS T*
FTIP1	*FT-INTERACTING PROTEIN 1*
GI	*GIGANTEA*
GIM1	*GAMMA-IRRADIATION AND MITOMYCIN C INDUCED 1*
GK	German plant genomics research program-Kölner Arabidopsis T-DNA lines (GABI-KAT)
GO	Gene Ontology
H_2O_2	Hydrogen peroxide
HIR	High Irradiance Response
Hpi	hours post induction
HR	Hypersensitive Response
HY5	*ELONGATED HYPOCOTYL 5*
IPCS2	*INOSITOL PHOSPHORYLCERAMIDE SYNTHASE 2*
ITS	Internal Transcribed Spacer
JA	Jasmonate
LD	Long day
LFR	Low Fluence Response
LFY	*LEAFY*
LHY	*LATE ELONGATED HYPOCOTYL*
LOL1	*LSD ONE LIKE 1*
LOX1	*LIPOXYGENASE 1*
LP	Left primer
LPS	Lipopolysaccharide
LRR	Leucine-Rich Repeat
*LSD*1	*LESION SIMULATING DISEASE 1*
LUX	*LUX ARRHYTHMO*
LYM1/3	*LYSM DOMAIN GPI-ANCHORED PROTEIN 1/3*
MAMPs	Microbe-Associated Molecular Patterns
MAPK	Mitogen-Activated Protein Kinase
MAX2	*MORE AXILLARY BRANCHING 2*
MC1	*METACASPASE 1*
MC2	*METACASPASE 2*
MIPS1/2	*MYO-INOSITOL-1-PHOSPHATE SYNTHASE 1/2*
MKK4/5	*MITOGEN-ACTIVATED PROTEIN KINASE KINASE 4/5*
MS medium	Murashige & Skoog medium
MULEs	Mutator-Like Elements
NahG	Encoding a *Pseudomonas sp*. salicylate hydroxylase
NASC	Nottingham Arabidopsis Stock Centre
NB	Nucleotide-Binding
NDR1	*NON RACE-SPECIFIC DISEASE RESISTANCE 1*
NLS	Nuclear Localisation Sequence
No-0	Nossen
NPR1	NONEXPRESSER OF PR GENES1
$O_2^{-\cdot}$	Superoxide
OUT	Operational Taxonomic Unit

PAD4	*PHYTOALEXIN DEFICIENT 4*
PAL	Phenylalanine Ammonium Lyase
PBG	Porphobilinogen
PCA	Principal Component Analysis
PCD	Programmed Cell Death
Pchlide	Protochlorophyllide
PCR/qRT-PCR	Polymerase Chain Reaction/ Reverse Transcription-quantitative PCR
PDF1.2a	*PLANT DEFENSIN 1.2A*
PDV1/2	*PLASTID DIVISION 1/2*
Pfr	Far-red light absorbing form of phytochrome
PGN	Peptidoglycans
Phy	Phytochrome
Pr	Red-light absorbing form of phytochrome
PR3	*PATHOGENESIS-RELATED 3*
PRRs	Pattern recognition receptors
Pst DC3000	*P. syringae* pv, tomato strain DC3000
PTI	Pattern-triggered Immunity
QC	Quality Control
RBOHA – F	*RESPIRATORY BURST OXIDASE HOMOLOGUE A to F*
RCD	Runaway cell death
REV	*REVOLUTA*
R gene	Resistance-gene
RLKs	Receptor-like Kinases
RNS	Reactive nitrogen species
ROS	Reactive oxygen species
RP	Right primer
RT	Room temperature
S3H	*SALICYLIC ACID 3-HYDROXYLASE*
SA	Salicylic Acid
SAG101	*SENESCENCE-ASSOCIATED GENE 101*
SALK	The Salk Institute for Biological Studies
SAR	Systemic Acquired Resistance
SBH2	*SPHINGOID BASE HYDROXYLASE 2*
SD	Short days
SID2	*SALICYLIC ACID INDUCTION DEFICIENT 2*
SPA	*SUPPRESSOR OF PHYTOCHROME A*
SUV2	*SENSITIVE TO UV 2*
T3SS	Type III Secretion System
TAIR	The Arabidopsis Information Resource
temp.	Temperature
TF	Transcription Factor
TIR	Toll-Interleukin Receptor
TOC1	*TIMING OF CAB EXPRESSION 1*
UVR2	*UV RESISTANCE 2*
UVR8	*UV RESISTANCE LOCUS 8*
VLFR	Very Low Fluence Response
ZT	Zeitgeber Time
ZTL	*ZEITLUPE*

1 GENERAL INTRODUCTION

Light is an essential environmental factor that is especially important for plants. Therefore, plants have an array of information-gathering photoreceptors to allow them to take maximum advantage of the light environment. The specific molecular mechanisms of light stimulus integration into the different light-dependent mechanisms of plants are not well understood. *FAR-RED ELONGATED HYPOCOTYL 3* (*FHY3*) and *FAR-RED IMPAIRED RESPONSE 1* (*FAR1*) are two genes that act downstream of the red light photoreceptors phytochromes A - E and, as found more recently, downstream of the UV-B light photoreceptor Ultraviolet-B receptor 8 (UVR8). FHY3 and FAR1 are two proteins that present a direct link between light signal perceiving mechanisms and the circadian clock central oscillator component *EARLY FLOWERING 4* (*ELF4*) that mainly acts at night (Siddiqui *et al*., 2016). Besides the important function of FHY3 and FAR1 in the circadian rhythm, both proteins additionally act in several other mechanisms such as chloroplast division, shoot branching and abscisic (ABA) signalling (Figure 1.1) (Gao *et al*., 2013; Stirnberg *et al*., 2012; Tang *et al*., 2013). FHY3 and FAR1 have also been suggested to act in cell division, control of DNA remodelling (euchromatin and heterochromatin formation) and floral development in Arabidopsis (Li *et al*., 2011; Wang and Wang, 2015). The broad range of FHY3 and FAR1-dependent mechanisms allows for investigations of the effect of light on these mechanisms.

An *FHY3* and *FAR1* loss-of-function was also found to result in severe alterations of the Arabidopsis phenotype that is mainly characterised by reduced growth and enhanced leaf-lesion formation that is reminiscent of defence response mediated HR. This phenotype is accompanied by increased ROS accumulation and a constitutively activated SA biosynthesis, which infers an involvement of *FHY3* and *FAR1* in plant defence response associated signalling (Ma *et al*., 2016). *fhy3 far1* mutant plants could, therefore, be utilised to investigate light regulation of plant defence mechanisms a well-documented but poorly-characterised phenomenon (Zhang *et al*., 2013; Shim and Imaizumi, 2014). *fhy3 far1* mutant plants could also be utilised to investigate plant defence responses without the collateral effects of plant pathogen infection assays. This thesis sought to address both possibilities.

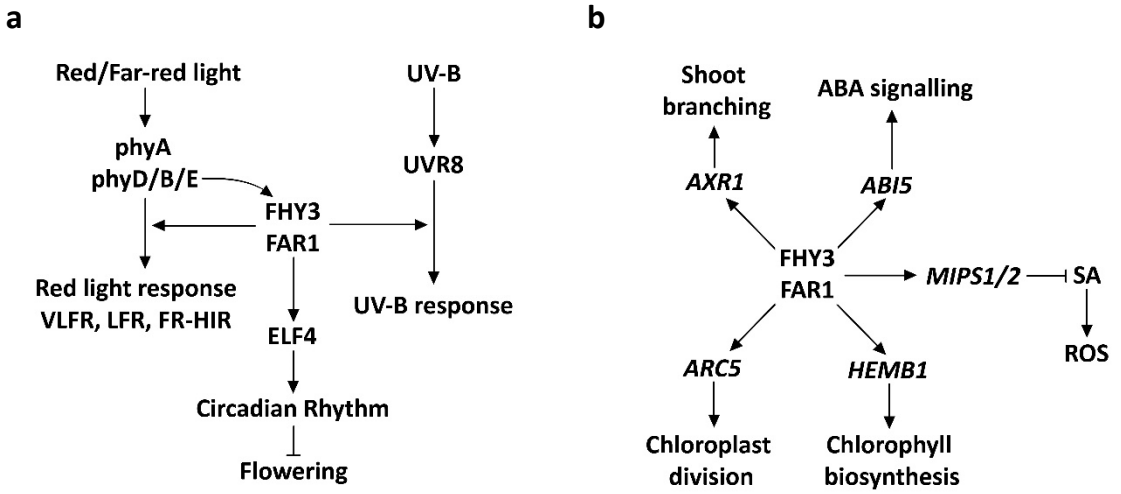

Figure 1.1: Schematic diagram summarizing the state of research on the involvement of FHY3 and FAR1 in a) red, far-red and UV-B light responses, light signal integration to the circadian clock and flowering, and in b) shoot branching, chloroplast division, chlorophyll biosynthesis, abscisic acid (ABA) and salicylic acid (SA) signalling (in reference to Li *et al*., 2011; Stirnberg *et al*., 2012; Gao *et al*., 2013; Tang *et al*., 2013; Wang and Wang, 2015; Ma *et al*., 2016).

1.1 *FAR-RED ELONGATED HYPOCOTYL 3* AND *FAR-RED IMPAIRED RESPONSE 1*

1.1.1 Discovery and characterisation of *FHY3* and *FAR1*

FAR-RED ELONGATED HYPOCOTYL 3 (*FHY3*) was first discovered by Whitelam *et al.* (1993), who investigated the red-light-sensitive phytochrome photoreceptors (phyA-E) and *A. thaliana* mutants that lost light-mediated inhibition of hypocotyl elongation. Right from the beginning, *FHY3* was hypothesised to play a role in the signal transduction from phytochrome A (phyA) in the far-red (Fr) light response pathway. When old *FHY3* loss-of-function mutant seedlings that were grown in darkness and were thereupon transferred to continuous far-red light they exhibited elongated hypocotyls in contrast to WT seedlings that did not show this characteristic. This is a phenomenon solely controlled by phyA. In *FHY3* loss-of-function mutant plants, phyA itself was detected at WT levels and the altered phenotype of loss-of-light-mediated inhibition of hypocotyl elongation occurred in far-red light, but not in white light, suggesting that *FHY3* is not a regulator of phyA but part of the phyA signal transduction pathway. *FAR-RED IMPAIRED RESPONSE 1* (*FAR1*) was first identified by Hudson *et al.* (1999), who investigated the early steps of phyA signal transduction and photomorphogenesis. *FAR1* loss-of-function mutant plants were also deficient in constant far-red light (FRc)-induced photomorphogenesis and displayed elongated hypocotyls; however, had WT levels of phyA.

Hudson *et al.* (1999) suggested that *FAR1* is one component of the phyA signalling pathway and that in *FAR1*'s absence other components of this pathway could (partially) compensate for it since the *far1* mutant seedling phenotype still inferred a substantial phyA signalling activity. Three days old *far1* and *phyA* mutant seedlings that were grown in darkness and were thereupon transferred to continuous far-red light exhibited elongated hypocotyls in contrast to WT seedlings that did not show this characteristic. *phyA* mutant seedlings, however, showed a much stronger phenotype of elongated hypocotyl than *far1* mutant seedling.

FHY3 (AT3G22170) and its paralogue FAR1 (AT4G15090) show considerable sequence homology to the transposases MURA and Jittery that are part of the mobile element superfamily of Mutator-like elements (MULEs) found in maize. MURA and Jittery were proposed to be the common ancestors of FHY3 and FAR1 (Figure 1.2) (Hudson *et al.*, 2003; Lin *et al.*, 2007; Wang and Wang, 2015). FHY3 and FAR1, however, do not show transposon-activity, due to missing terminal inverted repeats or other associated structures. The *FHY3* and *FAR1* genes are located in active single copy gene regions without other transposons, unlike MULEs that are found in heterochromatin (Hudson *et al.*, 2003; Lin *et al.*, 2007).

FHY3 and *FAR1* are members of the *FAR1-RELATED SEQUENCE* (*FRS*) family of transcription factors (TF) and are found in most angiosperms. The family encompasses 14 members, *FHY3*, *FAR1* and *FAR1-RELATED SEQUENCE 1* to *12* (*FRS1* to *FRS12*) that all show sequence homology. All family members form a conserved secondary structure, suggesting overlapping functions in light-signalling pathways (Lin and Wang, 2004).

FHY3 and *FAR1* are located on chromosome 3 and 4, respectively, in the *A. thaliana* genome. According to Gene Ontology (GO), both genes are associated to response to far-red light and its signalling pathway, positive regulation of circadian rhythm and transcription (biological processes) (Berardini *et al.*, 2004).

The plant membrane protein databases ARAMEMNON (Schwacke *et al.*, 2003) and UniProt (The UniProt Consortium, 2015) list two alternatively spliced isoforms representing *FHY3*: (1) AT3G22170.1 with 839 AA and (2) AT3G22170.2 also with 839 AA, and one for *FAR1*: (1) AT4G15090.1 with 827 AA. *FHY3* and *FAR1* are described to be expressed throughout almost all plant structures, including hypocotyl (Lin and Wang, 2004). The proteins localise to the nucleus (shown by GUS-FHY3 fusion protein construct), which is consistent with the presence of a nuclear localisation sequence (NLS) in *FAR1* and a putative NLS in *FHY3* (Hudson *et al.*, 1999; Wang and Deng, 2002; Lin and Wang, 2004; Lin *et al.*, 2007).

FHY3 and FAR1 show considerable similarities to the transposase of transposons. Transposable elements or transposons are DNA sequences that change their position in the genome. In maize, the *Mutator* (*Mu*) transposable elements consist of autonomous (*MuDRs*) and nonautonomous members (*Mu1* – *Mu8*) (Raizada, 2001). Both have flanking terminal inverted repeats but only the autonomous *MuDRs* contain the genes *mudrA* and *mudrB*. *mudrA* codes for the transposase MURA that is essential for the transposition of autonomous as well as nonautonomous *Mu* elements. The function of the *mudrB* encoded protein is unclear (Lisch *et al*., 2001 and 2015). It was suggested that transposases of *Mu*-like elements (MULE) that are widespread in plants including rice and Arabidopsis have been "domesticated" to form the transcription factors FHY3 and FAR1. Despite their structural similarities to transposases (Figure 1.2), FHY3 and FAR1 lack terminal inverted repeats and most probably have lost their transposase activity. However, similar to MURA and other transposase that positively transcriptionally regulate their own expression or, for certain classes of transposases, the expression of adjacent genes, FHY3 and FAR1 directly bind the FHY3-FAR1-Binding Site (FBS) “CACGCGC” in promoters of their downstream genes and activate their expression. Similar to MURA, whose C2H2 zinc finger motif was predicted to be involved in binding the terminal inverted repeats of the transposon in the process of position change in the genome, FHY3 and FAR1 bind the FBS with their N-terminal C2H2 zinc-finger domain. Both TF deploy their transcriptional activation activity via their central core transposase and C-terminal SWIM zinc-finger domains. Both domains show sequence similarity with the core transposase and SWIM domains of MURA and Jittery (Figure 1.2). The core transposase and SWIM zinc-finger domains were also proposed to mediate protein-protein interactions during homodimerisation of FHY3s or FHY3s and heterodimerisation of FHY3 with FAR1 or other FRS proteins). Mutation of the core domain (amino acid substitutions) was shown to partially reduce the transcriptional activation activity of FHY3, as well as its ability to homo- and heterodimerise with FAR1. Mutation of the SWIM domain (amino acid substitutions) in FHY3 led to a complete elimination of its transcriptional activation activity and ability to homo- and heterodimerise with FAR1 (Lin *et al*., 2008). The detailed molecular mechanisms of the transcriptional activation mediated by FHY3 and FAR1 are, however, elusive (Lin *et al*., 2008 a; Wang and Wang 2015).

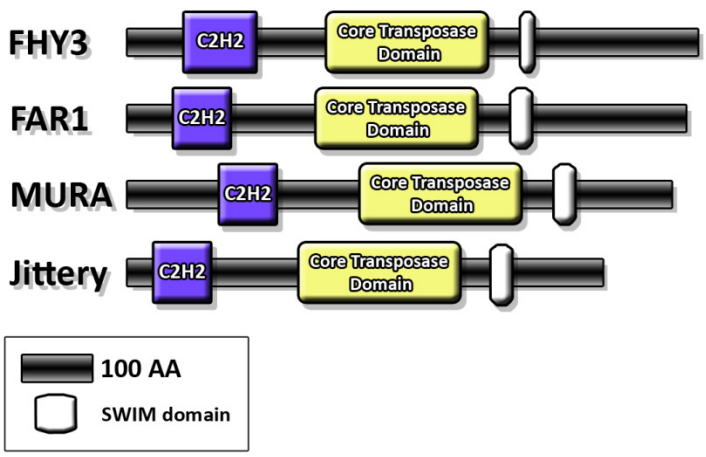

Figure 1.2: Protein structure of FHY3, FAR1, MURA and Jittery. FHY3 and FAR1 show structural similarities to the MULE transposases MURA and Jittery (in reference to Wang and Wang, 2015).

Lin *et al*. (2007) conducted a genome wide analysis, which showed that the FBS motif was present in the promoters of 602 *A. thaliana* genes (PatMatch analysis against the *A. thaliana* promoter database at). 30 % of the genes containing an FBS showed a cycling transcript pattern over time in in at least one of the tested circadian or diurnal conditions at the web-interface Diurnal (Mockler *et al.*, 2007). 12 % of the putative FHY3/FAR1-targets showed a cycling transcript pattern over time in most of the tested circadian or diurnal conditions (Lin *et al.*, 2007; Li *et al.*, 2011; Ouyang *et al.*, 2011).

Overall, the importance of the TFs *FHY3* and *FAR1* is illustrated by the extensive number of target genes and several different mechanisms they are involved in. Loss-of-function of both genes affects light-dependent and light-independent mechanisms in Arabidopsis that include resetting of the circadian clock, flowering and chloroplast division, and leads to a severely altered phenotype with increased leaf-lesion formation.

1.1.2 *FHY3* and *FAR1* in red light-signalling

A n essential light-dependent mechanism is the photoreceptor-mediated seedling transition from skoto- to photomorphogenesis.

Skotomorphogenesis and photomorphogenesis are opposite developmental programs of plants. Since plant seeds are mostly buried in the soil seedlings need to grow through soil, that is, in darkness, after germination. Skotomorphogenesis is the program a seedling adapts in darkness and it is characterised by hypocotyl elongation. The limited resources of the seedling are allocated to growth processes in order to reach photosynthetically active light. During this elongation process the apical hook remains folded to protect the cotyledons and apical

meristem. When the seedling reaches photosynthetically active light, it transitions to photomorphogenesis. This developmental program is mainly characterised by inhibition hypocotyl elongation, expansion of cotyledons, differentiation of chloroplasts and chlorophyll biosynthesis. The transition from skoto- to photomorphogenesis is induced by far-red, red, blue and UV-B light (Josse and Halliday, 2008).

In plants, several photoreceptors and their activity spectrum are known: Cryptochromes and phototropins absorb blue and UV-A light, phytochromes absorb red and far-red light.

The dimeric photoconvertible phytochromes B, C, D and E (phyB-E) are located in the cytoplasm in their inactive and red light absorbing Pr form. After irradiation with red light, they conformationally change to their active far-red light absorbing Pfr form and translocate into the nucleus, where they regulate transcription. For phyB-E, a significant proportion of these phytochromes are required to be in the Pfr form to trigger responses. Irradiation with far-red light photoreverses those into the Pr form, so that only 3 % stay as Pfr, which is, however, insufficient to observe the responses triggered by these phytochromes (Mancinelli, 1994).

PhyA is an exception amongst the phytochromes, as even very low levels of Pfr are sufficient to trigger responses (Mancinelli, 1994). It was shown to be active in red light (sufficient Pfr is formed to trigger responses), far-red and even blue light. However, it is, in contrast to the relatively stable phyB-E, light-labile in its Pfr form and degrades at a fast pace. After activation, phyA associates with *FAR-RED-ELONGATED HYPOCOTYL 1* (*FHY1*) and *FAR-RED-ELONGATED HYPOCOTYL 1-LIKE* (*FHL*), two phyA-specific signal transducers, and translocate as complexes to the nucleus. Here, they, if phyA is subsequently photo-converted back to the Pr form, disassociate and FHY1/FHL eventually exit the nucleus (Whitelam *et al.*, 1993; Hiltbrunner *et al.*, 2005; Lin *et al.*, 2007; Rausenberger *et al.*, 2011). PhyA Pfr subsequently induces the transcription of genes specific to responses in *A. thaliana,* as following: (1) Very Low Fluence Response (VLFR) and (2) High Irradiance Response (HIR). Both depend on the phytochromes photo-conversion for activation.

Like the name implies, VLFR only requires a short, low dose red-light pulse (between 10^{-6} and 10^{-3} μmol m^{-2} total fluence) for activation (Pr to Pfr). Its activation is not photoreversible, since sufficient Pfr can be formed in either red or far-red light. VLFR promotes seed germination (recognition of soil disturbance) and inhibits further hypocotyl elongation during the skoto- to photomorphogenic seedling transition stage (Figure 1.3).

Activation of HIR needs continuous irradiation with a high intensity of light for longer periods (on the order of hours). Its activation is also not photoreversible. It is a result of phyA cycling between Pr and Pfr forms, which maximises the rate of FHY1 and FHL recycling so that they

continue to be available to further import phyA Pfr into the nucleus and increase the nuclear phyA pool (Rausenberger *et al.*, 2011). In seeds, far-red-induced HIR (FR-HIR) inhibits germination. In skotomorphogenic seedlings, it results in activation of anthocyanin biosynthesis, inhibition of hypocotyl elongation, opening of apical hook, expansion of cotyledons and far-red preconditioned blocking of greening (Franklin and Quail, 2010) (Figure 1.3).

Low Fluence Response (LFR) is mediated by phyB to phyE, with phyB being the predominant phytochrome. LFR only requires a very brief red light pulse of 1 - 100 µmol m^{-2} of total fluence for activation, but is photoreversible by far-red light, since it requires a relatively high level of Pfr. LFR promotes seed germination and seedling transition to photoautotrophy (Figure 1.3) (Smith, 1995; Casal, 2000; Franklin and Quail, 2010).

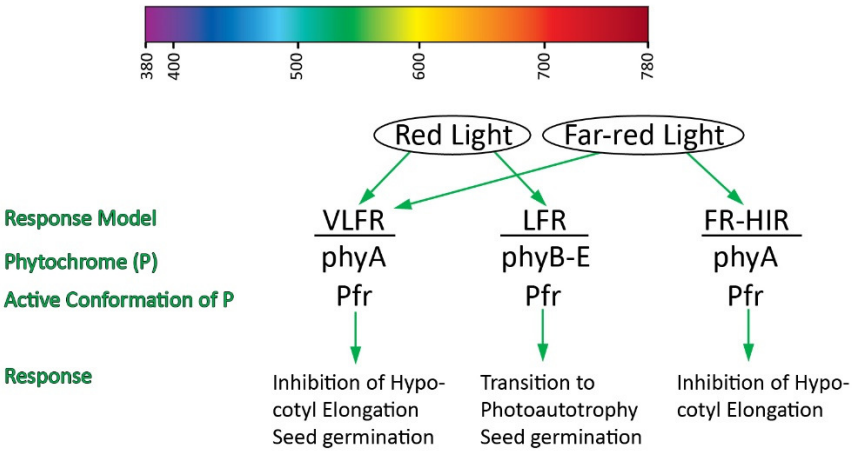

Figure 1.3: Red and far-red light-mediated response models in seedlings and involved phytochromes with their active conformation. VLFR = Very Low Fluence Response, LFR = Low Fluence Response, FR-HIR = far-red-induced High Irradiance Response.

Plant seeds that are usually buried in soil become sensitive to light and possibly accumulate phyA in the process of breaking dormancy. Disturbance of soil leads to (brief) light exposure that triggers seed germination mediated by phyA, as well as phyB - E, representing the function of VLFR and LFR.

After seed germination and the initial elongation, the seedling could be under a dense canopy that absorbs the photosynthetically active blue and red light, leaving a high amount of far-red light, and thereby a low red to far-red light ratio. A low red to far-red light ratio activates the shade avoidance response that leads to stem elongation amongst others (skotomorphogenesis) in order to surpass the shade and receive photosynthetically active light. FR-HIR, mediated by

phyA, counteracts the shade avoidance response, and is triggered by far-red but also by red light. Significantly, red light is photosynthetically active and in shade with a higher amount of red light plants do not necessarily have to further elongate to surpass the canopy. Linked to this inhibition of hypocotyl elongation, higher levels of red light also trigger LFR, mediated by phyB–E, that activates the transition from skoto- to photomorphogenesis, which includes chlorophyll biosynthesis and leaf growth.

FHY3 and *FAR1*'s crucial involvement in FR-HIR can be observed in loss-of-function mutant phenotypes. The *fhy3 far1* double mutant develops elongated hypocotyls and does not show anthocyanin accumulation when irradiated with FRc, inferring that FR-HIR was not activated. This phenotype resembles the *PHYA* loss-of-function phenotype. *phyA* mutant plants are also less responsive to high-irradiance with FRc. The difference is that *fhy3 far1* double mutant plants have WT levels of phyA, inferring that both genes are part of the downstream signalling from phyA. In terms of single mutations, *fhy3* displays a more pronounced effect than *far1*, and the double mutant shows the strongest deviation from the WT phenotype. Cotyledon and apical hook opening, as well as preconditioned block of greening by FRc are affected in *fhy3* but not in *far1* plants. It seems both genes can compensate the loss-of-function of the other gene to a certain degree in FR-HIR (Hudson *et al.*, 1999; Wang and Deng 2002; Lin and Wang 2004; Allen *et al.*, 2006; Li *et al.*, 2011).

Further molecular biological investigation into both mutations revealed that the localisation of phyA to the nucleus (shown as GFP fusion protein) was reduced in *fhy3* mutants, but almost disappeared in the *fhy3 far1* double mutant. That suggested a cooperation of both proteins for nuclear phyA accumulation. The FHY3- and FAR1-regulated accumulation of phyA in the nucleus is mediated by FHY1 and FHL. FHY3 and FAR1 are activators of *FHY1* and *FHL* expression (both genes contain FBS) and therefore indirectly regulate this light-dependent mechanism of FHY1-FHL-phyA complex translocation to the nucleus. Additionally, *ELONGATED HYPOCOTYL 5* (*HY5*) was found to be a repressor of *FHY1* and *FHL* expression by steric hindrance (FBS and ACGT containing element (ACE) motifs are very close together) and by direct interaction with FHY3/FAR1, therefore preventing their activational activity on *FHY1*/*FHL*. This co-regulation fine-tunes *FHY1* and *FHL* expression (Figure 1.4) (Rausenberger *et al.*, 2011; Hiltbrunner *et al.*, 2005; Lin *et al.*, 2007).

Interestingly, expression of *FHY3*, and to a lesser degree of *FAR1*, decreased rapidly after Fr irradiation in WT plants, where phyA is functional (shown by qRT-PCR investigation over

12 h). In *PHYA* loss-of-function mutants, on the other hand, *FHY3* and *FAR1* expression remained relatively stable on the same level after irradiation with Fr (over 12 h). This suggests a regulation of *FHY3*, *FAR1* and *PHYA* in a negative feedback loop (Lin *et al.*, 2007; Wang and Wang, 2015). Taken together, it was found that nuclear accumulation of phyA negatively regulates *FHY3* and *FAR1* expression. Reduced expression of *FHY3* and *FAR1* in turn leads to reduced nuclear accumulation of phyA. In this way, the homeostasis of phyA-signalling is maintained.

1.1.3 *FHY3* and *FAR1* in UV-B-signalling

UV-B light is highly energetic and causes DNA damage, production of Reactive Oxygen Species (ROS) and inhibition of photosynthesis in plants, when it occurs in high-fluence and shorter wavelength. UV-B light with low-fluence and longer wavelength, on the other hand, activates seedling transition to photomorphogenesis with the above stated characteristics. Upon UV-B perception, the photoreceptor UV RESISTANCE LOCUS 8 (UVR8), which is present as a homo-dimer in the cytoplasm, conformational changes and separates into monomers. The UVR8 monomers interact with CONSTITUTIVE PHOTOMORPHOGENESIS 1 (COP1) and together translocate into the nucleus. COP1 is actually an E3 ubiquitin-protein ligase and targets TFs such as HY5 that promote red and white light-induced photomorphogenesis, for degradation in darkness. COP1 is inactivated by phytochrome and cryptochrome photoreceptor action via SUPPRESSOR OF PHYTOCHROME A (SPA). Its inactivation then results in a derepression of photomorphogenesis in red and white light. However, upon UV-B irradiation, the UVR8-monomer interacts with COP1 and thereupon they activate the expression of HY5 by an unknown mechanism (instead of repression of HY5 activity via COP1). This subsequently activates the expression of UV-B-induced photomorphogenic genes (Oravecz *et al.*, 2006; Favory *et al.*, 2009).

FHY3 along with HY5 are two of the core TF of this mechanism. *FHY3* is induced in response to UV-B irradiation, binds *COP1* via the FBS in its promoter and activates *COP1* expression, similar to HY5 that binds to the ACE promoter motif of *COP1* to activate its expression. Both of these light responsive TFs, therefore, form a positive feedback loop on *COP1*-expression and UV-B responses, as COP1 also promotes *HY5* expression (Figure 1.4). Mutant plants lacking *HY5* or *FHY3* show impaired UV-B responses (Lin *et al.*, 2007; Huang *et al.*, 2012; Ulm and Jenkins, 2015).

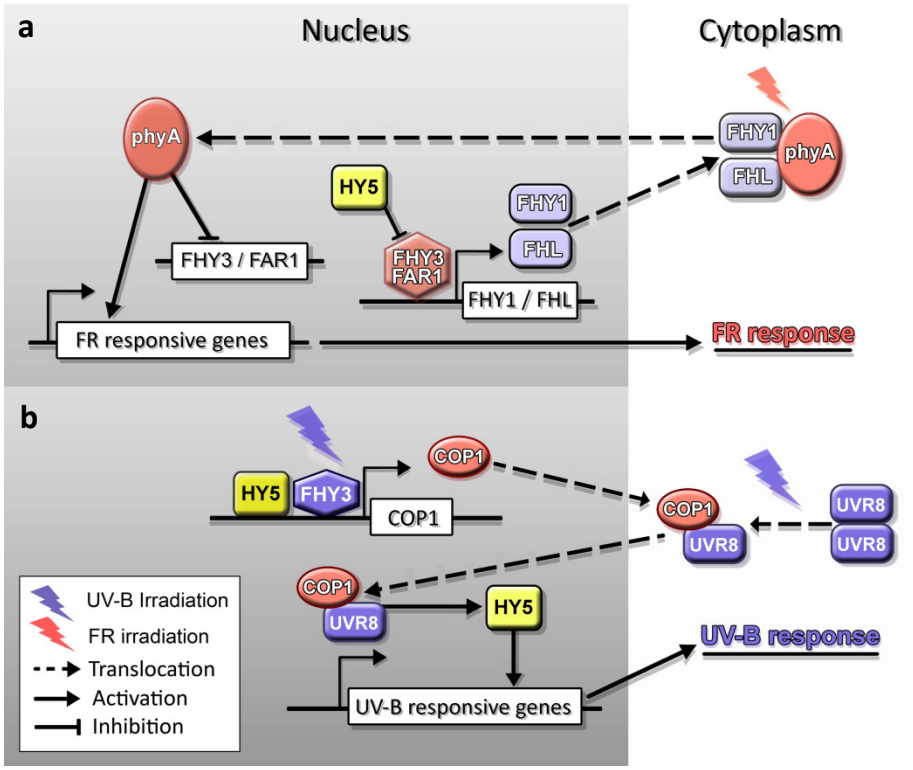

Figure 1.4: FHY3 and FAR1 in FR-signalling (a), where both TF transcriptionally activate *FAR-RED ELONGATED HYPOCOTYL1* (*FHY1*) and *FHY1-LIKE* (*FHL*) expression, FHY1 and FHL interact with phyA via protein-protein interaction, thereupon translocate from the cytoplasm to the nucleus. In the nucleus, FHY1 and FHL dissociate from phyA and phyA interacts with transcription factors (protein-protein interaction) to, on one hand, transcriptionally activate the expression of FR responsive genes and, on the other hand, transcriptionally repress *FHY3* and *FAR1* expression. HY5 inhibits FHY3's and FAR1's activational activity on *FHY1* and *FHL* by steric hindrance at their binding sites in the promoter region or by protein-protein interaction, thereby sequestering FHY3 and FAR1 and inhibiting their activational activity. FHY3 and FAR1 in UV-B signalling (b), where FHY3 and HY5 transcriptionally activate the expression of *CONSTITUTIVE PHOTOMORPHOGENIC1* (*COP1*) expression. Upon translocation from the nucleus to the cytoplasm, COP1 interacts with the UVB-RESISTANCE8 (UVR8) monomer (protein-protein interaction) and as a complex they translocate to the nucleus. Here, COP1 acts in stabilising HY5 protein that, in turn, transcriptionally activates the expression of UV-B responsive genes (in reference to Wang and Wang, 2015).

1.1.4 *FHY3* and *FAR1* in the circadian rhythm and its entrainment

FHY3 and FAR1 transcriptionally activate and physically interact with several genes and products (protein-protein interaction) of the circadian clock central oscillator and directly and indirectly modulate the circadian rhythm in plants.

1.1.4.1 Circadian rhythm overview

Plant's sessile character and consequent need to adapt to a changing environment made it necessary to have mechanisms evolved to anticipate and prepare for reoccurring changes by timing of biological processes, to a higher degree than in animals. This mechanism is called the circadian rhythm and was first coined by Franz Halberg in the 1950s. It is defined as a capability most eukaryotes and even some prokaryotes have to retain a 24 h rhythm without being exposed to environmental stimuli that indicate the daytime (endogenous generation). It evolved as adjustment to the earth´s axial rotation and resulting 24h cycles, as well as to facilitate adjustment to the axial tilt and resulting four seasons. The circadian rhythm is modulated by environmental cues, called "Zeitgeber" (e.g. change of light intensity), so the plant can adjust to the constantly changing environment. Otherwise, a delay or advance relative to the environment, due to the clock not having a perfect 24-hour period, would result in the occurrence of biological processes at an inappropriate and suboptimal time. This process of adjustment is called "entrainment" and affects processes of constant repetition, such as petal opening, and up to one-time-only processes, such as induction of flowering (Hamer *et al.*, 2001; Millar, 2004).

On a molecular level, the circadian rhythm is comprised of three parts: (1) the central oscillator, which generates the rhythm, (2) input pathways that are receiving and conveying signals from the environment, and (3) output pathways that have a modulating feedback on the central oscillator and synchronise the cells circadian rhythm. Regulation of the circadian rhythm is complex and takes place through multiple positive and negative factors that are interacting in transcriptional and post-translational feedback loops (Hsu and Harmer, 2013).

For regulation of the circadian clock, the phenomenon of "gating" is of crucial importance. It refers to "closing a gate" and therefore preventing, for example, light from resetting the clock during the middle of the day. "Gating" restricts the circadian rhythm's sensitivity to occurring daily fluctuations. Resetting of the clock takes place during dawn and dusk, indicating that these time points are when the plant´s circadian rhythm has the highest sensitivity to environmental stimuli. The resetting of the circadian clock is necessary and beneficial for the plant to adjust to the always changing day length throughout the seasons of the year. Also, the circadian rhythm does not follow exactly 24h, so daily resetting is required (Hamer *et al.*, 2001; Allen *et al.*, 2006). Investigations in the circadian rhythm-regulated pathways by global transcript analysis of multiple circadian rhythm microarray experiments found that approximately one-third of

A. thaliana genes are circadian regulated, depicting the magnitude of its importance (Yakir *et al.*, 2007; Covington *et al.*, 2008; de Montaigu *et al.*, 2010).

In general, the circadian clock regulates many processes, such as hypocotyl growth shortly after germination, elongation of hypocotyl, stems and roots at later developmental stages, stem circumnutation [1.1], cotyledon and leaf movement. It regulates the opening of petals and stomata as the major influences on phenotypical changes, but also stress responses, such as light, cold, salt and drought stress responses. The circadian clock also regulates metabolic pathways, such as starch degradation during the night, as well as pathogen defence response *in A. thaliana* (Yakir *et al.*, 2007; Harmer *et al.*, 2000; Graf *et al.*, 2010).

1.1.4.2 Central oscillator of the circadian rhythm

The main genes of the central oscillator are *CIRCADIAN CLOCK ASSOCIATED 1* (*CCA1*)*, LATE ELONGATED HYPOCOTYL* (*LHY*)*, TIMING OF CAB EXPRESSION 1* (*TOC1*)*, PSEUDO-RESPONSE REGULATOR 5, 7* and *9* (*PRR5, PRR7, PRR9*)*, EARLY FLOWERING 3* and *4* (*ELF3, ELF4*), and *LUX ARRHYTHMO* (*LUX*).

CCA1 encodes a transcriptional repressor with a single Myb domain. It is light induced with a particular responsiveness to light during the subjective night but with only little or no responsiveness to light during the subjective day. Subjective, in this case, refers to the phases of the endogenous rhythm normally associated with day and night in plants kept in constant light. *LHY* is a paralogue of *CCA1* and also contains a single Myb domain. It behaves similar as *CCA1* in response to light. CCA1 and LHY translocate to the nucleus, where they form a heterodimer and regulate the circadian rhythm (Ovadia *et al.*, 2010).

TOC1 and its paralogues *PRR5, PRR7* and *PRR9* encode transcriptional repressors. They contain two conserved domains (N-terminal: response regulator receiver domain; C-terminal: CCT domain with motifs similar to motifs present in *CONSTANS* (*CO*)) that are separated by one variable domain (Farre and Liu, 2013).

ELF3 and *ELF4* are nuclear proteins and part of the phyB-signalling pathway. Together with *LUX* that encodes a TF with a Myb domain, they form the "Evening Complex" (EC) (Khanna *et al.*, 2003; Hazen *et al.*, 2005; Nusinow *et al.*, 2011).

[1.1] Bowing or bending in different directions of the growing tip of the stem.

1.1.4.3 Transcriptional and post-translational regulation of the central oscillator and FHY3's and FAR1's function in integration of red light signal to the central oscillator

The central oscillator genes were proposed to be regulated in a repressilator, a regulatory network in which genes are interconnected in a negative feedback loop. They are expressed during certain time periods of the day and repress the preceding genes in the loop (Pokhilko *et al.*, 2012; Huang *et al.*, 2012).

In the repressilator model, the TFs *CCA1* and *LHY* are expressed during the night with peak expression at dawn (light onset). During this time, they repress the factors *ELF3*, *ELF4* and *LUX*. During the day *CCA1* and *LHY* are in turn repressed by *PRR9*, *PRR7*, *PRR5,* and *TOC1* (also known as *PRR1*). All of these four repressors peak in sequence to maintain *CCA1* and *LHY* repression throughout the day. *CCA1*, *LHY*, *PRR9*, *PRR7* and *PRR5* are expressed during the morning / daytime. The whole negative feedback loop closes as *PRR9, PRR7, PRR5* and *TOC1* are repressed by the EC during the evening hours / early night, which additionally results in a de-repression of *CCA1*/*LHY* and their rising levels during the night (Figure 1.5) (Pokhilko *et al*., 2012; Pokhilko *et al.*, 2013).

CCA1 and LHY both promote the expression of *PRR9, PRR7* and *PRR5* that act as repressors on *CCA1* and *LHY* and thereby additionally facilitate their repression during daytime (Pokhilko *et al.*, 2012).

The occurring post-translational degradation mainly involves GIGANTEA/ZEITLUPE (GI/ZTL) and COP1. The light-dependent GI stabilises ZTL during the day, which controls the degradation of TOC1 via proteasome on one hand and brings F-box proteins in the vicinity of the EC for its degradation on the other hand. The light-dependent COP1 degrades ELF3 during the day, thereby reducing the levels of EC. As a result of the reduced EC levels, a de-repression of the *PRRs* takes place, which in turn repress *CCA1*/*LHY* during the day (Figure 1.5). These light-dependent post-translational steps targeting the evening-phased proteins allow the clock to more-accurately maintain the correct timing in relation to dusk (Pokhilko *et al.*, 2012).

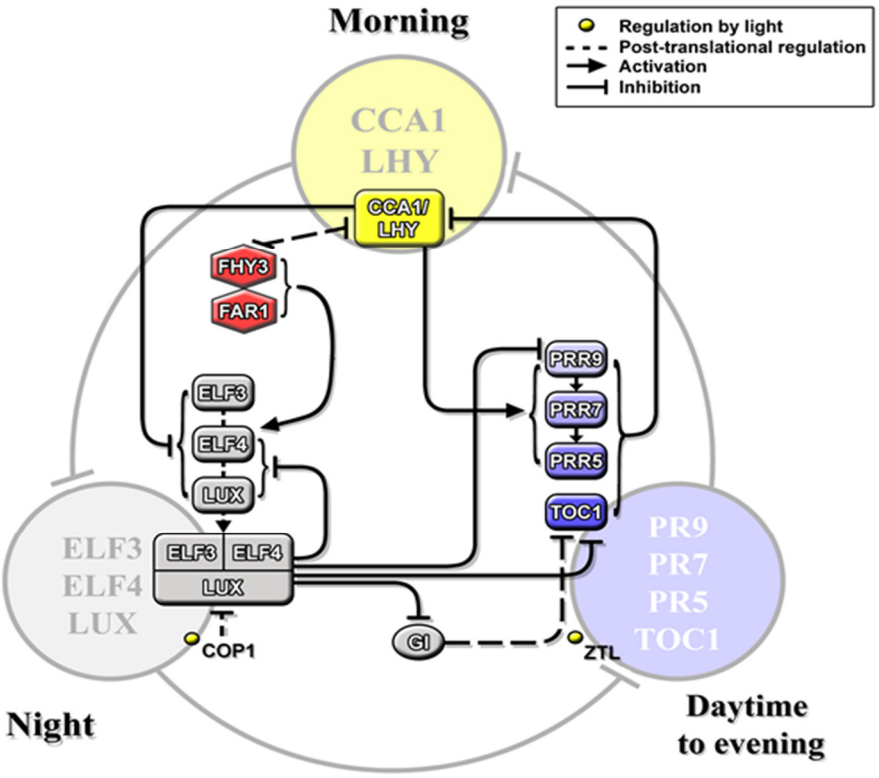

Figure 1.5: Network of feedback loops containing the main genes of the central oscillator and the involvement of FHY3 and FAR1 (in reference to Pokhilko *et al*., 2012 and Siddiqui *et al*., 2016).

The input pathways of the circadian rhythm that receive and convey signals from the environment are based on phytochromes and cryptochromes as the most important photoreceptors. *FHY3* and *FAR1* were shown to interact with components of the central oscillator (Figure 1.5). Loss-of-function of these two genes leads so substantial alterations in central oscillator gene expression: almost no *ELF4* expression and significantly reduced levels of *CCA1* and *LHY* after two days of continuous white light (in a free-running assay), as well as arhythmicity of *TOC1* expression (Li *et al.*, 2011).

Siddiqui *et al.* (2016) demonstrated *FHY3*'s and *FAR1*'s light-dependent activational activity on *ELF4* via FBS shortly after subjective dusk. At dawn, the TFs CCA1 and LHY directly suppress *ELF4* expression and the activational activity of FHY3 and FAR1 on *ELF4*. CCA1 and LHY were shown to continue to suppress *ELF4* expression later in the night and also to directly bind FHY3-protein, thereby reducing the amount of the TF that would otherwise activate *ELF4* (Li *et al.*, 2011).

The biological reason for light-dependent FHY3 and FAR1 promotion of *ELF4* expression around dusk was initially unclear. *ELF4* expression in both, WT and *fhy3 far1* mutants, tracks dusk in

short days (SD), 12 h light / 12 h darkness and long day (LD) conditions, showing a drop in expression after onset of darkness. Important is that *ELF4* expression in WT resembles more a sine curve, and in *fhy3 far1* mutants, it shows rather a sharp drop directly after onset of darkness. Its drop in expression becomes more obvious as the light phase shortens. Thus, FHY3 and FAR1 play an important role in maintaining this sinusoidal pattern of *ELF4* expression following dusk. As mentioned earlier, FHY3 and FAR1 were characterised as phyA signal transduction components. It is unlikely that promotion of *ELF4* expression via FHY3 and FAR1 is mediated by phyA after dusk, as phyA Pfr quickly degrades and no further phyA Pfr is formed in darkness. *ELF4* transcript levels, however, stay higher beyond dusk in WT. This *ELF4* pattern is maintained in red light / darkness cycles, but not in blue light / darkness cycles, suggesting that *ELF4* activation is dependent on the light-stable Pfr forms of phyB, phyD and phyE after dusk, rather than on phyA. This was confirmed by irradiation with an end of day far-red light pulse (EODFR), which largely inactivates photoconvertible phyB-E by converting Pfr back to Pr. WT plants lost their sinusoidal *ELF4* expression pattern (EODFR had no effect in *fhy3 far1* mutants). Furthermore, light stable phytochrome Pfr was shown to act via stabilisation of FHY3 protein levels. Therefore, it was concluded that *FHY3* and *FAR1* act downstream of phyB, phyD and phyE to buffer *ELF4* expression following dusk to prevent a sudden sharp drop in SD. This sinusoidal pattern of *ELF4* expression is important for the correct regulation of EFL4's downstream targets (Siddiqui *et al.*, 2016).

In LD conditions, CCA1- and LHY levels rise after onset of darkness and they rapidly supress *ELF4* expression, regardless of *FHY3*-mediated activation. In SD, however, darkness occurs before the accumulation of CCA1/LHY starts, enabling FHY3 and FAR1 to positively regulate *ELF4* expression after dusk (Li *et al.*, 2011).

1.1.5 *FHY3* and *FAR1* in flowering

Flowering is the plant's transition from vegetative to reproductive development by developing inflorescence meristems from shoot apical meristems. Flowering is strongly dependent on the environment, especially on the time of year and the change of photoperiod, besides temperature and availability of nutrients (Ó'Maoiléidigh *et al.*, 2013).

In the light of this work, the photoperiod is of most interest. In the transition model to form flowers, *FLOWERING LOCUS T* (*FT*) is activated in companion cells of the phloem in leaves by inductive photoperiods. FT binds *FT-INTERACTING PROTEIN 1* (*FTIP1*) at the membrane of the

endoplasmic reticulum and is transported to the conducting cells through which FT translocates to the shoot apical meristem. Here FT interacts with a receptor to enter the nucleus, where they associate with FLOWERING LOCUS D (FD) to form the Florigen Activation Complex (FAC). The FAC activates floral meristem identity genes like *APETALA1* (*AP1*) and *LEAFY* (*LFY*), leading to flower formation (Andrés and Coupland, 2012; Taoka *et al.*, 2013).

A. thaliana is a facultative LD plant that flowers earlier in LD than in SD conditions. The molecular mechanisms of the photoperiod-dependent regulation of flowering involve the zinc-finger TF encoded by *CO*.

In LD, *CO* expression is low during the first half of the day and peaks at around ZT12 to ZT16. Post-translational degradation of CO during the day is mediated by phyB, amongst others. However, as the day progresses, *CO* expression inhibitors are light-dependently degraded by the interacting factors GI and FLAVIN KELCH F BOX 1 (FKF1). Also during this time, CO degradation by a complex of COP1 and SUPPRESSOR OF PHYTOCHROME A (SPA1) is inhibited by phyA and cryptochrome 2 (encoded by *CRY*2). The subsequently increased CO levels in the afternoon lead to increased activation of *FT* expression at this time. FT in turn feeds into the formation of the FAC.

In SD conditions, the CO transcription repressors are not inhibited by the GI/FKF1 complex. *GI* and *FKF1* transcript levels peak at around ZT10 and are therefore expressed in darkness, since irradiation stopped at ZT8. In darkness, however, GI and FKF1 do no form an active complex. Also, even though *CO* transcript levels rise during the night, CO is post-transcriptionally repressed, due to cessation of COP1/SPA1-inhibition by phyA and cry2, which is light-dependent (Andrés and Coupland, 2012).

FHY3 was shown to protect phyA (after they associate) from recognition by the same protein degradation complex that acts on CO (COP1/SPA1) during the night. This suggests a flowering induction effect by *FHY3*. However, *fhy3*- and *far1*-single mutant plants were observed to transition to flowering much earlier than WT plants. This, in contrast, rather suggests repressive activity on flowering induction by *FHY3* and *FAR1*. It is possible that this effect very likely relates to the regulation of *ELF4* expression by FHY3 and FAR1, as *ELF4* loss-of-function mutant plants, similarly, flower early (Ouyang *et al.*, 2011; Neff and Chory, 1998; Li *et al.*, 2011).

1.1.6 *FHY3* and *FAR1* in chloroplast division and chlorophyll biosynthesis

Another layer of *FHY3's* and *FAR1's* multi-functionality is found in the chloroplast and chlorophyll biosynthesis. Multiple genes encoding for chloroplast-localised proteins, such as *ACCUMULATION AND REPLICATION OF CHLOROPLASTS 3, 5* and *6* (*ARC3, 5, 6*), were identified to be essential for the chloroplast division machinery. ARC5 is essential to constrict the outer chloroplast membrane during chloroplast-division. A loss-of-function of *ARC5,* as well as of *FHY3* and its homologue *FRS4,* resulted in enlarged dumbbell-shaped chloroplasts. The severity of this phenotype increased from *frs4* over *fhy3* to *arc5* mutants.
FHY3 and FAR1 were found to have a low ability to bind the *ARC5* promoter (via FBS), but after doing so, they did activate *ARC5* expression. FRS4, on the other hand, strongly bound to the *ARC5* promoter but did not show activational activity. The heterodimerisation of FHY3 and FRS4 was proposed to combine both features; binding and activation of *ARC5* (unknown if similar for FAR1). This would point to *FHY3* as a possible positive regulator of chloroplast division (Ouyang *et al.*, 2011; Gao *et al.*, 2013).

Linked to the chloroplast, *FHY3* and *FAR1* were suggested to be involved in the regulation of chlorophyll biosynthesis. Chlorophyll is the major pigment for photosynthesis and is synthesised from δ-Aminolevulinic acid (δ-ALA) via several intermediates to protoporphyrin IX, the point where the biosynthesis pathway divides into chlorophyll and heme biosynthesis. *HEMB1*, the gene encoding the enzyme ALA dehydratase (ALAD) that catalyses the reaction of δ-ALA to Porphobillinogen (PBG), was found to be directly activated by FHY3, and to lesser degree by FAR1. It was proposed that in darkness, when *FHY3* (and *FAR1*) is not activated, *HEMB1* expression is not induced; leading to low protochlorophyllide (Pchlide) levels at night. After irradiation and activation of phyA-signalling, FHY3 (and FAR1) would induce HEMB1 expression and thereby the conversion of δ-ALA to PBG. This, subsequently, would lead to Pchlide production and the following conversion to Chlorophyll (via Chlorophyllide). FHY3 (and possibly FAR1) was proposed to be a positive regulator of chlorophyll biosynthesis in this mechanism (Tang *et al.*, 2012). These findings, however, originate from a study in seedlings that transitioned from skoto- to photomorphogenesis. They should not simply be conferred to night-day transitioning plants of later developmental stages. 21 days old *fhy3 far1* mutant plants, for instance, that would lack this FHY3-mediated promotion of chlorophyll biosynthesis, did not exhibit reduced greening of true leaves. Chlorophyll biosynthesis in *fhy3 far1* mutants is either not impaired or functional compensational mechanisms are in place.

1.1.7 *FHY3* and *FAR1* in shoot branching and plant architecture

A. thaliana has an apical shoot meristem but can also form lateral shoot meristems. The apical shoot meristem allows the plant to increase in length (primary growth), whereas the lateral shoot (or axillary) meristems are the basis for lateral shoot production. The formation of the lateral shoot meristem from cells in the leaf axil is induced by specific TF, such as REVOLUTA (REV) (class III homeodomain leucine-zipper). Here, small lateral buds develop from the lateral shoot meristem, but mostly stay dormant. In response to environmental and endogenous signals, these dormant lateral buds can be re-activated and form lateral shoots. This process is mediated by plant hormones. The basipetal [1.2] transported Auxin and acropetal [1.3] transported Strigolactones inhibit the growth of lateral buds, and therefore inhibit branching. The acropetal transported cytokinins on the other hand promote branching.

Two genes that are important in regulation of branching are *MORE AXILLARY BRANCHING 2* (*MAX2*) and *AUXIN RESISTANT 1* (*AXR1*). *MAX2,* which encodes an F-box leucine-rich repeat protein, mediates signals from strigolactones and plant growth regulating Karrikins. *MAX2* loss-of-function mutant plants show increased lateral branching. *AXR1* encodes the subunit an enzyme that regulates activity of the Skp1-Cullin-Fbox protein degradation complexes. *AXR1* loss-of-function mutants have reduced Auxin-response and display moderately increased lateral branching.

One feature of the *FHY3* loss-of-function was found to be reduced lateral shoot branching. Interestingly, the *fhy3* mutation was able to supress the high branching phenotypes of *max2* and other strigolactone signal mutants, but not the one of *axr1.* This suggested that *AXR1* is epistatic to *FHY3*. The moderately increased branching phenotype of *axr1* mutant plants was associated with reduced Auxin response of the lateral buds, due to increased Auxin biosynthesis, reduced Strigolactone biosynthesis that is induced by Auxin, and reduced suppression of Cytokinin biosynthesis. The increased Auxin biosynthesis is accompanied with increased canalisation and removal of Auxin (as inhibitor of shoot branching) from later buds, activating lateral shoot branching. *FHY3* was proposed to be involved in the *AXR1*-dependent regulation of Auxin homeostasis and to be a promoter of branching. It possibly mitigates Auxin-mediated growth inhibition of lateral buds. Here it could act in the Auxin-mediated negative feedback loop on

[1.2] basipetal = from apex towards the base

[1.3] acropetal = from base towards the apex

Auxin biosynthesis itself and thus reducing Auxin levels to keep homeostasis, rather than on Cytokinin- or Strigolactone accumulation. *AXR1* was not found to contain a FBS, which led to the conjecture of an indirect *FHY3*-dependent regulation of *AXR1*.

The hypothesis of *FHY3*'s function in shoot branching was confirmed in *REV* loss-of-function mutants. These mutants are impaired in forming and maintaining lateral and floral meristem, caused by a defective Auxin transport and accumulation. A combination of both mutations, *fhy3* and *rev*, enhanced the *rev*-phenotype of reduced lateral branching (Stirnberg *et al.*, 2012).

1.1.8 *FHY3* and *FAR1* in Abscisic Acid signalling

Abscisic acid (ABA) is a phytohormone that shows overlaps or crosstalk with light-signalling in certain regulative processes, such as germination and seedling development. ABA has inhibitory function on seed germination (in unfavourable environment, high ABA levels lead to seed dormancy), seedling growth, and induces stomata closure. A group of ABA-responsive genes, *ABA INSENSITIVE 1 to 5* (*ABI1 to 5*), has been identified that is essential for the regulation of these processes. *ABI5* encodes a basic leucine zipper domain TF that is expressed in mature seeds and young seedlings. A loss-of-function results in seed germination and seedling growth in the presence of high levels of ABA, which prompted the proposal that *ABI5* is an ABA-dependent inhibitor of seed germination (Tang *et al.,* 2013).

ABI5 was found to contain an FBS and to be activated by FHY3 and/or FAR1. That suggested that FHY3 and/or FAR1 are part of ABA-signalling, and possibly activators of seed germination. Investigations of *fhy3 far1* double mutant seeds, as well as the respective single mutant seeds, showed a decreased sensitivity to ABA in terms of inhibition of seed germination. This led, after treatment with ABA, to increased germination rates of the *fhy3 far1* mutant seed compared to WT. ABA-marker genes were also downregulated in imbibed mutant seeds. The overexpression of *ABI5*, however, rescued the *fhy3* seed germination defect in the presence of ABA. Overall, the *fhy3* single mutation often showed more dramatic effects than the *far1* mutation, but was surpassed by the *fhy3 far1* double mutation (Tang *et al.,* 2013).

A link between ABA- and red light-signalling has been shown, where red light decreases and far-red light increases ABA levels. *FHY3* and *FAR1* were proposed to function at the intersection of both signalling pathways to integrate them during seed germination and early seedling stages. This is consistent with the finding that both TF, as well as *ABI5,* were induced in response to light and ABA-treatment (Tang *et al*., 2012; Chen *et al*., 2008). Tang *et al.* (2013) hypothesised a

regulatory mechanism in which *FHY3* and *FAR1* are induced in response to abiotic stress and then induce ABA-responsive and stress-associated genes, such as *ABI5*. These genes in turn positively modulate ABA-signalling to subsequently regulate plant growth and development.

1.1.9 Summary

In its entirety, *FHY3* and *FAR1* show multifunctional modes of action that are dependent on light-labile (phyA) and light-stable phytochromes (phyB-E), or are independent of phytochrome. These modes of action also differ during plant development stages, comprising of early seedling functions, such as HIR and transition to photomorphogenesis, later established plant functions, such as transition from vegetative to reproductive development, as well as continuous functions, such as nuclear import of phyA, circadian rhythm entrainment, regulation of stress responses and branching.

Table 1.1: Characteristics of the FHY3 and FHY3 FAR1 loss-of-function mutant phenotypes and the associated impaired molecular functions.

Phenotypic characteristic	Molecular mechanism	Reference
Elongated hypocotyl and reduced anthocyanin accumulation, *fhy3* mutants have a more pronounced phenotype than *far1* mutants in far-red light, phenotype is most pronounced in *fhy3 far1* double mutants in far-red light	Impaired phyA signalling / FR-HIR	Whitelam *et al*., 1993; Hudson *et al*., 1999; Wang and Deng, 2002
Early-flowering in *fhy3* and *far1* single mutant plants	Impaired *EARLY FLOWERING 4* (*ELF4*) expression	Li *et al*., 2011
Enlarged dumbbell-shaped chloroplasts in *fhy3* mutant plants	Impaired *ACCUMULATION AND REPLICATION OF CHLOROPLASTS5* (*ARC5*) expression that is essential to constrict the outer chloroplast membrane	Gao *et al*., 2013
Reduced lateral shoot branching in *fhy3* mutant plants	Impaired *AUXIN RESISTANT1* (*ARX1*)-dependent regulation of Auxin homoeostasis	Stirnberg *et al*., 2012
fhy3 and far1 single mutant, and *fhy3 far1* double mutant plants have decreased sensitivity to ABA in the mechanism of inhibition of seed germination	Impaired *ABA INSENSITIVE5* (*ABI5*) expression that is involved in ABA signalling	Tang *et al*., 2013

1.2 Plant biotic stress response pathways

1.2.1 Lesion formation in *fhy3 far1* mutant plants

In *A. thaliana, FHY3* and *FAR1* loss-of-function results in formation of extensive spontaneous lesions on rosette leaves, particular in SD conditions, that resemble lesions formed in response to pathogen attack, or the lesion mimic phenotype (Brooks *et al.*, 2004; Lorrain *et al.*, 2003). Stirnberg *et al.* (2012) observed this phenomenon as part of their analysis of the role of *FHY3* in the control of branching. They suggested it may represent an aspect of defective circadian regulation of preparedness for photosynthetic stress, resulting in increased ROS production, or alternatively represent a defective ROS tolerance. They proposed that the previously-demonstrated defective downregulation of protochlorophyllide oxidoreductase (POR) gene expression in *fhy3* (Barnes *et al*., 1996) may mean that Pchlide that accumulates in darkness would not be fully converted to chlorophyll upon subsequent illumination. Excess Pchlide generates ROS upon illumination. Short days would include a longer period of darkness and, therefore, a greater Pchlide accumulation, greater ROS production and increased lesion formation. However, Tang *et al.* (2012) showed that *fhy3* single and *fhy3 far1* double mutants actually coped better with photosynthetic stress following darkness, due to their reduced Pchlide production as well. In their investigations, 5 days old *fhy3 single* and *fhy3 far1* double mutant seedlings that were grown in darkness and thereupon transferred to light, contained less ROS, showed less photobleaching and cell death after their transfer from darkness to light. These results of seedlings that transitioned from skoto- to photomorphogenesis, however, should not be simply conferred to day-night transitioning plants of later developmental stages (1.1.6 FHY3 and FAR1 in chloroplast division and chlorophyll biosynthesis).

Following on from the findings that FHY3 and FAR1 play a key role in light input to the clock after dusk in SD, this project sought to further analyse the possibility that a circadian-regulated moderation of wider biotic or abiotic stress response pathways might be disrupted in *fhy3 far1* mutants in SD, explaining the leaf-lesion formation.

1.2.2 Introduction to plant biotic stress response

Plants represent a rich living source of nutrients that is desired by microorganisms, which are ubiquitous and of diverse characteristics. These microorganisms can be commensal, symbiotic or pathogenic, and can even switch between these characteristics.

To prevent exploitation, plants have developed an array of structural and chemical defence response mechanisms against infestation with pathogens. These pathogens are divided into biotrophs, necrotrophs and hemibiotrophs. Biotrophic pathogens keep their hosts alive while feeding on them. Necrotrophs produce degrading enzymes to release plant nutrients and thereby kill the host. Hemibiotrophs behave in their early stages of infection like biotrophs but eventually when the affected cell dies/is dead they start feeding on the released compounds, and effectively become necrotrophic (Freeman and Beattie, 2008).

1.2.3 Inducible plant defence responses

1.2.3.1 Overview

A well-established model of plants' inducible innate immunity was proposed by Jones and Dangl (2006) and explains the interaction of plant and pathogen in a zig zag model. This model describes the possible interactions between plants and pathogens as two-pathed and four-phased, as follows.

The first path consists of cell surface-localized transmembrane pattern recognition receptors (PRRs) that perceive conserved microbial features, called microbe-associated molecular patterns (MAMPs) and this path is called pattern-triggered immunity (PTI) (also primary immune response).

The second path is located mostly inside the cell and consists of (R)-gene-encoded products that interact with pathogenic avirulence factors, encoded by avirulence (Avr) genes. It is called effector-triggered immunity (ETI) (also secondary immune response).

In the first phase, the plant recognises MAMPs and activates PTI to stop pathogen growth and colonisation. In the second phase, successful pathogens use effectors that interfere with the plant's PTI, leading to effector-triggered susceptibility (ETS) in the plant and these effectors, thereby, increase the pathogen's virulence. If the plant recognises these microbial effectors with (R) gene-encoded products, then the third phase is triggered, activating ETI. In the fourth phase, natural selection favours the pathogens which have abandoned or modified their recognized

effectors, or alternatively gained unrecognised effectors, by possible horizontal gene transfer, meaning that the pathogens suppress ETI, again leading to ETS (Figure 1.6). It has to be clarified that all phases could be considered as evolutionary adjustments to increase virulence on the pathogen side and immunity on the plant side. It could be compared to an “arms race” on an evolutionary timescale.

Recently, however, this model was criticised since it is based on the plant's interaction with biotrophic microbes and lacked integration of symbiotic interactions, or the response to necrotrophic pathogens where HR would rather be a favourable result. Also, the environmental context such as water availability, heat and cold, photoperiod, previous encounters with pathogens, presence of beneficial microbes, etc. have not been considered in the model. In the zig zag model, inducible plant defence response is defined as a mechanism in which perception of MAMPs and microbial effectors result in immunity (PTI/ETI) or susceptibility (ETS). However, it was suggested that plant defence response should rather be defined as a mechanism that integrates various signals and results in different outcomes which cannot simply be categorised into ETI, PTS and PTI (Pritchard and Birch, 2014). An alternative model to describe inducible plant defence response has been proposed by Cook *et al*. (2015) with the invasion model. In this model, plant defence response-eliciting compounds that also include plant-derived compounds are not categorised into the strict categories of MAMPs or effectors but into a continuum of invasion patterns (IPs). These IPs are not defined from the point of perception and response by the host plant, but from the point of their main function in the microorganism or plant itself. Perception of IPs by the host plant's ligand perceiving receptors termed invasion pattern receptors (IPRs) indicate an invasion. IPs include external microbial-derived ligands such as chitin and flg22 but also host-derived modified-self ligands that indicate an invasion. Modified-self ligands are for example damage associated molecular patterns (DAMPs) such as compounds from the extracellular matrix that are released after wounding. Well described DAMPs are pectin fragments (oligogalacturonides) that are released from the cell wall after damage, for instance after penetration by an appresorium. However, the main function if pectin is in plant cell wall structure and not as indicator of invasion. Oligogalacturonides are perceived by the plant's RLK *Wall-associated kinase 1* (*WAK1*) that mediates resistance to *B. cinerea* in Arabidopsis and rice (Ferrari *et al*., 2013). DAMPs play an important role in plant defence responses but have not been integrated in the zig zag model.

A classification of defence response eliciting compounds into MAMPs or effectors is objected to in the invasion model, since some defence response eliciting microbial compounds have been found to not fit into the categories of MAMPs and effectors. One example are Nep1-like proteins

(NLPs) that are found in plant-associated bacteria, fungi and oomycetes. NLPs are secreted compounds that contribute to virulence of the microorganism and have mainly cytotoxic properties, thus, would be classified as effectors. *Nep1-like protein 24* (*nlp24*), however, a conserved region of NLPs that strongly induces ethylene production and is sufficient to elicit defence responses in Arabidopsis (Oome *et al*., 2014) would represent a pattern and therefore be classified as a MAMP. Different from the conserved fragment of *flagellum* flg22, for instance, that is sufficient to elicit defence response, *nlp24* does not fit in the definition of defence response eliciting structural components of microbes (MAMPs), since it is secreted and utilised as effector.

Contrary to the zig zag model, in the invasion model the host plant's responses are not classified into PTI or ETI, but into IP triggered responses (IPTRs). The difference is that perception of IPs results in a) continued symbiosis between invader and host plant, or b) end of symbiosis of invader and host plant, instead of immunity (PTI/ETI) or susceptibility (ETS) as conceptualised in the zig zag model. These outcomes of continuation or discontinuation of symbiosis are determined by the overall effect of elicited host responses that can be synergistic and/or antagonistic. From the invader perspective, mechanisms that lead to 1) the failure to supress IPTR, 2) the suppression of IPTR (for example by biotrophic invaders), or 3) the utilisation of IPTR (for example by necrotrophic invaders) determine if the symbiosis with the host plant is either continued or discontinued. Invaders may deploy IPs such as *P. syringae*'s *avr* proteins to influence the outcome of the symbiosis by manipulating IPTRs. When these IPs are used or the symbiosis is continued, further IPs could be released such as modified-self ligands that in turn could be perceived by IPRs and lead to a discontinuation or continuation of the symbiosis, depending on the triggered plant responses (Cook *et al*., 2015).

In the zig zag model, plant defence response and resistance are associated with HR, which, however, would rather result in a susceptibility to necrotrophic microorganisms instead of resistance. In the invasion model, invasion by necrotrophs leads to the release of DAMPs such as pectin fragments, resulting in triggering of appropriate defence responses. Additionally, pro-death mechanisms utilised by necrotrophic microorganisms such as specific toxins to hijack the plants defence response did not really fit in the zig zag model but are integrated in the invasion model. Victorin for instance, produced by *Cochliobolus victoriae,* targets LOV1 in Arabidopsis. LOV1 guards defence response-associated thioredoxin h5 (TRXh5) and an activation of LOV1 was found to results in PCD, which in turn benefits the necrotrophic *C. victoriae.* In the invasion model, Victorin represents an IP that utilize the IPTR to promote symbiosis (Cook *et al*., 2015).

Mutualistic and beneficial interactions with microbes are, similar to interactions with

pathogens, also shaped by microbial compounds. Here, lipochitooligosaccharide (LCO) Myc factors for example that are chitin derivatives produced by arbuscular mycorrhiza are perceived by cell membrane receptors. CERK1 in rice that is in general associated to chitin-triggered defence response was shown to be necessary for arbuscular mycorrhizal symbiosis. Symbiosis with beneficial/mutualistic microbes also depends on IPs (effectors) that suppress the plants defence response. *Rhizophagus irregularis,* which is an arbuscular mycorrhiza fungus, deploys an effector (SP7) that attenuates ETI-mediated defence responses. This, however, does not represent susceptibility of the host plant (ETS) in a narrow sense and, therefore, does not really fit into the zig zag model. In the invasion model on the other hand, arbuscular mycorrhiza fungi like *R. irregularis* deploy IPs that suppress IPTRs that would lead to a discontinuation of symbiosis (Cook *et al*., 2015).

Despite the shortcomings of the zig zag model for induced plant defence responses and the proposal of an alternative model, the zig zag model is still widely utilised and its terms MAMPs and effectors are prevailing and commonly used in the literature. Thus, these terms will be used to describe interactions and mechanisms in this thesis.

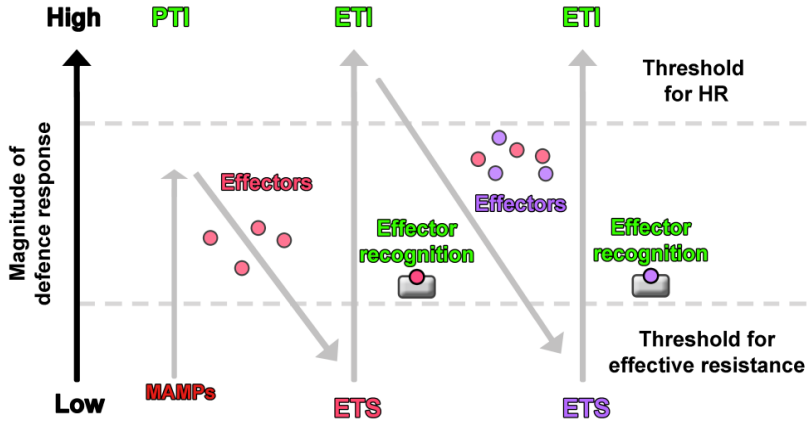

Figure 1.6: Zig Zag model of *A. thaliana* defence response and immunity against pathogens (in reference to Jones and Dangl, 2006).

1.2.3.2 Pattern-triggered immunity

Foliar pathogenic bacteria enter through stomata, and other openings such as wounds, into the plant's apoplast where they proliferate. Fungi enter directly into epidermal cells or penetrate the plant with their hyphae between and through cells. At this point, the plant's membrane-standing PRRs, which are mainly receptor-like kinases (RLKs), perceive MAMPs with their

extracellular leucine-rich repeat (LRR) domain, and transduce a signal to the cell with their intracellular domain via mitogen-activated protein kinase (MAPK) cascades. RLKs have a wide range of roles in plants. More than 600 RLKs were found in *A. thaliana*, but only a small part of them are involved in MAMP-recognition (Jones and Dangl 2006; Pel and Pieterse 2013; Yeh *et al.*, 2015).

The best described MAMPs are fungal chitin (N-acetylglucosamine oligomers), bacterial peptidoglycans (N-acetylglucosamine and N-acetylmuramic acid (PGN)) and lipo-polysaccharides (lipid attached to polysaccharide (LPS)), bacterial flagellin (or the derived peptide flg22) and elongation factor Tu (EF-Tu, or the derived peptides elf18/elf26) (Quirino and Brent 2003; Freeman and Beattie 2008; Yeh *et al.*, 2015). MAMPs are in general abundance and their nature is essentiality for microorganisms. Fungal chitin is an essential integral component of fungal cell walls and estimated to be the second most abundant polysaccharide in the world; bacterial peptidoglycans are essential integral components of bacterial cell walls; lipopolysaccharides are membrane components of Gram-negative bacteria; bacterial flagellin is a component of the bacterial flagellum (widespread among different species). This essential character often requires evolutionary conservation and selective pressure for adaptation could involve a loss of microbial fitness and virulence for pathogens. The flagellum for example is not essential for bacterial survival, but contributes strongly to the virulence of bacterial pathogens (Pel and Pieterse 2013).

Activation of PTI characteristically triggers ROS production, expression of pathogen-resistance genes, callose deposition in the plant´s cell walls and stomatal closure as the main reactions to adjust the plant to pathogen attacks (Quirino and Brent 2003; Freeman and Beattie 2008; Jones and Dangl 2006).

1.2.3.3 Effector-triggered immunity

Pathogens additionally use effectors (virulence factors[1.4]) to alter the plants immune response, and mask their presence. Effectors increase the plant's susceptibility, enhance microbial fitness, and can cause nutrient leakage for nutritional purposes of the pathogen (Jones and Dangl, 2006; Doehlemann and Hemetsberger, 2013; Pel and Pieterse 2013).

[1.4] Virulence factors were formerly termed Avr gene-encoded avirulence factors, because a recognition by the plant leads to plant resistance.

At this point, microbial effectors may be either directly or indirectly recognised by R gene products, which are mainly represented by nucleotide-binding leucine-rich repeat (NB-LRR) proteins, activating ETI.

There are two hypotheses that describe the recognition of microbial effectors by plant's NB-LRR proteins. The first states that NB-LRR proteins and R gene products in general directly recognise microbial effectors, and this is called the gene-for-gene hypothesis. The second, called the guard hypothesis, describes indirect effector recognition by NB-LRR proteins. Effectors manipulate plant components as their targets and, rather than being recognised directly, NB-LRR proteins recognise the resultant alteration of the targeted components. Therefore NB-LRR proteins 'guard' specific components and recognise a 'modified-self'. This way, a limited set of NB-LRR proteins can cover a wider range of microbial effectors. Most R genes encode NB-LRR proteins and only approximately 150 NB-LRR genes are found in *A. thaliana*; a number that would be insufficient to cover all known and potential microbial effectors. This supports the guard hypothesis. For example, *Pseudomonas syringae* and its multiple strains are estimated to produce more than 150 effectors alone (Dangl and Jones 2001; Min Gab Kim *et al.*, 2005; Coll *et al.*, 2011; Alfano and Collmer 2004).

NB-LRR proteins are divided into two main classes: (1) CC-NB-LRRs that contain, at the N-terminal, a coiled-coil domain (CC), and (2) TIR-NB-LRRs that contain, at the N-terminal, a domain homologous to the intracellular Toll/Interleukin receptor (TIR) domain of mammalian Toll-like receptors (TLRs) (Coll *et al.*, 2011).

In plants CC-NB-LRR-dependent effector recognition is mediated by the NON RACE-SPECIFIC DISEASE RESISTANCE 1 (NDR1) protein, and TIR-NB-LRR-dependent effector-recognition by a complex of ENHANCED DISEASE SUSCEPTIBILITY 1 (EDS1) and PHYTOALEXIN DEFICIENT 4 (PAD4) (Coll *et al.*, 2011) (Figure 1.7).

NDR1 is a plant plasma membrane-localised protein that induces SA biosynthesis via activation of *SID2* upon its own activation (Figure 1.6). *NDR1* loss-of-function mutant plants showed susceptibility to *P. syringae* strains *Pst* DC3000 *avrB*, *Pst* DC3000 *avrRpt2*, *Pst* DC3000 *avrRpm1* and *Pst* DC3000 *avrPphB*, whose effectors, *avrB*, *avrRpt2*, *avrRpm1* and *avrPphB*, are recognised by CC-NB-LRR proteins, but not to the *P. syringae* strain *Pst* DC3000 avrRps4, as this effector, *avrRps4*, is recognised by a TIR-CC-NB-protein (Lee *et al.*, 2006; Chisholm *et al.*, 2006).

EDS1 and *PAD4* encode lipase-like genes. Both proteins directly interact with each other and together they activate and amplify SA-signalling and ROS production, as well as repress JA-signalling. *EDS1* and *PAD4* loss-of-function mutants showed abolished and strongly reduced SA levels, respectively, in response to *Pst* DC3000 *avrRps4*, but not in response to

Pst DC3000 *avrRpm1*, which makes EDS1 and PAD4 components of the CC-NB-TIR-mediated defence response signalling pathway (Koornneef and Pieterse, 2008; Wang *et al.*, 2016; Feys *et al.*, 2001) (Figure 1.7).

SID2 encodes the chloroplast-localised isochorismate synthase I (also called ICS1) that converts chorismate to isochorismate; therefore, channelling chorismate one step further downstream on its conversion to SA that is an essential signalling molecule of the plant defence response. Chorismate can also be channelled into a pathway of SA biosynthesis via phenylalanine that is converted to cinnamic acid. This process is catalysed by phenylalanine ammonium lyase, encoded by *PAL1* to *4*. Further reactions convert cinnamic acid to SA. *sid2* mutants were shown to be strongly impaired in their disease resistance (versus *Erysiphe* and *P. syringae*), caused by their compromised pathogen-induced SA biosynthesis that was only 5 - 10 % of WT levels. Another study found 25 % to 50 % of WT basal and pathogen-induced SA levels in plants with loss-of-function in all four *PAL* genes (*pal1/2/3/4*), but not in single, double or triple mutants, where the SA levels were similar to WT (Yu *et al.*, 2010; Wildermuth *et al.*, 2001; Wang *et al.*, 2016; Fu and Dong 2013; Huang *et al.*, 2010 a).

Elicitors that elicit ETS include the *P. syringae* genes, AvrPto and AvrPtoB (that are delivered by the type III secretion system (T3SS) described below). AvrPto binds to receptors for flagellin, EF-Tu and chitin perception and blocks their signal transduction. AvrPtoB has ubiquitin ligase activity and targets the flagellin perception receptor FLS2 for degradation. These examples demonstrate the effect of effectors on PTI to trigger ETS (Pel and Pieterse, 2013).

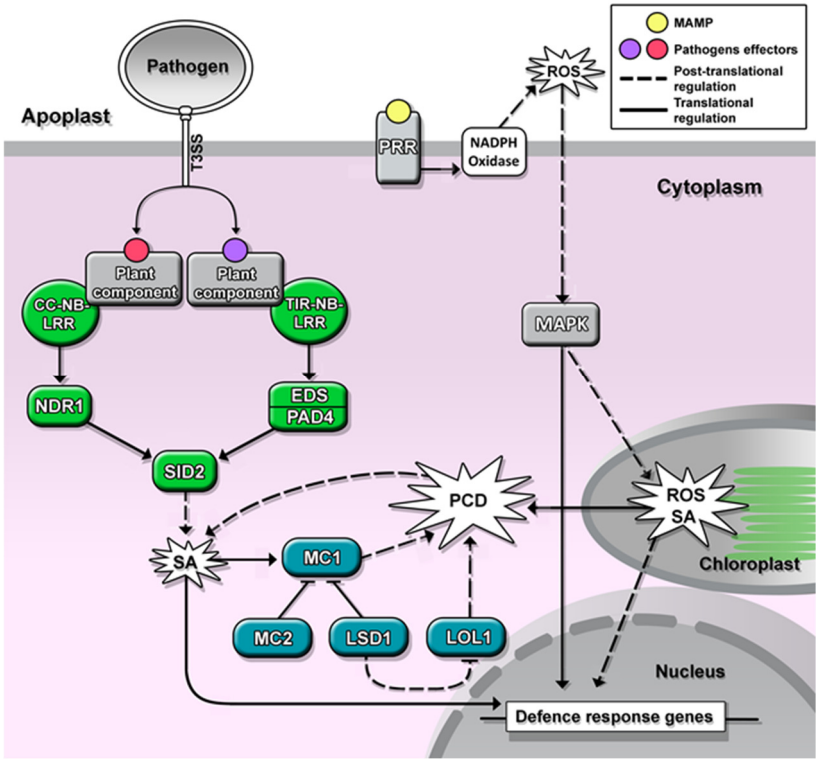

Figure 1.7: Schematic of SA-mediated effector-triggered and pattern-triggered immunity.

PTI is understood to be the first line of defence against the majority of pathogens, mainly triggering weaker and rather localised defence responses, such as ROS accumulation, while ETI is more specific and triggers mainly stronger responses, such as hypersensitive response (HR) and systemic acquired resistance (SAR). However, the reversed case is not excluded and suggests that the specific character of the MAMP or effector, as well as their quantity and exposure time, together modulate a specific defence response (Nishimura and Dangl, 2010; Doehlemann and Hemetsberger, 2013).

1.2.4 Virulence, avirulence, host and non-host

Avirulence describes a pathogen`s state, in which its Avr gene products (effectors) are recognised by plant-resistance R gene products (like NB-LRR proteins), resulting in activation of ETI and failure of the pathogen to cause disease. In this case, the interaction between Avr and R gene products is incompatible and the plant is resistant. In case the microbial Avr gene products are not recognised, due to absence of Avr gene products and/or absence of perceiving R gene

products, ETI is not activated, the pathogen is virulent and the plant is susceptible (pathogen-host-interaction is compatible) (Kim *et. al*, 2005)

In addition, most biotrophic and hemibiotrophic plant pathogens possess a high specificity to certain plant species and are unable to infect species other than these due to another phenomenon, known as non-host resistance, which is still poorly understood (Freeman and Beattie, 2008).

1.2.5 Defence response signalling pathways

1.2.5.1 Overview

Plants need to modulate their defence response to appropriately adjust the outcome to the nature of the infecting pathogen. Defence responses are classified in two main response types: (1) against biotrophs and (2) against necrotrophs.

Biotrophic pathogens try to avoid eliciting the host plant's defence response while they feed on living cells. Their effectors, therefore, often aim to supress the plant's HR, a defence response mechanism that leads to far-reaching programmed cell death (PCD) and, hence, deprivation of the pathogen of nutrients and water. Necrotrophic pathogens, on the other hand, often try to induce PCD and necrotic tissue formation in their host plants to feed on the released nutrients and water. Effectors for this induction are toxins, cell wall degrading enzymes and biosynthesis-interfering components (see 3.1.3 Fumonisin B1), amongst others (Coll *et al.*, 2011).

Plant defence responses are modulated by signalling pathways that mainly utilise SA as the main signalling molecule in response to biotrophic pathogens, and ethylene and jasmonate (ET/JA) as the main signalling molecules in response to necrotrophic pathogens (Torres *et al.*, 2006; Coll *et al.*, 2011).

It makes sense that the differentiation of biotroph from necrotroph mainly takes place during ETI (and not PTI), when microbial effectors operate. In this thesis, more emphasis is placed on ETI.

1.2.5.2 SA-mediated defence signalling in response to biotrophs

When biotrophic microbes gain access to the plant's apoplast, their MAMPs are recognised by PRRs. For example, in *A. thaliana*, fungal chitin is perceived by the PRR CHITIN ELICITOR RECEPTOR KINASE 1 (CERK1), the major and most-studied chitin-perceiving receptor. CERK1 is able to directly bind chitin, chito-oligomers and chitosan[1.5], resulting in phosphorylation of its intracellular domain and further signal transduction. *cerk1* mutants were not only shown to be more susceptible to fungal pathogens, but also to *P. syringae*, suggesting that it recognises multiple ligands, including PGN. CERK1 forms a receptor complex with LYSM DOMAIN GPI-ANCHORED PROTEIN 1 and 3 (LYM1 and 3), two chitin oligosaccharide elicitor binding proteins, for PGN-perception and intracellular signal transduction, which is different from chitin-perception, where CERK1 acts on its own (Petutschnig *et al.*, 2010; Newman *et al.*, 2013).

Upon MAMP recognition, an oxidative burst is triggered via membrane-bound NADPH-oxidases and cell wall peroxidases, such as RESPIRATORY BURST OXIDASE HOMOLOGUE A to F (RBOHA – F[1.6]). However, this oxidative burst is observed in response to biotic and abiotic stress in general. Nevertheless, the produced apoplastic ROS trigger intracellular signal transduction pathways (MAPKs, amongst others) and are also imported into the cell. The process of signal transduction is poorly understood, but eventually leads to a transcriptional response of defence-associated genes. Besides targeting of the apoplastic ROS signals to the nucleus, they are also conveyed to the chloroplast where, again, ROS and SA are produced. Chloroplastidal ROS is involved in HR, and, together with SA, in activation of defence response gene expression. These mechanisms include feedback loops, whereby HR as a downstream outcome, itself, promotes SA production (Coll *et al.*, 2011; Glazebrook 2005; Shapiguzov *et al.*, 2012)

The deployment of effectors by biotrophs to induce ETS is mediated by the T3SS of many Gram-negative bacteria. The T3SS consists of a basal body that is located partly in the cytoplasm and spans through the cell membrane. A needle complex represents the extra-cellular part and is connected to the basal body. At its extracellular tip, there is the translocon, which is responsible for forming a channel through the plant cell's plasma membrane. In its entirety, the T3SS provides a passage or channel for effectors into the host cytoplasm (Büttner and He, 2009).

[1.5] Chitosan is a partially de-acetylated and water-soluble derivative of chitin (Igarashi, 2013).

[1.6] Rbohs oxidize NADPH in the cytoplasm and transport the released electrons across the cell membrane. The electrons then reduce oxygen to superoxide ($O_2^{-\cdot}$). Superoxide then again reacts to hydrogen peroxide (H_2O_2) (Shapiguzov *et al.*, 2012).

In response to biotrophic bacteria, *A. thaliana* induces the production of the phytoalexin, camalexin, for example. Phytoalexins are a group of plant compounds that are toxic for bacteria, but also for fungi and nematodes (Falcon-Rodriguez, 2012; Glazebrook, 2005)
An example for defence response components against fungal pathogens is the production of chitinases, which are localized in the vacuole and apoplast. Apoplastic chitinases inhibit hyphae growth, lyse fungal cells and subsequently activate additional defence mechanisms in response to the released fungal elicitors (Ebrahim *et al.*, 2011).

1.2.5.3 Hypersensitive response

HR is the most investigated defence response outcome against biotrophic pathogens and needs to be addressed at this point. HR is a form of PCD that is triggered at the site of infection and characterised by rapid cell death. ROS play a very important role in HR as signalling molecules, as well as executing molecules, where they oxidise proteins, nucleic acids and membrane lipids. Here, chloroplasts are a central component for HR as a source for ROS (besides the apoplast). Significantly, light is often required for HR and effectors were shown to target chloroplasts (Torres *et al.*, 2006; Coll *et al.*, 2011).
Investigations of PCD in plants crystallised two distinct types: (1) vacuolar and (2) necrotic PCD. In principal, vacuolar PCD is characterised by, first, a decrease of cytoplasm volume and increase of lytic vacuole volume, followed by degradation of cytoplasm, massive release of hydrolases from lytic vacuoles and subsequent degradation of cell organelles. Vacuolar PCD is mostly seen during tissue and organ formation, and takes several days for completion. Necrotic PCD follows a different sequence. The cell initially gains in volume followed by a rupture of the cell membrane, leading to shrinkage of the protoplast and loosing of the intracellular content. This process takes from minutes to a day. HR shows signs of both, vacuolar and necrotic PCDs. It starts similarly to necrosis with an initial increase of cell volume and rupture of the plasma membrane but is accompanied by an increase of lytic vacuoles (Doorne *et al.*, 2011).
PCD is a final event for cells that needs to be tightly regulated. The main positive regulators to drive HR are SA and ROS. Upstream of SA biosynthesis, *NDR1*, *EDS1* and *PAD4* are necessary for defence response signal transduction to amplify SA accumulation. SA accumulation is negatively regulated through *LESION SIMULATING DISEASE 1* (*LSD1*), amongst others. LSD1 was shown (by yeast-two-hybrid assay) to interact with LSD ONE LIKE 1 (LOL1) and METACASPASE 2 (MC2) to inhibit the positive regulatory function of *NDR1*, *EDS1* and *PAD4* in PCD (Coll *et al.*, 2011), giving

an idea of the complexity involved to appropriately regulate SA and ROS accumulation. In fact, the importance of this control is demonstrated by the phenotype of SA overexpressing mutants. Durrant and Dong (2004) showed that *A. thaliana* mutants with permanent increased SA levels formed spontaneous HR-like lesions or exhibited severe morphological phenotypes such as dwarfing, that is often a result of the resource diversion to defence responses instead of growth (Balibi and Devoto, 2008).

1.2.5.4 Systemic acquired resistance

Another effect of activating SA-signalling is the development of resistance within the entire plant (unchallenged cells) to subsequent infections by pathogens that are sensitive to SA-regulated defence responses. This effect is called Systemic Acquired Resistance (SAR) and is long-lasting, sometimes for the lifetime of the plant (Freeman and Beattie 2008; Mahalingam 2003; Durrant and Dong, 2004).

On a molecular level, SAR is characterized by increased levels of endogenous SA, increased lignin deposition and increased expression of pathogenesis related (PR) genes, locally and systemically (Durrant and Dong 2004; Coll *et al.*, 2011).

ROS and SA were suggested to mediate SAR together as intercellular and/or intracellular messengers. The systemic transport of the SA signal is most likely done via the plant´s phloem, but movement through a different route is not excluded. Studies involving inhibition of ROS and SA showed an improbability of only ROS being the signal mediating SAR. ROS rather enhances SA-signalling through a signal amplification loop (Durrant and Dong, 2004; Torres *et al.*, 2006; Coll *et al.*, 2011).

1.2.5.5 JA/ET-mediated defence signalling in response to necrotrophs

SA-dependent defence response and subsequent increased PCD/HR would be a disadvantage for the plant when it has to respond to necrotrophic pathogens since necrotrophs feed on dying and dead cells. JA- and ET-dependent defence response, therefore, involves the expression of different defence response-associated genes such as *CORONATINE INSENSITIVE 1* (*COI1*) that is essential for JA-mediated defence response, and the JA/ET-dependent *PLANT DEFENSIN 1.2A* (*PDF1.2a*) that harbours antifungal activity, subsequently producing a different output. The loss-

of-function of *COI1* led to a block of JA-signalling and severely impaired the mutant's resistance to *Alternaria brassicicola*, a necrotrophic fungus, but at the same time did not affect its resistance to the hemibiotrophic oomycete *Phytophthora parasitica* (Freeman and Beattie, 2008; Mahalingam, 2003; Durrant and Dong, 2004; Coll *et al.*, 2011; Wang *et al.*, 2015; Koornneef and Pieterse, 2008).

Similar to biotrophic pathogens, necrotrophic pathogens are also recognised by PRRs in the apoplast. Here, *Botrytis cinerea,* as an example of necrotrophic fungi, utilises its cell wall degrading enzymes and degrades pectin as source for carbon, which, however, releases oligo-galacturonides that can be detected and elicit a defence response against the pathogen.

B. cinerea infection was found to alter the *A. thaliana* transcriptome fast and significantly, affecting one-third of all genes within 48 h (Windram *et al.*, 2012). JA- and ET-associated genes were the most important in terms of plant defence response (Windram *et al.*, 2012).

1.2.6 Pathway crossing and shared defence outcome

It is impossible to divide the discussed response pathways and signalling molecules into biotrophic and necrotrophic *per se*. An extensive interaction and crosstalk between SA-signalling and JA/ET- signalling was shown, integrating them in a complex signalling network that enables the plant to adjust and fine-tune its response to the specific characteristics of pathogens. In general, JA and ET together lead to a positive regulatory interaction, resulting in a synergistic induction of their targeted defence-related genes. SA and JA have a mutualistic inhibitory effect on each other, but genes induced by both exogenous SA and exogenous JA are also known (*LIPOXYGENASE 1* (*LOX1*) for example), as well as cases of negative interaction of ET and JA (PAL1 for example). SA and ET also show partly positive and partly negative regulatory interaction, making the defence-signalling in its entirety as very adaptable (Schenk *et al.*, 2000; Kunkel and Brooks 2002; Glazebrook 2005; Coll *et al.*, 2011).

1.2.7 Uncoupling of HR and biotrophic defence response

Based on contradicting results showing that proliferation of plant pathogens was not inhibited by plant cell death, and that plant resistance to pathogens was not affected by an inhibition of cell death in response to pathogens (shown by suppressing caspase-like activities in plants) (Coll *et al*., 2010 and 2011), a hypothesis was proposed that is different from the established understanding of HR. HR is understood as the plant´s strategy to prevent pathogen propagation from the site of infection to other parts of the plant during incompatible plant-pathogen interactions. Coll *et al.* (2010 and 2011) likewise showed that PCD itself does not inhibit pathogen proliferation. The researchers knocked out *MC1*, which resulted in reduced HR after *Pst* DC3000 (*avrRpm1*) infection (this *P. syringae* strain was chosen because *MC1* is activated by NB-LRR-mediated signalling). However, the reduced HR did not result in increased susceptibility to *Pst* DC3000 (*avrRpm1*). The proposed hypothesis by Coll *et al*. (2011) stated that HR is the consequence of an escalated signalling at the interface of plant-pathogen interactions, where the subsequent surge of toxic intermediates could cause plant cell death and pathogen cell death.

In conjunction with this, Igarashi *et al.* (2013) found that *Pst* DC3000 (virulent) growth was suppressed when the leaves were pre-treated with flg22 (1 day), and at the same time, HR was not visible. This suggests that a strong defence response is not necessarily accompanied by PCD.

1.2.8 The influence of the circadian rhythm, light and day length on ROS production and pathogen defence response

As stated earlier in the introduction of this thesis (1.1.4.1 Circadian rhythm overview), approximately one-third of *A. thaliana*'s genes were estimated to be circadian rhythm regulated. These genes are associated with a wide range of processes including the regulation of metabolic and developmental processes. This infers that defence responses are most probably partly circadian regulated as well. It has been found that an impaired expression of the central oscillator gene *CCA1* results in impaired resistance to the hemibiotrophic *P. syringae* and *Hyaloperonospora arabidopsis* (Hpa). One way of defence response regulation by *CCA1* was suggested to involve stomata closure. *CCA1* directly binds to the promoter and activates the transcription of *GLYCIN RICH PROTEIN 7* (*GRP*7) that regulates the stomata opening and closure.

Additionally, SA levels that peak at night, and JA/ET levels that peak during the day, antiphasic to SA, have been proposed to be circadian regulated (Zhang *et al*., 2013).

ROS were already shown to act as oxidising agents, but also as messengers in response to stress, showing their wide-ranging activity spectrum and importance. Lai *et al.* (2012) investigated the expression of ROS-responsive marker genes (by qPCR) in plants grown in 12 h light / 12 h darkness and found a time of day specific phases of increased expression for 39 % (50 genes) of all ROS-associated genes they investigated at ZT10 (approximately subjective evening). H_2O_2 levels were highest at ZT7 (also increased at ZT3), when photosynthesis-associated gene expression peaked. Catalase activity was also increased during the whole light phase, but peaked at ZT7, which was the suggested cause for the strongly decreased H_2O_2 levels at ZT11. LD entrained plants, when transferred to constant light, showed a similar result in which 75 % (100 genes) of the oxidative stress response marker genes showed peak expression at ZT10. This indicated a circadian clock-regulation of the ROS regulatory network, leading to an oscillating production that is sustained in constant light (Shim and Imaizumi, 2014).

CCA1 and *LHY* double loss-of-function mutations resulted in increased H_2O_2 production during the whole day in LD and constant light, accompanied by decreased catalase activity during the day in LD and subjective day in constant light. *CCA1* overexpression, however, led to decreased levels of H_2O_2 under both conditions. Interestingly, catalase activity was also decreased but only during the day in LD and subjective day in constant light (and was similar to WT during the night / subjective night, respectively), suggesting that *CCA1* (and possibly *LHY*) is involved in regulating ROS production and ROS-responsive gene expression. *CCA1* and *LHY* are circadian rhythm-dependently expressed at dawn and early part of the day and would only regulate these genes at these time points. During the night, when CCA1 levels are low, oxidative stress did not lead to regulation of these ROS-responsive genes. The genes following *CCA1* and *LHY* in the repressilator model, *PRR5*, *7*, and *9*, as well as *ELF3* and *LUX*, were also reported to be involved in ROS-regulation, as the loss-of-function mutants are hypersensitive to ROS (increased chlorosis after methyl viologen (oxidative stress causing agent) treatment). This, however, could be attributed to a resulting altered expression of *CCA1* and *LHY* in these mutant plants. In *LUX* loss-of-function mutants, for instance, the WT expression pattern of ROS-regulated genes was almost retained across 24 h. In *CCA1* overexpressor or *cca1/lhy* mutant plants, on the other hand, these ROS-regulated genes were constantly expressed or misregulated, respectively (Lai *et al.*, 2012; Shim and Imaizumi, 2015).

The highly reactive properties of ROS make a tight regulation necessary, partly through scavenging by catalases and antioxidants. Peroxisome-located catalases scavenge ROS during photorespiration, which is a major source for ROS. Three catalases are known *in A. thaliana* (*CAT1-3*) and all seem to be circadian rhythm regulated. CAT2 was established to be strongly circadian regulated and showed high expression at subjective early morning. Loss-of-function mutants develop lesions, which were LD specific. Catalases degrade due to irradiation, which becomes more obvious with irradiation length and could be an explanation of the LD-dependent phenotype of *cat*2, where the other catalases are not able to compensate for the loss as the day progresses. There also could be a pathway involved that is only active or more active in LD (Shim and Imaizumi, 2014; Nitschke *et al.*, 2016).

Plants show differences in ROS accumulation when grown in SD and LD. SD grown Arabidopsis plants accumulate H_2O_2 in leaves in contrast to plants grown in LD that was suggested to be linked to Pchlide accumulation in darkness. Here, the light dependent POR catalyses the reduction of Pchlide to chlorophyllide. In SD conditions when the dark period is long, Pchilde accumulates due to inactivity of POR and subsequently generates ROS upon illumination. In LD, where the dark period is short, less Pchilde accumulates and less ROS are generated upon illumination. *FHY3* loss-of-function mutants show a defective downregulation of POR expression, inferring increased Pchilde accumulation (Barnes *et al*., 1996). However, Pchilde accumulation has actually been found to be decreased in *fhy3* and *fhy3 far1* mutants, due to reduced *HEMB1* expression (encoding for 5-aminolevulinic acid dehydratase (ALAD)) in *fhy3* that encodes an enzyme that acts upstream of Pchilde in the chlorophyll biosynthesis pathway. It was hypothesised that the reduced Pchilde levels could even protect *fhy3* and *fhy3 far1* plants from oxidative stress upon light onset (Tang *et al.*, 2012) (Figure 1.8 a). However, these findings stem from seedlings that transitioned from skoto- to photomorphogenesis and cannot necessarily be transferred to day-night shift in older seedlings.

A secondary consideration could be the coinciding decreased levels of peroxisomal catalases that represent a ROS scavenging mechanism and, therefore, point to additionally increased peroxisomal H_2O_2 production in SD conditions. It was proposed that ROS accumulation in SD is controlled, whereas in LD oxidising components are completely quenched (Lepistö and Rintamäki, 2012; Gibon *et al*., 2004). The reduced activity of catalases and ascorbate peroxidases, as well as reduced glutathione levels (which is involved in detoxification and redox homoeostasis mechanisms) in SD grown Arabidopsis plants (Becker *et al*., 2006), however, could also result in higher levels of oxidative stress.

Light itself, in excess and as red light, can also trigger ROS production. Excessive light and red light cause changes in the redox state of the chloroplastidal plastoquinone pool, involving increased levels of reduced glutathione, and lead to a more oxidized environment that inactivates LSD1 by homo-dimerisation. LSD1 consequently does not inhibit *EDS1* expression. At the same time, phyB is also activated by red-light and translocates into the nucleus, where it interacts with HY5 to induce EDS1 expression. As a result, SA and ROS accumulation are activated, mediating PCD in red light. The loss-of-function mutant *phyB* exhibits decreased PCD, ROS and SA levels that conversely are increased in the PHYB overexpressor mutant. *HY5*'s contribution to this process can be seen in *hy5* mutants that have decreased PCD, ROS and SA production in response to red light, which is similar in *eds1* mutants. In total, excessive white light and red light regulate PCD/HR through at least these two pathways that converge on *EDS1* (Chai *et al*., 2015). It is, however, unknown if SD conditions and the associated change of redox state has a similar effect on LSD1-mediated *EDS1* expression. It could be speculated that the de-repression of *EDS1* due to cessation of LSD1 localisation into the nucleus leads to SA accumulation which, in turn, inhibit catalase activity (Sanchez-Casas and Klessig, 1994) (Figure 1.8 b). However, *LSD1* loss-of-function mutants that have increase SA levels (Huang *et al*., 2010 b) and reduced catalase activity (LSD1 directly binds and induces *CAT1/2/3* in Arabidopsis (Yi *et al*., 2013)) did not exhibit runaway cell death (RCD – a form of PCD) in SD but only in LD conditions (Yi *et al*., 2013). This could indicate mechanisms that prevent extensive PCD in SD grown plants that already have increased ROS levels and possibly increased SA levels. In LD, *lsd1* mutants developed lesions, even when catalases were overexpressed. This suggests that catalases do not reduce RCD in LD.

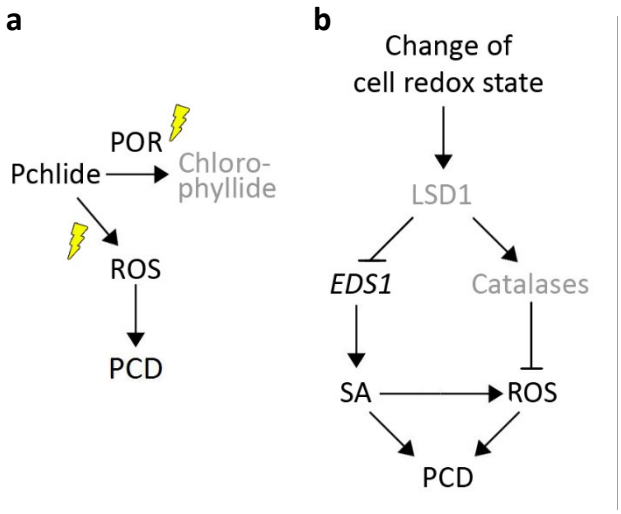

Figure 1.8: Scheme of ROS accumulation in SD conditions by a) accumulation of protochlorophyllide (Pchlide) due to long inactivation of light-dependent protochlorophyllide oxidoreductase (POR) in the chlorophyll biosynthesis pathway, and ROS generation upon light onset that could induce PCD, and b) change of the cells redox state could lead to LSD1-mediated de-repression of *EDS1* expression, resulting in SA accumulation, which could induce PCD but may be inhibited by PCD inhibiting mechanisms in SD conditions.

1.3 Aim and objectives of this project

The aim of this thesis was to investigate and determine the primary causes for the enhanced leaf-lesion formation in *fhy3 far1* mutants. *FHY3 FAR1* loss-of-function mutant plants have been subjected to several assays probing the involvement of both TFs in different mechanisms. The three original objectives were: 1) Analysing the defence response patterns of *fhy3 far1* mutants without and with treatments of a range of elicitors and plant pathogens, to investigate the effect of the *fhy3 far1* mutation on disrupting stress and defence response pathways; 2) Searching for altered stress, defence, or biosynthesis pathways in *fhy3 far1* mutants; and 3) Testing whether lesion formation may represent enhanced defence response to a normally commensal aspect of the microbial community on *A. thaliana*.

During the course of this investigation, two other groups also addressed the issue of the first two objectives. Wang *et al.* (2016) suggested the chlorophyll biosynthesis pathway as cause for the extensive leaf-lesion formation. FHY3, and to lesser degree FAR1, directly bind and activate *HEMB1* and were suggested to thereby promote chlorophyll biosynthesis. The loss-of-function of *FHY3* and *FAR1* was proposed to cause the accumulation of photosensitizing intermediates in darkness (no specific intermediates were stated), which could lead to ROS production upon light onset. Secondly, a constitutive accumulation of ALA (the substrate for HEMB1) in *fhy3 far1* mutants could act as a stress signal and lead to increased SA production in response to abiotic

stress. Increased SA levels activate ROS production and cause leaf-lesion formation. The group referred to their previously published paper (Tang *et al.*, 2012), where they discovered *FHY3*'s interaction with *HEMB1*. As mentioned above, that paper actually stated a prevention of light-induced damage in *fhy3 far1* mutants after transfer from darkness to light. Since the level of photosensitizing intermediate, Pchlide in this case, was confirmed to be lower in *fhy3 far1* mutants than in WT, it cannot be concluded that the double mutant phenotype is caused by increased levels of Pchlide and/or other pyrrole intermediates. No other evidence has been found that accumulation of chlorophyll biosynthesis intermediates upstream of HEMB1 would cause any oxidative damage (Tanaka *et al.*, 2011), so the proposal of Wang *et al.* (2015) remains controversial.

In the second publication, Ma *et al.* (2016) suggest a constitutively activated SA-dependent defence response in *fhy3 far1* mutant plants, due to an impaired light-induced *myo*-inositol biosynthesis, as the cause for the observed leaf-lesion formation. *Myo*-Inositol is the precursor for inositol derivatives that are essential for vesicle trafficking, phytohormone-signalling and response to biotic and abiotic stress. *MYO-INOSITOL-1-PHOSPHATE SYNTHASE 1* and *2* (*MIPS1* and *2*) are essential enzymes that act early in the inositol biosynthesis pathway and contain FBSs. This makes them targets for activation by FHY3 and FAR1. Therefore, the two TF are positive regulators of *myo*-inositol biosynthesis in *A. thaliana* (*MIPS1*-and *MIPS2* expression temporally follows the expression of *FHY3*/*FAR1* in WT). Antisense constructs for *MIPS1* and *2* resulted in leaf-lesion mimicking cell death, comparable to *fhy3 far1* leaf-lesions. *fhy3 far1* plants were found to accumulate high levels of SA because of reduced *myo*-inositol and/or inositol-derivate biosynthesis that would, in WT levels, indirectly prevent SA accumulation and subsequently prevent enhanced ROS production (enhanced ROS production was shown by means of DAB-staining and increased ROS marker gene expression in *fhy3 far1*).

Chaouch and Noctor (2010) investigated the ROS-scavenging *CATALASE 2* (*CAT2*) and showed that enhanced PCD in *cat2* mutants was prevented by *myo*-inositol application or by introducing a *SID2* loss-of-function mutation. *Myo*-inositol was found to supress *SID2* transcript accumulation, and as mentioned earlier, *SID2* is required for SA biosynthesis. This confirmed the connection between SA and *myo*-inositol and attributed an important role in this mechanism to *SID2*.

In *fhy3 far1* mutant plants grown in SD, the expression of *CAT1, CAT2* and *CAT3,* as well as the other ROS scavenging antioxidant-encoding genes *L-ascorbate peroxidase 1* (*APX1*) and *THYLAKOIDAL ASCORBATE PEROXIDASE* (*tAPX*) was not affected during the light period, which coincided with increased H_2O_2 accumulation at this time in the double mutant (Ma *et al*., 2016).

A transformation of *fhy3 far1* mutants with a construct constitutively overexpressing *SALICYLIC ACID 3-HYDROXYLASE* (*S3H*) resulted in a block of SA accumulation. In these plants, the extensive leaf-lesion formation was prevented and the dwarf phenotype of *fhy3 far1* mutants almost completely rescued, in both, LD and SD. Ma *et al.* (2016) proposed that *FHY3* and *FAR1* function in maintaining SA homoeostasis via induction of the *myo*-inositol biosynthesis (Figure 1.9 a). It is important to note that a constitutive overexpression of *MIPS1* in *fhy3 far1* background was not sufficient to completely rescue the mutant phenotype (especially in SD), suggesting that other *FHY3/FAR1*-dependent mechanisms are also impacted (Ma *et al*., 2016).

The hypothesised mechanism of increased ROS accumulation and resulting cessation of LSD1-mediated repression of *EDS1* expression in SD (1.2.8 Circadian rhythm and pathogen defence response) could possibly contribute to the increased leaf-lesion formation of *fhy3 far1* mutants in SD conditions. Increased SA levels in *fhy3 far1* mutants caused by absent repression of *SID2* via *myo*-inositol could be further increased by additional activation of *SID2* by *EDS1* in SD (Figure 1.9 b).

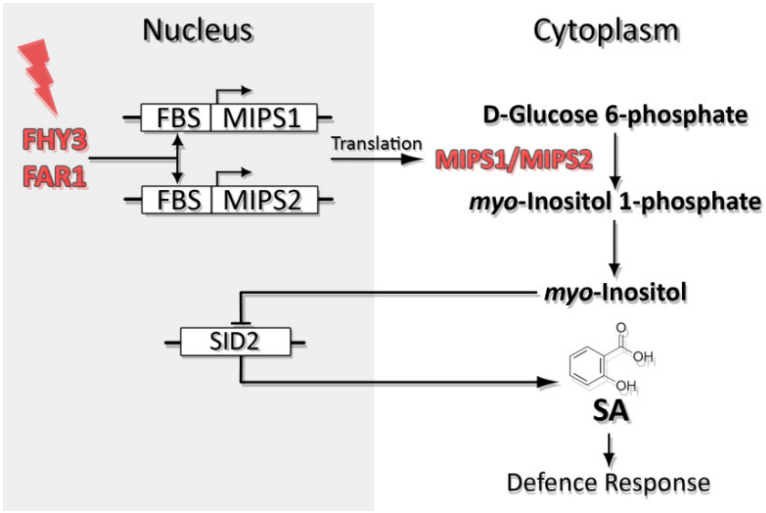

Figure 1.9: Regulating of *myo*-Inositol biosynthesis by FHY3 and FAR1 that bind *MIPS1* and *MIPS2* promoters and promote transcription (FHY3 is pre-dominant). MIPS1 and MIPS2 catalyse D-Glucose 6-phospate conversion to *myo*-Inositol 1-phospahte that is further converted to *myo*-Inositol. *myo*-Inositol in turn supresses SID2 transcription and subsequent SA accumulation (in reference to Ma *et al*., 2016).

Given these new findings of altered SA accumulation in *fhy3 far1* mutants, it is natural to expect an altered SA-dependent defence response of these plants. Thus, the question if the leaf-lesions are caused by impaired defence mechanisms is answered. As a result, the original third objective of this thesis was modified as below and so the objectives became the following: 1) Analysing the defence response patterns of *fhy3 far1* mutants without and with treatments of a range of elicitors and plant pathogens, to investigate the effect of the *fhy3 far1* mutation on disrupting stress and defence response pathways, 2) Searching for altered stress, defence or

biosynthesis pathways in *fhy3 far1* mutants, and 3) Analysing the phyllospheric microbial community (microbiota) of *fhy3 far1* mutant plants to investigate the effect of a constitutively activated SA-mediated defence response on the microbial community composition.

The discussion of the first two objectives is done in the light of the new findings by Ma *et al.* (2016).

For the different investigations, different plant growth stages and sampling time points were chosen. Table 1.2 summarises theses and states the reasons for their selection.

Table 1.2: Plant growth stages of *A. thaliana* WT, *fhy3 far1*, *METACASPASE 2* (*MC2*) loss-of-function and *CYSTEIN RICH KINASE 13* (*CRK13*) overexpression mutants when they were sampled for the investigations of this work and reasons for the selection of the respective growth stages.

Investigation	Plant growth stage and time when sampled	Reason for selection of plant growth stage and sampling times
Global transcript analysis by DNA microarray (3.2.3 Global transcript analysis of *fhy3 far1* (No-0) and WT (No-0))	9 days old seedlings were sampled during the night in SD (ZT12, 16, 20)	FHY3 and FAR1 have been shown to buffer *ELF4* expression at these time points (Siddiqui *et al.*, 2016). Li *et al.* (2011) also showed that these are the peak times of action of FHY3 and FAR1, suggesting that the expression of other genes is also affected at this time and would be misregulated in *fhy3 far1* mutant plants. Young seedlings were used to allow pooling of large numbers to get a more accurate representation of gene expression.
Biotic challenges investigations of WT, *fhy3 far1*, *mc2* and *CRK13*-ox mutants (3.2.4.2 Symptoms upon biotic challenges and histochemical staining, 3.2.4.5 Transcriptional changes upon biotic challenges, 4.2.5.1 Phenotypic changes and histochemical staining upon biotic challenge, 4.2.5.2 Transcriptional changes upon biotic challenges)	22 days old short day-grown plants (WT plants were at six rosette leaves development stage, *fhy3 far1* mutant plants at five to six rosette leaves development stage, *mc2* mutants at six rosette leaves development stage, and *CRK13*-ox mutants at six rosette leaves development stage)) were treated with biotic challenges by spraying during the daytime in SD, samples were harvested 3 dpi (at ZT4) for RT-qPCRs	Mutant plants clearly exhibited their phenotypes at this stage. Plants were treated with biotic challenges by spraying during the daytime in SD, thereby the time of higher susceptibility of the plants at least for *Pst* DC3000 (Zhang *et al*., 2013). Samples were harvested 3 dpi at ZT4 for RT-qPCRs, since the expression of all utilised defence response marker genes (3.2.4.4 Marker genes of defence response) was increased at this time of day in SD. The defence response marker gene expression was evaluated with the web-interfaces Diurnal (Mockler *et al.*, 2007)
Investigations of the phyllospheric microbiota of *fhy3 far1* mutant and WT plants (5.2.2 Culture-independent taxonomic identification of phyllospheric microbiota in short days)	35 days old short day-grown plants were sampled during the day (ZT4)	It was intended to use older plants, since the microbial community would have more time to establish a steady state.

2 MATERIAL AND METHODS

2.1 Plant material and growth conditions

2.1.1 Loss-of-function plant lines and genotyping

The *fhy3 far1* double mutant plant line of Arabidopsis with Nossen (No-0) ecotype was obtained from the Xing Wang Deng group at Yale University, New Haven, USA (Wang and Deng, 2002). It is a cross of the two mutant plant lines *fhy3-4* and *far1-2* that were produced via 1-Methylsulfonyloxyethane (EMS) mutagenesis by Hudson *et al.* (1999).

15 *MC2* loss-of-function lines were purchased from the Nottingham Arabidopsis Stock Centre (NASC). They consisted of 2 homozygous lines from The Salk Institute for Biological Studies, La Jolla, Canada (SALK_050076C and SALK_009045C) and 13 heterozygous T3 lines (segregating) that contained a 12-line set from the German plant genomics research program-Kölner Arabidopsis T-DNA lines (GABI-KAT (GK)), termed GK-537H06, and one heterozygous SALK line (SALK_084393). The heterozygous lines were grown to obtain homozygous progeny in case the already established homozygous lines would not grow successfully.

Lines from both institutions are based on T-DNA inserts that disrupt the ORF of *MC2*. The pROK2-vector integrated the *Neomycin phosphotransferase II* (*NTPII*)-marker to convey resistance to kanamycin and was used for SALK lines (Salk Institute Genomic Analysis Laboratory, 2003). GK lines were generated with a pAC161 vector that contained the *Sul1*-marker to convey resistance to sulfadiazine (GABI-Kat, 2014)).

The Dexamethasone (DEX)-inducible *CYSTEINE-RICH RECEPTOR-LIKE PROTEIN KINASE 13* overexpression (*CRK13*-Ox) lines, #26 and #33, were obtained from the Raina Lab at Syracruse University, USA. Both lines are based on T-DNA inserts, using the binary pTA7002-vector that additionally contained the *Hygromycin phosphotransferase II* (*HPTII*)-marker gene (Acharya *et al.*, 2007).

The *fhy3-12 far1* (allele number not stated for *far1*) double mutant plant line with Columbia (Col-0) ecotype was obtained from the Ottoline Leyser Group at The Sainsbury Laboratory, University of Cambridge, Cambridge, UK. It is a cross of the SALK_031652 *FAR1* loss-of-function mutant line and a line with disrupted *FHY3* ORF (by stop-codon), obtained by EMS-mutagenesis (Stirnberg *et al.*, 2012).

In order to genotype the plant lines, their DNA was extracted with the Qiagen DNeasy Plant Mini Kit (QIAGEN N.V., Manchester, UK), according to manufacturer's protocol. The DNA was used

for PCR amplification. PCRs were performed in volumes of 20 µl, with 1 x GoTaq Flexi Buffer (Promega UK, Southampton, UK), 1.5 mM $MgCl_2$, 200 µM dNTPs, 0.2 µM forward primer, 0.2 µM reverse primer, 1.25 units of GoTaq Flexi DNA Polymerase (Promega UK, Southampton, UK), ~ 200 ng template DNA and distilled water.

For the homozygous *mc2* SALK line SALK_050076C, a PCR with the primer pair LBb1.3 (ATTTTGCCGATTTCGGAAC) / RP (ACGGTACCACTATGACAAGCG) was used to identify the T-DNA insertion, and with the primer pair LP (TTTCTTCCTTGCCTTATTGGC) / RP (ACGGTACCACTATGACAAGCG) to identify the WT gene.
For the homozygous *mc2* SALK line SALK_009045C, PCRs with the primer pair LBb1.3 / RP (ATGACACCTGAAGTCCTGTGG) was used to identify the T-DNA and with the primer pair LP (TCCAAACTTCTGCAATGAAGG) / RP (ATGACACCTGAAGTCCTGTGG) to identify the WT gene.

For the *FAR1* loss-of-function (SALK_031652), PCRs with the primer pair LBb1.3 / RP (AGCTTCTCGCCAATCTAAACC) was used to identify the T-DNA insertion and with the primer pair LP (GCTTCTTGCAAATGTTTCCTG) / RP (AGCTTCTCGCCAATCTAAACC) to identify the WT gene. The *FHY3* loss-of-function was produced by a disruption of the *FHY3-12* ORF by a stop-codon. At codon 428, the TGG sequence was converted to the stop-codon TGA (EMS procedure) (Stirnberg *et al.*, 2012). In order to genotype the disrupted *FHY3-12* ORF, Stirnberg *et al.* (2012) recommended the utilisation of derived Cleaved Amplified Polymorphic Sequences (dCAPS) analysis. PCRs with the dCAPS primer pair 40CAPS-forward (GTAGGTTGGTGCCCATTTCT) / 40CAPS-reverse primer (GCAATCGGTGGACAAGCTC) were performed and the PCR amplicons digested by the restriction endonucleases FokI and XmnI (New England Biolabs, Hitchin, UK). The digests with both Fok1 and XmnI were carried out according to manufacturer's protocol.
FokI recognises the sequence 5'…GGATG$(N)_9$ …3' (3'…CCTAC$(N)_{13}$…5'), thereby, cutting the WT sequence, and XmnI recognises the sequence 5'…GAANNNNTTC…3' (3'…CTTNNNNAAG…5'), thereby, cutting the mutated sequence with the integrated stop-codon (Figure 2.1).

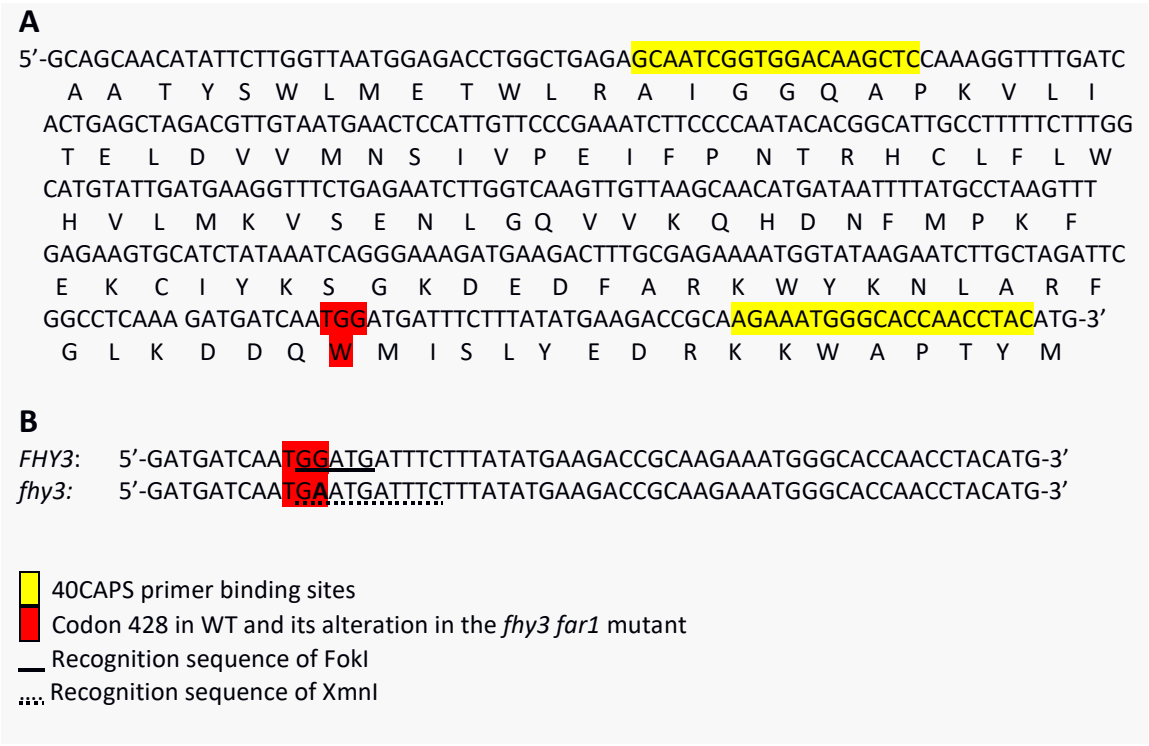

Figure 2.1: dCAPS analysis of *FHY3* loss-of-function, a) WT *FHY3* nucleotide sequence and translated amino acid sequence of PCR amplicon produced with *FHY3*-specific 40CAPS primer pair, b) sequences of *FHY3* in WT and *fhy3 far1* mutant with indicated recognition sites for the restriction enzymes FokI and XmnI (in reference to Stirnberg *et al.*, 2012).

The thermo cycler profile for the PCRs was as follows: initial denaturation at 94°C for 4 min, followed by 34 cycles of denaturation at 94°C for 30 sec., annealing at 60°C (for SALK lines) / 58°C (for dCAPS) for 30 sec., elongation at 72°C for 1 min. Final elongation was performed at 72°C for 7 min.

2.1.2 Induction of *CRK13* overexpression

Dexamethasone (Sigma-Aldrich Company Ltd., Dorset, UK) to induce *CRK13* overexpression, was dissolved in ethanol at 30 mM and diluted to 1 µM with distilled water (Aoyama and Chua 1997; Acharya *et al.*, 2007). The solution was applied to the plants by spraying.

2.1.3 Plant growth conditions

All plants were grown in white light at a Photon Flux Density of 164 µmol m^{-2} s^{-1}. SD conditions correspond to 8 h of light, followed by 16 h of darkness.

2.2 Phenotype analysis

For fresh weight of seedlings, the average weight of 20 individual six weeks old seedlings (after sowing that was followed by two days of cold stratification) grown in SD, weighed with the AL204 precision fine balance (Mettler-Toledo Ltd, Leicester, UK), was calculated.

2.3 Histochemical ROS staining assay

For *in situ* detection of hydrogen peroxide according to Xiao *et al.* (2013), three *A. thaliana* leaves from six independent plants (per treatment and genotype) were infiltrated with a staining solution containing DAB (1 mg/ml, pH 3.0), Tween 20 (0.05 % v/v) and Disodium phosphate (Na_2HPO_4, 10 mM, pH 7), in a six-well microtitre plate under vacuum for 5 min. Control treatment consisted of an infiltration with Disodium phosphate (10 mM) solution. The six-well microtitre plate was covered with aluminium foil, as DAB is light-sensitive. This was followed by shaking of the six-well microtitre plate at 100 rpm for 4 h. Afterwards, the staining solution was replaced with a bleaching solution, consisting of ethanol, acetic acid and glycerol in a 3:1:1 proportion. The microtitre plate was incubated in a water bath of 90 - 95 °C for 15 min. Subsequently, the bleaching solution was replaced by fresh one and the microtitre plate was incubated at RT for 30 min. Pictures of the stained leaves were taken with a stereo microscope (Leica Microsystems EZ4, Leica Microsystems (UK) Ltd, Milton Keynes, UK).

2.4 Microarray analysis

Before analysing the *fhy3 far1* microarray, genes on the *fhy3 far1* microarray that did not show a relative transcript value of more or equal to 10 in one out of six arrays (all WT and *fhy3 far1* sampling time points - three time points each) were omitted. This represented the cut-off expression, below which the expression values were considered to represent background noise.

2.4.1 Gene ontology analysis

The GO enrichment analysis (or statistical overrepresentation test) (3.2.3.2 Enrichment analysis of misregulated genes in *fhy3 far1* (No-0) mutants) was performed by the web-interface PANTHER (Protein ANalysis THrough Evolutionary Relationships) statistical overrepresentation test (Mi *et al.*, 2013). Here, all genes that showed a two-fold up- or downregulation in their mean relative transcript over the three sampling time points in *fhy3 far1* mutants were uploaded to PANTHER with their mean relative transcript values. These data were compared by PANTHER to a reference list with all genes of the *fhy3 far1* microarray. The test was statistically evaluated by the Mann-Whitney test.
The functional classification (3.2.3.3 Functional classification of misregulated genes in *fhy3 far1* (No-0) mutants) of genes that are two-fold up- or downregulation in their mean relative transcript over the three time points in *fhy3 far1* mutants was also performed with PANTHER. For this analysis, only the list of genes that are two-fold up- or downregulated was uploaded to the web-interface (option “Functional classification viewed in pie charts”). Results were returned in pie charts.

For the GO analysis of the *fhy3 far1* microarray (3.2.3.4 Misregulation of PCD and defence response signalling), all genes that showed a two-fold up- or downregulation in their mean relative transcript over the three time points in *fhy3 far1* mutant were compared to the GO-associated genes for the GO categories “Salicylic acid”, “Jasmonate and Ethylene” and “Systemic acquired resistance”. These were filtered from the *A. thaliana* ATH_GO_GOSLIM list (The Arabidopsis Information Resource, 2016). The gene list for GOs associated to “negative regulators of PCD” was obtained from GONUTS, the Gene Ontology Normal Usage Tracking System (GONUTS, 2016). This gene list is based on the reviewed computational analysis from Heyndrickx and Vandepoele (2012) and the genetic interaction analysis from Nagano *et al.*

(2009). This GO-analysis was statistically evaluated by z-test. Therefore, 20 lists of randomly selected genes were created with the Bio-Array Resource Random AGI ID List Generator Tool (Honys *et al.*, 2008) that contained the same number of genes as found to be associated to the respective, above stated, GO categories. These 20 lists were used to calculate a mean and standard deviation for GO term frequency in the background population of Arabidopsis genes. To determine the z-score, the mean population GO term frequency was subtracted from the GO term frequency in the up- or downregulated genes in *fhy3 far1* mutants, and the difference divided by the population standard deviation. All calculations were done in Microsoft Excel 2010. P-values based on z-scores were calculated with the web-interface "P Value from Z Score Calculator" (http://www.socscistatistics.com/pvalues/normaldistribution.aspx). Here, the individual z-scores were transferred to the web-interface (Setting: two-tailed hypothesis) (Social Science Statistics, 2016).

2.4.2 Evaluation of defence response marker genes for RT-qPCR

In order to select appropriate defence response marker genes for biotic challenges assays (subheadings 3.2.4.5 Transcriptional changes upon biotic challenges, and 4.2.5.2 Transcriptional changes upon biotic challenges), the in table 2.1 listed publicly available microarray data obtained from ArrayExpress (Kolesnikov *et al.*, 2015) were analysed.

Table 2.1: Publicly available microarray data that was used to select defence response marker genes for biotic challenges assays

Microarray ID	Title of microarray	Reason for selection
E-GEOD-5684	Transcription profiling by array of Arabidopsis after infection with *Botrytis cinerea*	For this microarray, *B. cinerea* treated WT (Col-0) plants were used, similar to the biotic challenges assay in the present thesis.
E-GEOD-19109	Transcription profiling of Arabidopsis thaliana wild type (Col-0) and *lht1* mutant leaves	For this microarray, *Pst* DC3000-infected WT plants were used, similar to the biotic challenges assay in the present thesis.
E-GEOD-5520	Transcription profiling by array of Arabidopsis after inoculation with *Pseudomonas syringae* pv. Tomato	For this microarray, *Pst* DC3000-infected WT plants were used, similar to the biotic challenges assay in the present thesis.
E-GEOD-5525	Transcription profiling by array of Arabidopsis after exposure to various pathogens and insects	For this microarray, *Alternaria brassicicola*-infected WT (Col-0) plants were used. *A. brassicicola* is a necrotrophic fungus and defence response against it was shown to depend on JA signalling, similar to *B. cinerea* (Thomma *et al*., 1998).
E-GEOD-50526	Responses of Arabidopsis immune signalling mutants to *Alternaria brassicicola* infection	For this microarray, *Alternaria brassicicola*-infected WT (Col-0) plants were used. *A. brassicicola* is a necrotrophic fungus and defence response against it was shown to depend on JA signalling, similar to *B. cinerea* (Thomma *et al*., 1998).
E-GEOD-13739	Transcription profiling by array of *Arabidopsis* mutant for *eds16* after infection with *Golovinomyces orontii*	For this microarray, *Golovinomyces orontii*-infected WT (Col-0) were used. *G. orontii* is a biotrophic powdery mildew and defence response against it was shown to depend on SA signalling (Dewdney *et al*., 2000).
E-GEOD-40973	Expression profiling of uninfected and *Golovinomyces orontii* infected *Arabidopsis thaliana* wild type Col-0 and *del1-1* mutant	For this microarray, *Golovinomyces orontii*-infected WT were used. *G. orontii* is a biotrophic powdery mildew and defence response against it was shown to depend on SA signalling (Dewdney *et al*., 2000).
E-GEOD-4746	Transcription profiling of response of *Arabidopsis* seedlings to chitooctaose treatment	For this microarray, chitooctaose (a chitin octamer)-treated WT (Col-0) plants were used similar to the biotic challenges assay in the present thesis.
E-NASC-22	Transcription profiling of *Arabidopsis* protoplasts are treated with 20mM Fumonisin B1 (FB1)	For this microarray, Fumonisin B1 (FB1)-treated WT (Col-0) protoplasts were used similar to the biotic challenges assay in the present thesis.

2.4.3 Analysis of disrupted gene expression in *fhy3 far1* mutants

For analysis of the *fhy3 far1* microarray, the web-interface "Patmatch" (The Arabidopsis Information Resource (n.d.) Patmatch. [online] Available from: [30.05.2014]) was utilised. "Patmatch" searches public *A. thaliana* sequence databases that are also used by TAIR Blast, such as GenBank (The Arabidopsis Information Resource. (n.d.) TAIR BLAST Help. [online] Available from: [30.05.2014]), for short (<20) nucleotides motifs, represented by the sequences

of FBS (CACGCGC), Evening Element (EE) (AAAATATCT) and CCA1 Binding site (CBS) (AAAAATCT). The nucleotide sequence of the FBS, EE, and CBS were entered in the web-interface and searched against the "TAIR10 Transcripts (-introns, +UTRs (DNA)" sequence database. 2-fold misregulated genes that contained these promoter elements were subjected to analysis with the web-interface "Classification SuperViewer" (Provart *et al*., 2003). Here, a gene list was uploaded to this web- interface that classified the genes according to their function (based on the GO database). The returned results were sorted according the categories "responses to biotic and abiotic stimuli", "stress response" and "developmental processes" in Microsoft Excel 2010. The genes involved in those processes were subsequently subjected to a simultaneous analysis with the web-interfaces "Diurnal" (Mockler *et al.*, 2007) and "NASCArrays Gene Swinger" (Craigon *et al.*, 2004). The conditions selected for the web-based tool "Diurnal" were "shortday" and "COL_SD" that represent the genes transcript pattern in *A. thaliana* plants with Landsberg-erecta and Columbia background, respectively, grown in short day conditions for seven days. The shortday conditions were selected based on the role FHY3 and FAR1 play in SD by regulating cycling genes after dusk (Siddiqui *et al*., 2016). For the criterion "Cutoff", a correlation of 0.7 was selected. For the data-mining tool "NASCArrays Gene Swinger", experimental treatments involving "pathogens", "stress" and "circadian rhythm" were selected.

2.5 Biotic stressors and challenge of *A. thaliana* plants

2.5.1 Biotic stressors

B. cinerea was obtained from infected strawberries (residential garden, Wokingham, UK) and cultured on Yeast Extract Agar (see Table S2 in supplementary data for ingredients) at 21°C. For molecular identification, DNA from colonies was extracted with the QIAGEN DNeasy Plant Mini Kit (QIAGEN N.V., Manchester, UK), according to manufacturer's protocol. For the subsequent PCR, the fungal ribosomal gene internal transcribed spacer (ITS)-region was targeted with the primer combination ITS1-F (CTTGGTCATTTAGAGGAAGTAA) / ITS4 (TCCTCCGCTTATTGATATGC) (Manter and Vivanco, 2007). The amplicons were sequenced (Sanger sequencing) at Eurofins MWG Operon (Eurofins Genomics, Ebersberg, Germany, Value Read service). These sequencing results were analysed with Ensemble genome annotation system BLAST search (EnsemblFungi) (Kersey et al., 2016) and showed 100 % alignment with *B. cinerea*.

B. cinerea conidia were microscopically observed with a Leica DM500 microscope (Leica Microsystems (UK) Ltd, Milton Keynes, UK) and the conidia showed the typical ellipsoid to obovoid shape known to be associated with *B. cinerea* (Sutton, 1998). Spore suspension for plant infection: *B. cinerea* was cultivated at 21°C for nine days, after which spores were collected by rinsing with 2 % glucose solution. The spore suspension was further diluted with 2 % glucose solution to generate a working suspension of 5 x 10^5 cfu/ml for plant infection (by counting with the Improved Neubauer Chamber BS748) (Torres *et al.*, 2005). The negative control for plant infection consisted of 2 % glucose solution.

Pst DC3000 was obtained from the Devoto-lab (Royal Holloway, University of London, School of Biological Sciences, Egham, UK) and was grown in liquid Nutrient Yeast Glycerol (NYG) medium (see Table S2 in supplementary data for ingredients) with Kanamycin (50 µg/ml) at 28°C, overnight. The concentration of the *Pst* DC3000 suspension was adjusted with Magnesium chloride ($MgCl_2$) solution (10 mM in water) at OD600 = 0.2 that corresponds to approximately 10^8 cfu/ml. The suspension was further diluted 250-times with 10 mM $MgCl_2$ to achieve a concentration of approximately 10^6 cfu/ml for plant infection (Liu *et al.*, 2015). The negative control for plant infection consisted of 10 mM $MgCl_2$ solution.

Fumonisin B1 (FB1) was purchased from VWR International Ltd. (Lutterworth, UK) and dissolved in methanol (99.8 %) for a 1000 µM stock-solution. The stock-solution was diluted with distilled water to the final concentrations of 5 and 50 µM for plant treatment (Igarashi *et al.*, 2013). The negative control for plant treatment consisted of a 0.5 % methanol (v/v) solution.

Chitin was purchased from Sigma-Aldrich Company Ltd. (Dorset, UK). Suspensions of 100 and 1.000 mg/L were prepared with distilled water for plant treatment (Zang *et al.*, 2002; Chen *et al.*, 2014). The negative control for plant treatment consisted of distilled water.

2.5.2 RT-qPCR for defence response marker genes in biotic stressor-challenged *A. thaliana* plants

Plants were treated with the respective stressor and approximately 20 plants per treatment were harvested three days post inoculation (dpi). RNA was extracted with the QIAGEN RNeasy kit, according to manufacturer's protocol, and reverse transcribed with the QIAGEN QuantiTect Reverse Transcription Kit, according to manufacturer's protocol. cDNA was diluted to 10 ng/µl and primers to 10 µM before qPCR reagents were mixed. qPCRs were performed in 20 µl reactions, with RNase-free water, 1 x SYBRGreen JumpStart *Taq* ReadyMix (Sigma-Aldrich

Company Ltd., Dorset, UK), 0.5 µM forward primer, 0.5 µM reverse primer and 20 ng template cDNA.

Since several different primer pairs for each defence response marker gene were found in the literature, the marker genes were subject to a DNA database alignment search using Primer-BLAST (Ye *et al.*, 2012). Final primer pairs from these BLAST results (Table 2.2) were selected according to similar length (nucleotides) between both primers of one pair, similar GC content in the range of 50 – 60 %, and low complementarity scores.

Table 2.2: Sequences of marker gene-specific primers utilised in RT-qPCR-investigation of *A. thaliana* plants challenged with biotic stressors.

Marker Gene	Primer combination and primer sequences	Primer-BLAST report				Reference
		Tm [°C]	GC [%]	Self	Self 3'	
PDF1.2a	Forward primer: CTTTGGTGCTAAATCGTGTGT Reverse primer: TGTAACAACAACGGGAAAATAAACA	57.1 58.14	42.86 32	4 5	0 0	Primer-Blast alignment result
PR3	PR3QCF: ACGGAAGAGGACCAATGCAA PR3QCR: AGCAGTCATCCAGAACCAAATC	59.6 59.62	50 47.83	4 2	2 0	Liu *et al.*, 2013 a
PAD4	Forward primer: ATCTTCTCCGCCGTCATTCC Reverse primer: CACGTGGCAGAAGTTGTGTG	59.89 59.97	55 55	3 6	0 1	Primer-Blast alignment result
EDS1	Forward primer: ACCTCATTTCAAGCTTCTGTGGA Reverse primer: GATTGCAGTTGCACCTCCTG	60.18 59.48	43.48 55	6 6	1 2	Primer-Blast alignment result
SID2	SID2RealF: TGGTTAGCGTTGCTGGTATC SID2RealR: CATTCAACAGCGATCTTGCC	57.98 57.82	50 50	3 6	2 2	Wang et al., 2015

Tm = melting temperature
Self = Self complementarity
Self 3' = Self 3' complementarity

The qPCR thermo cycler (QIAGEN Rotor-Gene Q, Model: 5-Plex) conditions used for the qPCRs were as follows: initial denaturation at 94°C for 2 min, followed by 45 cycles of denaturation at 94°C for 15 sec., annealing at 55°C for 60 sec. Final elongation was performed at 72°C for 20 sec. Subsequent qPCR results were processed with the Rotor Gene Q series software, Version 2.1.0 (Build 9).

RT-qPCRs were performed in two biological replicates (BRs) for each treatment and with two technical replicates for each BR.

2.6 Confirmatory RT-qPCRs of gene expression patterns found to be disrupted by the f*hy3* and *far1* mutations in *fhy3 far1* microarray analysis

RNA extraction, reverse transcription, qPCR reagents and conditions were performed and utilised as stated under heading 2.5.2 "RT-qPCR for defence response marker genes in biotic stressor-challenged *A. thaliana* plants". RT-qPCRs for the 11 candidate genes were performed in two BRs with two technical replicates each.

The utilised primer pairs were found by DNA database alignment search of the respective genes using Primer-BLAST; primer pairs are stated in Table 2.3.

Table 2.31: Sequences of qPCR-primers for 11 candidate genes with gene expression patterns that are disrupted by the *fhy3 far1* mutations. resist. = resistance.

Gene		Primer sequences
UVR2	(At1g12370)	Forward primer: ACTGACAGCAGATCCTCTATGG Reverse primer: ACATTCGCATGAAACCGTGC
ARD1	(At1g33560)	Forward primer: AACTGATACGTAACCATAAGATCCA Reverse primer: AAAGTGAGATGGTTGAGTGGT
Unnamed disease resist. protein (At4g11340)		Forward primer: AAGAAGGCTTGGGAGGATGC Reverse primer: CGAAGGTTGCTTGGTTGCTC
SUV2	(At5g45610)	Forward primer: TCCAACGTTTCTACCGGCTC Reverse primer: TGTTGTCCCGCTGAGGATTG
ATCSA-1	(At1g27840)	Forward primer: GAAGGTAGCTTTTGGCATGTGG Reverse primer: TCGTAGTGTCCACGAAGCAT
CRK13	(At4g23210)	Forward primer: GGAACTAGGCGAATTCTCGAT Reverse primer: GAGAAGCTCGTGTTCCTCTT
ERF6	(At4g17490)	Forward primer: CTCCGTTGCCTACTACTGCC Reverse primer: CCGGTTTGGGAGTGACGAG
MC2	(At4g25110)	Forward primer: CAGGACTTCAGGTGTCATCG Reverse primer: CATAGTTTCCGAGCCTGTCC
RbohD	(At5g47910)	Forward primer: CAGCTCCCGGAGACGATTAC Reverse primer: CCGTCGATAAGGACCTTCGG
GIM1	(At5g24280)	Forward primer: AACCCTTACCTGCCGAATGG Reverse primer: TCTCTAAGCCCGTAACCCGA
ERF4	(At3g15210)	Forward primer: TTGGCACTTTCGATACGGCT Reverse primer: AGGCACAACTAACGTCGGAG

2.7 Phyllospheric microbes

2.7.1 Extraction of phyllospheric microbes for trial run to test the PCR amplification procedure for high-throughput sequencing

In order to extract phyllospheric microorganisms from WT (No-0) and *fhy3 far1* (No-0) plants, 1.5 ml of autoclaved 0.2 % Tetrasodium pyrophosphate ($Na_4P_2O_7$) that acts as buffer was added to 0.1 g plant material in a sterile falcon tube and vortexed for 20 min. The suspension was allowed to settle for 20 min. 150 µl of the supernatant was transferred into a sterile falcon tube and 1.35 ml of sterile 0.9 % Sodium Chloride (NaCl) solution was added (Pryce-Williams R, 2009). After gentle mixing by inverting the falcon tube five times, 0.1 ml of this suspension was spread on the following growth medium plates: Potato Dextrose Agar (PDA), Malt Extract Agar (MEA), Reasoner´s 2 Agar (R2A), Yeast Extract Agar (YEA), Czapek Dox Agar (CDA) and Lysogen Broth (LB) agar (see table S2 in supplementary data for ingredients). The plates were incubated for 4 days at 28°C. Grown colonies were subsampled on fresh plates with the stated six growth media. Plates with bacteria were incubated at 28 °C and plates with filamentous fungi at 21°C.

2.7.2 Extraction of phyllospheric microbes for high-throughput sequencing

Phyllospheric microbes were washed off according to the protocol from Zhou *et al.* (1996). In detail: 100 mg above ground growing parts of WT and *fhy3 far1* mutant plants, 2.7 ml of DNA extraction buffer and 10 µl of proteinase K (10 mg/ml) were added in falcon tubes. The tubes were shaken horizontally at 225 rpm at RT for 30 min. 0.3 ml of 5 % SDS was added and the tubes were incubated at 65°C for 2 h, with gentle mixing by inverting the falcon tubes every 15 to 20 min. The samples were centrifuged at 6,000 g for 10 min at RT and the supernatants were collected. The pellets were extracted two more times by adding 0.8 ml of the extraction buffer and 20 µl of 5 % SDS. The tubes were vortexed for 10 sec., incubated at 65°C for 10 min and centrifuged as before. The supernatants from the three cycles of extractions were combined and mixed with an equal volume of chloroform-isoamyl alcohol (24:1, vol/vol). The aqueous phase was recovered by centrifugation and precipitated with 0.6 volume of isopropanol at room temperature for 1 h. The pellet of crude nucleic acids was obtained by centrifugation at 16,000 g for 20 min at RT. The pellet was washed with ice cold 70 % ethanol, dried at 37°C and resuspended in sterile deionized water for a final volume of 500 µl.

DNA extraction buffer contained 100 mM Tris-HCl (pH 8.0), 100 mM sodium EDTA (pH 8.0), 100 mM sodium phosphate (pH 8.0), 1.5 M NaCl and 1 % CTAB.

2.7.3 PCR and sequencing for trial run (colony-PCR)

Bacterial and fungal sub-sampled colonies (part of the individual colony was picked and cultivated on new medium) (2.7.1 Extraction of phyllospheric microbes for trial run to test the procedure) were picked (sterile toothpick) to remove a part of them. These respective parts were each suspended in 25 µl distilled water and the suspension directly used for PCRs. PCRs for bacteria and fungi were performed in volumes of 20 µl, with 1 x GoTaq Flexi Buffer, 1.5 mM $MgCl_2$, 200 µM dNTPs, 0.2 µM forward primer, 0.2 µM reverse primer, 1.25 units of GoTaq Flexi DNA Polymerase, 1 µl colony suspension and distilled water.

In order to amplify bacterial 16S rDNA and reduce mitochondria- and chloroplast-specific rDNA-amplicons, two separate PCRs were run as described by Sakai *et al.* (2004). A strong amplification of mitochondria- and chloroplast-specific rDNA-amplicons has been described when universal bacterial primers are utilised due to the homology of bacterial 16S, chloroplast 16S and mitochondrial 18S rRNA genes (Müller and Ruppel, 2014). The first PCR utilised the primer pair 63f (5'-CAGGCCTAACACATGCAAGTC-3') / 1492r (5'-GGCTACCTTGTTACGACTT-3') and resulted in amplification of bacterial-, mitochondria- and chloroplast-specific rDNA amplicons (Figure 2.2). However, mitochondria-specific 18S rDNA amplicons are larger (expected amplicons size of approximately 1850 bp) than bacterial 16S rDNA (expected amplicons size of approximately 1470 bp) and chloroplast 16S rDNA amplicons (expected amplicons size of approximately 1420 bp). After separation by gel electrophoresis on a 1 % agarose gel, showing one band at approximately 1800 bp (mitochondria-specific amplicons of 1850 bp) and one at approximately 1400 bp (bacteria-specific amplicons of approximately 1470 bp and chloroplast-specific amplicons of approximately 1420 bp), the smaller band was excised from the gel and processed with the QIAquick Gel Extraction Kit (QIAGEN V.N., Manchester, UK), according to the manufacturer's protocol, to recover the amplicons. The recovered DNA solution was adjusted to a concentration of 10 ng/µl and used as a template for a PCR with the primer pair 63f / 783r. Here, the degenerate primer 783r (5'-CTACCVGGGTATCTAATCCBG-3') is a mix of nine primers (783r-a1 (CTACCAGGGTATCTAATCCTG), 783r-b1 (CTACCGGGGTATCTAATCCCG), 783r-c1 (CTACCCGGGTATCTAATCCGG), and 783r-a2 (CTACCGGGGTATCTAATCCTG), 783r-b2

(CTACCCGGGTATCTAATCCCG), 783r-c2 (CTACCAGGGTATCTAATCCGG), and 783r-a3 (CTACCCGGGTATCTAATCCTG), 783r-b3 (CTACCAGGGTATCTAATCCCG), 783r-c3 (CTACCGGGGTATCTAATCCGG)). In general, degenerate primers are used to amplify a target gene in different organisms that is similar, however, most probably not identical in these organisms. Degenerate primers are used to identify uncultivated microorganisms and the mixture of very similar primers covers all permutations of the targeted sequence of the microorganismal DNA. In the present case, the degenerate primer 783r was designed to reduce amplification of chloroplast 16S rDNA due to primer mismatches and reduced annealing to chloroplast 16S rDNA (Figure 2.2).

The thermocycler profile for all bacteria- and fungi-specific PCRs was as follows: initial denaturation at 94°C for 4 min, followed of 20 cycles of denaturation at 94°C for 1 min, annealing at 50°C (63f/1492r and 63f/783r) or 55°C (for ITS1-F/ITS2) for 1 min and elongation at 72°C for 1 min. The final elongation step was performed at 72°C for 7 min.

Subsequently, PCR amplicons were separated by gel electrophoresis on a 1.5 % agarose gel to confirm successful amplification. PCR amplicons were purified with the Qiaquick PCR Purification Kit, according to the manufacturer's protocol. Amplicons were sent for Sanger sequencing to Eurofins MWG Operon.

The returned clipped sequences were subjected to a DNA database alignment search using BLAST. Here, the "Nucleotide collection (nr/nt) database was selected, and the alignment search optimised for "Somewhat similar sequences (blastn)". Identified microorganisms with highest identity and query cover were selected. Alignment results are shown on genus level.

***E. coli* 16S rDNA**

GTTTGATCATGGCTCAGATTGAACGCTGGCGGCAGGCCTAACACATGCAAGTCGAACGGTAACAGGAAGCAGCTTGCTGTTTCGCTGACGAGTG
GCGGACGGGTGAGTAATGTCTGGGAAACTGCCTGATGGAGGGGGATAACTACTGGAAACGGTAGCTAATACCGCATAACGTCGCAAGACCAAA
GAGGGGGACCTTCGGGCCTCTTGCCATCGGATGTGCCCAGATGGGATTAGCTAGTAGGTGGGGTAACGGCTCACCTAGGCGACGATCCCTAGC
TGGTCTGAGAGGATGACCAGCCACACTGGAACTGAGACACGCTCCAGACTCCTACGGGAGGCAGCAGTGGGGAATATTGCACAATGGGCGCAA
GCCTGATGCAGCCATGCCGCGTGTATGAAGAAGGCCTTCGGGTTGTAAAGTACTTTCAGCGGGGAGGAAGGGAGTAAAGTTAATACCTTTGCTC
ATTGACGTTACCCGCAGAAGAAGCACCGGCTAACTCCGTGCCAGCAGCCGCGGTAATACGGAGGGTGCAAGCGTTAATCGGAATTACTGGGCG
TAAAGCGCACGCAGGCGGTTTGTTAAGTCAGATGTGAAATCCCCGGGCTCAACCTGGGAACTGCATCTGATACTGGCAAGCTTGAGTCTCGTAG
AGGGGGGTAGAATTCCAGGTGATAGCGGTGAAATGCGTAGAGATCTGGAGGAATACCGGTGGCGAAGGCGGCCCCCTGGACGAAGACTGACG
CTCACGTGCGAAAGCGTGGGGAGCAAACAGGATTAGATACCCTGGTAGTCCACGCCGTAAACGATGTCGACTTGGAGGTTGTGCCCTTGAGGC
GTGGCTTCCGGAGCTAACGCGTTAAGTCGACCGCCTGGGGAGTACGGCCGCAAGGTTAAAACTCAAATGAATTGACGGGGGCCCGCACAAGCG
GTGGAGCATGTGGTTTAATTCGATGCAACGCGAAGAACCTTACCTGGTCTTGACATCCACGGAAGTTTTCAGAGATGAGAATGTGCCTTCGGGA
ACCGTGAGACAGGTGCTGCATGGCTGTCGTCAGCTCGTGTTGTGAAATGTTGGGTTAAGTCCCGCAACGAGCGCAACCCTTATCCTTTGTTGCCA
GCGGTCCGGCCGGGAACTCAAAGGAGACTGCCAGTGATAAACTGGAGGAAGGTGGGGATGACGTCAAGTCATCATGGCCCTTACGACCAGGG
TCTACACACGTGCTACAATGGCGCATACAAAGAGAAGCGACCTCGCGAGAGCAAGCGGACCTCATAAAGTGCGTCGTACTCCGGATTGGAGTCT
GCAACTCGACTCCATGAAGTCGGAATCGCTAGTAATCGTGGATCAGAATGCCACGGTGAATACGTTCCCGGGCCTTGTACACACCGCCCGTCACA
CCATGGGAGTGGGTTGCAAAAGAAGTAGGTAGCTTAACCTTCGGGAGGGCGCTTACCACTTTGTGATTCATGACTGGGGTGAAGTCGTAACAA
GGTAACCGTAGGGGAACCTGCGGTTGGATCACCTCCTTACCTTAAAGAAGCGTTCTTTGCAGTGCTC

***A. thaliana* mitochondrial 18S rDNA (ATMG01390.1)**

ATCATAGTCAAAAGAAGAGTTTGATCCTGGCTCAGAAGGAACGCTAGCTATATGCTTAACACATGCAAGTCGAACGTTGTTCTCGGGGAGCTAG
GCAGAAGGAAAAGAGGCTCCTAGCTCAAGGTAGCTTGTCTCGCCCAGGAGGCGGGAAGAGTTGAGAACAAAGTGGCGAACGGGTGCGTAAGG
CGTGGGAATCTGCCGAACAGTTCGGGCCAAATCCTGAAGAAAGCTAAAAAGCGCTGTTTGATGAGCCTGCGTAGTATTAGGTAGTTGGTTAGGT
AAAGGCTGACCAAGCCAATGATGCTTAGCTGGTCTTTTCGGATGATCAGCCACACTGGGACTGAGACACGGCCCGGACTCCCACGGGGGGCAG
CAGTGGGGAATCTTGGACAATGGGCGAAAGCCGATCCAGCAATATCGCGTGAGTGAAGAAAGGCAATGCCGCTTGTAAAGCTCTTTCGTCGAG
TGCGCGATCATGACAGGACTCGAGGAAGAAGCCCCGGCTAACTCCGTGCCAGCAGCCGCGGTAAAACGGGGGGGGCAAGTGTTCTTCGGAAT
GACTGGGCGTAAAGGGCACGTAGGCGGTGAATCGGGTTGAAAGTGAAAGTCGCCAAAAAGTGGCGGAATGCTTTCGAAACCAATTCACTTGAG
TGAGACAGAGGAGAGTGGAATTTCGTGTGGAGGGGTGAAATCTACAGATCTACGAAGGAACGCCAAAAGCGAAGGCAGCTCTCTGGGTCCCTA
CCGACGCTGGGGGTGCGAAAGCATGGGGGAGCGAACGGGATTAGATACCCTGGTAGTCCATGCCGTAAACGATGAGTGTTCGCCCTTGGTCTA
CGCAGATCAGGGGCTCAGCTAACGCGTGAACACTCCGCCTGGGGAGTACGGTCGCAAGACCAAAACTCAAAGGAATTGACGGGGGCCTGCACA
AGCGGTGGAGCATGTGGTTTAATTCGATACAACGCGCAAAACCTTACCAGCCCTTGACATATGAACAACAAAACCTATCCTTAACGGGATGGTAC
TCACTTTCATACAGGTGCTGCATGGCTGTCGTCAGCTCGTGTCGTGAGATGTTTGGTCAAGTCCTATAACGAGCGAAACCCTCGTCTTGTGTTGCT
CAGACATGCGCCTAAGGAGAAAGGCTTGAAAACCGAAGTGAGCCAAGGAGCCGAGTGACGTGCCAGACCTAGTAATTGAGTGACAGCAACTA
GCTCTGCTCTCAGTAAGAAGGGAGACGGCGCCTTTCCAAGCCCTTTCTAGTCTGCGCTTGAGTTTGATTGCAGCTAGCGCCGCGCTTTACTAAGA
AGTGCGAAAGGGCTTTTCTCGCTTGTTTAGTAAAGTCAAGTTTTTGACCCAGGTGACGACGACGTCGAGTTGGCGGCGGAGAAAGACTCGGCAT
TCAGGCGAGCCGCCCGGTGGTGTGGGACGAAGTAAGTGGGTTTAGTACGCCCTGCCAAAACGGCTCCGAAACAAACAAAAAGGTGCGTGCCGC
ACTCACGAGGGACTGCCAGTGATATACTGGAGGAAGGTGGGGATGACGTCAAGTCCGCATGGCCCTTATGGGCTGGGCCACACACGTGCTACA
ATGGCAATTACAATGGGAAGCAAGGCTGTAAGGCGGAGCGAATCCGGAAAGATTGCCTCAGTTCGGATTGTTCTCTGCAACTCGGGAACATGA
AGTTGGAATCGCTAGTAATCGCGGATCAGCATGCCGCGGTGAATATGTACCCGGGCCCTGTACACACCGCCCGTCACACCCTGGGAATTGGTTTC
GCCCGAAGCATCGGACCAATGATCACCCATGACTTCTGTGTACCACTAGTGCCACAAAGGCTTTTGGTGGTCTTATTGGCGCATACCACGGTGGG
GTCTTCGACTGGGGTGAAGTCGTAACAAGGTAGCCGTAGGGGAACCTGTGGCTGGATTGAATCC

***A. thaliana* chloroplast 16S rDNA (ATCG00920.1)**

TCTCATGGAGAGTTCGATCCTGGCTCAGGATGAACGCTGGCGGCATGCTTAACACATGCAAGTCGGACGGGAAGTGGTGTTTCCAGTGGCGGA
CGGGTGAGTAACGCGTAAGAACCTGCCCTTGGGAGGGGAACAACAGCTGGAAACGGCTGCTAATACCCCGTAGGCTGAGGAGCAAAAGGAGG
AATCCGCCCGAGGAGGGGCTCGCGTCTGATTAGCTAGTTGGTGAGGCAATAGCTTACCAAGGCGATGATCAGTAGCTGGTCCGAGAGGATGAT
CAGCCACACTGGGACTGAGACACGGCCCAGACTCCTACGGGAGGCAGCAGTGGGGAATTTTCCGCAATGGGCGAAAGCCTGACGGAGCAATG
CCGCGTGGAGGTAGAAGGCCTACGGGTCCTGAACTTCTTTTCCCAGAGAAGAAGCAATGACGGTATCTGGGGAATAAGCATCGGCTAACTCTGT
GCCAGCAGCCGCGGTAATACAGAGGATGCAAGCGTTATCCGGAATGATTGGGCGTAAAGCGTCTGTAGGTGGCTTTTTAAGTCCGCCGTCAAAT
CCCAGGGCTCAACCCTGGACAGGCGGTGGAAACTACCAAGCTTGAGTACGGTAGGGGCAGAGGGAATTTCCGGTGGAGCGGTGAAATGCGTA
GAGATCGGAAAGAACACCAACGGCGAAAGCACTCTGCTGGGCCGACACTGACACTGAGAGACGAAAGCTAGGGGAGCGAATGGGATTAGATA
CCCCAGTAGTCCTAGCCGTAAACGATGGATACTAGGCGCTGTGCGTATCGACCCGTGCAGTGCTGTAGCTAACGCGTTAAGTATCCCGCCTGGG
GAGTACGTTCGCAAGAATGAAACTCAAAGGAATTGACGGGGGCCCGCACAAGCGGTGGAGCATGTGGTTTAATTCGATGCAAAGCGAAGAACC
TTACCAGGGCTTGACATGCCGCGAATCCTCTTGAAAGAGAGGGGTGCCTTCGGGAACGCGGACACAGGTGGTGCATGGCTGTCGTCAGCTCGT
GCCGTAAGGTGTTGGGTTAAGTCCCGCAACGAGCGCAACCCTCGTGTTTAGTTGCCACCGTTGAGTTTGGAACCCTGAACAGACTGCCGGTGAT
AAGCCGGAGGAAGGTGAGGATGACGTCAAGTCATCATGCCCCTTATGCCCTGGGCGACACACGTGCTACAATGGCCGGGACAAAGGGTCGCGA
TCCCGCGAGGGTGAGCTAACTCCAAAAACCCGTCCTCAGTTCGGATTGCAGGCTGCAACTCGCCTGCATGAAGCCGGAATCGCTAGTAATCGCC
GGTCAGCCATACGGCGGTGAATTCGTTCCCGGGCCTTGTACACACCGCCCGTCACACTATGGGAGCTGGCCATGCCCGAAGTCGTTACCTTAACC
GCAAGGAGGGGGGTGCCGAAGGCAGGGCTAGTGACTGGAGTGAAGTCGTAACAAGGTAGCCGTACTGGAAGGTGCGGCTGGATCACCTCCTT

63f:	5’-**CAGGCCTAACACATGCAAGTC**-3’
1492r:	5’-**GGCTACCTTGTTACGACTT**-3’
783r:	5’-CTACCVGGGTATCTAATCCBG-3’

Figure 2.2: Segment of *E. coli* (strain BL21) 16S rDNA (GenGank:X80721.1), *A. thaliana* chloroplast 16S rDNA (TAIR Accession:1009068753) and mitochondrial 18S rDNA sequence (TAIR Accession: 1009068297), showing binding sites of 63f, 1492r and 783r primers.

2.7.4 PCR for high-throughput sequencing and sequencing analysis

Genomic DNA of phyllospheric microbes (2.7.2 Extraction of phyllospheric microbes for high-throughput sequencing) was extracted and subjected to PCRs. Here, PCR reagents for bacteria- and fungi-specific amplification, as well as the PCR thermocycler profile, were used as stated under heading 2.7.3 "PCR and sequencing for trial run (Colony-PCR)". PCR amplicons for fungi (ITS1-F/ITS2) and bacteria (63f/783r) were combined (equal volumes) for each genotype (WT and *fhy3 far1*), representing one BR. For both genotypes two BRs were done.

Eventually, the PCR amplicons were sent for high-throughput sequencing using the Illumina MiSeq single read platform (Department of Epidemiology and Biostatistics, Institute for Computational Biology, Case Western Reserve University, Ohio, USA). 200 ng of DNA per sample, as requested by the Department of Epidemiology and Biostatistics, were sent for high-throughput sequencing.

The quality of the returned sequencing data was reviewed with the program FastQC (Andrews, 2010) (5.2.2 Culture-independent taxonomic identification of phyllospheric microbiota in short days). Subsequently, sequencing data were submitted to SILVAngs - high quality ribosomal RNA database web interface (Quast et al. 2013) for analysis. SILVAngs allows classification of prokaryote 16S rRNA (or Eukaryote 18S RNA) sequences but is not designed to analyse fungal intergenic spacer (ITS) sequences. However, in addition to identifying prokaryote sequences to genus level, it was also used to separate out fungal ITS sequences for separate analysis on the basis that it could identify the 18S fragment included in the ITS.

As expected, the number of sequences varied greatly from replicate to replicate in the sequencing results. However, it was found that the proportion of fungal and bacterial sequences found in each sequence file (from Illumina MiSeq) also varied greatly. Sequence files were rarefied prior to upload to ensure a relatively consistent number of bacterial or fungal sequences were classified for each BR, an important requirement for subsequent community structure analysis. In terms of fungal sequences, this required only a simple rarefaction of the total number of sequences submitted for each BR be equal to the minimum number of sequences returned for any replicate. The total number of sequences for *fhy3 far1* BR1 that were returned by MiSeq high-throughput sequencing was 63,968. All of them were uploaded to SILVAngs for analysis. This analysis found 21,000 fungal sequences in *fhy3 far1* BR1. An upload of 64,000 MiSeq high-throughput sequences for *fhy3 far1* BR2, WT BR1 and WT BR2 found a similar number of fungal sequences, which allowed for further comparative analysis between the WT and *fhy3 far1* microbiota in terms of fungal sequences.

The upload of 63,968 MiSeq high-throughput sequences for *fhy3 far1* BR1 found approximately 19,000 bacterial sequences. An upload of 64,000 MiSeq high-throughput sequences for WT BR1, however, yielded a much lower number of bacterial sequences. An upload of 128,000 MiSeq high-throughput sequences for WT BR1, in turn, yielded a similar number of bacterial sequences (approximately 22,000) as found in the 63,968 MiSeq high-throughput sequences for *fhy3 far1* BR1. An upload of 64,000 MiSeq high-throughput sequences for *fhy3 far1* BR2 yielded approximately 7,000 bacterial sequences. However, an upload of the full complement of 150,000 MiSeq high-throughput sequencing for WT BR2 was necessary to yield a similar number of bacterial sequences (approximately 8,000) as found in *fhy3 far1* BR2 (5.2.2 Culture-independent taxonomic identification of phyllospheric microbiota in short days). Thus, since it was impossible to upload additional WT BR2 sequences, community analysis for the second BR was carried out based on these lower numbers of bacterial sequences. Overall, the similar numbers of bacterial sequences found in WT BR1 and *fhy3 far1* BR1, and WT BR2 and *fhy3 far1* BR2 allowed a justifiable comparison between WT BR1 and *fhy3 far1* BR1, and WT BR2 and *fhy3 far1* BR2, however not between both BRs, since the number of sequences differed too much. The alignment results from SILVAngs for bacteria were returned in several file formats. Here, the “Krona” files (Microsoft Excel files that included an additional function to generate pie charts (Ondov *et al.*, 2011, seen in Figure 5.4) contained the operational taxonomic units (OTUs) (Sequences with 97 % sequence similarity were grouped in one OTU) and their corresponding alignment results and abundance of sequences in each OTU. These results were used to generate rarefaction curves using the “R” Vegan package rarefaction function according to Jacobs (2011) (Figure 5.3), to calculate Shannon’s diversity and Buzas and Gibson's evenness indices (Table 5.3).

Hierarchical clustering was done with the PAST suite, Version 3.13 (Hammer *et al.*, 2001) (Figure 5.6), and XL-Stat extension for Windows Excel, version 2014.6.02 to generate PCA plots (Figure 5.7), and Microsoft Excel 2010 to generate heatmaps (Figure 5.8). For Shannon’s diversity and Buzas and Gibson's evenness indices, hierarchical clustering, PCA plot and heatmap, the bacterial and fungal abundances were normalised to the corresponding WT BR1 data. The calculated relative change of abundances for all samples was, therefore, on the same scale. The data to generate the heatmaps (for bacterial and fungal communities) represents the proportional amount (in percentage) of the individual genera of the total abundance of genera. Since SILVAngs aligned eukaryotic sequences to an 18S rDNA-based reference database, where the18S region only accounted for a short part of the PCR amplicons that were used for sequencing (5.2.2 Culture-independent taxonomic identification of phyllospheric microbiota in

short days) OTUs were often classified as simply “eukaryotic”. In the “fna” files that were returned by SILVAngs, the listed OTUs were stated with their alignment results and a representative sequence for each individual OTU. The representative sequence of the OUTs that were aligned to “eukaryotic” sequences were subjected to a SILVAngs-independent DNA database alignment search using BLAST. Here, the “Nucleotide collection (nr/nt)” database was selected as reference database, and the alignment search optimised for “Somewhat similar sequences (blastn)”. The alignment results, which consisted of the NCBI accession IDs and various scores such as bit score, query cover and identity scores, were evaluated according to the bit-score (S). Alignment results were selected when $S \geq 200$, which indicated a good alignment. A maximum of 10 alignments was selected per sequence. Subsequently, the alignment results with their NCBI accession IDs were uploaded to the web interface Batch Entrez ((www.ncbi.nlm.nih.gov/sites/batchentrez) to retrieve a taxonomic identification on genus level. The alignment results were then sorted by identity, and for each sequence, the best alignment, among those alignments which gave a defined genus, was kept. Where a genus was not identified, the alignment result that gave the most detailed taxonomic level was selected. A minimum cut-off that required an identity of at least 97 % was also applied (Stackebrandt and Goebel, 1994). The final alignment results on genus level with their number of sequences, which represented the abundance of the genus, were transferred to “Krona”-files and used to generate rarefaction curves (Figure 5.5). Shannon’s diversity and Buzas and Gibson's evenness indices (Table 5.3), hierarchical clustering (Figure 5.6), the PCA plot (Figure 5.7) and heatmap (Figure 5.8) were calculated and generated in the same way as was done for bacterial results.

In order to obtain the number of chloroplast and mitochondrial sequences, SILVAngs files that were labelled “fingerprint” and contained the total number of sequences for each sample and their alignment result, were sorted for “chloroplast” and “mitochondria” using Microsoft Excel 2010.

3 TRANSCRIPTIONAL PROFILING AND PHENOTYPE INVESTIGATIONS

3.1 Introduction

As discussed, the *fhy3 far1* mutant displays extensive leaf lesion formation. It was considered that *fhy3 far1* mutant plants' extensive leaf-lesion formation could possibly be linked to the double mutants' response to pathogens (1.3 Aim and objectives of this project). It was proposed that the leaf-lesions may represent either a constitutively activated defence response or, alternatively, an inappropriately activated (or non-supressed) defence response to common microbial triggers. Global gene expression profiling offers an ideal opportunity to address the question of which pathways may be particularly affected. In addition, comparison of defence-related gene expression in healthy versus infected plants of WT and *fhy3 far1* mutants would form a good approach to look both for a constitutively activated defence response and for loss of suppression of the normal defence response. Infective microorganisms can, essentially, be classified into different classes: biotrophic, hemibiotrophic or necrotrophic pathogens. Biotrophic and hemibiotrophic pathogens are rather associated with SA signalling-dependent defence response, whereas necrotrophic pathogens rather with JA/ET signalling-dependent defence response (Glazebrook, 2005). *fhy3 far1* mutant plants could have developed leaf-lesions in response to an activation of defence against (hemi-) biotrophic pathogens, representing HR, or could have been caused by activation of defence against necrotrophic pathogen; or a combination of both. The ideal infection study would, therefore, include (hemi-) biotrophic and necrotrophic pathogens in addition to more generic microbial effectors. Widely-known and commonly used pathogens are the hemibiotrophic *Pseudomonas syringae* and necrotrophic *Botrytis cinerea.*

3.1.1 *Pseudomonas syringae*

P. syringae is a Gram-negative, mastigote[2.1] bacterial plant pathogen that is seed-borne or spreads by water drops during rain, with over 50 different pathovars; *P. syringae* pv, tomato strain DC3000 (*Pst* DC3000 from here on) is probably the best known.

[2.1] Possessing a flagellum.

P. syringae enters into leaf tissue through stomata/wounds and forms colonies between mesophyll cells. The caused disease symptoms are necrotic spots on leaves and fruits, called bacterial speck, that also seem to severely curl affected leaves. *P. syringae* also causes flower blast, brown to black flowers and flower buds (Zipfel and Robatzek, 2010; Moore, 1988).

Pst DC3000 is an effective hemibiotrophic pathogen of *A. thaliana* as its effectors are not recognised to trigger R protein-mediated resistance. However, it will still trigger an HR gene expression response as part of infection. Inoculation of *A. thaliana* with *Pst* DC3000 at a concentration of 5 x 10^6 cfu/ml (considered high concentration) led to chlorosis 2 days post inoculation (dpi). Inoculation with a concentration of 10^5 cfu/ml (considered a low concentration) led to chlorosis 4 dpi (Whalen *et al*., 1991; Ishiga *et al*., 2011). This strain was, therefore, ideal for the study of the leaf-lesion formation phenotype of the *fhy3 far1* mutant plants. In particular, it may help to address whether the *fhy3 far1* mutation disrupts SA-mediated defence response pathways against *P. syringae* (Liu *et al*., 2013 a).

3.1.2 *Botrytis cinerea*

B. cinerea is a conidia-producing necrotrophic fungus that kills host plant cells very early during infection, leading to grey pre- and postharvest rot of flowers, leaves, shoots, fruits (such as grapes and strawberries) and soil storage organs (such as cabbage and broccoli). Most severely damaged are vegetables, small fruit crops and cut flowers of over 50 host plants (Williamson *et al.*, 2007). The primary source for infection of crop plants is conidiophores and their airborne conidia.

After germination of the *B. cinerea* conidia, the fungus forms appressoria to secrete enzymes, like cutinases, lipases and superoxide dismutase, to breach the plant surface and enter the apoplast. The fungus deploys enzymes for pectin decomposition (endo-polygalacturonases, amongst others), phytotoxic metabolites (Botrydial) and effectors (NEP1-like proteins) to drive necrosis (Williamson *et al.*, 2007; Windram *et al.*, 2012).

B. cinerea is an effective necrotrophic pathogen of *A. thaliana* and causes leaf-lesions upon infection (Ingle and Roden, 2014). Resistance to this pathogen is dependent on JA- and ET-signalling (Thomma *et al*., 1998; Thomma *et al*., 1999). *B. cinerea* was, therefore, also ideal for the study of the leaf-lesion formation phenotype of the *fhy3 far1* mutant plants. It will help to address whether JA/ET-mediated pathways are specifically affected in the double mutant.

3.1.3 Fumonisin B1

Although the plant will tend to avoid triggering PCD in response to a necrotrophic pathogen, many necrotrophic fungi use elicitors to locally induce PCD, possibly promote host senescence, by hijacking plant signalling pathways. The elicitor Fumonisin B1 (FB1) is one such example. It is produced by necrotrophic *Fusarium* species and disrupts the sphingolipid biosynthesis, more precisely inhibits a ceramide synthase (sphingonine N-acetyl transferase), in plants. Ceramides are an essential part of membranes and a disruption in biosynthesis by FB1, suggests a disruption of vacuolar membrane integrity, resulting in PCD. This would benefit the necrotrophic *Fusarium* species by killing plant cells. However, other modes of action cannot be excluded, as FB1-mediated PCD could not be rescued by ceramide application. The increased occurrence of PCD resembles HR and involves ROS production, requires JA/ET- and SA-mediated signalling, leads to callose-deposition in cell walls, phytoalexin production and PR-gene expression, such as *PR1* and *PDF1.2a* (Asai *et al.*, 2000; Stone at al., 2000; Kuroyanagi *et al.*, 2005; Berkey *et al.*, 2012; Igarashi *et al.*, 2013). FB1 treatment will help to address whether the leaf-lesion formation in *fhy3 far1* mutants could be caused by sensitivity to elicitors of necrotrophic fungi.

3.1.4 Chitin

Fungal chitin is an essential integral component of fungal cell walls and estimated to be the second most abundant polysaccharide in the world; it is a polymer of β-1,4 linked N-acetyl glucosamine. Chitin is recognised by membrane standing receptors containing extracellular LysM domains (Zang *et al*., 2009), such as CERK1 in *A. thaliana* (Petutschnig *et al.*, 2010). Chitin treatment of *A. thaliana* results in ROS accumulation, activation of defence response-associated MAPKinase-and JA/ET-signalling (Miya *et al*., 2007; Le *et al*., 2014).

The aim of this chapter was to characterise the leaf-lesion formation and defence response signalling of *fhy3 far1* mutant plants. In connection with the leaf-lesion formation phenotype, an increased accumulation of ROS was ascertained. Global transcript analysis based on an Affymetrix chip revealed a downregulation of negative regulators of PCD in the double mutant, but unexpectedly also a downregulation of SA- and JA/ET-associated genes. A subsequent assay for transcriptional changes upon challenge with biotic stressors showed a differential defence response associated gene expression in *fhy3 far1* mutant contrary to WT plants. These results

prompted the proposal of negative feedback on SA- and JA/ET-signalling-dependent defence response in *A. thaliana,* which is enhanced in *fhy3 far1* mutants.

3.2 Results

3.2.1 Lesion formation phenotype of *fhy3 far1* mutants with Nossen ecotype

The phenotypic characteristic that prompted the investigations for this thesis is an increased leaf-lesion formation of FHY3 and FAR1 loss-of-function mutant plants. SD-grown mutant plants with Nossen ecotype (No-0) showed more enhanced leaf-lesion formation, affecting the majority of all rosette leaves, compared to LD grown mutant plants, where they occurred more rarely. Nonetheless, mutant plants grown in both light conditions eventually develop leaf-lesions that extend further as time progressed. (Representative plants are shown in Figure 3.1 a). Approximately 100% of the leaves are smaller, and approximately 50% show lesions.

Also, *fhy3 far1* (No-0) mutant plants displayed a dwarf phenotype in SD, while in LD, the size was only slightly reduced. (Representative plants are shown in Figure 3.1 b). The dwarfing was reflected in the fresh weight that was decreased by approximately 90 % in six weeks old *fhy3 far1* mutant plants when grown in SD (Figure 3.1 c).

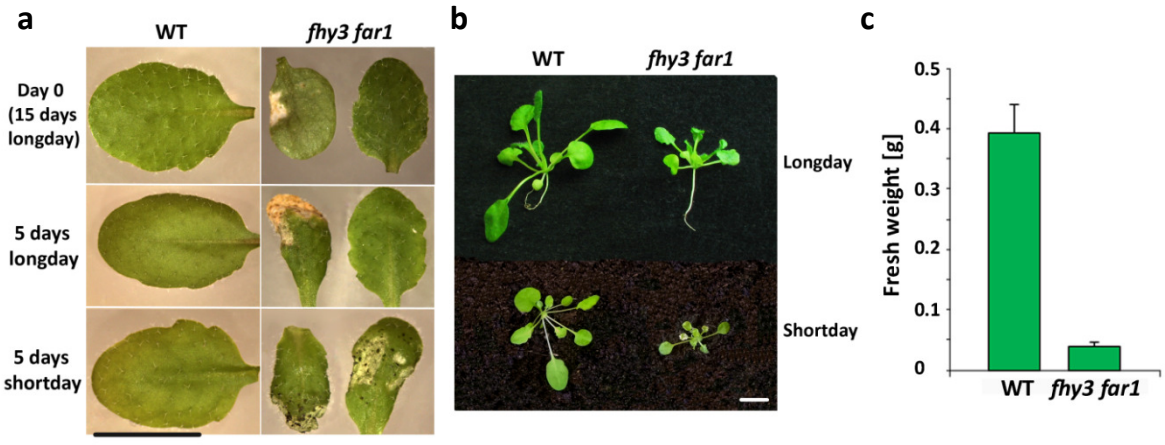

Figure 3.1: Phenotypic characteristics of WT (No-0) and *fhy3 far1* (No-0) mutant plants, a) plants were grown in LD for 15 days and pictures of their leaves taken (Day 0). Plants were then either kept at LD (16 hours of light followed by 8 hours of darkness) or transferred to SD (8 h of light followed by 16 h of darkness). Pictures of their leaves were taken after 5 days in LD or SD, scale bar: 2 mm, b) 4 weeks old plants grown in LD and SD, scale bar: 5 mm, and c) average fresh weight of 20 WT and *fhy3 far1* plants each grown in SD for 6 weeks, error bars represent standard error.

3.2.2 ROS assay of *fhy3 far1* (No-0) mutant plants

The leaf-lesion formation of *fhy3 far1* (No-0) mutant plants is reminiscent of HR cell death, which would suggest an increased ROS production, possibly including H_2O_2, potentially triggering PCD. The highly reactive nature of H_2O_2 allows an *in situ* colorimetric detection by forming a water-insoluble brown precipitate after reaction with 3,3'-Diaminobenzidine (DAB). This assay is commonly used to assess H_2O_2 content in *A. thaliana* rosette leaves (Xiao *et al.*, 2013). Therefore, leaves of 21 days old *fhy3 far1* mutant and WT plants, grown on soil in SD, were subject to this assay. 21 days represent the time before the biotic challenges investigations of *fhy3 far1* and WT plants, where 22 days old plants were challenged with biotic stressors and sampled 3 dpi.

WT (No-0) rosette leaves showed only a low level of staining across the entire leaf with small patches of more intense DAB staining (Figure 3.2). This was in contrast to the more intense, whole-leaf staining of the majority *fhy3 far1* (No-0) rosette leaves, indicating increased H_2O_2 production (Figure 3.2). However, some of the *fhy3 far1* mutant plant leaves did not show any staining, indicating decreased H_2O_2 production. This observation was not restricted to size or age of the leaves.

This aberration could be caused by environmental factors that vary across the individual plant. Such an environmental factor could be the phyllospheric microbiota that can vary between different parts of the plant (Whipps et al., 2008; Lindow and Brandl, 2008). Specific microbes could affect the leave phenotype especially in already stressed plants such as *fhy3 far1* mutants.

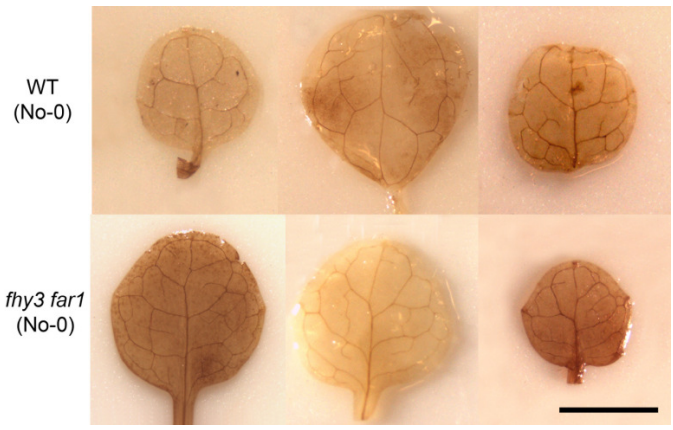

Figure 3.2: DAB staining assay of 21 days old WT (No-0) and *fhy3 far1* (No-0) mutant plants, grown on soil in SD (8 hours of light followed by 16 hours of darkness). Representative of ten leaves where eight mutant leaves showed intense staining and two no staining. Scale bar: 2mm.

3.2.3 Global transcript analysis of *fhy3 far1* (No-0) and WT (No-0)

3.2.3.1 Overview

I was kindly provided with DNA microarray data (Affymetrix chip, from now on called *fhy3 far1* microarray) for *fhy3 far1* (No-0) mutants compared to WT (No-0) by Dr Paul Devlin. RNA for the *fhy3 far1* microarray was prepared by the postdoctoral fellow at that time, Dr Hamad Siddiqui. The data of the *fhy3 far1* microarray represents one biological replicate (BR). Plants were grown in LD for seven days and then transferred to SD. Samples for the data were collected at three time points: 36, 40 and 44 hours after onset of SD conditions (i.e. after 4, 8 and 12 hours of darkness in the second day of SD, representing ZT12, ZT16, and ZT20 - Figure 3.3), which represent the time of day and beyond when *FHY3* and *FAR1* most strongly affect target gene expression in SD (Siddiqui *et al*., 2016).

The *fhy3 far1* microarray data were validated by RT-qPCRs for a selection of genes shown in chapter 4. Here, transcript patterns of *ATCSA-1 UVR2, SUV2 GMI1*, *CRK13* and *MC2*, found by RT-qPCR, were in overall accordance to the *fhy3 far1* microarray data.

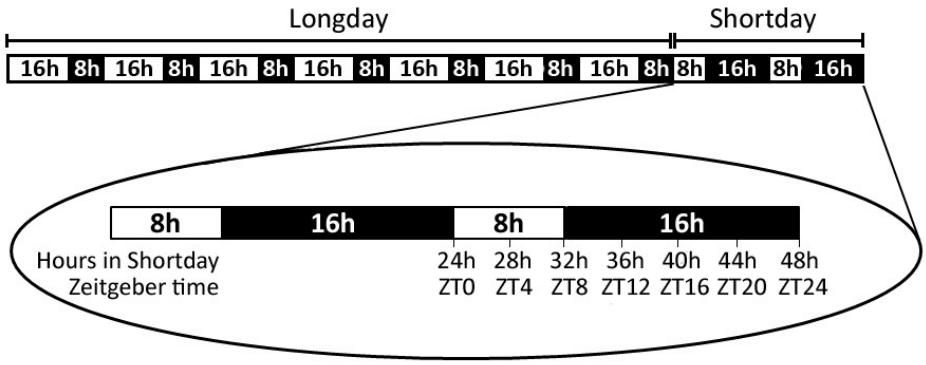

Figure 3.3: Time points of sampling for the microarray experiment. Plants were grown in LD (16 hours of light followed by 8 hours of darkness) for 7 days in order to reach bigger size than in SD (8 hours of light followed by 16 hours of darkness). Thereupon; plants were transferred to SD for two days for entrainment and harvest during the night of the second day in SD at 36h (ZT12), 40h (ZT16), and 44h (ZT20), which represent the time of day and beyond when FHY3 and FAR1 most strongly affect target gene expression in SD (Siddiqui *et al*., 2016).

For the *fhy3 far1* microarray, a series of global gene expression investigations were designed to establish the impact of the *FHY3* and *FAR1* loss-of-function on the leaf-lesion formation phenotype of *A. thaliana* plants in SD. Genes that showed a two-fold up- or down-regulation in their mean relative transcript over the three time points in *fhy3 far1* mutants, compared to WT,

were selected. This identified 1,967 out of 20,855 genes as misregulated by two-fold, of which 754 are upregulated and 1,213 are downregulated.

The analyses are based on Gene Ontology (GO), which classifies genes (and their products) into specific terms of molecular function, biological process and cellular component, thereby categorising them (Guo, 2010). The starting point was a GO overrepresentation analysis, which is a statistical test (binomial test and Bonferroni correction for multiple testing, $p<0.05$) to determine how frequently misregulated genes appear in particular GOs, and, therefore, whether the misregulated genes in *fhy3 far1* mutants in SD are overrepresented or enriched in certain processes.

Based on the results of these overviews, an *fhy3 far1* microarray analysis for the behaviour of entire gene sets associated to specific GO categories for the two-fold misregulated genes in *fhy3 far1* mutants followed. The utilised GO categories are connected to the observed leaf-lesion formation, such as negative regulators of PCD.

3.2.3.2 Enrichment analysis of misregulated genes in *fhy3 far1* (No-0) mutants

The GO enrichment analysis (or statistical overrepresentation test) was performed by the PANTHER (Protein ANalysis THrough Evolutionary Relationships) statistical overrepresentation test (Mi *et al.*, 2013). It used a list of the misregulated genes in *fhy3 far1* (No-0) mutants and compared it to a reference list, which contained all the genes of the *fhy3 far1* microarray. It functionally classified genes in the overrepresented biological processes of “toxin catabolic process”, “defence response”, and “response to other organism”. Underrepresented biological processes were “RNA processing” and “ribosome biogenesis” (Table 3.1).

GO enrichment analysis for molecular functions revealed a significant enrichment of differentially expressed genes in “oxygen binding” and “heme binding”. Underrepresented cellular components were “protein binding”, “RNA binding” and “structural constituent of ribosome” (Table 3.1).

GO enrichment analysis for cellular components showed an overrepresentation of the “extracellular region”, and underrepresentation of “chloroplast stroma”, “chloroplast envelope”, as well as “Golgi apparatus part”, “vacuolar membrane”, “endosome”, “nucleolus”, amongst others (Table 3.1).

The overrepresented GO terms for biological processes and molecular functions in *fhy3 far1* mutants point to increased ROS activity, which is consistent with the extended leaf lesions.

Table 3.1: GO overrepresentation analysis of up- and downregulated genes of *fhy3 far1* (No-0) mutant compared to WT (No-0) plants grown in SD. The analysis is categorised into biological processes, molecular functions and cellular components, including respective calculated fold-enrichment (Fold-Enrich) and significance (p-value).

GO biological process complete	Fold-Enrich	p-value
toxin catabolic process	3.94	4.31E-02
response to organo-nitrogen compound	2.51	4.23E-02
defence response	1.72	1.90E-06
response to other organism	1.57	2.71E-02
translation	0.34	2.74E-03
RNA processing	0.25	5.02E-04
ribosome biogenesis	< 0.2	1.42E-02
GO molecular function complete	**Fold-Enrich**	**p-value**
oxygen binding	2.3	1.93E-02
heme binding	2.22	7.20E-04
protein binding	0.74	2.36E-02
RNA binding	0.48	4.43E-03
structural constituent of ribosome	< 0.2	1.57E-04
structural molecule activity	0.37	3.34E-02

GO cellular component complete	Fold-Enrich	p-value
extracellular region	1.67	9.97E-13
chloroplast stroma	0.45	1.65E-02
organelle subcompartment	0.42	9.22E-04
chloroplast envelope	0.39	2.98E-03
Golgi apparatus part	0.39	1.13E-02
vacuolar membrane	0.31	2.82E-05
transferase complex	0.31	1.89E-02
membrane protein complex	0.28	6.06E-04
cytosolic ribosome	0.25	2.70E-02
endosome	0.24	2.18E-03
nucleolus	0.22	4.50E-03
nucleoplasm part	< 0.2	1.08E-02
ribosomal subunit	< 0.2	2.13E-03

3.2.3.3 Functional classification of misregulated genes in *fhy3 far1* (No-0) mutants

A functional classification of the up- and downregulated genes separately in *fhy3 far1* (No-0) mutants, based on general ontology terms, was performed with PANTHER. This method highlights the proportions of the misregulated genes in the specific processes these genes are associated to. This allows further dissection of the nature of the involved genes (Figure 3.4). Analyses of three processes, apoptotic and developmental processes, as well as response to stimulus, were particularly revealing (Figure 3.4, level 1). These processes were selected based on the GO enrichment analysis that suggested increased ROS activity and defence response / response to organisms of *fhy3 far1* mutants. A number of downregulated genes were

categorised in “apoptotic process” (1.6 % / 18 of the mapped downregulated genes). Downregulated genes within this process mainly consist of negative regulators of the apoptotic process (child ontology term). A number of downregulated genes were also categorised in “development” (2.2 % / 24 genes). These include mainly “death”-associated genes. Finally, a number of downregulated genes were also categorised in “response to stimuli” (6.8 % / 75 genes). More than one-quarter of these were defence response to bacteria-associated genes. Upregulated genes showed a very similar distribution. They are categorised in “apoptotic process” (1.3 % / 9 genes) and were also mainly negative regulators of apoptosis. Upregulated genes categorised in “development” (2 % / 14 genes) also include a high amount of “death”-associated genes. Upregulated genes categorised in “response to stimuli” (5.4 % / 38 genes) also consist of a large number of defence response to bacteria-associated genes (Figure 3.4).

There is a higher proportion of negative regulators of PCD that is downregulated than upregulated in *fhy3 far1*, possibly suggesting an impaired prevention of PCD in *fhy3 far1* mutant plants. The observations also suggest that this could be connected with the defence response to bacteria in particular.

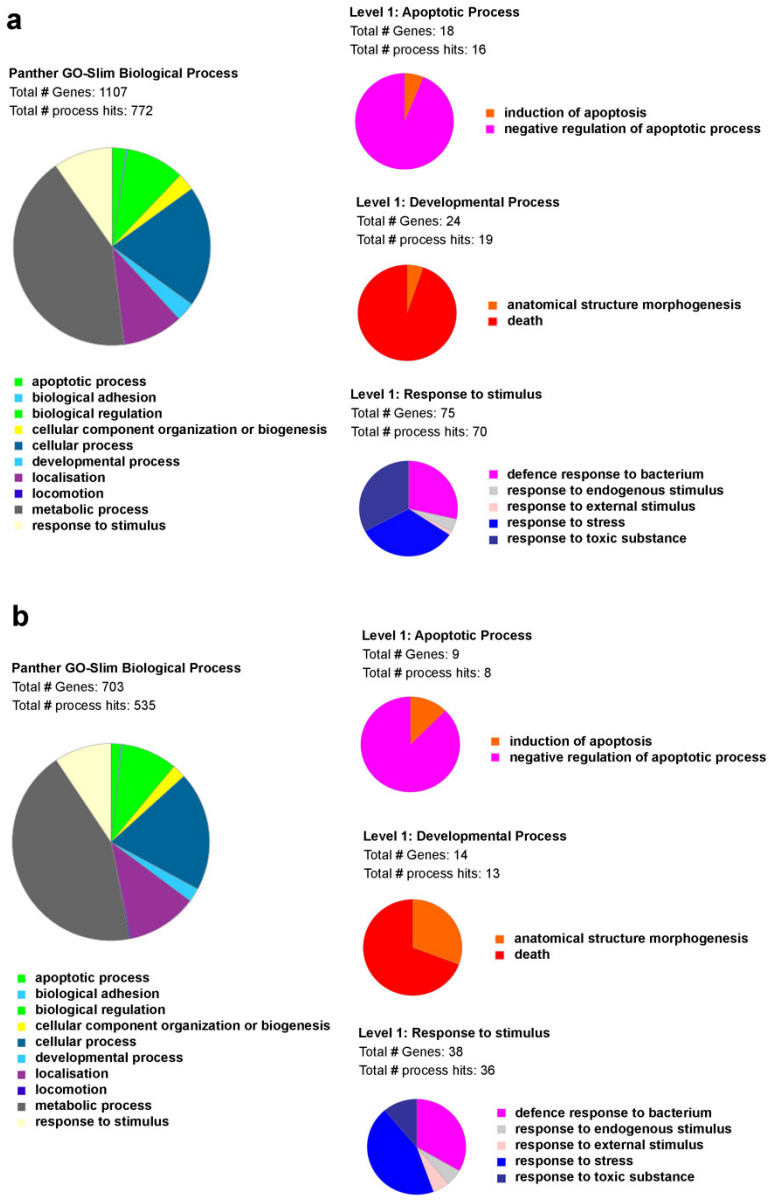

Figure 3.4: PANTHER functional classification of misregulated genes during the night, in *fhy3 far1* mutant plants grown in SD: a) downregulated genes, and b) upregulated genes. "Total # Genes" represents the number of genes that were mapped (others are un-classified) and "Total # process hits" represents the number of biological PCD processes these genes are categorised in (one gene can be allocated to more than one biological process (Mi *et al.*, 2013)).

3.2.3.4 Misregulation of PCD and defence response-signalling

Given the results from the GO overrepresentation analysis and classification, an *fhy3 far1* microarray analysis for the behaviour of entire gene sets associated to specific GO categories was performed in order to gain information in greater detail and thereby possibly explain the leaf-lesion formation. The GO categories of interest were: (1) negative regulators of PCD, (2) SA, (3) JA and ET, and (4) SAR (for a complete list of genes for each GO, see supplementary data Table S1).

Since the GO functional classification results showed a downregulation of negative regulators of PCD, further investigation of these was prompted. The GO analyses also showed an enrichment of defence response-associated genes and a functional classification of misregulated genes of defence response to bacterium in *fhy3 far1*, suggesting altered SA- and JA/ET-signalling pathways that also could be responsible for the increased ROS accumulation in the double mutant. This prompted further investigation of SA- and JA/ET-signalling pathway-associated genes.

The already mentioned 1,967 genes on the *fhy3 far1* microarray that were misregulated in the *fhy3 far1* mutant compared to the WT (3.2.3.1 Overview), were used to generate a heatmap in order to compare *fhy3 far1* and WT data. Here the relative transcript values from the three sample time points for each genotype were normalised to a WT mean of 100 for the three time points, and subsequently logarithmic transformed (Log_2) for visualisation by conditional formatting. The majority of the misregulated genes in *fhy3 far1* mutants, 61.6 % (1213 genes), were at least two-fold downregulated, whereas 38.4 % (154 genes) were at least two-fold upregulated (Figure 3.5 a).

However, the mean relative transcript (non-logarithmic transformed) for each sampling time point of all misregulated genes revealed significantly higher values in *fhy3 far1* mutants than in the WT, which is not obvious judging from the heatmap (Figure 3.5 b). This shows that out of all misregulated genes, a smaller number are upregulated in the double mutant, they nevertheless strongly impact the mean transcript level.

The first analysis for the behaviour of entire gene sets associated to specific GO categories was for the category “negative regulators of PCD”, which contained 163 genes in total. 14.1 % of the genes (23 genes) were downregulated ($p<0.00001$ based on z-test), and 0.6 % / 1 gene was upregulated ($p=0.84$ based on z-test, though), suggesting reduced PCD-prevention during the night.

GO analysis for SA-associated genes showed a downregulation of 11.8 % of all associated genes (27 out of 229 genes - $p<0.00001$ based on a z-test) and an upregulation of 0.5 % (1 gene - $p=0.65$ based on z-test, though). As SA performs different functions in plants, the question was how many of the misregulated genes are actually associated to defence response. According to the GO terms (defence - GO:0006952 and immune response - GO:0006955) and the genes annotations, it were at least 42.9 % of all associated misregulated genes in *fhy3 far1* mutants, including the downregulated gene. These results suggest a downregulation of SA-mediated defence response in SD-grown *fhy3 far1* mutant plants during the night.

11.5 % of all JA- and ET-associated genes (94 out of 815 genes - $p<0.00001$ based on a z-test) were downregulated, and 1.4 % (11 genes) were upregulated ($p<0.00001$ based on a z-test). In total, 37.1 % of the misregulated genes (39 out of 105 genes) were associated to defence response, according to GO analysis (defence - GO:0006952 and immune response - GO:0006955) and their annotations. These results also suggest a downregulation of JA/ET-mediated defence response in SD-grown *fhy3 far1* mutant plants during the night.
14 % (12 out of 86 genes) of the SAR-associated genes were misregulated in *fhy3 far1* and all were downregulated ($p<0.00001$ based on a z-test). Since SAR is a SA signalling-mediated systemic defence and the misregulated SA-mediated defence response genes in *fhy3 far1* were all downregulated, this result was not surprising and confirmed the overall inhibited defence response gene expression in *fhy3 far1* mutants.

The comparison of the mean relative transcript levels (non-logarithmic transformed) of all misregulated genes to the mean relative transcript levels of the SA-, JA/ET-, and SAR-associated genes showed that the mean relative transcript levels of the SA-, and SAR-associated genes were gradually downregulated as the night progressed in SD-grown WT. JA/ET associated genes, by contrast, showed a steady mean expression level throughout the night (Figure 3.5b).
fhy3 far1 mutants on the other hand showed a behaviour, where the mean relative transcripts of the SA-, JA/ET-, and SAR-associated genes were all significantly lower than the mean relative transcript of the same genes in WT (Figure 3.5 b). This further points to an inhibited defence response in SD-grown *fhy3 far1* mutant plants during the night.

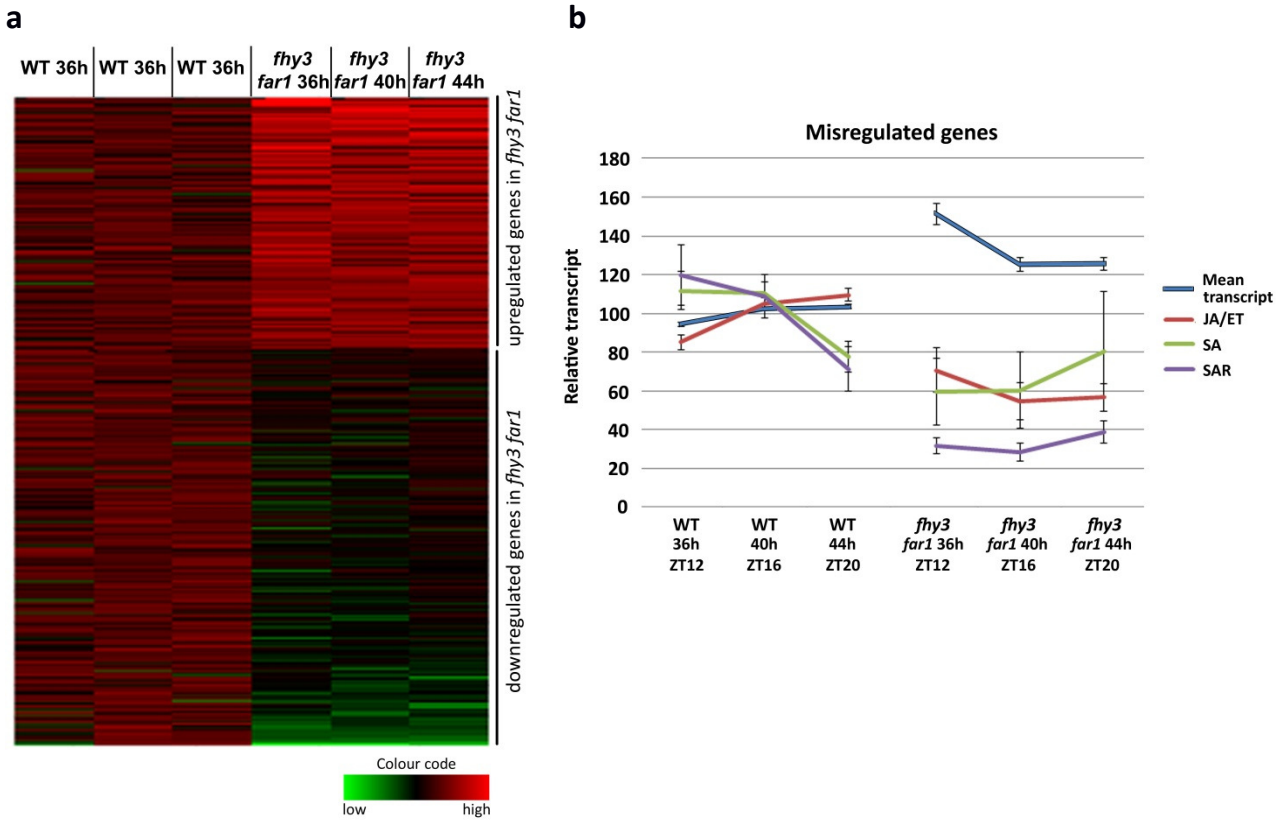

Figure 3.5: Misregulated genes in *fhy3 far1* mutants compared to WT, after growth in SD for 36, 40 and 44 h. Heatmap for all misregulated genes in *fhy3 far1*, indicating the manually-selected, two-fold upregulated and downregulated gene clusters in *fhy3 far1* mutants compared to WT. Each row represents a gene. Genes were normalised to WT and logarithmic transformed prior to colouring. Highest relative transcript for each is labelled red, lowest green, midpoint black (a). Mean relative transcripts (non-logarithmic transformed) of all misregulated genes and PCD-, SA-, JA/ET-, and SAR-associated genes, *fhy3 far1* microarray investigation was done in one BR, error bars represent standard error (b).

3.2.4 Biotic challenges of *fhy3 far1* mutants

3.2.4.1 Overview

The *fhy3 far1* mutant was further transcriptionally characterised to determine the contextual relationship between PCD in connection with ROS accumulation, and defence response in connection with its main signalling pathways. Biotic challenges in the form of the microbial pathogens *B. cinerea* and *Pst* DC3000, as well as the defence response-elicitors FB1 and chitin, were chosen to intentionally trigger (further) responses. They represent a range of different triggers: necrotroph, hemibiotroph, inducer of PCD and MAMP, respectively.

The response to these biotic challenges was investigated histochemically by DAB assay for ROS production and transcriptionally by RT-qPCR, for which appropriate defence response marker genes were selected beforehand.

3.2.4.2 Symptoms upon biotic challenges and histochemical staining

The challenged WT and *fhy3 far1* mutant plants had a Nossen (No-0) ecotype, consistent with the plants used for the *fhy3 far1* microarray, and were grown for 22 days in SD (WT plants were at six rosette leaves development stage, and *fhy3 far1* mutant plants at five to six rosette leaves development stage) before they were subject to treatment with *B. cinerea* suspension at 5 x 10^5 colony forming units (cfu), *Pst* DC3000 suspension at concentrations of 10^6 and 10^8 cfu, FB1-solution at 5 and 50 µM, and chitin suspension at 100 and 1,000 mg/L. Pictures were taken three days post treatment, when DAB staining for *B. cinerea*- and *Pst* DC3000-treated plants was also utilised to assess ROS accumulation upon biotic challenge. In the literature, it has been shown that plants developed disease symptoms after two to seven dpi with *B. cinerea* at which time points samples were taken (Windram *et al*., 2012; Veronese *et al*., 2006; Torres *et al*., 2005), two to four dpi with spray-/dip-inoculated *Pst* DC3000 (Zipfel *et al*., 2004; Ishiga *et al*., 2011). Plants showed PCD after three to seven dpi with FB1 (Zhang *et al*., 2015; Stone *et al*., 2000; Asai *et al*., 2000), and increased H_2O_2 production when tested nine dpi with chitin (Pastor *et al*., 2013). The sampling time point in this investigation were intended to be uniform between treatments with biotic challenges. After three dpi for all treatments, plants showed disease symptoms. It was expected that *fhy3 far1* mutant plants would be more sensitive to biotic challenges due to their reduced "health status" and that the sampling time point would be dependent on the disease symptom development of *fhy3 far1* mutant rather than WT plants.
B. cinerea was isolated from infected strawberries, a common host for the necrotroph. The fungus was from a residential garden in Wokingham, United Kingdom, which made it necessary to confirm its identity. This was done on the basis of sequencing of the fungal ribosomal gene internal transcribed spacer (ITS) region. The sequencing results were analysed by Ensemble genome annotation system BLAST search (Kersey *et al.*, 2016) and showed 100 % alignment with *B. cinerea*. Additionally, microscopic observation found the conidia to have the typical ellipsoid to obovoid shape known to be associated with *B. cinerea* (Sutton, 1998).
Pst DC3000 was kindly provided by the Devoto-lab (Royal Holloway, University of London, School of Biological Sciences, Egham, United Kingdom).

B. cinerea treatment (5 x 10^5 cfu) resulted in leaf-chlorosis on WT and *fhy3 far1* mutant plants that was much more severe and comprehensive in the double mutant, whereas WT was less affected. *Pst* DC3000 treatment (10^6 cfu) resulted in much more severe leaf chlorosis in WT compared to *fhy3 far1* mutant plants, to a point where plants partly collapsed, whereas double

mutant plants only showed severe chlorosis. (Representative plant responses are shown in Figure 3.6). The symptoms were not observed to be dose-dependent for *Pst* DC3000 (10^8 cfu). DAB-staining and therefore H_2O_2 production followed the same given trend. *B. cinerea* infection led to accumulation of H_2O_2 in spots of necrotic lesions that seemed to encompass similar area sizes in both genotypes. (Representative plant responses are shown in Figure 3.7). *Pst* DC3000-treatment also promoted H_2O_2 generation in the whole WT leaf and appeared additionally in darker patches. *fhy3 far1* mutant plants showed a slightly more intense DAB staining but were in general very similar to mock treatment. (Representative plant responses are shown in Figure 3.7).

FB1-treatment led to a dose-dependent increase of leaf chlorosis and PCD that was much more pronounced in *fhy3 far1* mutants. WT plants showed only little effect when treated with 5 µM FB1 solution, whereas *fhy3 far1* mutant plants displayed increased chlorosis compared to mock treatment. (Representative plant responses are shown in Figure 3.6). At high concentration (50 µM), both genotypes showed severe chlorosis that affected the majority of plants, albeit less severe in WT.

Chitin-treatment induced chlorosis in WT plants, which was much more severe in *fhy3 far1* to a point of leaf collapse. (Representative plant responses are shown in Figure 3.6). The symptoms were observed to be dose-independent, thus similar in degree at higher concentration (1,000 mg/L).

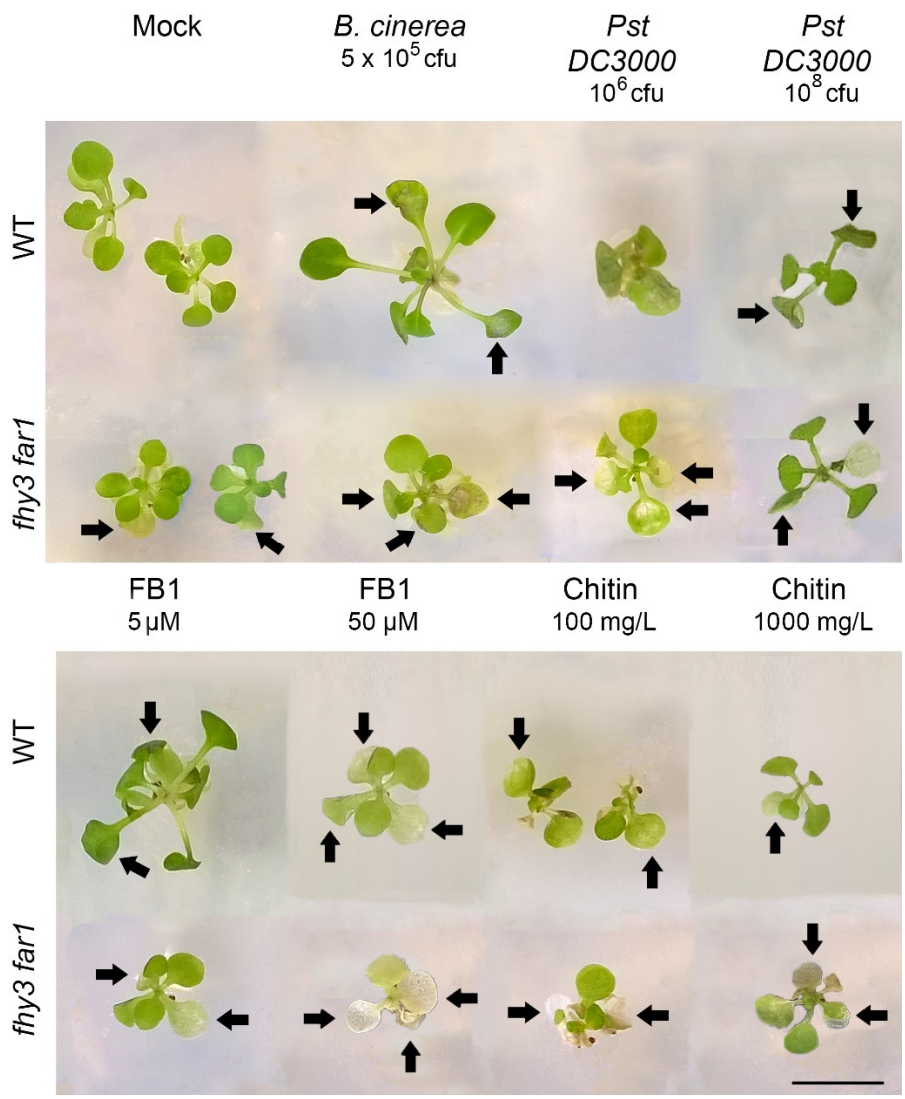

Figure 3.6: Representative responses in WT (No-0) and *fhy3 far1* (No-0) mutant plants grown for 22 days on MS agar in SD, treated with either mock, *B. cinerea* suspension (5 x 10^5 cfu), *Pst* DC3000 suspension (10^6 cfu), FB1 solution (50 µM) or chitin suspension (100 mg/L), and photographed 3 dpi. Arrows indicate chlorosis. Scale bar: 5 mm.

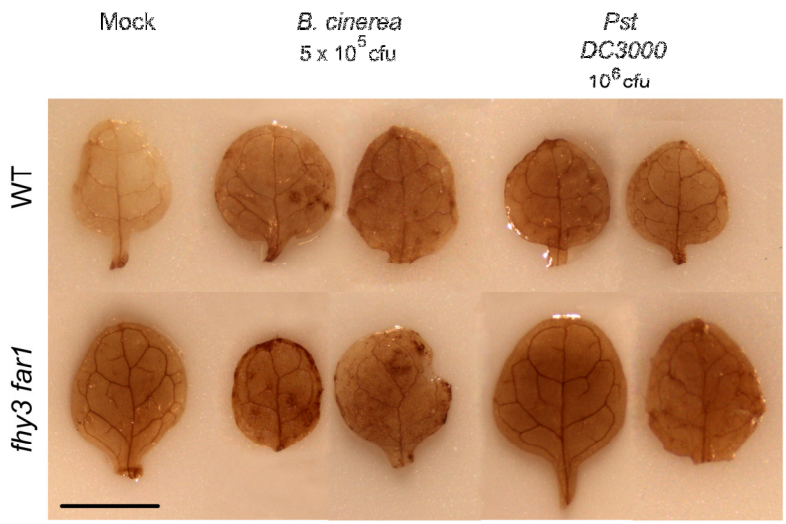

Figure 3.7: Representative DAB-staining of WT (No-0) and *fhy3 far1* (No-0) mutant plants grown for 22 days on soil in SD, treated with either mock, *B. cinerea* (5 x 10^5 cfu) or *Pst* DC3000 (10^6 cfu) suspension, and photographed 3 dpi. Scale bar: 2 mm.

Overall, *fhy3 far1* mutant plants seemed to be more susceptible to *B. cinerea* than WT plants, which could be attributed to the already increased PCD in the double mutant, seen as leaf-lesions (3.2.1 Lesion formation phenotype of *fhy3 far1* mutants with Nossen ecotype), representing advantageous conditions for the necrotrophic fungi. *fhy3 far1* mutant plants seemed less susceptible to the hemibiotroph *Pst* DC3000 than WT, probably also on account of increased basal PCD and ROS accumulation. Nevertheless, both pathogens caused disease in both genotypes.

The fungal PCD-inducing FB1 caused more severe chlorosis in *fhy3 far1* mutant than in WT plants, consistent with the findings of *B. cinerea* treatment. Treatment with the MAMP chitin also led to stronger disease symptoms in *fhy3 far1*, possibly linked to the strong reaction observed upon treatment with (necrotrophic) fungal and fungi-originating stressors.

3.2.4.3 Sphingolipid biosynthesis

The *fhy3 far1* mutant was phenotypically much more sensitive to FB1 than WT. FB1 disrupts sphingolipid biosynthesis, amongst other things, to cause PCD. Sphingolipids are essential components of the plant cell membrane and are required for the plant viability as well as growth (Chen *et al.*, 2006). For instance, loss-of-function of *LAG1 Homolog 1* (*LOH1*), which is part of the sphingolipid biosynthesis, was shown to lead to a leaf-lesion phenotype in *A. thaliana* that is SD-

specific (Ternes *et al.*, 2011). This finding prompted the hypothesis of an impaired sphingolipid biosynthesis in *fhy3 far1* mutants that could add to the explanation for the leaf-lesion and dwarf phenotype of the double mutant. GO analysis for the category "sphingolipid" revealed that the relative transcript (non-logarithmic transformed) for each sampling time point of two misregulated sphingolipid-associated genes *INOSITOL PHOSPHORYLCERAMIDE SYNTHASE 2* (*IPCS2*) and *SPHINGOID BASE HYDROXYLASE 2* (*SBH2*) was reduced compared to the mean relative transcript of the complete set of associated genes in *fhy3 far1* mutants; but not in WT (Figure 3.8). Overall, however, there was not strong evidence that the whole sphingolipid biosynthesis pathway is affected.

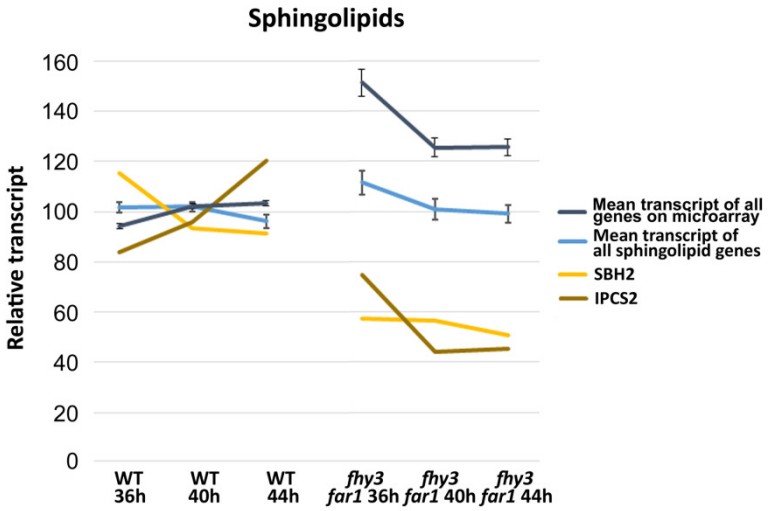

Figure 3.8: Mean relative transcript of all genes on the *fhy3 far1* microarray and of all sphingolipid-associated genes, compared to the relative transcript of *IPCS2* and *SBH2* in *fhy3 far1* mutants compared to WT, after growth in SD for 36, 40 and 44 h, error bars represent standard error.

3.2.4.4 Marker genes of defence response

It is of utmost importance to select appropriate *A. thaliana* defence response marker genes to assess the respective transcriptional alterations of the plant's defence regulatory mechanisms in response to biotic challenges. The contemplable marker genes had to be established as such and an eventual utilisation was evaluated based on the *fhy3 far1* microarray and available microarray data at ArrayExpress (Kolesnikov *et al.*, 2015) shown in Table 3.2.

Table 3.2: Publicly available microarray data that was used to select defence response marker genes for biotic challenges assays

Microarray ID	Title of microarray	Development of plants (if stated????) and time points of sampling for data that was considered
E-GEOD-5684	Transcription profiling by array of Arabidopsis after infection with *Botrytis cinerea*	**4 weeks** old *A. thaliana* plants (Col-0) grown in SD were treated with 5 µl drops of *B. cinerea* conidia suspension (5 x 10^5 conidia/ml) on four to five fully expanded rosette leaves per plant and assayed 18 and 48 hpi. For the heatmap, only the 48 hpi data was considered since it was temporarily closer to the 3 dpi sampling time point for the assay of biotic challenges (subheading 3.2.4.5)
E-GEOD-19109	Transcription profiling of Arabidopsis thaliana wild type (Col-0) and *lht1* mutant leaves	**3 weeks** old *A. thaliana* plants (Col-0) grown in SD were treated with *Pst* DC3000 (10^5 cfu/ml) by syringe infiltration and assayed 48 hpi.
E-GEOD-5520	Transcription profiling by array of Arabidopsis after inoculation with *Pseudomonas syringae* pv. Tomato	**5 weeks** old *A. thaliana* plants (Col-0) grown in SD were treated with *Pst* DC3000 (*avrRpt2*) (10^7 cfu/mL) by syringe infiltration and assayed 12 and 24 hpi. The data of this microarray was not used for the generation of the heatmap (Figure 3.9) since Pst DC3000 (*avrRpt2*) was utilised, however, the data was considered when defence response marker genes were selected.
E-GEOD-5525	Transcription profiling by array of Arabidopsis after exposure to various pathogens and insects	**5 weeks** old *A. thaliana* plants (Col-0) grown in SD were treated with 3 µl drops of *Alternaria brassicicola* conidia suspension (10^6 conidia/ml) all fully expanded rosette leaves per plant and assayed at 24 and 48 hpi.
E-GEOD-50526	Responses of Arabidopsis immune signalling mutants to *Alternaria brassicicola* infection	**3 weeks** old *A. thaliana* plants (Col-0) grown in 12 h light/12 h darkness were treated with 10 µl droplet of *Alternaria brassicicola* conidia suspension (10^5 conidia/ml) and assayed at 9 and 24 hpi. In order to generate the values for the heatmap, the 24 hpi data of this microarray and the 24 hpi data of microarray E-GEOD-5525 were combined since these were the common denominator and close to the 3 dpi sampling time point for the assay of biotic challenges (subheading 3.2.4.5).
E-GEOD-13739	Transcription profiling by array of *Arabidopsis* mutant for *eds16* after infection with *Golovinomyces orontii*	**4 weeks** old *A. thaliana* plants (Col-0) grown in 14 h photoperiod were treated with *Golovinomyces orontii* and assayed at 6 hpi, 1, 3, 5 and 7 dpi.
E-GEOD-40973	Expression profiling of uninfected and *Golovinomyces orontii* infected *Arabidopsis thaliana* wild type Col-0 and *del1-1* mutant	**4 weeks** old *A. thaliana* plants (Col-0) grown in 12 h light/12 h darkness were treated with *Golovinomyces orontii* and assayed at 5 dpi. In order to generate the values for the heatmap, the 5 dpi data of this microarray and the 5 hpi data of microarray E-GEOD-13739 were combined since these were the common denominator and close to the 3 dpi sampling time point for the assay of biotic challenges (subheading 3.2.4.5).
E-GEOD-4746	Transcription profiling of response of *Arabidopsis* seedlings to chitooctaose treatment	**14 days** old *A. thaliana* plants (Col-0) grown in constant light were treated with 1 µM chitooctaose and assayed at 30 minutes pi.
E-NASC-22	Transcription profiling of *Arabidopsis*	*A. thaliana* plants (Col-0) protoplasts were treated with 20 mM FB1 and assayed 5 dpi.

	protoplasts are treated with 20mM Fumonisin B1 (FB1)	

Microarrays testing the response to the necrotrophic fungus *A. brassicicola* and the biotrophic powdery mildew *G. orontii* were taken into account for the selection of marker genes. Resistance to *A. brassicicola* was shown to dependent on JA-signalling, similar to *B. cinerea* (Thomma *et al*., 1998), and resistance to *G. orontii* was shown to dependent on SA (Dewdney *et al.*, 2000). These arrays were chosen with the aim of selecting genes that may be generic markers for defence response to biotrophs or necrotrophs.

Overall, these microarray data represent the effect of biotrophic, hemibiotrophic and necrotrophic microbes, the fungal PCD-inducing toxin FB1, as well as the MAMP chitin, on *A. thaliana* WT plants. According to these data, in combination with the *fhy3 far1* microarray data, 77 potential marker genes were evaluated for further transcriptional investigations of the SA- and JA/ET-mediated defence response signalling pathways of WT and *fhy3 far1* mutants upon biotic challenges. The potential marker genes were also selected according to literature, and included WRKY TF, PR genes, chitinases, plant Defensins and NBS-LRR genes, amongst others.

Eventually, *PATHOGENESIS-RELATED 3* (*PR3*), *PDF1.2*, *PAD4*, *EDS1* and *SID2* were chosen as the most appropriate marker genes for the infection assay.

PDF1.2a (AT5G44420) encodes a plant defensin and is most probably mainly involved in ROS production and, secondly, in the formation of pore-like membrane defects of pathogens that allow efflux of essential ions and nutrients. Its expression is induced by JA/ET-mediated signalling pathways, but not by SA and was described previously to have been utilised as a marker gene for JA/ET-mediated defence responses to necrotrophs (*A. brassicicola* and *B. cinerea*) (Vriens *et al.*, 2014; Zimmerli *et al.*, 2001). According to the investigated microarrays, *PDF1.2a* showed a strong activation in response to *B. cinerea* and *A. brassicicola,* activation by *Pst* DC3000, but no activation in response to *G. orontii.* Its expression was slightly downregulated by chitin and FB1 treatment (Figure 3.9). Therefore, it was concluded that *PDF1.2a* could be used as marker for JA/ET-mediated defence response, and thus would be a good marker for *B. cinerea* infection. In addition, *PDF1.2a* has been shown to be a marker for more-generic ROS accumulation (Tierens *et al*., 2002).

PR3 (AT3G12500) encodes a basic chitinase and its expression is induced by SA- and JA/ET-mediated signalling pathways (Vieira Dos Santos *et al.*, 2003). According to the investigated microarrays, *PR3* showed a trend of strong induction by *B. cinerea* and *A. brassicicola,* but no

induction in response to *Pst* DC3000 and *G. orontii*. FB1 and chitin treatment also did not induce *PR3* expression (Figure 3.9). It was concluded that *PR3* could be used as a marker for JA/ET-mediated signalling and, therefore, mainly for *B. cinerea* infection.

PAD4 (AT3G52430) encodes a lipase-like gene, functioning in R gene-mediated defence response. *PAD4* was shown to directly interact with *EDS1* and together they activate and amplify SA-signalling and ROS production (Rustérucci *et al.*, 2001). According to the investigated microarrays, *PAD4* was not affected by treatment with *B. cinerea* and slightly downregulated in response to *A. brassicicola* and FB1 treatment. *Pst* DC3000, *G. orontii* and chitin, on the other hand, induced its expression (Figure 3.9). Consequently, it was concluded that *PAD4* could be used as a marker for SA-signalling-mediated defence response and, therefore, possibly, for *Pst* DC3000 infection, as well as for chitin.

EDS1 (AT3G48090) encodes a lipase-like gene that is part of R gene-mediated defence response and directly interacts with the disease resistance signalling protein *PAD4* (Feys *et al.*, 2001). According to the investigated microarrays, *EDS1* was slightly repressed in response to treatment with *A. brassicicola* and not affected by *B. cinerea* or FB1, but induced by *Pst* DC3000, *G. orontii* and chitin (Figure 3.9). It was concluded that *EDS1* could be used as a marker for SA-mediated defence response to *Pst* DC3000 and to chitin.

SID2 (AT1G74710) encodes a protein with isochorismate synthase activity, crucial for SA biosynthesis. Wildermuth *et al.* (2001) showed that in *sid2* mutants pathogen-induced SA levels were massively reduced (5 - 10 % of WT levels) and that the mutant plant had a strongly impaired defence response, especially SA-mediated SAR. According to the investigated microarrays, *SID2* was not affected by treatment with *B. cinerea*, chitin or FB1, but upregulated in *Pst* DC3000- and *G. orontii*-treated plants. *A. brassicicola* treatment led to a slight downregulation of *SID2* expression (Figure 3.9). It was concluded that *SID2* could be used as a marker for SA-signalling and defence response to *Pst* DC3000.

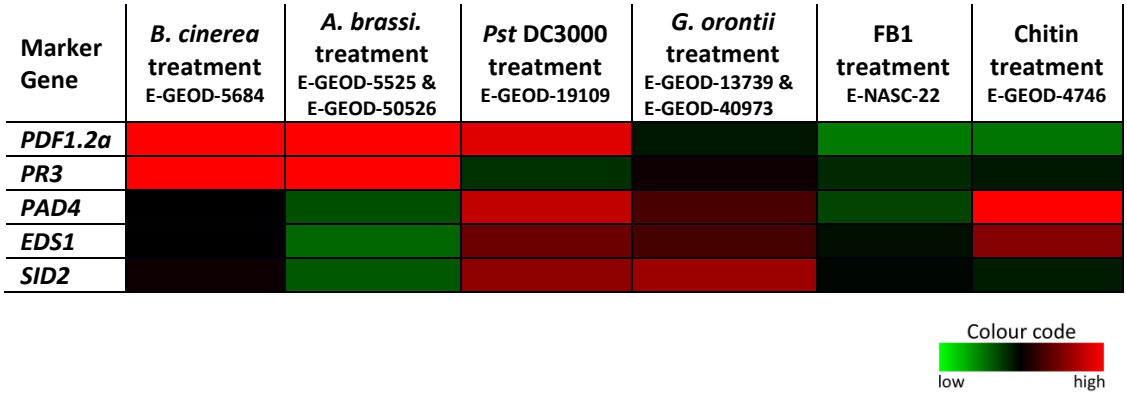

Figure 3.9: Degree of defence marker gene response relative to mock treatment (rather than the absolute levels of transcript) from published microarray data (Microarray IDs stated) investigating challenges of *A. thaliana* plants with *B. cinerea*, *A. brassicicola* (*A. bras.*), *Pst* DC3000 (*Pst*), *G. orontii*, chitin and FB1. For *Pst* DC3000, *A. brassicicola* and *G. orontii* treatment, two microarrays each were utilised for analysis. Here, the average of the relative defence marker gene transcript was used to calculate their degree of response. Highest relative response for the whole table is labelled red, lowest green, midpoint black. *A.brassi. = A. brassicicola*.

3.2.4.5 Transcriptional changes upon biotic challenges

22 days old SD-grown WT and *fhy3 far1* mutant plants were treated with *B. cinerea* (10^5 cfu), *Pst* DC3000 (10^6 and 10^8 cfu), FB1 (5 and 50 µM) and chitin (100 and 1,000 mg/L). Samples were collected 3 dpi at ZT4 and the transcriptional regulation of the selected defence response marker genes investigated by RT-qPCR. WT and mutant plants had Nossen (No-0) ecotype.

Figure 3.10 depicts the transcript levels of the marker genes *PDF1.2a*, *PR3*, *EDS1*, *PAD4* and *SID2* upon treatment with *B. cinerea*, *Pst* DC3000, FB1 and chitin in *fhy3 far1* and WT plants. For each treatment, approximately 20 plants were sampled and their RNA extracted for RT-qPCR. The respective marker gene transcript was analysed with the "2-[delta] [delta] Ct method" and the result was normalised to its mock-treated WT marker gene transcript, and is shown as the average of two BRs. The error bars represent standard error. Defence response marker genes expression in general was found as predicted in WT based on the microarray analysis summarised in the Figure 3.9. Some different results, however, were observed. *Pst* DC3000 treatment in either concentration did not affect *EDS1* expression, whereas it was upregulated according to the investigated microarrays. *PAD4* and *SID2* were only activated when *Pst* DC3000 was applied in high concentration (10^8 cfu/ml). Also, *PAD4* and *EDS1* were slightly upregulated in response to FB1 treatment in both concentrations. High concentration of FB1 activated

PDF1.2a, PR3 and *SID2*. According to the investigated microarray, all five marker genes showed no effect or a slight downregulation in response to FB1. Chitin treatment at a concentration of 1.000 mg/L resulted in no change of *PDF1.2a* expression (and activation with 1,000 mg/L), but was downregulated according to the investigated microarray. *PR3* was downregulated upon chitin treatment (1.000 mg/L), whereas it was not affected by chitin according to the microarray. For the SA-responsive *PAD4*, chitin led to a downregulation instead of an upregulation, and a downregulation of *SID2* instead of no change according to the microarray.

These discrepancies between the RT-qPCR data and data from the microarrays (Figure 3.9) could be caused by many factors, such as photoperiod (not all plants for the microarrays were grown in SD - Table 3.2), different light intensities during plant growth, developmental stage of the *A. thaliana* plants (Table 3.2), and treatment time point and treatment methods. For instance, spray/drop infiltration of Arabidopsis with *Pst* DC3000 has been shown to result in higher degree of susceptibility when performed during the day, and syringe infiltration resulted in higher degree of susceptibility when performed during the night (Zhang *et al*., 2013)).

In all cases in this assay, melt curves for the PCR products generated, indicated the presence of a single PCR product, confirming the specificity of the primers used.

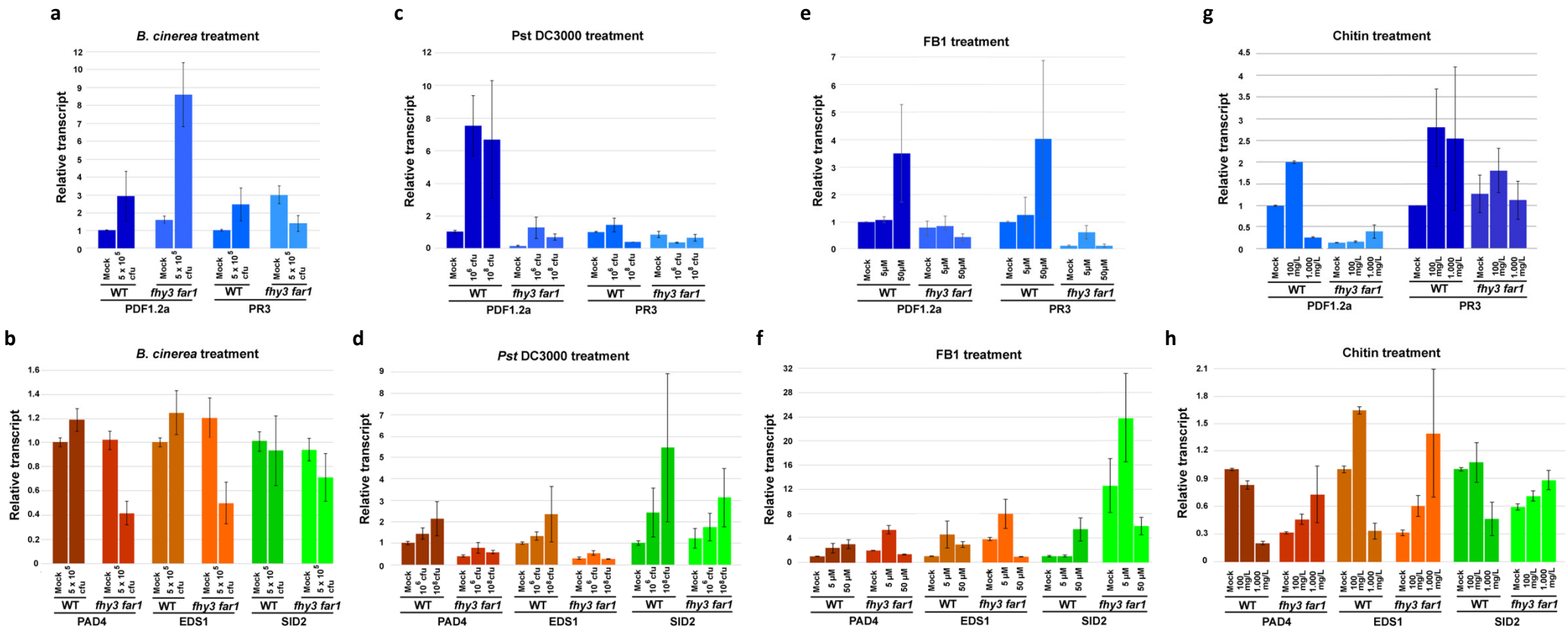

Figure 3.10: Transcriptional changes (absolute levels of transcript) 3 dpi in 25 days old SD-grown WT (No-0) and *fhy3 far1* (No-0) mutant plants after treatment with FB1 solution (a and b), *B. cinerea* spore suspension (c and d), *P. syringae* cell suspension (e and f), and chitin solution (g and h) in respective concentrations. a), c), e) and g) depict transcript levels of *PR3* and *PDF1.2a*, and b), d), f) and h) depict transcript levels of *SID2*, *PAD4* and *EDS1*. Approximately 20 plants for each genotype and treatment were sampled for RT-qPCRs. Investigations were done in two BRs and error bars represent standard error.

Table 3.2 represents the overall results of marker gene transcript changes in WT and *fhy3 far1* mutants upon biotic challenges, rather than the absolute levels of transcript as seen in Figure 3.10. The heatmap data is based on the individual biological replicate results and the stated concentrations of treatment are the major influences, i.e. Pst DC3000, 10^6 cfu/ml treatment for example was the basis for the heatmap, but the Pst DC3000, 10^8 cfu/ml treatment results were also considered in the depiction of the regulation. The aim of the heatmap was to present what the weight of evidence suggests and to get an idea what the effects of the biological challenges on the defence response marker gene expression are. In order to show clear trends in marker gene expression for each treatment, several additional biological replicates would have been necessary (big standard errors in some RT-qPCRs in Figure 3.10). Since Ma *et al*. (2016) found the cause of the enhanced leaf-lesion phenotype of *fhy3 far1* mutants in increased accumulation of SA (see 3.3 - Discussion), an expansion in terms of BRs was not pursued. Nonetheless, marker gene transcript levels in SD-grown *fhy3 far1* mutant plants upon mock treatment were similar to the results from the *fhy3 far1* microarray. In both investigations, expression of the JA/ET-responsive marker gene *PDF1.2a*, as well as the SA-responsive marker genes *PAD4, EDS1* and *SID2*, was downregulated. This suggests that the downregulation of SA- and JA/ET-mediated defence signalling in *fhy3 far1* mutants occurs during the day and during the night. The downregulation of *PDF1.2a*, which is also a marker for more-generic ROS accumulation, could point to a possible downregulation of ROS accumulation in *fhy3 far1* mutants.

Pst DC3000 treatment results suggest an induction of SA-signalling, seen by the upregulation of the SA-responsive markers *PAD4* and *SID2*. JA/ET-signalling also seemed induced, seen by the upregulation of the JA/ET-responsive markers *PDF1.2a* and *PR3*. *PDF1.2a* upregulation again could also point to a possible induction of ROS accumulation in WT. Similar to WT, an induction of SA-signalling was found in *fhy3 far1* mutants (upregulation of the SA markers *PAD4, EDS1* and *SID2*), occurring to the same extent as found in WT. However, JA/ET-signalling showed a mixed response. *PDF1.2a* was increased similar as seen in WT, but *PR3* actually showed a decrease. This might suggest that JA/ET response is suppressed in *fhy3 far1*. *PDF1.2a* could possibly be activated only as a response to later ROS accumulation associated with the SA-mediated responses to *Pst* DC3000.

B. cinerea challenge results indicate induced defence response-related JA/ET-signalling, as well as possibly ROS accumulation, but no differential regulation of SA-signalling in WT. However, the *B. cinerea* challenge results suggest a repression of SA-, as well as JA/ET-signalling in *fhy3 far1* mutants, whereas ROS accumulation seemed to be induced to the same extent as in WT.

FB1 treatment results suggest an induction of defence response-related SA-signalling and possibly ROS accumulation in WT, with potentially no induction of defence response-related JA/ET-signalling. In *fhy3 far1* mutants, there is a clear repression of SA-signalling related marker gene transcripts and little response for JA/ET-signalling and ROS accumulation.

The chitin treatment results suggest a repression of defence response-related SA-signalling and possibly ROS accumulation in WT, but a possible induction of JA/ET-signalling. *fhy3 far1* mutants, on the other hand, seemed to have SA-signalling and ROS accumulation induced in response to chitin.

Overall, this points to a complex picture, with *fhy3 far1* behaving in a quite different manner than WT upon challenge with a number of stressors. There is no clear enhancement of any one class of response. In fact, similar to the *fhy3 far1* microarray data, this defence response marker gene expression suggests that *fhy3 far1* mutants show a negative feedback on SA- and JA/ET-defence response pathways.

Table 3.2: Relative defence marker gene expression. Degree of defence marker gene response in WT and *fhy3 far1* mutants relative to their mock treatment (rather than the absolute levels of transcript shown in Figure 3.10) upon challenges with *Pst* DC3000 (10^6 cfu), *B. cinerea* (5 x 10^5 cfu), FB1 (50 µM) and chitin (1.000 mg/L). Data is based on the majority results of the individual biological replicate results. *fhy3 far1* mock versus WT mock data represents the average of the differences in all mock treatments that were used. Again, data is based on the majority results of the individual biological replicate and treatment level results.

Gene	Function (responsiveness)	*fhy3 far1* mic, night	*fhy3 far1*, mock vs WT mock	WT *Pst* resp.	*fhy3 far1 Pst* resp	WT *B. c.* resp.	*fhy3 far1 B. c.* resp.	WT FB1 resp.	*fhy3 far1* FB1 resp.	WT Chi resp.	*fhy3 far1* Chi resp.
PDF1.2a	Defensin (JA/ET and ROS)										
PR3	Chitinase (JA/ET and SA)										
PAD4	Lipase-like (SA)										
EDS1	Lipase-like (SA)										
SID2	ICS (SA)										

Upregulationed (more than 2-fold)

Some upregulation (1.5 to 2-fold)

Downregulationed (more than 2-fold)

Some downregulation (1.5 to 2-fold)

No change

B. c.= *B. cinerea* treatment
chi = chitin treatment
mic = Microarray
night = mean transcript of sampling time points 36, 40, 44h after transfer to SD (ZT12, 16, 20)
Pst = *Pst* DC3000 treatment
resp = response (*fhy3 far1* treated versus *fhy3 far1* mock)

3.3 Discussion

The aim of the investigations in this chapter was to characterise the misregulated defence response of *fhy3 far1* mutant plants to gain insight if it is constitutively or inappropriately activated, and to determine its possible contextual relation to the double mutant's leaf-lesion formation.

3.3.1 Disrupted *myo*-inositol biosynthesis causes constitutively activated SA-mediated defence response in *fhy3 far1* mutants

Towards the end of the investigations for this thesis, a paper by Ma *et al.* (2016) was published, also concerning *FHY3 FAR1* loss-of-function in *A. thaliana*, that addressed similar questions as the ones of this thesis. The group demonstrated increased SA accumulation in *fhy3 far1* mutants, caused by the cessation of *MIPS1*- and *MIPS2*-dependent *myo*-inositol biosynthesis. The group's microarray GO analysis (microarray based on SD-grown plants) displayed an upregulation of defence- and/or SA-response genes (PR1, PR2, PR5, EDS1, EDS5, PAD3, SID2, etc.) in *fhy3 far1* at ZT4, therefore during the day. In WT, FHY3 and FAR1 protein levels show a peak at dawn, when they activate *MIPS1* and *MIPS2* expression, seen by an expression peak of both genes at ZT4 in SD. *MIPS1* and *2* activate the *myo*-inositol biosynthesis pathway, which again represses *SID2* as component of the SA-signalling pathway, therefore representing a negative regulation of SA accumulation. This mechanism is missing in *fhy3 far1* mutants and leads to a constitutively activated SA-mediated defence response.
The findings in this chapter are discussed in light of this paper.

3.3.2 Initial analysis of *fhy3 far1* mutants

Defence response

The GO overrepresentation analysis of the *fhy3 far1* microarray data for biological process highlights that, among misregulated genes in *fhy3 far1*, there is an enrichment of genes associated with "defence response" and "response to other organism", as well as the over-represented cellular component "extracellular region". Extracellular regions are, of course, the main location of pathogens, and microbes in general (Turner *et al.*, 2013). This suggests an inappropriately regulated defence response in *fhy3 far1* mutants, at least at the time points

analysed during the night. Also, the enrichment of genes in the category “toxin catabolic process” (enriched GO children “secondary metabolite catabolic process” and “secondary metabolic process”) could be attributed to the necessity of a cleansing of excessively deployed toxic defence compounds by the plant. However, GO analysis showed that approximately 12 % of SA-associated genes were misregulated in *fhy3 far1* mutants, actually almost all down-regulated. Approximately 40 % of these downregulated genes are positive regulators of defence response, which points to a downregulation of SA-mediated defence response. Here, it has to be kept in mind that the significant differential expression is based on the average of three time points during the night in SD (ZT 12, 16 and 20). At night, defence response in plants was reported to be less active (Bhardwaj *et al.*, 2011; Zhang *et al.*, 2013; Zhou *et al.*, 2015) so differences could vary from those that might be observed during the daytime. Correspondingly, Ma *et al*. (2016)’s GO analysis of their microarray data found that positive regulators of defence and/or SA-responsive genes were upregulated during the day in SD. This could suggest that mechanisms regulating the SA-signalling pathway might be amplified during the night to compensate for an enhanced activation of the SA-signalling pathway during the day in *fhy3 far1* mutants. That could cause the downregulation of SA-dependent genes during the night, found in the *fhy3 far1* microarray analysis.

Amplified inhibiting mechanisms could also act on JA/ET-signalling pathways, as most of the misregulated JA-and ET-associated genes, which represent 13 % of the total number of JA-and ET-associated genes, are downregulated in *fhy3 far1* mutants. Approximately 39 % of these genes are also associated to defence response and are predominantly positive regulators. Even though Ma *et al*. (2016) did not do a GO analysis for JA/ET-associated genes, they provided their microarray data for misregulated genes that were at least two-fold up- or downregulated. GO analysis showed an upregulation of most of the misregulated JA- and ET-associated genes in *fhy3 far1* mutants during the daytime (7 % of the total number of JA-and ET-associated genes). This could imply a mitigation of a possibly increased defence response as a whole in *fhy3 far1* mutants during the night.

All of the SAR-associated misregulated genes (14 % of total number of SAR-associated genes) in *fhy3 far1* mutants were downregulated in the *fhy3 far1* microarray. GO analysis for Ma *et al*. (2016)`s microarray data for misregulated genes showed an upregulation of most of the misregulated SAR-associated genes in *fhy3 far1* mutants during the daytime (20 % of the total number of SAR-associated genes). This again suggests the presence of compensatory feedback to mitigate extensive SA accumulation and subsequent activation of SAR during the night.

The Panther classification tool indicated that for the misregulated genes in the *fhy3 far1* mutant, within the category "response to stimulus", a large number of genes fell into the category "defence response to bacterium". This also points to a misregulated SA-mediated defence response in the double mutant. Most pathogenic bacteria are of biotrophic nature (Kraepiel and Barny, 2016), which mainly activates SA-signalling, while the largest group of pathogenic fungi is of necrotrophic nature (Wang *et al.*, 2014).

Programmed Cell Death

GO analysis revealed an almost exclusive downregulation of the misregulated negative regulators of PCD in *fhy3 far1* mutants during the night. This is consistent with the increased PCD in the double mutant.

This observation is also consistent with the two hypotheses that *fhy3 far1* mutant plants could have 1) an inappropriate defence response, or 2) a defence response that is activated constitutively. In the first hypothesis, the always present microbial community, which mainly consist of commensal and beneficial microbes, could activate defence response mechanism in *fhy3 far1* mutant that would not be activated it in WT plants. Speculatively, an inappropriate activation could take place at the first path of defence response, when MAMPs of the microbial community are perceived (Jones and Dangl, 2006). Here signal transduction could be misregulated, leading to SA-mediated HR. In the second hypothesis, defence response mechanisms are always activated, independently of microbes. Speculatively, mechanism of the second path of defence response (ETI), responsible for the accumulation of the defence response signalling molecules SA and ROS, could be affected, leading to activation of HR.

Ma *et al*. (2016)'s investigations showed that *fhy3 far1* mutants have a constitutively activated defence response. The disrupted *myo*-inositol biosynthesis in the double mutant leads to a cessation of *SID2* repression by *myo*-inositol (Chaouch and Noctor, 2010), resulting in the accumulation of high levels of SA. The group suggested these high SA levels as cause for the extensive leaf-lesion formation in *fhy3 far1* mutant plants.

The observed increase of PCD would be dependent on ROS and reactive nitrogen species (RNS), as well as signalling mediated by components of these two categories (Glazebrook 2005; Wang *et al.*, 2013). The overrepresented molecular functions "oxygen binding" and "heme binding" among genes misregulated in *fhy3 far1* could, therefore, point to mechanisms counteracting increased ROS and RNS levels (Minibayeva and Beckett, 2015). The PANTHER classification tool displayed more upregulated genes in the categories "induction of apoptosis" and "death" than

downregulated ones, also consistent with increased PCD, but at the same time pointing to at least some possible mitigating effects, due to the downregulated genes. This suggests that increased ROS accumulation is the main cause for leaf-lesion formation (ROS as PCD-executing molecules) in *fhy3 far1* mutant plants. One particularly interesting aspect of the *fhy3 far1* phenotype is the SD-specific enhancement of the lesion phenotype, as this phenotype has previously been observed in another lesion mutant, *loh1*. A potential contributing cause, which was, therefore, investigated, was an impaired sphingolipid biosynthesis. *LOH1* encodes a ceramide synthase that is essential for the production of ceramides containing very long chain fatty acid (VLCFA-ceramides). The *LOH1* loss-of-function mutant exhibits spontaneous cell death when grown in SD. In this condition, *loh1* mutant plants show reduced levels of ceramide species with C20 - C28 fatty acids, but high levels of trihydroxy sphingoid bases and ceramide species with C16 fatty acid. Accumulation of the latter was suggested to trigger PCD (Ternes *et al*., 2011). However, the overall pattern of expression of sphingolipid-associated gene did not suggest any misregulation of this pathway.

Another contributing cause to the enhanced leaf-lesion formation in *fhy3 far1* mutants was suggested to be an impaired Tetrapyrrole/Chlorophyll biosynthesis pathway (Wang *et al*., 2016). Chlorophyll is synthesised from δ-Aminolevulinic acid (δ-ALA) via several intermediates to protoporphyrin IX, the point where the pathway divides into chlorophyll and heme biosynthesis. Wang *et a*l. (2016) investigated HEMB1, which encodes one of two δ-Aminolevulinic acid dehydratases (ALAD) in *A. thaliana,* that catalyses the condensation of δ-ALA to porphobilinogen (PBG). A *HEMB1* loss-of-function mutant (produced by artificial microRNA of *HEMB1*) that had a 40 % - 50 % reduced HEMB1/ALAD production and strongly reduced ALAD activity, exhibited increased ROS accumulation and a lesion mimic phenotype. Wang *et al*. (2016) found that *HEMB1* is directly activated by FHY3 and that *fhy3 far1* mutants showed decreased expression of *HEMB1*. It was argued that, due to the reduced ALAD activity, photosensitizing intermediates could accumulate in *fhy3 far1* and *hemb1* mutants in darkness (no specific intermediates were stated), which then could lead to ROS production and photobleaching upon light onset. The shortcoming of the study, in the light of this thesis, is that it was done with 5 - 7 days old seedlings and the changes in darkness and changes in transition from darkness to light (skoto- to photomorphogenesis) were investigated. *fhy3 far1* mutant plants grown in light did not display photobleaching at this developmental stage, and leaf-lesion started to form at later development stages of the plant (Figure 3.1). This is underpinned by the greening of *fhy3 far1* plants. So, either the chlorophyll biosynthesis is not impaired or functional compensational mechanisms are in place. Also, no evidence has been found that pyrrole intermediates upstream

of ALAD would cause any oxidative damage (Tanaka *et al*., 2011). In the group's previously published paper (Tang *et al*., 2012), they discovered a direct binding of FHY3 (and FAR1) to HEMB1 and argued that light-induced damage after transfer from darkness to light is actually prevented in *fhy3 far1* mutants. In the chlorophyll biosynthesis pathway, several intermediate after protoporphyrin IX, protochlorophyllide (Pchlide) is converted to chlorophyllide. In darkness, there is a block at this step, as the responsible enzyme, NADPH:protochlorophyllide oxidoreductase (POR), is light-dependent. Since the accumulation of Pchlide and/or other pyrrole intermediates could lead to ROS production after light onset, possibly resulting in photobleaching of cotyledons and even excessive cell death, transcriptional and post-transcriptional mechanisms are in place to prevent damage. These mechanisms regulate Pchlide quantity in darkness, and ALA levels are one check point. Tang *et al*. (2012)'s hypothesis stated that **in darkness**, *FHY3* (and *FAR1*) are not activated and do not induce *HEMB1*, leaving the Pchilde pool at a small level. **After irradiation**, FHY3 (and FAR1) induce *HEMB1* expression and thereby the conversion of ALA to porphobilinogen (PBG), subsequently leading to Pchlide- and Chlorophyll biosynthesis. The *fhy3 far1* double mutant would accumulate less Pchlide, which the group confirmed, and/or other pyrrole intermediates during darkness. This could lead to less ROS production after light onset, and would result in less photobleaching of cotyledons and less cell death. Both studies (Tang et al., 2012 and Wang et al., 2016) were done in seedlings that transitioned from skoto- to photomorphogenesis and not in plants of later developmental stages when leaf-lesion formation occurred in *fhy3 far1* mutants. The results by Wang *et al*. (2016) and Tang *et al*. (2012) should not simply be conferred to night-day transitioning plants of later developmental stages. Photomorphogenic *fhy3 far1* mutant plants of 10 days (as used for the *fhy3 far1* microarray) and 22 days (as used for the biotic challenges investigation) that would lack this FHY3-mediated promotion of chlorophyll biosynthesis, however, did not exhibit reduced greening of true leaves. Misregulated mechanisms of the chlorophyll biosynthesis are unlikely to contribute to the leaf-lesion formation in *fhy3 far1* mutant plants.

The double mutant showed an interesting pattern of DAB staining. Some leaves strongly accumulated H_2O_2 and others surprised with almost a complete absence of dark brown precipitate that suggest no accumulation of H_2O_2 (Figure 3.2). Leaves with almost no H_2O_2 accumulation were an exception, but this aberration was not quantified. The *FHY3 FAR1* loss-of-function was suggested to lead to a misregulated HR response, including loss of downregulation of HR via the MIPs pathway (Ma *et al*., 2016). It could be hypothesised that a certain threshold has to be reached before a RCD (HR) is triggered, giving an all or nothing staining effect.

Furthermore, studies in animal models and humans have shown a very comprehensive effect of the microbiota on its host and vice versa. For example, the gut microbiota is directly and indirectly connected to the brain and immune system, exhibiting a bidirectional communication. Alterations of the gut microbiota are associated to profound effects on the host, seen by inflammatory bowel disease for example, where abnormal gut microbiota compositions were found (Dinan *et al.*, 2015; Carding *et al.*, 2015). A similar comprehensive effect of the plant's microbiota on host leaves could be possible. Interestingly, individual leaves of one plant have been shown to differ in their microbial community size and composition (Whipps *et al.*, 2008; Lindow and Brandl, 2008). The presence of particular microbial factors on some leaves, which may not be present on all leaves, could dramatically affect the H_2O_2 accumulation in *fhy3 far1* mutant plants. This could be consistent with the hypotheses of an inappropriately and constitutively activated defence response in *fhy3 far1* mutant plants.

Instead of triggering inappropriately activate defence response mechanisms, including H_2O_2 accumulation, the plant's signalling molecule SA could be degraded by microbes, which would also affect a constitutively activated defence response. The *U. maydis Shy1*, which encodes a salicylate hydroxylase, is transcriptionally induced during the biotrophic phase of the fungus' life cycle. Rabe *et al*. (2013) found that *U. maydis* uses SA as carbon source, which could lower SA levels in plants. The fungus particularly grows along the phloem (in corn) that is the plant structure through which SA is mainly distributed systemically (Rocher *et al*. 2006). However, *U. maydis* did not show altered virulence after *shy1* loss-of-function. Ambrose *et al*. (2014) found a putative salicylate hydroxylase in *Epichloe festucae*, an endophytic fungal symbiont. However, the group did not find evidence suggesting that the SA degradation by the fungus would be a factor in the prevention of activation of plant defence response. Similar levels of SA were observed in endophyte-infected and endophyte-free plants. Yet, neither group investigated ROS accumulation so a potential effect on it cannot be excluded.

Development

Furthermore, the underrepresented biological processes "RNA processing" and "ribosome biogenesis", in combination with the molecular functions "RNA binding" and "structural constituent of ribosome", as well as the cellular components "cytosolic ribosome" and "ribosomal subunit" could be attributed to resource allocation to possibly increased defence response mechanism during the day. Hence, a lack for developmental processes in the mutant during the night, when growth mainly takes place (Smith and Stitt, 2007), could cause the dwarf phenotype of *fhy3 far1* mutant plants. The constitutively activated SA-mediated defence

response in *CONSTITUTIVE EXPRESSOR OF PATHOGENESIS RELATED GENES 1* (*CPR1*) loss-of-function mutants, for example, results in a higher resistance to various pathogens, but at the cost of a dwarf phenotype (Heidel *et al.*, 2004).

Underrepresentation of the molecular function "protein binding", and the cellular components "Golgi apparatus part" as cellular distributor of proteins, "endosome" as cellular sorter, and "vacuolar membrane", all intracellular components, could again be ascribed to impaired developmental processes, caused by reduced protein biosynthesis and protein transport to cellular components.

Underrepresentation of the cellular component "chloroplast stroma", with its child ontologies "plastid stroma", "plastid part" and "intracellular organelle", could be attributed to the impaired chloroplast biosynthesis in *fhy3 far1* mutant plants, demonstrated by Gao *et al.* (2013).

3.3.3 Transcriptional changes upon biotic challenges

Plants for the assay to test the transcriptional changes in WT and *fhy3 far1* mutants upon biotic challenges were sampled at ZT4, therefore representing the marker gene behaviour during the day. GO analysis of Ma *et al.* (2016)'s microarray data suggested an activated SA-mediated defence response at this time. Consequently, SA-associated defence response genes were expected to be upregulated at this time. The double mutant, however, showed opposite defence response marker gene expression results (RT-qPCR result), with a downregulation of both, SA- and JA/ET-dependent pathways, therefore agreeing more with the *fhy3 far1* microarray findings for night time, rather than with the daytime findings of Ma *et al*. (2016). This could point to the existence of a certain threshold for the activation of defence response-signalling pathways that is reached and results in a negative feedback on defence response marker genes, rather than an upregulation of those markers. Alternatively, other compounding stressors could have been affecting the plants. Plants for both, the *fhy3 far1* microarray and challenge with biotic stressors investigation were grown in the same conditions (same growth chamber and same light conditions). These stressors could have tipped the *fhy3 far1* system over the proposed threshold, activating the negative feedback to contain excessive defence response mechanisms and possible ensuing damages.

The fungal toxin FB1 induces PCD by disrupting the sphingolipid biosynthesis and requires plant defence response pathways (SA, JA/ET), suggesting that FB1-mediated PCD and HR share certain

mechanisms (Kuroyanagi *et al.*, 2005; Berkey *et al.*, 2012). FB1 treatment strongly induced defence marker gene expression in WT. It may be that this upregulation of defence response gene expression is partly induced by ROS stress; high concentrations of FB1 induce stronger PCD than lower concentrations, seen by the more severe leaf-chlorosis. In *fhy3 far1* mutants, treatment with low FB1 concentration led to increased chlorosis and increased defence response gene expression; however, high FB1 concentration led to severe chlorosis, but a downregulation of marker gene expression. This suggests the presence of a negative feedback on defence response gene expression, triggered by reaching a ROS threshold due to the combination of endogenous ROS stress and added ROS stress caused by high concen-trations of FB1.

For treatments with pathogens, the degree of infection was not measured, but the chlorotic appearance of the leaves and the necrotic lesion formation demonstrate the occurrence of infection in both WT and *fhy3 far1*.
Infection with *B. cinerea* resulted in necrotic leaf-lesions and triggered only JA/ET-responsive genes in WT, which was expected following the infection by a necrotroph. *fhy3 far1* mutants showed more severe necrotic leaf-lesion, in combination with a downregulation of the SA- and JA/ET-responsive marker gene *PR3*. Birkenbihl *et al.* (2012) found an accumulation of H_2O_2 in *A. thaliana* leaves upon infection with *B. cinerea* that, on top of that, produces ROS (H_2O_2) itself to degrade plant tissue. Increased ROS accumulation in *fhy3 far1* mutants, as well as in WT, is also suggested by the upregulation of the ROS production-associated gene *PDF1.2a*. This perhaps suggests that in *fhy3 far1* a ROS-mediated negative feedback on defence response pathways in general is triggered by *B. cinerea* infection, as was proposed for FB1. Here, the increase ROS triggers reach a certain threshold and lead to a negative regulation of SA- and JA/ET-signalling (as seen by the downregulated SA- and JA/ET-associated markers in *fhy3 far1*).

Infection by *Pst* DC3000 resulted in severe chlorosis of WT leaves and triggering of defence response marker genes for both, SA-induction and JA/ET-response. *fhy3 far1* mutants showed less susceptibility to the hemibiotrophic pathogen, seen by less severe chlorosis than in WT, and yet it retained the induced response of ROS and SA-marker genes. However, *fhy3 far1* showed reduced JA/ET-associated gene expression in response to *Pst* DC3000. This also suggests an activation of negative feedback on JA/ET-associated defence response marker genes, seen in PR3 repression. The enhanced resistance of *fhy3 far1* mutant plants to *Pst* DC3000 also agrees

with the observations of Ma *et al*. (2016). It was proposed that the constitutively activated SA-signalling pathway leads to a very effective constitutive antibacterial defence.

The most abundant MAMP, chitin, was used to investigate PTI-activation in WT and *fhy3 far1* mutant plants. It induced some leaf-chlorosis and the downregulation of most defence response genes in WT. Chitin has been shown to yield quite different gene expression profiles from other defence responses. Ramonell *et al.* (2002) showed that approximately 50 % of SA- or JA-inducible genes are downregulated in response to chitin, in accordance with the findings of this assay. However, this expression pattern in WT was partly contrary to expectations, based on published chitin microarray studies in Columbia-ecotype plants, where *EDS1* and *PAD4* were induced (Wan *et al.*, 2008). ROS accumulation upon chitin treatment in WT (No-0) could have reached the proposed threshold and led to a negative regulation of SA- and JA/ET-signalling. Chitin-responsive genes have not been extensively studied before in the Nossen ecotype and the present findings strongly indicate ecotype-specific differences. Conversely, severe chitin-induced leaf chlorosis and upregulation of most defence response genes in *fhy3 far1* suggest that the misregulated SA-signalling pathway in *fhy3 far1* mutants interfere with the normal defence response-related SA- and JA/ET-signalling upon chitin-treatment.

The lesion formation and dwarf phenotype of *fhy3 far1* (No-0) mutant plants was also observed by Ma *et al.* (2016), who observed an increase in severity of the phenotype when mutant plants were grown in SD. DAB staining likewise showed H_2O_2 accumulation in *fhy3 far1*, but not in WT (No-0) in their study. The group demonstrated enhanced accumulation of SA in the double mutant, and were able to rescue the leaf-lesion formation in SD and in LD by a block of SA accumulation via overexpression of S3H (encodes a SA accumulation-blocking enzyme). It was concluded that excessive SA plays an essential role in *fhy3 far1* mutant response to oxidative stress/PCD and the associated leaf-lesion formation. The proposed negative feedback on SA-mediated defence response gene expression in this thesis is not inconsistent with Ma *et al.* (2016)'s findings.

3.4 Conclusion

The leaf-lesion forming *fhy3 far1* mutant plants were found to over-accumulate ROS in leaves and were shown to transcriptionally downregulate negative regulators of PCD in the *fhy3 far1* microarray analysis performed here. This agrees with the very-recently published findings of Ma *et al*. (2016), which showed that increased PCD in *fhy3 far1* was due to increased SA accumulation. This accumulation is caused by the cessation of *MIPS1*- and *2*-dependent *myo*-inositol biosynthesis that would normally suppress SA biosynthesis. The additional repression of SA- and JA/ET-signalling associated genes in the *fhy3 far1* microarray analysis, however, contradict the findings of Ma *et al*. (2016). Ma *et al*. (2016) showed increased defence response-associated gene expression in *fhy3 far1*. The *fhy3 far1* microarray data of this thesis is based on plants sampled during the night, when FHY3 and FAR1 affect the gene expression of *ELF4* during the early night in SD, whereas Ma *et al*. (2016)'s microarray is based on plants sampled during the day. The differences observed at this time prompted the hypothesis of differential feedback mechanisms that may exist specifically in the night time. Alternatively, it was hypothesised that additional stressors present in the local growth conditions such as light, humidity and seed-borne microbes that grew on the plant – even though the seeds were surface-sterilised before sowing it is almost impossible to grow sterile plants - may have pushed the *fhy3 far1* system over the threshold at which negative feedback prevents potentially very-damaging excessive defence responses.

The investigations in this chapter also assessed the response of *fhy3 far1* mutant plants to a range of biotic challenges. These challenges resulted in a differential response of plant defence-associated marker genes in *fhy3 far1* mutants contrary to WT. Here, a negative regulation of defence response-associated gene expression was often observed in *fhy3 far1*. This is perhaps, again, consistent with the proposed hypothesis of a threshold that has been reached, and at which negative feedback occurs to prevent potentially very-damaging excessive defence responses. It suggests the existence of SA- and ROS-mediated negative feedbacks on SA- and JA/ET-signalling dependent defence response. It is even conceivable that the proposed negative feedback could differ in threshold-setting during day and night, showing a lower setting during the latter for reasons of resource allocation to development.

Overall, this, if nothing else, demonstrated that the plant defence response is extremely complex and not merely based on simple upregulation of associated genes.

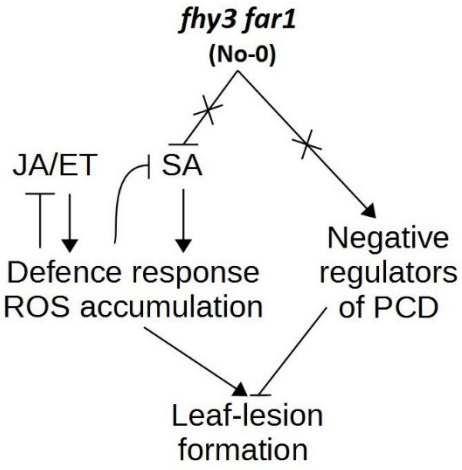

Figure 3.11: Mechanisms in *fhy3 far1* (No-0) mutants that lead to leaf-lesion formation including the hypothesised negative feedback mechanism on SA- and JA/ET-associated defence response signalling.

4 DEFENCE PATHWAY DISSECTION OF *FHY3 FAR1* MUTANTS

4.1 Introduction

The loss-of-function mutations of *FHY3* and *FAR1* result in increased ROS accumulation (3.2.2 ROS assay of *fhy3 far1* (No-0 mutant plants), impeded negative regulation of PCD and perturbed SA-mediated regulatory mechanisms in *A. thaliana* plants (3.2.3.4 Misregulation of PCD and defence response signalling). These features point to a possibly impaired defence response as the cause for the observed enhanced leaf-lesion formation of *fhy3 far1* mutant plants. The work presented in this chapter aimed to more-specifically identify the role of *FHY3* and *FAR1* in these processes. The plant immune response involves several key steps involving recognition, then initiation and moderation of the subsequent response.

The initial step of defence response, pathogen recognition, requires receptors such as membrane-bound RLKs that act in MAMP recognition, and intracellular R genes that act in avirulence factor recognition (pathogenic Avr gene product). RLKs are mostly represented by LRR subclass members, such as FLS2 that is involved in flg22 recognition, and lysine motif subclass members, such as CERK1 that is involved in chitin recognition (Goff and Ramonell, 2007; Dangl *et al*., 2013). RLKs are represented to a lesser extent by the cysteine-rich receptor-like kinases (CRKs) subclass, consisting of 44 members, such as CRK13 (Acharya *et al.*, 2007). Once pathogens are recognized by these receptors, signals are conveyed by downstream signal transduction cascades and, according to which, eventually gene expression is regulated, and thereby the plant's response. PCD, as one of the responses, is positively regulated by ROS and SA (Coll *et al.*, 2011). Since PCD is a final event for cells, it needs tight regulation. Coll *et al.* (2011) reported that the regulation of PCD downstream of SA accumulation involves the three positive regulators LSD-ONE-LIKE PROTEIN 1 (LOL1), ARABIDOPSIS THALIANA BASIC LEUCIN ZIPPER 10 (AtbZIP10) and METACASPASE 1 (MC1), as well as the two negative regulators LSD1 and MC2. The latter two factors negatively regulate PCD by repressing MC1 activity.

Metacaspases (MCs) are structurally related to caspases in animals that are the key initiators of apoptosis there. Loss-of-function of, for instance, *MC4* and *MC8* in *A. thaliana* was found to result in decreased occurrence of PCD, whereas an overexpression of *MC4* or *MC8* induced PCD in response to oxidative stress (treatment with H_2O_2 or the oxidative-stress causing agent methyl viologen) (Lam and Zhang, 2012).

In the preceding chapter, global transcript analysis of *fhy3 far1* mutant plants (3.2.3.4 Misregulation of PCD and defence response signalling), as well as an investigation of the double mutants' response to biotic stressors (3.2.4.5 Transcriptional changes upon biotic challenges),

suggested an inappropriate activation of its SA-dependent defence response. The investigations of this chapter aimed to find specific elements, including elements of plant defence response, which are impaired in the double mutant and could indicate the primary mechanism by which *FHY3* and *FAR1* could be involved in the regulation of leaf-lesion formation. This involved a more detailed analysis of the *fhy3 far1* microarray for misregulated biotic and abiotic stress-, as well as development-related genes that could be directly regulated by FHY3 and FAR1. This analysis pointed to two genes in particular. The upregulation of the defence response-related and PCD-inducing *CRK13,* as well as the downregulation of the PCD-inhibiting *MC2* indicated both genes as possible contributors to the leaf-lesion formation in *fhy3 far1* mutant plants. Their misregulation across 24 h in *fhy3 far1* mutants was consequently confirmed by RT-qPCR. A subsequent transcriptional analysis of *CRK13* overexpression (*CRK13*-Ox) and *mc2* mutant plants was carried out looking at induction of defence response markers upon challenge with the biotic stressors *Pst* DC3000, *B. cinerea*, FB1 and chitin. This, however, revealed little similarity between *CRK13*-Ox and *mc2* mutant responses and those of *fhy3 far1* mutants.

4.2 Results

4.2.1 *fhy3 far1* microarray analysis for disrupted FHY3 and FAR1 target genes involved in the defence response

The *fhy3 far1* microarray, with 20,855 distinctively assigned genes in total, was analysed with the objective to find specific misregulated genes in the *FHY3 FAR1* loss-of-function mutant that could give indications of the primary mechanism by which FHY3 and FAR1 could be involved in the regulation of leaf-lesion formation. Therefore, a series of analysis techniques, as follows, was utilised. Out of all genes, 1,967 genes were misregulated in their mean relative transcript over the three time points of 36, 40 and 44 h after onset of SD in *fhy3 far1*, of which 754 genes were two-fold up- and 1,213 two-fold downregulated. These misregulated genes were screened for the presence of the specific promoter binding sites, which would make them direct or indirect targets of FHY3 and FAR1, thereby, possibly linking their misregulation to the *fhy3 far1* phenotype. The promoter binging sites are FBS, Evening Element (EE) and CCA1-binding site (CBS) within the 3000 bp region of their promoters, using the web-interface Patmatch. This web-interface searches public *A. thaliana* sequence databases for short nucleotides (<20) and returned 759 genes that contain at least one of these binding sites. FBS is a direct target of FHY3 and FAR1 and genes containing this element are activated by both TFs. CCA1 and LHY act as

repressors on genes containing an EE, as well as activators on genes containing a CBS (Lin *et al.* 2007; Li *et al.* 2011; McWatters and Devlin 2011). FBS was selected, since genes regulated via this element might be expected to be downregulated in *fhy3 far1.* EE and CBS were selected due to the finding that CCA1 and LHY bind FHY3 (Li *et al.*, 2011), thereby reducing the activity of all three TFs. Genes regulated via the CBS might be expected to be upregulated in *fhy3 far1,* as FHY3 would no longer titrate out the positive action of CCA1 and LHY at the CBS. Accordingly, genes regulated via the EE might be expected to be upregulated in *fhy3 far1,* as FHY3 would no longer titrate out the negative action of CCA1 and LHY at the EE. Nonetheless, all of these promoter elements were searched for in both, upregulated and downregulated genes at this stage.

The next criterion of gene selection was an annotation of the gene for an involvement in responses to biotic and abiotic stimuli, stress response in general and developmental processes. The 759 genes containing either of the above stated binding sites were analysed with the web-interface "Classification SuperViewer" (Provart *et al*., 2003). This tool classifies genes according to their function (based on the GO database). This facilitated the selection of 187 genes. These were subsequently subjected to a simultaneous analysis with the web-interfaces Diurnal (Mockler *et al.*, 2007) and NASCArrays Gene Swinger (Craigon *et al.*, 2004). Diurnal displays the transcript pattern of *A. thaliana* genes over the course of 48 hours (in 4h intervals) under different growth conditions, such as SD (the condition which enhanced the lesion phenotype of *fhy3 far1*), and is based on results from multiple DNA microarray replicates. The gene selection criterion here was the consistent repeat of a 24-hour transcript pattern that suggests a circadian or diurnal regulation. This criterion was applied on the basis that FHY3 and FAR1 have been shown to play a specific role in SD via regulation of cycling genes after dusk (Siddiqui *et al*., 2016). Selection was based on correlation ($R > 0.7$) to one of a number of possible pre-set cycling patterns. NASCArrays Gene Swinger is a data-mining tool based on the Nottingham Arabidopsis Stock Centre microarray database. It identified the specific experiments and, hence, the biological contexts, in which genes of interest vary the most in expression. The tool is similar to GO tools but rather than categorising gene functions, it categorises experimental treatments which activate expression of genes. By extension of this, it could be proposed that changes in expression level of these genes might disrupt the pathways involved in response to those treatments. One gene selection criterion was a recording of a significant change in expression of the gene in response to experimental treatments involving pathogens or stress in general. In addition, any genes recording a significant change in expression between time points in any

circadian rhythm assay were also selected. Eventually, 36 genes out of the previous 187 genes met the criteria of one or both of these two analyses.

Finally, taking into account the literature on these genes, eight genes were identified for further study on the basis that firm experimental evidence had also previously associated these genes with potential pathways of interest, with respect to lesion formation. However, in parallel, an additional search was carried out among the misregulated genes in *fhy3 far1* for any which had previously been shown to directly affect leaf-lesion formation or suppression, when misregulated. This identified three additional candidate genes, which were added to this list. Eventually, a total of 11 genes were selected as the most interesting and promising for further analysis aimed at shedding light on the mechanisms underlying the leaf-lesion formation phenotype of *fhy3 far1* mutant plants. Six genes were identified as being involved in defence response and control of ROS/PCD, four genes in DNA damage response (loss-of-function of DNA damage recognising factors has been shown to elicit PCD (Furukawa *et al.*, 2010)), and one in regulation of cell proliferation in response to infection. Figure 4.1 displays the workflow of his investigation, and Table 4.1 lists the 11 candidate genes and summarises the selection criteria according to which the genes were selected.

After the selection of *CRK13* and *MC2* out of the candidate genes, and after the subsequent investigations (4.2.5.1 Phenotypic changes and histochemical staining upon biotic challenge, 4.2.5.2 Transcriptional changes upon biotic challenges) it was discovered that the Patmatch search for the nucleotide sequence of the FBS, EE, and CBS was done against the “TAIR10 Transcripts (-introns, +UTRs (DNA)” sequence database, which does not represent the promoter region of genes but the transcripts including predicted sequences and untranslated regions. A Patmatch search against the 3000 bp region upstream of the genes translational start (“TAIR10 Loci Upstream Sequence – 3000 bp (DNA)”), in retrospect, showed a different occurrence of FBS, EE, and CBS binding sites (“Cis-element” column in table 4.1 was amended according to new findings).

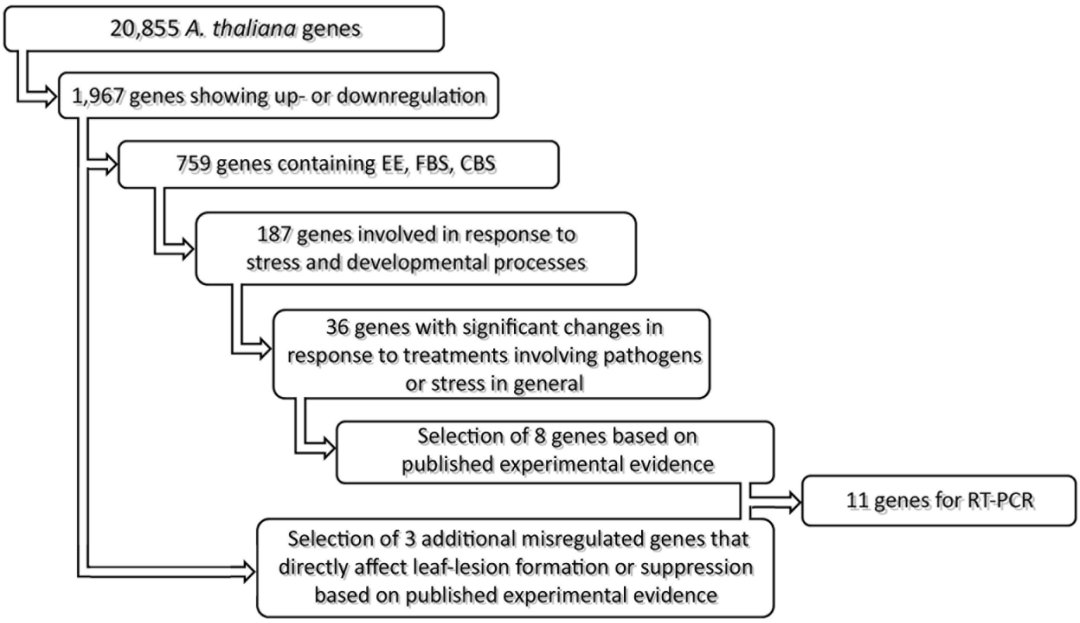

Figure 4.1: Workflow of *fhy3 far1* microarray analysis used to select the eventual 11 genes, which showed disrupted expression in *fhy3 far1* mutant plants, and which were identified as possible cause of the leaf-lesion phenotype.

Table 4.1: 11 candidate genes that are misregulated in the *fhy3 far1* mutant and the criteria according to which they were selected in the course of the *fhy3 far1* microarray analysis.

Gene	Regulation in *fhy3 far1*	Cis-elements in promoter	Function	Diurnal regulation	Inducing treatment	Description
UV RESISTANCE 2 (*UVR2*), At1g12370	2.5 times upregulated	EE	Stress response and response to abiotic and biotic stimulus	Diurnal regulation in SD	Not rep. in relevant treatment	Encodes a photolyases and loss-of-function mutants are UV-B sensitive and have a decreased ability to remove cyclobutane pyrimidine dimers (Kaiser *et al*., 2009)**.**
ACTIVATED DISEASE RESISTANCE 1 (*ADR1*), At1g33560	2.4 times upregulated		Stress response and response to abiotic and biotic stimulus	Diurnal regulation in SD	Pathogen-rel., Circ. rhythm-rel., DNA-repair-rel.	Encodes a NB-LRR disease resistance protein that is suggested to regulate signal transduction leading to SA accumulation. Over-expression leads to constitutively activated defence response (Bonardi *et al*., 2011).
Unnamed-disease resistance protein, At4g11340	2.3 times upregulated	EE CBS x 2	Stress response	Diurnal regulation in SD	Not rep. in Geneswinger database	Encodes a disease resistance protein of TIR-NB-LRR class (The Arabidopsis Information Resource. (n.d.) Locus: AT4G11340. [online] Available from: https://www.arabidopsis.org/servlets/TairObject?id=128491&type=locus [01.06.2014])
SENSITIVE TO UV 2 (*SUV2*), At5g45610	2.2 times upregulated	EE x 3 CBS x 2	Stress response	Diurnal regulation in SD	Not rep. in Geneswinger database	Encodes a protein homologous to ATR-interacting protein in mammals. Loss-of-function leads to UVB- and γ-irradiation hyper-sensitivity and defect in DNA damage response (Sakamoto *et al*., 2009).
AT COCKAYNE SYNDROME A PROTEIN-1 (*ATCSA-1*), At1g27840	2.2 times upregulated		Stress response and response to abiotic and biotic stimulus	Diurnal regulation in SD	Not rep. in relevant treatment	Encodes a protein that interacts with DNA DAMAGE-BINDING PROTEIN 1A and is necessary for UV-B tolerance, as well as for maintaining genome integrity. Loss-of-function and overexpression leads to UV-B hypersensitivity (Biedermann and Hellman, 2010)
CYSTEINE-RICH RECEPTOR-LIKE KINASE 13 (*CRK13*), At4g23210	2.1 times upregulated	EE CBS x 2	Stress response and response to abiotic and biotic stimulus	Diurnal regulation in SD	Pathogen-rel.	Encodes a protein that, when overexpressed, leads to PCD, increased SA accumulation and induction of defence response against pathogens (Acharya *et al*. 2007).
ETHYLENE RESPONSIVE ELEMENT BINDING FACTOR 6 (*ERF6*), At4g17490	6.7 times **down-**regulated	EE x 2 CBS FBS x 2	Stress response	Diurnal regulation in SD	Pathogen-rel., Stress-rel., Circ. rhythm-rel.	Encodes a TF that is involved in ROS and light stress response. Loss-of-function leads to increased sensitivity to photo-damage (Wang *et al.,* 2013).

METACASPASE 2 (*MC2*), At4g25110	3.6 times **down-**regulated	CBS x 5	Response to abiotic and biotic stimulus	Diurnal regulation in SD	Pathogen-rel.	Encodes a protein that antagonistically controls PCD (Coll *et al*., 2010).
RESPIRATORY BURST OXIDASE HOMOLOGUE D (*RbohD*), At5g47910	2.6 times **down-**regulated	CBS x 2	Stress response and response to abiotic and biotic stimulus	Diurnal regulation in SD	Pathogen-rel., Stress-rel., Circ. rhythm-rel., DNA-repair-rel.	Encodes a NADPH-oxidase that is involved in fine-tuning of ROS production and HR in and around pathogen infection sites (Torres *et al.,* 2005).
GAMMA-IRRADIATION AND MITOMYCIN C INDUCED 1 (*GMI1*), At5g24280	2 times **down-**regulated	EE CBS x 2	Stress response and response to abiotic and biotic stimulus	Diurnal regulation in SD	Stress-rel., DNA-repair-rel.	Encodes a protein of the SMC-hinge domain containing protein family that is involved in double strand break repair mechanisms. *GMI1* loss-of-function in *ataxia telangiectasia-mutated* (*atm*) background (*atm gmi1*) has been shown to lead to γ-irradiation sensitivity (Böhmdorfer *et al*., 2011).
ETHYLENE RESPONSIVE ELEMENT BINDING FACTOR 4 (*ERF4*), At3g15210	2 times **down-**regulated	CBS FBS x 2	Stress response and response to abiotic and biotic stimulus	Diurnal regulation in SD	Pathogen-rel., Stress-rel., Circ. rhythm-rel., DNA-repair-rel.	Encodes a TF that negatively regulates JA-mediated defence response gene expression and resistance to the necrotrophic *F. oxysporum (*McGrath *et al.,* 2005).

CBS AAAATCT
EE AAATATCT
FBS CACGCG
Cir. = Circadian
rel. = related pathways
rep. = Represented

4.2.2 Confirmatory RT-qPCRs for the transcript pattern of 11 candidate genes selected in *fhy3 far1* microarray analysis for disrupted FHY3 and FAR1 target genes

WT (No-0) and *fhy3 far1* (No-0) plants were investigated in order to confirm the *fhy3 far1* microarray expression pattern of the 11 candidate genes listed in Table 4.1. For that, plants were grown in the same growth conditions as used for the *fhy3 far1* microarray, yet samples (approximately 20 plants) were taken every 4 h across a 24 h period (7 samples). Extracted RNA was reverse transcribed to obtain cDNA for RT-qPCRs, which was done in two BRs for each gene and time point. Following RT-qPCR, the transcript patterns of the 11 genes in WT and *fhy3 far1* mutants were compared to those in the *fhy3 far1* microarray data.

CRK13 is a cysteine-rich receptor-like kinase acting in defence response. Overexpression of *CRK13* has been shown to cause leaf-lesion formation (Acharya *et al.*, 2007). Examination of the "Diurnal" web tool demonstrated that *CRK13* is expressed with a diurnal rhythm in WT plants in SD and peaks at ZT8 (32 h) and ZT16 (40 h), spanning dusk and the early part of the night (Figure 4.2 c). The expression of *CRK13* was strongly increased relative to WT at all three time points tested (ZT12 - ZT20) in the *fhy3 far1* microarray (Figure 4.2b). In the confirmatory RT-qPCR, expression of *CRK13* in WT plants approximately followed that observed via the "Diurnal" web tool, showing a rise towards ZT8 (32 h) and a night time peak at TZ12 (40 h) in SD. The transcript pattern of *CRK13* in *fhy3 far1* mutants showed higher levels than in WT essentially over the whole course of 24 h, specifically between ZT8 (32 h) and ZT16 (40 h) (Figure 4.2 a). Thus, the RT-qPCR transcript pattern closely resembled the transcript pattern revealed by the *fhy3 far1* microarray (Figure 4.2 e).

MC2 is a metacaspase acting in the HR pathway. *MC2* loss-of-function has been shown to cause deregulation of leaf-lesion formation (Coll *et al*., 2010). Examination of the "Diurnal" web tool demonstrated that the gene is expressed with a diurnal rhythm in WT plants in SD and peaks at ZT16, in the middle of the night (Figure 4.2 f). *MC2* expression was strongly reduced relative to WT at all three time points tested (ZT12 - 20) in the *fhy3 far1* microarray (Figure 4.2 e). In the confirmatory RT-qPCR, expression of *MC2* in WT plants approximately followed that observed via the "Diurnal" web tool, showing a slightly earlier night time peak at ZT12 (36 h) in SD. The transcript pattern of *MC2* in *fhy3 far1* mutants followed the WT pattern with a peak at ZT12 (36 h), whereas the *fhy3 far1* levels were almost constantly lower over the whole course of 24 h (Figure 4.2 d). Thus, the RT-qPCR transcript pattern also closely resembled the transcript pattern revealed by the *fhy3 far1* microarray (Figure 4.2 e).

ATCSA-1 is an ortholog of Cockayne Syndrome type-A protein found in mammals and acts in induction of repair of UV-B-caused DNA-damage. Overexpression of *ATCSA-1* has been shown to lead to UV-B hypersensitivity (not tolerance!) (Biedermann and Hellmann, 2010). Examination of the Diurnal web tool demonstrated that the gene is expressed with a diurnal rhythm in WT plants in SD (Figure 4.3 c). *ATCSA-1* expression *in fhy3 far1* mutants was increased relative to WT at all three time points tested (ZT12 - 20) in the *fhy3 far1* microarray (Figure 4.3 b). In the confirmatory RT-qPCR, expression of *ATCSA-1* in WT plants did not follow that observed via the "Diurnal" web tool. The gene showed a rather constant expression in SD that does not suggest diurnal regulation. The transcript pattern of *ATCSA-1* in *fhy3 far1* mutants was higher than in WT during the first part of the night time and peaked at ZT12 (36 h) (Figure 4.3 a). Thus, the RT-qPCR transcript pattern resembled the transcript pattern revealed by the *fhy3 far1* microarray (Figure 4.3 b). Due to the probable non-circadian regulation of *ATCSA-1* inferred from the gene's expression in WT, it was not further pursued.

UVR2 is a photolyase acting in DNA-repair. *UVR2* loss-of-function leads to UV-B sensitivity and reduced ability to remove cyclobutane pyrimidine dimers (Kaiser *et al*., 2009)**.** The web tool "Diurnal" demonstrated that the gene is expressed possibly with a diurnal rhythm in WT plants in SD with night time peaks at ZT16 and ZT24 (Figure 4.3 f). *UVR2* expression was increased relative to WT at all three time points tested (ZT12 - 20) in the *fhy3 far1* microarray (Figure 4.3 e). In the confirmatory RT-qPCR, expression of *UVR2* in WT plants approximately followed that observed via the "Diurnal" web tool, showing a trough in expression at ZT12 (36h) in SD. The transcript pattern of *UVR2* in *fhy3 far1* mutants essentially followed the WT pattern with slightly earlier peaks at ZT0 (24 h) and ZT16 (40 h), whereas the *fhy3 far1* levels were higher than in WT at the first part of the night (Figure 4.3 d). Thus, the RT-qPCR transcript pattern resembled the transcript pattern revealed by the *fhy3 far1* microarray (Figure 4.3 e). Due to the small difference of *UVR2* expression in *fhy3 far1* relative to WT and inconsistency between BRs (resulting in large error bars), which could point to less specificity of the utilised primers to *UVR2*, as well as the uncertainty of a real diurnal expression, it was not further pursued.

GMI1 is a structural maintenance of chromosomes (SMC)-hinge domain containing protein acting in DNA-repair. *GMI1* loss-of-function in *ataxia telangiectasia-mutated* (*atm*) background (*atm gmi1*) has been shown to lead to γ-irradiation sensitivity (Böhmdorfer *et al*., 2011). Examination of the "Diurnal" web tool demonstrated that *GMI1* is expressed with a diurnal rhythm in WT plants in SD, peaking at ZT8, at the end of the day time (Figure 4.3 i).

GMI1 expression was strongly reduced relative to WT at ZT12 and ZT16 (36 and 40 h) in the *fhy3 far1* microarray (Figure 4.2 h). In the confirmatory RT-qPCR, expression of *GMI1* in WT plants did not followed that observed via the Diurnal web tool in SD. Also, the RT-qPCR transcript pattern did not infer a diurnal regulation of the gene in WT. The transcript pattern of *GMI1* in WT was higher than in the *fhy3 far1* mutants at ZT12 (36 h), then dropped below the *fhy3 far1* level later in night (Figure 4.2 g). Thus, the RT-qPCR transcript pattern supports the *fhy3 far1* microarray data (Figure 4.2 h). Eventually, *GMI1* was not further pursued, due to a probable non-diurnal regulation and inconsistency between BRs (resulting in large error bars).

SUV2 is a homologue to ATR-interacting protein (ATRIP) involved in DNA-repair. Loss-of-function leads to UVB- and γ-irradiation hypersensitivity and defect in DNA damage response (Sakamoto *et al*., 2009). Examination of the "Diurnal" web tool demonstrated that the gene is expressed with a diurnal rhythm in WT plants in SD, peaking at ZT8, at the end of the day time (Figure 4.3 l). *SUV2* expression was strongly increased relative to WT at ZT16 and ZT20 (40 and 44 h) in the *fhy3 far1* microarray (Figure 4.3 k). In the confirmatory RT-qPCR, expression of *SUV2* in WT plants approximately followed that observed via the "Diurnal" web tool, showing a slightly later day time peak at ZT4 (28 h) in SD. The transcript level of the gene in *fhy3 far1* mutants peaked at ZT12 (36 h) and was higher than in WT during the early night (Figure 4.2 j). Thus, the RT-qPCR transcript pattern resembled the transcript pattern revealed by the *fhy3 far1* microarray (Figure 4.2 k). Eventually, the gene was not pursued due to its inconsistent expression in *fhy3 far1* mutants in relation to WT (expression is decreased during the daytime and later parts of the night and increased during the early part of the night in *fhy3 far1*). Also, *SUV2* misregulation has not been reported to directly cause lesion formation in *A. thaliana*.

ERF4 is a TF containing an APETALA2/ERF domain acting in defence response. *ERF4* loss-of-function leads to increased defence response gene expression and resistance to *F. oxysporum* (McGrath *et al.,* 2005). *ERF6* is also a TF containing an APETALA2/ERF domain and is involved in ROS and light stress response. *ERF6* loss-of-function leads to increased sensitivity to photo-damage (Wang *et al.,* 2013). *ERF4* and *ERF6* expression in WT showed a diurnal rhythm in the examination of the "Diurnal" web tool. In the confirmatory RT-qPCRs, expression of both genes in WT plants did not followed those observed via the "Diurnal" web tool, inferring no diurnal regulation. The RT-qPCR results of *ERF4* and *ERF6* in WT and *fhy3 far1* mutants also conflicted with the *fhy3 far1* microarray data. Both genes are part of a large gene family and the utilised primers were suspected to be not specific enough for *ERF4* and *ERF6*.

For the genes *ADR1*, Unnamed-disease resistance protein (At4g11340) and *RbohD*, the selected primers showed poor specificity.

According to the initial analysis, none of the candidate genes quite fit with the expected patterns based on the promoter elements. *SUV2* and *UVR2* contain EEs but were upregulated, contrary to the expectation of a downregulation, while *GMI1* contains CBSs but was downregulated, contrary to the expectation of an upregulation. *ATCSA-1, MC2* and *CRK13* have no promoter elements of interest. Thus, the eventual choice was not based on the presence of any elements of interest. The eventual reason to select *CRK13* and *MC2* out of the six candidate genes was that both genes showed the greatest and most consistent difference between WT and the double mutant. Both genes have also been shown to directly affected lesion formation (Acharya *et al*., 2007; Coll *et al*., 2010).

Based on the retrospective analysis for promoter elements, the candidate genes also partly did not quite fit with the expected transcript patterns. *SUV2* only contains an EE but was upregulated, contrary to the expectation of a downregulation, while *RbohD* and *MC2* contain CBSs but were downregulated, contrary to the expectation of an upregulation. *ADR1* and *ATCSA-1* have no promoter elements of interest. Unnamed-disease resistance protein, *SUV2*, and *CRK13* contain EEs and CBSs, and were upregulated. This may be explained by an increased binding of CCA1 and LHY to CBS rather than EE, but it must also be considered that *GMI2* also contains both promoter elements and was downregulated. Thus, unknown mechanisms must be involved in the regulation of at least one of these genes. *ERF6* and *ERF4* contain FBSs, EEs and a CBS, and FBSs and a CBS, respectively. The downregulation of both genes cannot be explained only according to the presence of promoter elements, and unknown mechanisms must be involved in their regulation.

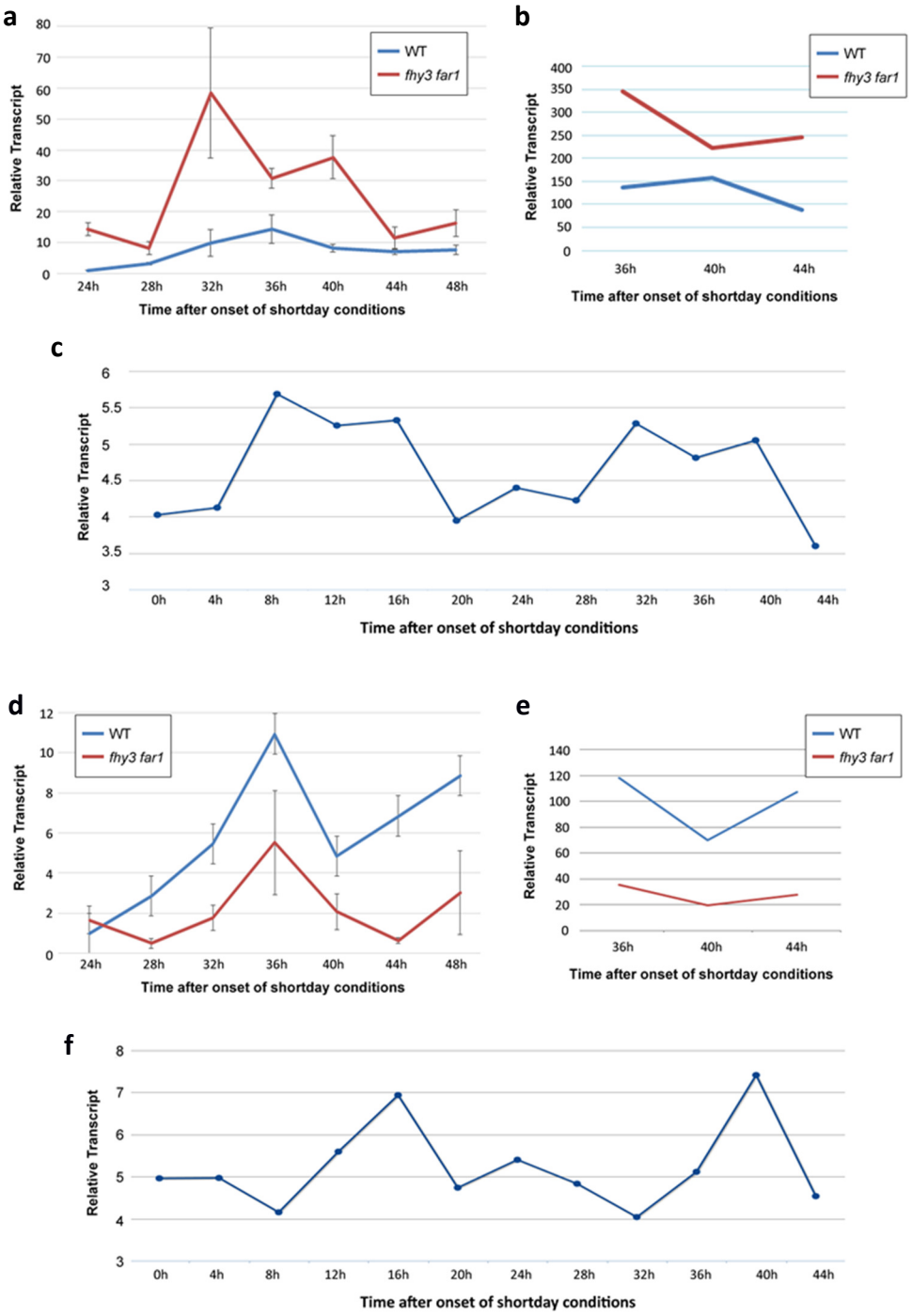

Figure 4.2: Comparison of transcript pattern in WT (No-0) and *fhy3 far1* mutants (No-0): a) RT-qPCR measurement of relative *CRK13* expression in SD in WT and *fhy3 far1* mutant plants (data represent the average of two BRs), b) microarray measurement of relative *CRK13* expression in SD in WT and *fhy3 far1* seedlings, c) data from the Diurnal web tool showing relative *CRK13* expression in SD-grown WT (Col-0) plants, d) RT-qPCR measurement of relative *MC2* expression in SD in WT and *fhy3 far1* mutant plants (data represent the average of two BRs), e) microarray measurement of relative *MC2* expression in SD in WT and *fhy3 far1* mutant plants, f) data from the Diurnal web tool showing relative *MC2* in SD-grown WT (Col-0) plants. RT-qPCRs were done in two BRs and error bars represent standard error.

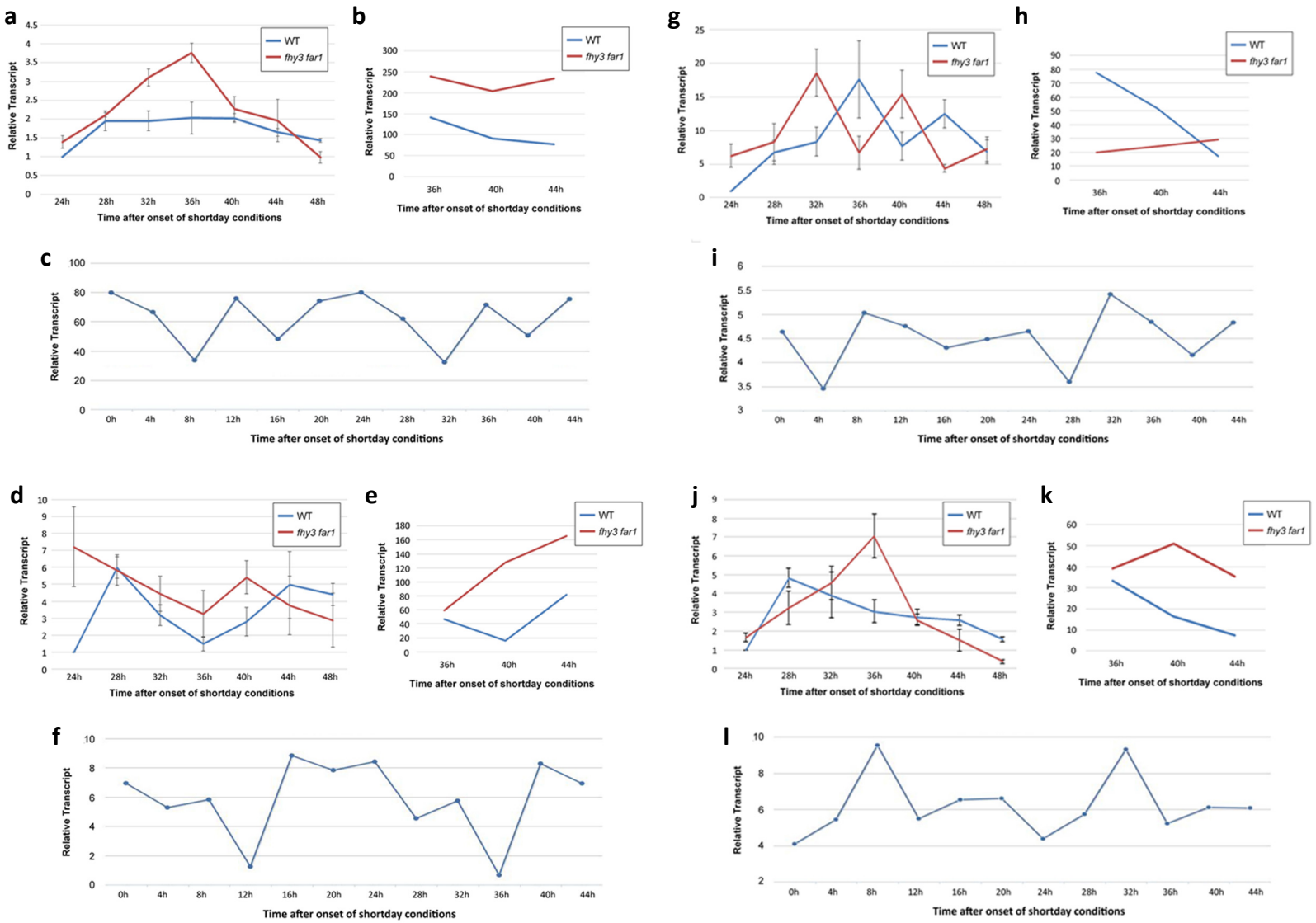

Figure 4.3: Comparison of transcript pattern in WT (No-0) and *fhy3 far1* mutants (No-0): a) RT-qPCR measurement of relative *ATCSA-1* expression in SD in WT and *fhy3 far1* mutant plants (data represent the average of two BRs), b) microarray measurement of relative *ATCSA-1* expression in SD in WT and *fhy3 far1* seedlings, c) data from the Diurnal web tool showing relative *ATCSA-1* expression in SD-grown WT (Col-0) plants, d) RT-qPCR measure-ment of relative *UVR2* expression in SD in WT and *fhy3 far1* mutant plants (data represent the average of two BRs), e) microarray measurement of relative *UVR2* expression in SD in WT and *fhy3 far1* mutant plants, f) data from the Diurnal web tool showing relative *UVR2* in SD-grown WT (Col-0) plants, g) RT-qPCR measurement of relative *GMI1* ex-pression in SD in WT and *fhy3 far1* mutant plants (data represent the average of two BRs), h) microarray measurement of relative *GMI1* expression in SD in WT and *fhy3 far1* seedlings, i) data from the Diurnal web tool showing relative *GMI1* expression in SD-grown WT (Col-0) plants, j) RT-qPCR measurement of relative *SUV2* expression in SD in WT and *fhy3 far1* mutant plants (data represent the average of two BRs), k) microarray measure-ment of relative *SUV2* expression in SD in WT and *fhy3 far1* mutant plants, l) data from the Diurnal web tool showing relative *SUV2* in SD-grown WT (Col-0) plants. RT-qPCRs were done in two BR and error bars represent standard error.

4.2.3 Overexpression and loss-of-function mutant lines

The RT-qPCR investigations confirmed the upregulation of *CRK13* and downregulation of *MC2* in the *fhy3 far1* mutant. Initially, none of the expression patterns of the eleven selected genes in the *fhy3 far1* mutant corresponded to those expected based on the promoter elements present. This suggests that none are likely to be misregulated due to direct effects of loss of the FHY3 and FAR1 TFs. It must, therefore, be presumed that FHY3 and FAR1 act indirectly on *CRK13* and *MC2*. Based on the retrospective analysis for promoter elements, *MC2* was found to contain CBSs. Genes with a CBS are expected to be upregulated in *fhy3 far1* mutants, but *MC2* was downregulated, which suggests regulation of *MC2* by additional mechanisms. *CRK13* contains EEs and CBSs and was upregulated. *CCA1/LHY* mediate opposite effects on gene expression when bound to these promoter elements, which makes it hard to speculate on the regulatory mechanisms. These findings, however, are still consistent with the presumption that *MC2* and *CRK13* are indirectly affected by FHY3 and FAR1. Nonetheless, *A. thaliana* lines with a misregulated *CRK13* and *MC2* have been shown to display deregulated PCD in a manner similar to that seen in *fhy3 far1*. This is consistent with these genes acting downstream of FHY3 and FAR1. Both genes are valid candidate genes for investigations to determine how early in the signal transduction pathway downstream of FHY3 and FAR1 they act, and if their misregulation in *fhy3 far1* mutants could be part of the primary cause for extended leaf-lesion formation in the double mutant. It is proposed that if these genes form early components of the signal transduction pathway downstream of FHY3 and FAR1 then the majority of the other aspects of the *fhy3 far1* mutant defence response phenotype might also be observed in *A. thaliana* lines with misregulated *CRK13* and *MC2*. This proposal prompted an investigation of *CRK13*-Ox and *MC2* loss-of-function mutant plants.

4.2.3.1 Identification of mutant lines

15 *MC2* T-DNA mutant lines were purchased from The Nottingham Arabidopsis Stock Centre (NASC) (http://arabidopsis.info/), consisting of 2 homozygous lines from The Salk Institute for Biological Studies, La Jolla, Canada (SALK) and 13 heterozygous T3 lines that contained a 12-line set from the German plant genomics research program-Kölner Arabidopsis T-DNA lines (GABI-KAT (GK)) and one heterozygous SALK line. The heterozygous lines were grown to obtain homozygous progeny in case the already-established homozygous lines would not grow

successfully. Lines from both institutions are based on T-DNA inserts that disrupt the ORF of *MC2*.

Two DEX-inducible *CRK13*-Ox lines, #26 and #33, were obtained from the Raina lab at Syracuse University, Department of Biology and were also generated by *A. tumefaciens* transformation (Acharya *et al.*, 2007).

4.2.3.2 Selection of homozygous mutant lines

In order to determine the zygosity of the purchased *mc2* mutant plant lines, they were genotyped by PCR with primers that specifically yield amplicons for the WT gene and the gene with T-DNA insert. For SALK lines, the WT sequence was PCR amplified using left primer (LP) and right primer (RP). Both primers were generated specifically for respective SALK line at the Salk Institute Genomic Analysis Laboratory homepage (SIGnAL Salk Institute Genomic Analysis Laboratory, 2005). For PCR amplification of the T-DNA insert, the insert-specific left border primer LBb1.3 and a primer for the respective genomic RP (same as for WT) were used. The expected amplicon for WT was estimated to be between 900 and 1100 bp (dependent on the respective line), and the insert amplicon to be of approximately 700 bp length. Homozygous mutant lines would only have one amplicon of approximately 700 bp, whereas heterozygous lines would have two amplicons, one of approximately 700 bp and one of 900 to 1100 bp (Figure 4.4).

The line SALK_009045C (NASC ID: N669682), donated by Joseph R. Ecker from The Salk Institute for Biological Studies, where the T-DNA was inserted into exon 2 of the *MC2* gene, showed a homozygous amplicon (Figure 4.4) and was chosen over the homozygous line SALK_050076C (Figure 4.4), as the seeds germinated to a higher degree. (No phenotypic differences between both lines were observed). The *mc*2 mutant phenotype did not differ from the WT phenotype, which was expected, since *mc2* enhances PCD rather than initiating it.

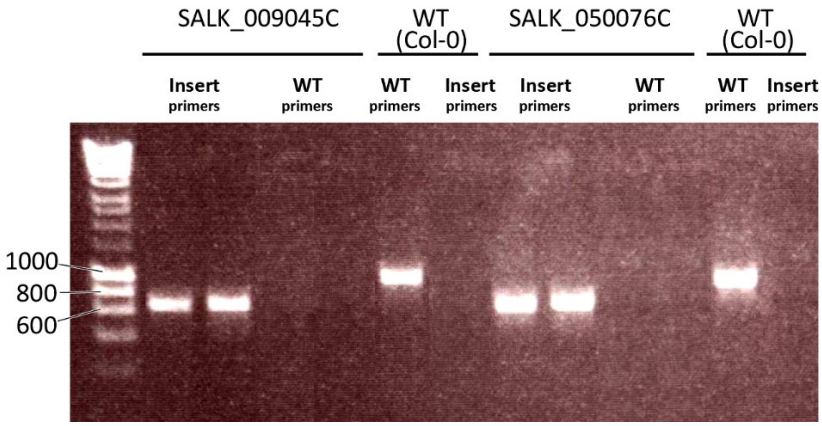

Figure 4.4: Genotyping of *MC2* loss-of-function lines SALK_009045C, and SALK_050076C. PCRs with WT-specific primers (labelled as WT primers) resulted in no amplification in these two plant lines, and PCRs with T-DNA insert-specific primers (labelled Insert primers) resulted in amplicons of approximately 700 bp. For WT (Col-0), as control, PCRs with WT-specific primers resulted in amplicons of approximately 1000 bp, and PCRs with T-DNA insert-specific primers resulted in no amplification.

Acharya *et al.* (2007) established DEX-inducible *CRK13*-Ox lines and reported increased *CRK13* transcription levels 4 hours post inoculation (hpi) that remained increased for at least 48 hpi. The group also reported a tissue collapse similar to HR within 24 hpi. DAB staining showed a brown precipitate in the collapsed tissue area (lesions), indicating increased presence of H_2O_2 as a possible cause.

For the investigations in the present thesis, the method of induction of *CRK13* overexpression by DEX was modified from syringe infiltration, as performed by Acharya *et al.* (2007), to spray inoculation instead. Leaf-lesion formation was found to be less extensive when spray-inoculated with a 1 µM DEX solution on a daily basis (Figure 4.5 a), compared to syringe infiltration with 1 µM (Figure 4.5 b). This method of DEX application was selected to reduce stress to the more fragile SD-grown *fhy3 far1* mutant plants used for comparison in the subsequent investigations and ensure their survival during the three days of inoculation with biotic stressors.

Cell death in *CRK13*-Ox did not occur in distinct lesions as was seen for *fhy3 far1* mutant plants, but rather seemed to apply to the whole leaf (Figure 4.5 a).

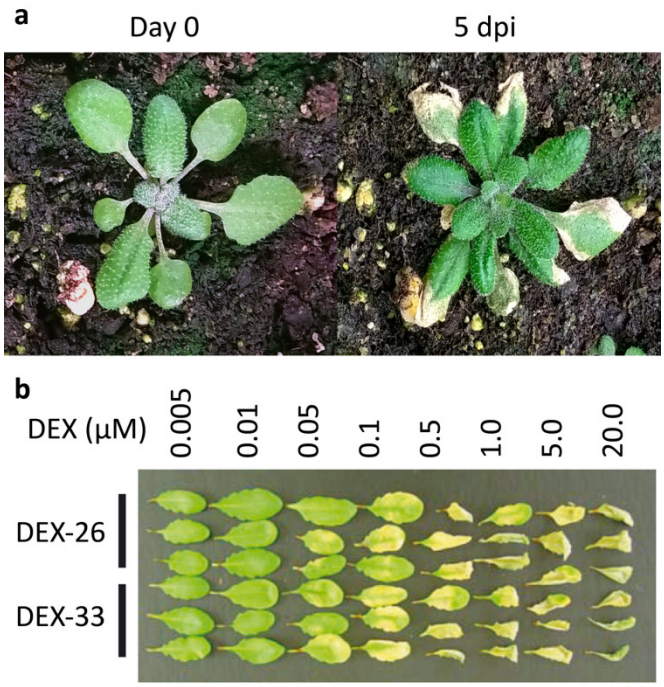

Figure 4.5: DEX-induced *CRK13* over-expression in *CRK13*-Ox (Col-0) mutant plants, a) 30 days old plants before induction (Day 0) and 5 dpi with daily spray inoculation with 1µM DEX, and b) leaves of 30 days old plants 1 day post syringe infiltration with different concentrations of DEX and the resulting HR/PCD. DEX-26 and DEX-33 are *CRK13* overexpression lines generated by Acharya *et al.* (2007).

At this point it is important to notice that all selected mutant lines had a Col-0 background, in contrast to the WT and *fhy3 far1* mutant plants that were used up to this point that had a No-0 background. Differences between both ecotypes have already been reported, especially in terms of defence responses (Korolev *et al.*, 2008; Zheng *et al.*, 2008), which made it necessary to use WT and *fhy3 far1* mutant plants with Col-0 background in the following investigations to establish a common ground and justify comparisons of WT (Col-0) and *fhy3 far1* (Col-0) mutants to *CRK13*-Ox (Col-0) and *mc2* (Col-0) mutants.

4.2.3.3 *fhy3 far1* mutants with Columbia ecotype

An *fhy3 far1* line with Col-0 ecotype was obtained from Ottoline Leyser's Group at The Sainsbury Laboratory, University of Cambridge, Bateman Street, CB2 1LR Cambridge, UK and was already used in the investigations for a published article by Stirnberg *et al.* (2012). The double mutant is a cross of two separate lines. The *FAR1* loss-of-function mutant originated from a SALK line that, similar as in the above stated *MC2* loss-of-function lines (4.2.3.2 Selection of homozygous mutant lines), contained a T-DNA insert in exon 5, disrupting the FAR1 ORF (SALK_031652). In order to confirm the *FAR1* loss-of-function, the PCR utilised for genotyping followed the same

principal as that used for genotyping the *mc2* mutants (4.2.3.2 Selection of homozygous mutant lines).

The *FHY3* loss-of-function in the obtained *fhy3 far1* (Col-0) mutants was produced via a disruption of the FHY3 ORF via a stop-codon by Stirnberg *et al.* (2012). Here, the TGG sequence at codon 428 was converted to the stop-codon TGA, in the course of a EMS procedure. In order to genotype this conversion, and therefore confirm the *FHY3* loss-of-function, the derived Cleaved Amplified Polymorphic Sequences (dCAPS) analysis was chosen (in reference to Stirnberg *et al.*, 2012). This method is based on the introduction of a restriction endonuclease recognition site to detect polymorphic nucleotides (Neff *et al.*, 1998). The PCR amplicon produced with the 40CAPS-specific primers was digested with the restriction endonucleases FokI and XmnI. FokI cuts the WT sequence, and XmnI the mutated sequence with the integrated stop-codon.

The *FAR1*-targeted PCR yielded amplicons with a size of between 800 and 1,000 bp (expected size was between 600 and 900 bp) when the *FAR1* insert specific primer combination was used, whereas the WT specific primer combination yielded no PCR amplicons. This inferred homozygous T-DNA insertions and a loss-of-function of *FAR1* (Figure 4.6 a).

PCR with the 40CAPS primer pair resulted in an amplicon of approximately 300 bp (317 bp was expected) that was purified, treated with the restriction endonuclease FokI and run on gel. No digestion was observed; as only one band was visible (sequences of 272 and 45 bp were expected in case WT sequence would have been present) (Figure 4.6 b). Digestion with the restriction endonuclease XmnI resulted in two bands on the gel, one between 200 and 300 bp and one below 100 pb (Figure 4.6 b). This confirmed the presence of the XmnI restriction endonuclease recognition site at codon 428 and, therefore, the presence of the stop-codon TGA. In conclusion, the received seed line with Col-0 ecotype was affirmed to contain *FHY3* and *FAR1* loss-of-function mutations.

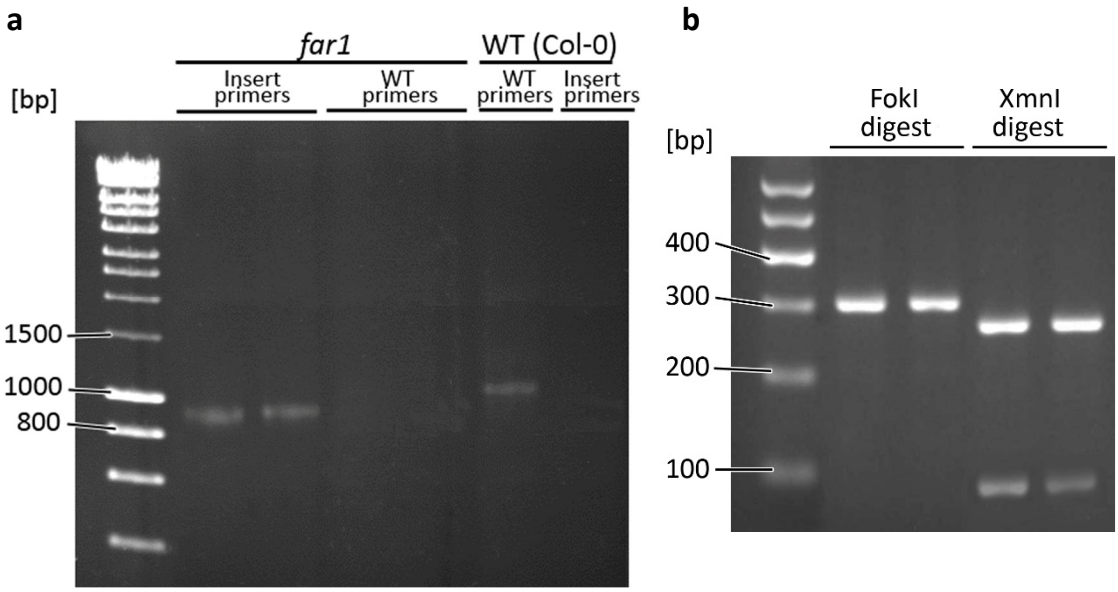

Figure 4.6: Genotyping of *FHY3 FAR1* loss-of-function lines. *FAR1*-targeted PCR amplicons with primers specific to *FAR1* insert (labelled Insert primers), resulting in a band between 800 to 1,000 bp, and primers specific for WT sequence (labelled WT primers), resulting in no amplification (a). Digest of *FHY3*-targeted amplicons produced with 40CAPS primers. Utilisation of restriction endonuclease FokI did not result in a digest, showing one amplicon of approximately 300 bp. Utilisation of restriction endonuclease XmnI resulted in a digest, showing one band between 200 and 300 bp and one band at approximately 100 bp (b).

4.2.4 Phenotype comparison of Nossen and Columbia ecotype plants

Phenotypic comparisons of SD-grown plants showed that *fhy3 far1* mutant plants with No-0 ecotype developed a more extensive leaf-lesion formation than those with Col-0 ecotype (Figure 4.7). The dwarf phenotype was also more pronounced in mutant plants with No-0 ecotype (Figure 4.6). In general, plants with No-0 ecotype seemed to be smaller than those with Col-0 ecotype. Given these phenotypic differences, results from the subsequent molecular investigations using WT and *fhy3 far1* mutant plants in Col-0 and No-0 should be compared to each other with reservation.

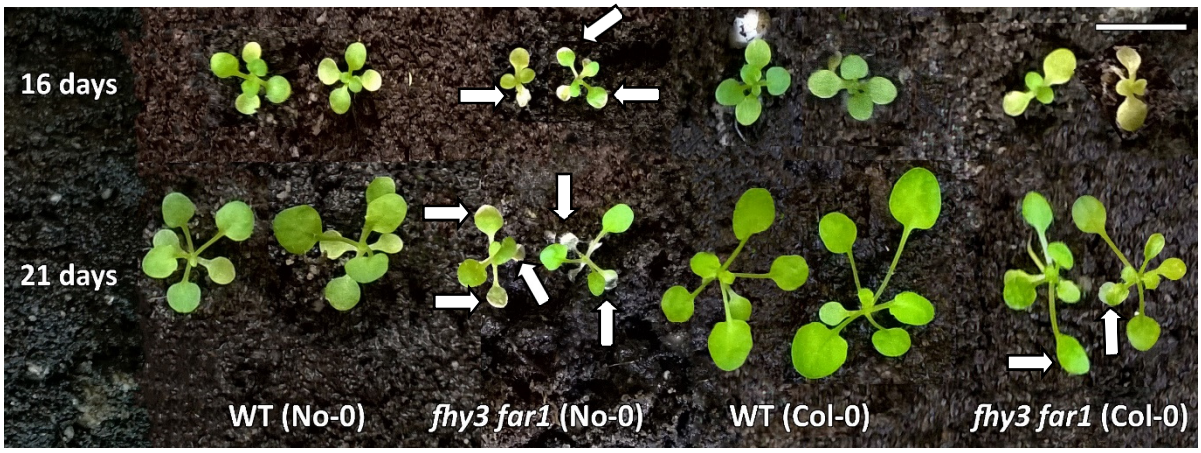

Figure 4.7: Comparison of Representative WT and *fhy3 far1* mutant plants with Col-0 and No-0 ecotype, after 16 days and 21 days of growth on soil in SD. Lesion formation is indicated by arrows, scale bar: 5 mm.

4.2.5 Defence response elicitation assay of plants with Columbia background

WT, as well as *fhy3 far1*, *CRK13*-Ox and *mc2* mutant plants with Col-0 ecotype were subjected to challenges with biotic stressors in the form of the fungal necrotroph *B. cinerea*, the bacterial hemibiotroph *Pst* DC3000, the PCD-eliciting mycotoxin FB1 and the MAMP chitin. Seeds were surface sterilised and grown on MS agar to minimise the number of microbes and, therefore, possible additional stressors that could affect defence response marker gene expression. Analysis of the subsequently activated defence responses could be used to potentially draw conclusions about the involvement of misregulation of *CRK13* and *MC2* in *fhy3 far1* mutant's leaf-lesion formation.

The plants responses were assayed by histochemical ROS staining with DAB and RT-qPCR, utilising the described defence response marker genes *PDF1.2a, PR3, PAD4, EDS1* and *SID2* (see chapter 3).

4.2.5.1 Phenotypic changes and histochemical staining upon biotic challenge

As expected, DEX-induced *CRK13*-Ox mutant plants displayed chlorosis even in response to mock treatment. This chlorosis seemed to be enhanced in the overexpressor beyond even that seen in *fhy3 far1* mutant plants. (Representative plant responses are shown in Figures 4.8 to 4.11). DAB staining also demonstrated increased H_2O_2 accumulation in both *CRK13*-Ox and *fhy3 far1* mutant plants compared to WT. Here, a darker staining was observed in *CRK13*-Ox compared to

fhy3 far1 mutants. No chlorosis phenotype was observed for the *mc2* mutant in response to mock treatment. DAB-staining of *mc2* mutants also appeared to be similar to WT. (Representative plant responses are shown in Figures 4.8 to 4.11).

Treatment with the necrotrophic pathogen *B. cinerea* (5 x 10^5 cfu) resulted in enhanced leaf chlorosis in all genotypes. (Representative plant responses are shown in Figures 4.7 to 4.10). DAB staining showed increased H_2O_2 accumulation in WT and *mc2* mutants. However, it resulted in no change of the already high levels of H_2O_2 in the *CRK13*-Ox or *fhy3 far1* mutants (no pictures present for *fhy3 far1*). (Representative plant responses are shown in Figures 4.8 to 4.11).

Treatment with the hemibiotrophic pathogen *Pst* DC3000 (10^6 cfu) resulted in leaf chlorosis that was strongest and most extensive in WT. (Typical plant responses are shown in Figures 4.7 to 4.10). DAB staining again displayed increased H_2O_2 levels in WT and *mc2* mutants. However, it resulted in no change of the already high levels of H_2O_2 in *fhy3 far1* and *CRK13*-Ox mutant plants. (Representative plant responses are shown in Figures 4.8 to 4.11).

FB1 treatment resulted in leaf chlorosis in all genotypes, but was strongest in *CRK13*-Ox mutants. (Representative plant responses are shown in Figures 4.8 to 4.11). These results point to a strong PCD-eliciting effect of FB1 on *CRK13*-Ox plants. This effect was less severe in the other genotypes.

Chitin treatment resulted in severe chlorosis in all genotypes with the most severe symptoms again in *CRK1*3-Ox mutant plants. (Representative plant responses are shown in Figures 4.8 to 4.11). The MAMP chitin seems to trigger PCD-activating mechanisms in all genotypes, affecting *CRK13*-Ox plant the most.

Overall, the physiological responses of the *CRK13*-Ox mutants to biotic challenges showed a degree of similarity with those of *fhy3 far1*, in that the *CRK13*-Ox plants showed a constitutive HR-like PCD phenotype. *mc2* mutants, on the other hand, showed high phenotypic similarity to WT. *MC2* loss-of-function was found to enhance PCD following induction of PCD-eliciting pathway but not to cause constitutive PCD. Consequently, no phenotype would be expected for mock treated *mc2* plants but an enhanced physiological response to biotic challenge might be expected, including possible enhanced PCD due to the missing inhibitory function of MC2 on

PCD-inducing MC1 (Coll *et al*., 2011; 1.2.5.3 Hypersensitive response). However, *mc2* mutant plants showed little difference compared to WT in any conditions. The overt physiological responses of the *mc2* plants, therefore, are inconsistent with *fhy3 far1* responses. A consistency was expected, which would have indicated that the misregulation of *MC2* in *fhy3 far1* mutants is part of the primary cause for leaf-lesion formation in the double mutant. However, it remains possible that aspects of the molecular response of *fhy3 far1* may still be apparent in the *mc2* mutant.

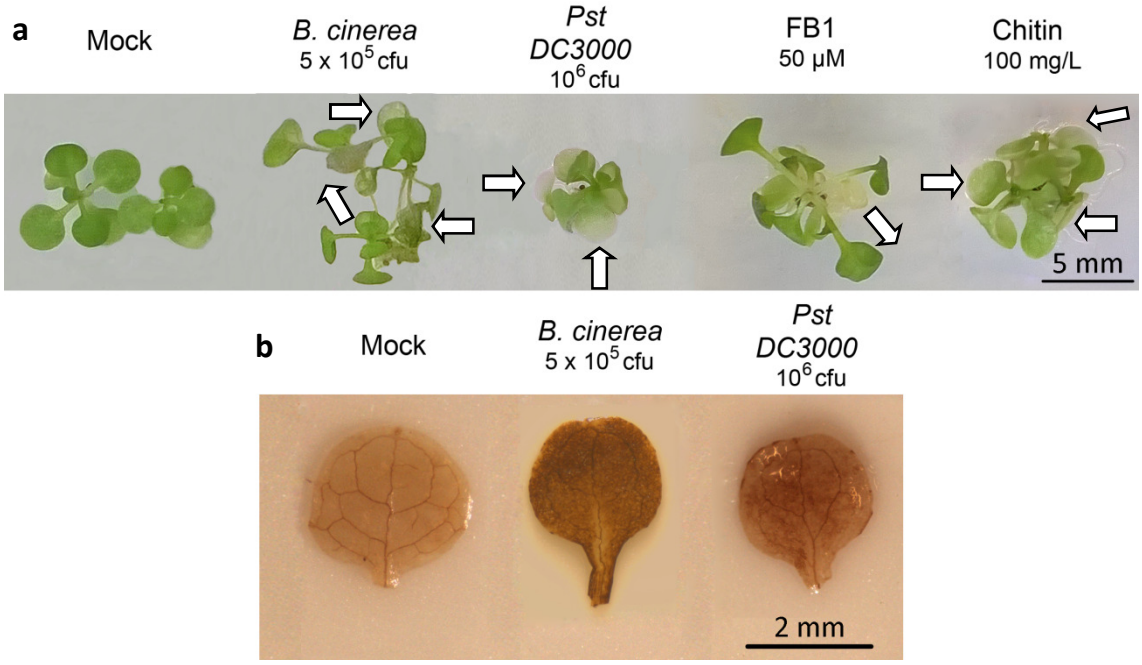

Figure 4.8: a) Representative responses of WT (Col-0) plants, grown for 22 days on MS agar in SD, photographed 3 days post-treatment with either mock, *B. cinerea* suspension (5 x 10^5 cfu), *Pst* DC3000 suspension (10^6 cfu), FB1 solution (50 µM), or chitin suspension (100 mg/L) (arrows indicate chlorosis), and b) DAB staining of WT (Col-0) plants, grown for 22 days in SD, 3 days post-treatment with either mock, *B. cinerea* suspension (5 x 10^5 cfu), or *Pst* DC3000 suspension (10^6 cfu).

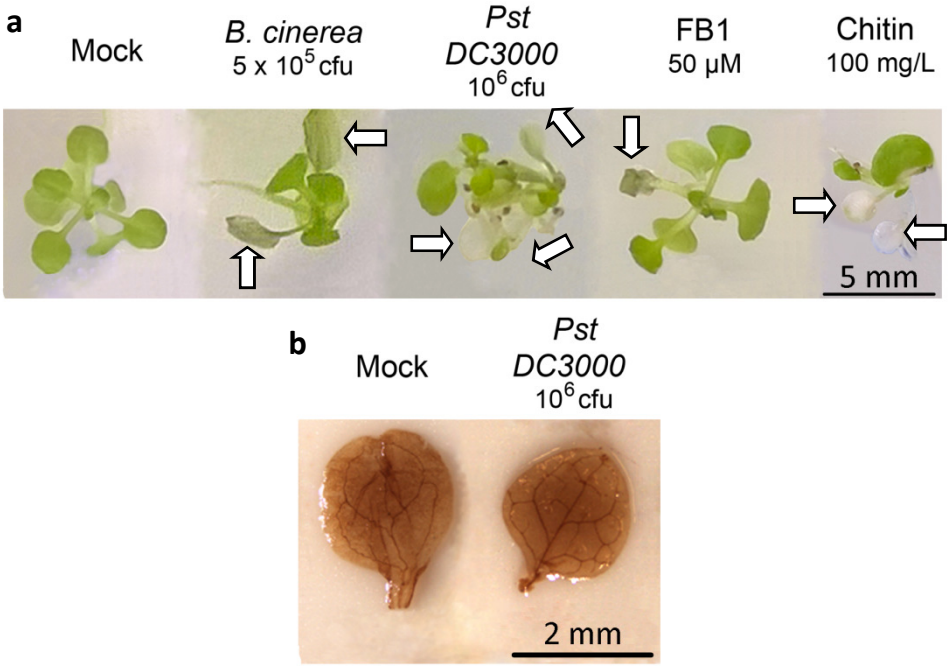

Figure 4.9: a) Representative responses of *fhy3 far1* (Col-0) mutant plants, grown for 22 days on MS agar in SD, photographed 3 days post-treatment with either mock, *B. cinerea* suspension (5 x 10^5 cfu), *Pst* DC3000 suspension (10^6 cfu), FB1 solution (50 µM), or chitin suspension (100 mg/L) (arrows indicate chlorosis), and b) DAB staining of *fhy3 far1* (Col-0) mutant plants, grown for 22 days in SD, 3 days post-treatment with either mock, *B. cinerea* suspension (5 x 10^5 cfu), or *Pst* DC3000 suspension (10^6 cfu).

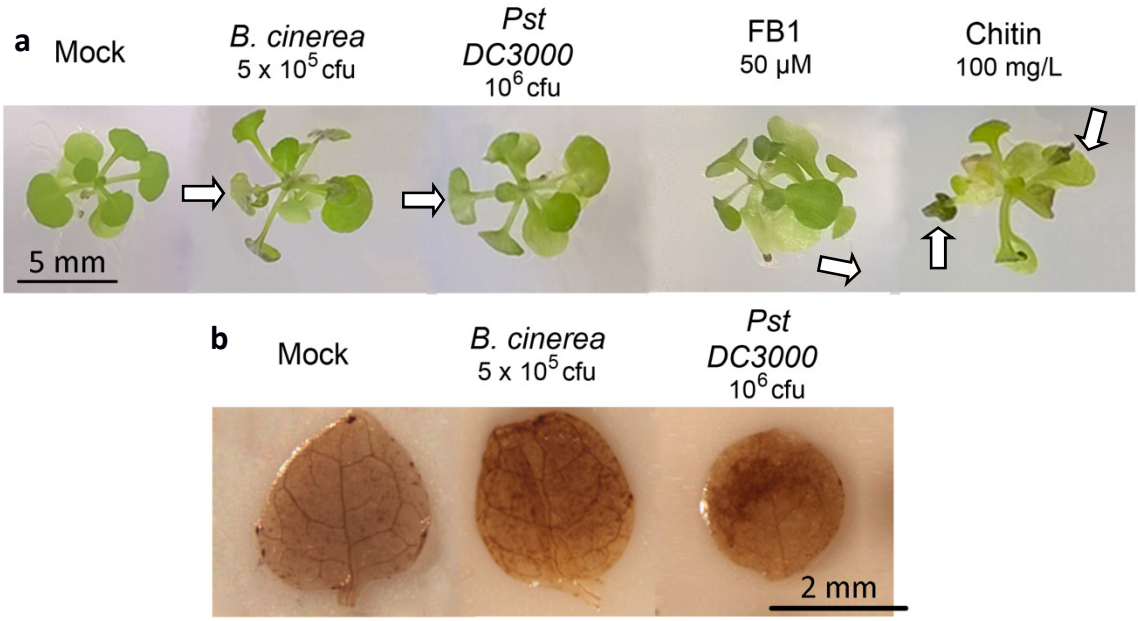

Figure 4.10: a) Representative responses of *mc2* (Col-0) mutant plants, grown for 22 days on MS agar in SD, photographed 3 days post-treatment with either mock, *B. cinerea* suspension (5 x 10^5 cfu), *Pst* DC3000 suspension (10^6 cfu), FB1 solution (50 µM), or chitin suspension (100 mg/L) (arrows indicate chlorosis), and b) DAB staining of *mc2* (Col-0) mutant plants, grown for 22 days in SD, 3 days post-treatment with either mock, *B. cinerea* suspension (5 x 10^5 cfu), or *Pst* DC3000 suspension (10^6 cfu).

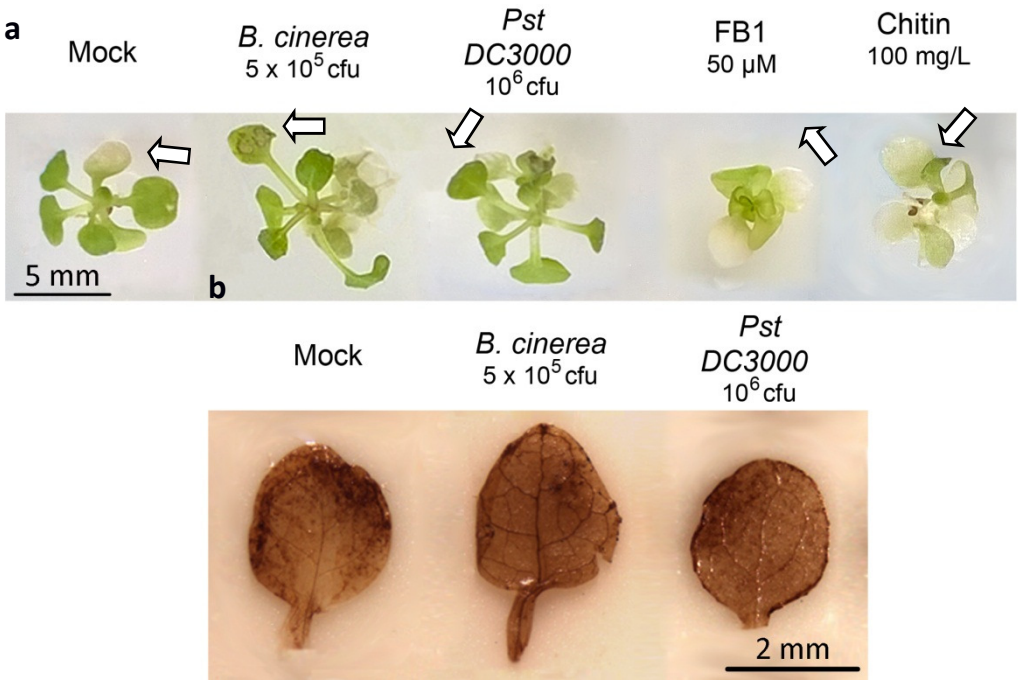

Figure 4.11: a) Representative responses of *CRK13*-Ox (Col-0) mutant plants, grown for 22 days on MS agar in SD, photographed 3 days post-treatment with either mock, *B. cinerea* suspension (5 x 10^5 cfu), *Pst* DC3000 suspension (10^6 cfu), FB1 solution (50 µM), or chitin suspension (100 mg/L) (arrows indicate chlorosis), and b) DAB staining of *CRK13*-Ox (Col-0) mutant plants, grown for 22 days in SD, 3 days post-treatment with either mock, *B. cinerea* suspension (5 x 10^5 cfu), or *Pst* DC3000 suspension (10^6 cfu).

4.2.5.2 Transcriptional changes upon biotic challenges

Identical to the investigation of transcriptional changes of WT and *fhy3 far1* mutant plants in No-0 background upon biotic challenges (3.2.4.5 Transcriptional changes upon biotic challenges), 22 days old SD-grown WT, as well as *fhy3 far1,* DEX-induced *CRK13*-Ox and *mc2* mutant plants were treated with *B. cinerea* (10^5 cfu), *Pst* DC3000 (10^6 and 10^8 cfu), FB1 (5 and 50 µM) and chitin (100 and 1,000 mg/L). Samples (approximately 20 plants per genotype and treatment) were collected 3 dpi at ZT4 and the transcriptional regulation of the selected defence response marker genes investigated by RT-qPCR in two BRs. WT and mutant plants had Col-0 ecotype.

Figures 4.12 and 4.13 depict the transcript levels of the marker genes *PDF1.2a*, *PR3*, *EDS1*, *PAD4* and *SID2* in WT, *fhy3 far1*, *mc2* and *CRK13*-Ox plants upon treatment with *B. cinerea*, *Pst* DC3000, FB1 and chitin. The respective marker gene transcript was normalised to its mock-treated WT marker gene transcript, and represent the averages of two BRs.

Defence response marker genes in general behaved as predicted in WT, based on the microarray analysis summary in chapter 3 (Figure 3.9). Some different results, however, were observed. In response to *Pst* DC3000 treatment, *PR3* was upregulated in WT in this assay but was not affected according to the investigated microarrays (Figures 3.9 and 4.13). Also, *PAD4* was expected to be induced in WT according to the investigated microarrays, but was not affected by *Pst* DC3000 treatment in the present investigation.

FB1 treatment was expected not to affect the marker genes in WT according to the investigated microarrays, but induced, in at least the 5 µM concentration, all of them in the present investigation.

Chitin treatment induced *PDF1.2a* and *EDS1* expression in WT in this assay, but both genes were downregulated upon chitin treatment according to the investigated microarrays. Also, *PAD4* expression was expected to be induced in WT according to the investigated microarrays, but was not affected in the present investigation.

These differences may highlight issues with the specificity of probes used on the investigated microarrays. In all cases in this assay, melt curves for the PCR products generated indicated the presence of a single PCR product, confirming the specificity of the primers used.

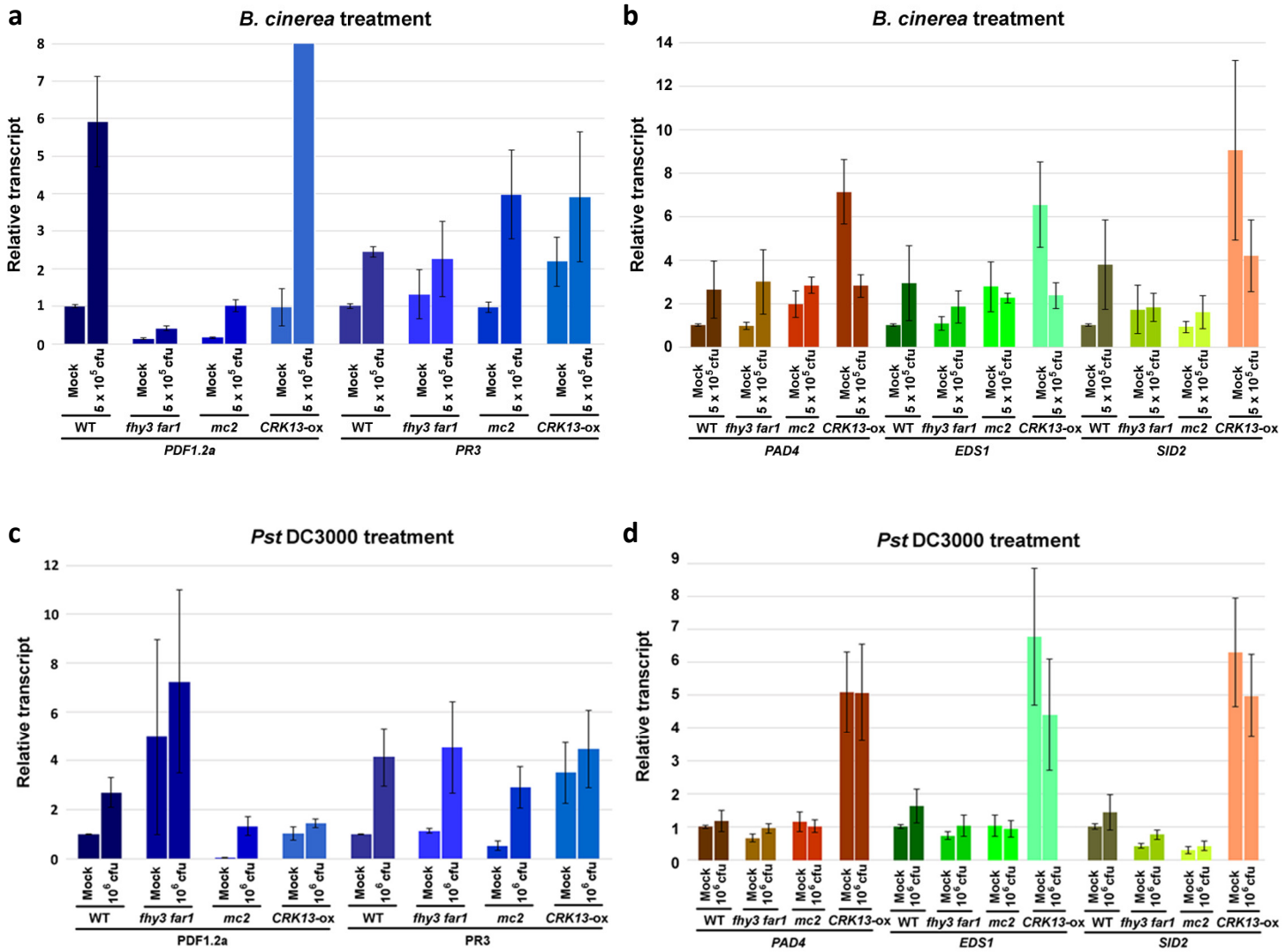

Figure 4.121: Transcriptional changes 3 dpi in 25 days old SD-grown WT, *fhy3 far1*, *mc2* and *CRK13*-Ox mutant plants, all with Col-0 ecotype, after treatment with a - b) 5 x 10^5 cfu *B. cinerea*-suspension, c - d) 10^6 cfu *Pst* DC3000-suspension, depicting transcript levels of the marker genes *PR3* and *PDF1.2a* (a and c), *PAD4*, *EDS1* and *SID2* (b and d). Approximately 20 plants for each genotype and treatment were sampled for RT-qPCRs. Investigations were done in two BRs and error bars represent standard error.

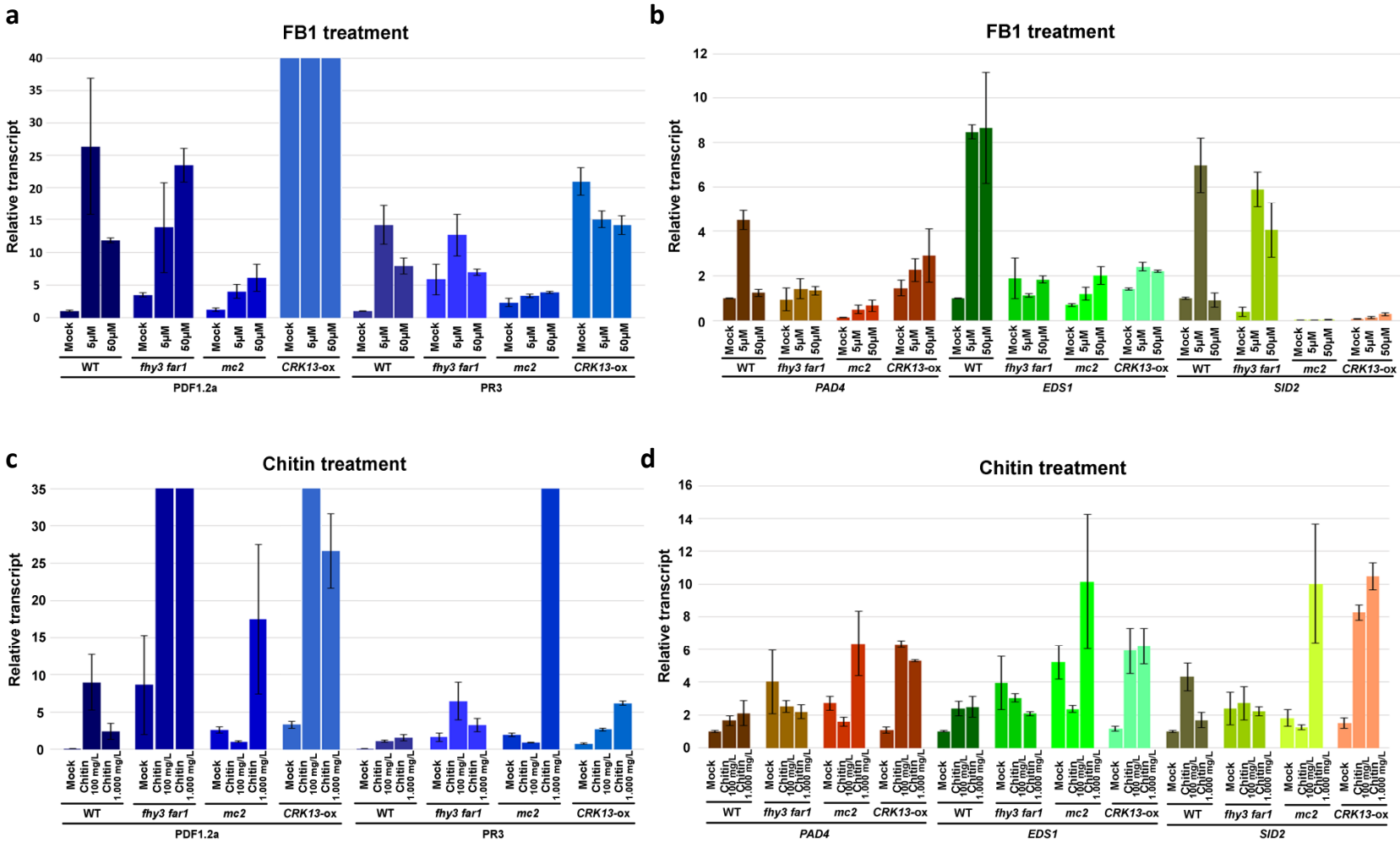

Figure 4.13: Transcriptional changes 3 dpi in 25 days old SD-grown WT, *fhy3 far1*, *mc2* and *CRK13*-Ox mutant plants, all with Col-0 ecotype, after treatment with a - b) 5 and 50 µM FB1-solution, c - d) 100 and 1,000 mg/L chitin-solution, depicting transcript levels of the marker genes *PR3* and *PDF1.2a* (a and c), *PAD4*, *EDS1*and *SID2* (b and d). Approximately 20 plants for each genotype and treatment were sampled for RT-qPCRs. Investigations were done in two BRs and error bars represent standard error.

Relative levels of defence marker gene expression (rather than the absolute levels of transcript as seen in Figures 4.12 and 4.13) for WT, *fhy3 far1*, *mc2* and *CRK1*3-Ox mutants upon biotic challenges compared to mock treatments are shown in the heatmap in Table 4.2. The heatmap is based on the individual biological replicate results and the stated concentrations of treatment are the major influences for the generation of the heatmap, i.e. FB1, 50 µM treatment for example was the basis for the heatmap, but the FB1, 5 µM treatment results were also considered for the depicted regulation. The aim of the heatmap was to present what the weight of evidence suggests and to get an idea what the effects of the biotic challenges on the defence response marker gene expression are. Data for differences in mock-treated mutant lines relative to mock-treated WT are based on the mean of the mock treatment data of all four biotic challenge assays. These mean data were used for comparison of basal levels of defence marker gene expression in the mutant lines. The transcripts of the JA/ET-responsive marker genes *PDF1.2a* and *PR3* in SD-grown *mc2* and DEX-induced *CRK13*-Ox mutant plants upon mock treatment were similar to those of *fhy3 far1* mutants, suggesting an activation of JA/ET-mediated defence signalling. The upregulation of *PDF1.2a*, which is also a marker for more-generic ROS accumulation, could point to a possible upregulation of ROS accumulation in all three genotypes. The SA-mediated defence response markers *PAD4*, *EDS1* and *SID2*, however, only seemed to be activated in *mc*2 and *fhy3 far1* mutant plants.

Responses to *B. cinerea* treatment pointed to an activation of SA- and JA/ET-mediated defence response in WT, *fhy3 far1* and *mc2* mutants. The strongest induction of JA/ET-mediated defence gene expression was displayed by *mc2* mutants that, in combination with the lower induction of the full set of SA-mediated genes, possibly points to a stronger resistance. SA-mediated PCD induction could be present to a lesser extent, thereby, creating less favourable conditions for the necrotrophic pathogen. WT and *fhy3 far1* showed an induction of both defence response signalling pathways. Conversely, *fhy3 far1* may be more susceptible by extension of the same argument that it already suffered from increased PCD (favourable conditions for *B. cinerea*). *CRK13*-Ox mutants also seemed to have an upregulated JA/ET-signalling, which, combined with a downregulation of SA-mediated defence marker expression, suggested higher resistance to *B. cinerea*. This, however, is in contrast with the mutant's actual increased occurrence of PCD. Crucially, though, in showing a reduction in SA-related gene expression in response to *B. cinerea*, *CRK13*-Ox mutants are quite distinct from *fhy3 far1* mutants, suggesting that *CRK13* overexpression may not be a primary cause of the *fhy3 far1* leaf-lesion formation phenotype.

Pst DC3000 treatment results suggested the induction of SA- and JA/ET-signalling, as well as possibly increased ROS accumulation, in WT and *fhy3 far1* mutants. In *mc2, Pst* DC3000 induced

strong JA/ET-related gene expression, but SA-signalling was only induced in part. *CRK13*-Ox mutants showed little response overall to *Pst* DC3000, possibly suggesting a degree of constitutive resistance. *CRK13*-Ox mutants reacted with a partial upregulation of JA/ET-signalling, but, if anything, showed a slight downregulation of SA-mediated defence response. Again, though, *CRK13*-Ox and *mc2* mutants are quite distinct from *fhy3 far1* mutants, suggesting that *MC2* loss-of-function or *CRK13* overexpression may not be a primary cause of the *fhy3 far1* leaf-lesion formation phenotype.

The FB1 treatment results suggested an induction of defence response-related JA/ET- and SA-signalling in WT. *fhy3 far1* mutants showed increased SA-mediated defence response and a partial activation of JA/ET-signalling. The response of *mc2* mutants also suggest the activation of both signalling pathways, but differed slightly in the pattern of marker gene expression from WT and *fhy3 far1* mutants. The response of *CRK13*-Ox mutants, on the other hand, suggested a downregulation of JA/ET- mediated defence response and induction of SA-mediated defence response. On the basis of high induction of SA-signalling marker genes, the results are perhaps consistent with the observed PCD in all four genotypes in response to FB1. The *CRK13*-Ox mutant results also suggested that the observed stronger induction of PCD in the *CRK13*-Ox mutant may be due to repression of JA/ET-signalling, which normally counteracts the PCD-induced activation of SA-signalling. Crucially, again the data show a clear difference between the *CRK13* overexpressor and the *fhy3 far1* mutant at molecular level.

The chitin treatment responses suggested an induction of JA/ET- and SA-mediated defence response in WT, *mc2* and *CRK13*-Ox mutants. In *fhy3 far1* mutants, JA/ET-signalling seemed to be induced and SA-signalling repressed. These results suggest an overall strong defence response in WT, *mc2 and CRK13*-Ox mutants, seen by the broad induction of all defence marker genes. In contrast, only JA/ET-mediated defence response was found in *fhy3 far1* mutants upon chitin challenge, again, making it quite distinct from the *mc2* and *CRK13*-Ox mutants at the molecular level.

Overall, it was expected that the responses of *mc2* and *CRK13*-ox mutants upon biotic challenges would have resembled the responses in *fhy3 far1* mutants more closely. This would have indicated that the misregulation of *MC2* and *CRK13* in *fhy3 far1* mutants would be part of the primary cause for leaf-lesion formation in the double mutant.

Table 4.2: Relative defence marker gene expression. Change in defence marker gene expression in WT, *fhy3 far1*, *mc2* and *CRK13*-Ox mutants relative to their mock treatment (rather than the absolute levels of transcript shown in Figures 4.11 and 4.12). Data is based on the majority results of the individual biological replicate results. WT, *fhy3 far1*, *mc2* and *CRK13*-Ox mutants were challenged with *Pst* DC3000 (10^6 cfu), *B. cinerea* (5 x 10^5 cfu), FB1 (50 µM) and chitin (1,000 mg/L). Data for differences in mock-treated mutant lines relative to mock-treated WT are based on the mean of the mock treatment data of all four biotic challenge assays. Again, data is based on the majority results of the individual biological replicate results. Marker gene transcripts in WT upon the respective biotic challenges from publicly available microarrays ("Pub mic WT") are also included. These are based on the "Marker Genes of Defence Response" investigation in chapter 3 (section 3.2.4.4) and are included as a comparison for the response of WT, *fhy3 far1*, *mc2* and *CRK13*-Ox mutant plants observed in this assay.

Gene	**Function (responsive-ness)**	***fhy3 far1* mock vs WT mock**	***mc2* mock vs WT mock**	***CRK13*-Ox mock vs WT mock**	**Pub mic, *Pst***	**WT *Pst* resp.**	***fhy3 far1*, *Pst* resp.**	***mc2*, *Pst* resp.**	***CRK13*-Ox, *Pst* resp.**	**Pub mic WT, *B. c.* resp.**	**WT, *B. c.* resp.**	***fhy3 far1*, *B. c.* resp.**	***mc2*, *B. c.* resp.**	***CRK13*-Ox, *B. c* resp.**	**Pub mic WT, FB1 resp.**	**WT, FB1 resp.**	***fhy3 far1*, FB1 resp.**	***mc2*, FB1 resp.**	***CRK13*-Ox, FB1 resp.**	**Pub mic WT, Chi resp.**	**WT, Chi resp.**	***fhy3 far1*, Chi resp.**	***mc2*, Chi resp.**	***CRK13*-Ox, Chi resp.**
PDF1.2a	Defensin (JA/ET)																							
PR3	Chitinase (JA/ET and SA)																							
PAD4	Lipase-like (SA)																							
EDS1	Lipase-like (SA)																							
SID2	ICS (SA)																							

Strong Upregulation (more than 3-fold)

Upregulation (2 to 3-fold)

Some upregulation (1.5 to 2-fold)

Downregulation (more than 2-fold)

Some Downregulation (1.5 to 2-fold)

No Change

B. c. = *B. cinerea* treatment
Chi = Chitin treatment
Pst = *Pst* DC3000 treatment
Pub mic WT = WT transcript levels from publicly available microarray
Resp. = Response (challenged versus mock treatment)
WT = Transcript levels from challenged WT

4.3 Discussion

This chapter aimed to identify components of the defence response pathways which are misregulated in the *fhy3 far1* mutant and which might form key players in the leaf-lesion formation phenotype observed in *fhy3 far1* mutant plants.

4.3.1 *fhy3 far1* microarray analysis for disrupted elements and selection of mutant plants

The *fhy3 far1* microarray displayed that 9.4 % of all distinctively assigned *A. thaliana* genes (1,965 out of 20,855 genes) were two-fold misregulated in the *fhy3 far1* mutant during the middle of the night in SD conditions, the time at which FHY3 and FAR1 are known to act. These misregulated genes would naturally contain both, direct targets of the two TF and genes that are indirectly affected by the *FHY3* and *FAR1* loss-of-function. Analysis for the presence of promoter elements which may allow regulation by FHY3 and FAR1 was, therefore, carried out. In addition, gene lists were scanned for association with pathways, which may result in leaf-lesion formation. A comparison of the number of two-fold misregulated genes in *fhy3 far1* identified in the present study with the additional microarray investigation of Ouyang *et al.* (2011) showed an interesting result. Ouyang *et al.* (2011) found 643 genes in total to be two-fold misregulated in *fhy3 far1* in darkness and 197 of them to contain an FBS. The *fhy3 far1* microarray in the present investigation of this thesis found 1,965 genes to be two-fold misregulated and 138 of them to contain an FBS (out of the combined 759 genes with FBS or EE or CBS). In the experimental setup used by Ouyang *et al.* (2011), samples were 4 days old *fhy3* (No-0) single mutant plants, that were harvested at an unspecified time point, compared to the 9 days old *fhy3 far1* double mutant plants, sampled during the night, for the *fhy3 far1* microarray in the analysis of this thesis. These differences could explain the discrepancy in numbers of misregulated genes. The influence of developmental stages, growth conditions and sampling time point on the differential gene expression can also be seen in Ma *et al.* (2016)'s microarray experiment. Here, *fhy3 far1* (No-0) mutant plants were grown for 3 weeks in SD and sampled at ZT4 (during the middle of the light phase). Only 399 genes were two-fold misregulated, pointing to the direct regulation and indirect influence of far fewer genes by FHY3 and FAR1 during the day compared to the night in SD.

Taken together, the number of genes that are affected by a loss-of-function of *FHY3* and *FAR1* was not surprising, given the broad spectrum of regulations *FHY3* and *FAR1* are involved in,

namely circadian clock entrainment, flowering, chloroplast division and chlorophyll biosynthesis, ROS homeostasis and PCD, shoot branching and plant architecture, ABA-signalling and defence response against pathogens. Therefore, it was also not surprising that 187 two-fold misregulated genes that contain an FBS, CBS or EE were associated with stress response and developmental processes.

In the search for impaired pathways in *fhy3 far1* mutant plants, 11 differentially expressed candidate genes were eventually selected. The two NBS-LRR class genes, unnamed protein (At4g11340) and *ARD1*, were upregulated. *RbohD,* which acts early in pathogen recognition and ROS production, was also upregulated. Two ET-responsive genes were downregulated; *ERF4*, encoding a negative regulator of JA-mediated defence genes against fungal necrotrophs, and *ERF6*, a repressor of cell proliferation and expansion. Three UV-light protection and DNA damage repair-associated genes, *SUV2, UVR2* and *ATCSA-1*, were upregulated. Also, *GMI1*, a gene associated with somatic homologous recombination, was downregulated. Finally, the gene *MC2*, involved in suppression of PCD, was downregulated and the gene *CRK13,* involved in upregulation of PCD, was upregulated.
Although the majority of these 11 genes possessed relevant promoter elements, some were selected on the basis that not all FHY3 targets were shown to possess such elements (and to be indirect targets). Ouyang *et al.* (2011) performed a chromatin immunoprecipitation-based sequencing (ChIP-seq) and estimated 1,783 genes in the *A. thaliana* genome to be potential direct targets of FHY3 alone, whereby 1,559 genes are bound by FHY3 in darkness (light receptor-independent) and 1,009 genes in constant FR conditions. Approximately half of the total number of these genes was estimated to contain an FBS.

After confirmation of the transcript patterns by RT-qPCR over 24 h, *CRK13* and *MC2* were selected for further study as potential key components acting downstream of FHY3 and FAR1 in the regulation of lesion formation (Figure 4.14). RT-qPCR results of both genes display highest accordance to the *fhy3 far1* microarray data, and showed most significant difference in *fhy3 far1* mutants compared to WT.
The *CRK13* transcript pattern showed an upregulation during the day and majority of the night in *fhy3 far1* mutants. The gene's function in enhancing PCD/HR and its high expression levels in *fhy3 far1* conforms to the double mutant phenotype. The WT transcript pattern acquired from "Diurnal" also showed a repeating 24h cycle of transcript level in SD, suggesting a regulation by diurnal rhythm. According to the RT-qPCR data, between ZT4 and ZT12 the transcript level of

CRK13 rises in both WT and *fhy3 far1* mutant plants, consistent with the presence of CCA1/LHY. *CRK13* transcript levels remain high up to ZT16, after which *CRK13* transcript levels decrease. NASCArrays Gene Swinger, which shows the experimental treatments associated with the greatest expression changes in a gene of interest, found that *CRK13* showed the greatest expression changes associated with pathogen response experiments, fitting the gene in the initial aim and objectives of this chapter.

MC2 transcript levels are reduced in *fhy3 far1* mutant plants (*fhy3 far1* microarray) and these levels were confirmed by RT-qPCR to be downregulated during the course of the day (except during the first morning hours). The gene's function in *LSD1*-dependent prevention of PCD and its low expression level in *fhy3 far1* conform to the double mutant's phenotype. The "Diurnal" and RT-qPCR WT transcript pattern additionally suggest a circadian regulation, showing peak expression during the early part of the night, when *FHY3* (and *FAR1)* are stabilised by light stable phyB, phyD and phyE and unfold their activational activity (Siddiqui *et al.*, 2016). Due to loss-of-function of both TFs, *MC2* transcript levels decrease, mostly at evening and night. NASCArrays Gene Swinger found that the *MC2* showed the greatest expression changes in experiments associated with response to pathogens, also fitting *MC2* in the initial aim and objectives of this chapter. Interestingly, *MC2* was found to be directly bound by FHY3, even though it does not possess an FBS. However, this binding occurred in an exon (Ouyang *et al.*, 2011).

4.3.1.1 *CYSTEINE-RICH RECEPTOR-LIKE PROTEIN KINASE 13*

CRK13 encodes a 673 AA CRK, which belongs to a sub-family of RLKs that consists of 44 transmembrane proteins. Pivotal for their name is the abundance of cysteine. CRK13 is predicted to occur mainly in the extracellular region of the plasma membrane, in particular at plasmodesma, and is involved in defence response to bacterium, response to chitin and molecules of bacterial origin, defence response-associated respiratory burst and HR in plants, according to GO. The protein is expressed in cauline leaves, central cells (embryo sac), rosette leaves, cotyledons, guard cells, hypocotyl, petals, sepals, stamen, stem and vascular leaves (The Arabidopsis Information Resource. (n.d.) Locus: AT4G23210. [online] Available from: https://www.arabidopsis.org/servlets/TairObject?id=127532&type=locus [01.06.2014]; Acharya *et al.*, 2007).

CRK13 contains a Cystein (C)-X8-C-X2-C motif that belongs to the extracellular part of the protein, as well as a transmembrane domain and an intracellular kinase domain. The conserved cysteines function in maintaining of the protein's tertiary structure, but likewise

could form a zinc finger motif to mediate protein-protein interactions, or form disulphide bridges to sense and regulate redox changes in the apoplast (Acharya *et al.*, 2007; Zhanga *et al.*, 2013; Ederli *et al.*, 2014).

Ohtake *et al.* (2000) showed an upregulation of RLKs with C-X8-C-X2-C motif in response to exogenous SA and predicted their involvement in SA-mediated defence responses in *A. thaliana*. CRK13, as a receptor-like kinase, could be involved in transmitting information from signal perception to effector gene. Acharya *et al.* (2007) showed *CRK13*'s induction upon challenge with virulent *Pst* DC3000 and avirulent *Pst* DC3000 (avrRpm1) in WT (Col-0) plants, which was confirmed by the online tool eFP browser (based on AtGenExpress Consortium data (Winter *et al.*, 2007)). The necrotroph *B. cinerea* on the other hand did not induce *CRK13* expression.

CRK13-Ox mutants (DEX-induced) developed extensive HR-like lesions and showed an approximately 20-fold reduced growth of *Pst* DC3000 and 10-fold reduced growth of *Pst* DC3000 (avrRpm1). Upon infection, SA levels were found to be induced 100-fold compared to WT and uninfected lines. Combined with the observation of increased *SID2* expression and no induction of *PAL1/2/3*, it was concluded that the higher SA levels were biosynthesised by means of chorismate (and not phenylalanine). *CRK13*-Ox in a *sid2* background or in combination with the transgene *NahG* (encoding a *Pseudomonas sp*. salicylate hydroxylase), which both lead to reduced SA levels, showed a reduced occurrence of HR-like leaf-lesions (Acharya 2007). This suggests a *SID2*-dependent activity of CRK13.

Transcriptome comparison (by custom microarray with 199 *A. thaliana* genes) of DEX-induced *CRK13*-Ox mutant and *Pst* DC3000 (avrRpm1)-challenged WT (Col-0) plants revealed that 60 % of the induced genes in *CRK13*-Ox mutants were also induced in challenged WT plants. This suggested that the induction of *CRK13*-Ox mimics the plant's response to pathogens and suggested the characterisation of *CRK13* as an early induced gene for bacterial pathogen challenges (Acharya *et al.*, 2007).

Loss-of-function investigations by Wrzaczek *et al.* (2010) showed a two-fold upregulation of *CRK13* expression in the JA biosynthesis-impaired *FATTY ACID DESATURASE 3*/*7*/*8* loss-of-function triple mutant (*fad3*/*7*/*8*). This suggested a negative regulation of *CRK13* by JA. Acharya *et al.* (2007) did neither find a differential regulation of *CRK13* expression in response to avirulent *Pst* DC3000 (avrRpm1) in *npr1*, *sid2*, *eds1, eds5, ndr1, pad4*, or lesion mimic mutant *lsd1*, nor in response to exogenous SA in WT. This prompted the group to suggest that CRK13 is situated downstream of these defence response-associated genes and upstream of SA biosynthesis (Figure 4.14. b).

CRK13 could be part of early signal transduction in response to biotrophic bacteria recognition, given that it is a membrane-bound protein, and induces SA-signalling. Its expression does not seem to be part of a positive feedback by SA, since Acharya *et al.* (2007) did not find an induction by exogenous SA, but could be negatively regulated by JA (Wrzaczek *et al.*, 2010) in order to mitigate excessive SA-signalling and induction of PCD.

4.3.1.2 *METACASPASE 2*

MC2 encodes a cysteinyl-aspartate specific protease of 418 AA, related to caspases that are found in plants, fungi and protozoa. *A. thaliana* expresses three known type I metacaspases, namely *MC1*, *MC2* and *MC3*, and six type II metacaspases, namely *MC4-MC9*. On a structural level, type I MCs differ from type II MCs by an extension with a proline-rich prodomain at the N-terminal domain, but lack the type II MC's long linker region between the putative catalytic subunits p10 and p20 (Coll *et al.*, 2010).

According to "The plant membrane protein databases aramemnon" (Schwacke *et al.*, 2003), MC2 is predicted to be mainly found in chloroplasts. Other investigations, however, showed that MC proteins in general lack organelle-targeting sequences, localising them most probably in the cytoplasm. They display different pH optima, which suggest that changes of pH in the cytosol are required for their functionality. These pH changes could be caused by ion exchanges as a result of pathogen recognition (Cox, 2011; Kwon and Hwang, 2013).

MC2 is predicted to be expressed in cauline leaves, rosette leaves, cotyledons, guard cells, root, stamen, stem and vascular leaves, and to be involved in defence response, negative regulation of PCD and proteolysis, according to GO (The Arabidopsis Information Resource. (n.d.) Locus: AT4G25110. [online] Available from: https://www.arabidopsis.org/servlets/TairObject?id=126927&type=locus [01.06.2014]).

Metacaspases hold a conserved histidine-cysteine catalytic dyad as the active site and a caspase hemoglobinase fold, cleaving peptide bonds C-terminal of arginine or lysine (via cystein), as well as a *LSD1*-like zinc-finger domain, potentially used for oligomerisation in order to activate MC2's activity (Coll *et al.*, 2011; Kwon and Hwang 2013). The presence of a LSD1-like zinc-finger domain gives some indication of MC2's mechanism of action. Cytoplasm-localised LSD1 sequesters positive regulators of cell death, such as LOL1 and MC1, and represses apoplastic ROS-induced stress responses. Loss-of-function of *LSD1* leads to a dwarf phenotype and a specific HR in leaves, termed runaway cell death (RCD), as it is defined by sharp borders that separate living and dead

tissue. In contrast, *mc2* mutant plants (as well as *mc1*) do not differ phenotypically from WT. A double mutation of *lsd1* and *mc2* results in an enhanced HR and a dwarf phenotype that is more severe than the *lsd1* single mutant phenotype. By introducing an *MC1* loss-of-function, the *lsd1* phenotype was rescued. This points to an epistatic connection and an upstream localisation of both metacaspases in relation to *LSD1*. Interdependency was confirmed by overexpression constructs in the *lsd1* background. Here, *MC2* overexpression mimics the WT phenotype. The molecular function of *MC2* was concluded to be repression or counteraction of *MC1*'s PCD-inducing activity, which, in turn, is activated by apoplastic ROS and the NB-LRR pathway, and depends on *LSD1* (Coll *et al.*, 2010; Coll *et al.*, 2011; Kwon and Hwang, 2013). The investigation by Coll *et al.* (2010) of PCD/RCD (by electrolyte leakage assay to determine membrane deterioration) showed accelerated PCD/RCD in *lsd1* mutants, but not in WT, *mc1*, *mc2*, or *mc1 mc2* plants, upon treatment with the SA analogue Benzo-(1,2,3)-thiadiazole-7-carbothioic acid S-methyl ester (BTH). Additionally, BTH supressed electrolyte leakage in *lsd1 mc1* and rescued the double mutant's dwarf phenotype on one hand, and, on the other hand increased electrolyte leakage in *lsd1 mc2* and enhanced dwarfing in *lsd1 atmc2* mutants. This confirmed the proposed regulatory functions of *MC1* and *MC2*.

MC1 and MC2 showed an interesting expression pattern in response to *Pst* DC3000 (avrRpm1) and the biotrophic oomycete *Hyaloperonospora arabidopsidis.* Both pathogens elicit defence response via TIR-NB-LRR and CC-NB-LRR receptors, subsequently inducing PCD/RCD. Cells in the infected leaf area, designated to undergo PCD, were shown to have upregulated *MC1* expression. That was opposed by the surrounding uninfected area, where cells showed an upregulation of *MC2* expression. Infection with the necrotrophic pathogen *A. brassicicola* did not result in a change of *MC1* or *MC2* expression; nor did flg22. On the basis of these results, it was hypothesised that the CC-NB-LRR- and TIR-NB-LRR-mediated pathways converge via SA accumulation into one PCD/PCD output that is mediated by regulatory interaction of LSD1, MC1 and MC2 (Coll *et al.*, 2010; Coll *et al.*, 2011; Kwon and Hwang 2013) (Figure 4.14 c).

In general, plant pathogen resistance could be understood as a system of stimuli integration and respective modulation of responses by the plant. MAMP recognition would be the first factor to influence the defence output. Distinction between fungi, bacteria and oomycete, in terms of microorganisms, takes place by multiple receptors that also show overlaps like CERK1, which binds multiple ligands, including chitin and PGN (Newman *et al.,* 2013). Nonetheless, signals are mainly integrated into JA-, ET- and SA-signalling pathways, modulating them according to the entirety of perceived MAMPs. Here, a complex feedback system allows for a robust and precise

signal transduction (Tsuda *et al.*, 2013). Subsequently, the signalling molecules induce or repress specific defence response genes, thereby adjusting plant defence to the nature of the pathogen (bacterium, fungus, oomycete). This most probably also takes place in a feedback system, underpinned by the presence of multiple TF binding sites in genes. *CRK13* for instance contains a W-box and a MYB1 binding site, both suggested to convey SA-dependent activation[74.1] (Ederli *et al.*, 2011), as well as a proposed ROS promoter element (RBOH-dependent), where SA is supposed to act as negative regulator and JA/ET as positive regulators (Wrzaczek *et al.*, 2010). This point represents the first step in the zig zag model, namely PTI (Jones and Dangl, 2006).

The arms race between plant and pathogen starts with the deployment of microbial effectors to modulate the host plant's defence response, leading to ETS. The consequent signals in the host plant are integrated, again mainly via the three signalling pathways (SA-, JA- and ET-dependent), into the subsequent modulation of the defence response, conceivably thereby adjusting it further to specific types of microorganisms (commensal, biotrophic, necrotrophic), leading to ETI.

CRK13 and *MC2* represent two genes that are probably part of the defence response regulatory mechanisms up- and downstream of SA/JA/ET.

[4.7] W-box is known to be recognized by WRKY TFs that are established to play roles in plant defence response-regulation, and MYB1-binding site could potentially be involved in a SA-dependent induction (Ederli *et al*., 2011).

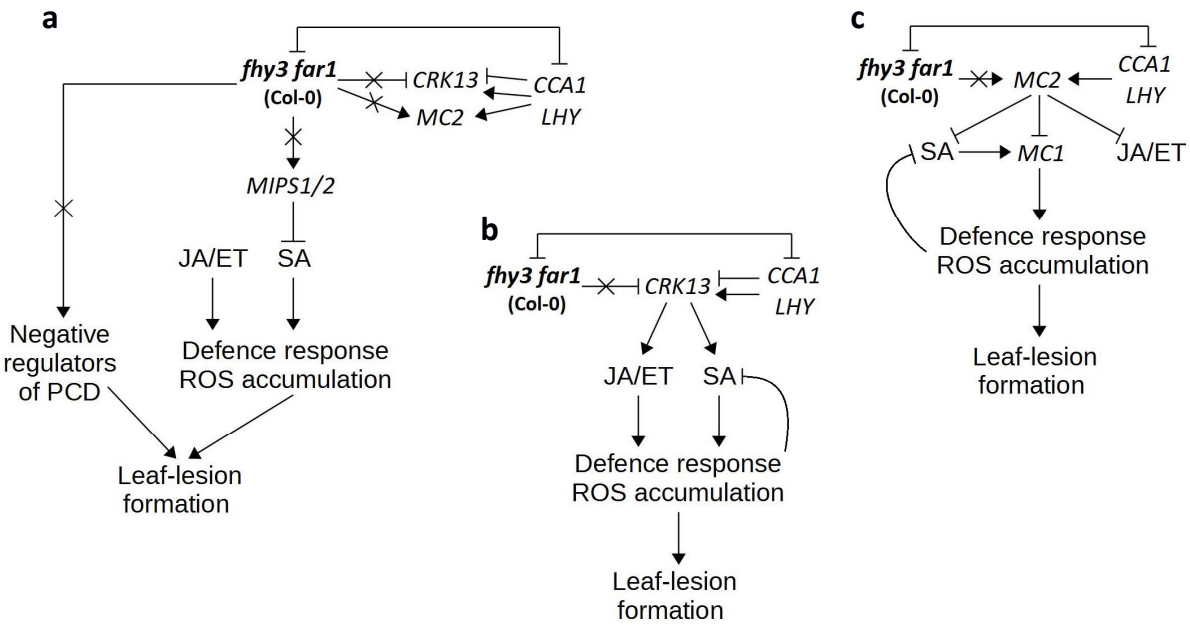

Figure 4.14: Schematic depiction of mechanisms in *fhy3 far1* (Col-0) mutants that a) result in leaf-lesion formation and affect *CRK13* and *MC2* expression, b) detail the effect of *CRK13* on lesion formation, and c) detail the effect of *MC2* on lesion formation (in reference to Acharya *et al.*, 2007; Coll *et al.*, 2010, 2011).

4.3.2 Transcriptional changes upon biotic challenges in plants with Columbia ecotype

4.3.2.3 Differences in transcriptional changes upon biotic challenges between No-0 and Col-0 ecotypes

Phenotypic differences between SD-grown WT and *fhy3 far1* mutant plants in No-0 and Col-0 ecotype were found in the investigations of this chapter. *fhy3 far1* mutant plants with No-0 ecotype developed a more extensive leaf-lesion formation than those with Col-0 ecotype (Figure 4.6). Double mutant plants with No-0 ecotype also showed a more pronounced dwarf phenotype (Figure 4.6). In general, plants with No-0 ecotype seemed to be smaller than those with Col-0 ecotype.

Investigations of SD-grown WT and *fhy3 far1* mutant plants with the No-0 ecotype in chapter 3 suggested the existence of negative feedback on SA- and JA/ET-signalling dependent defence response. To conjecture on a similar mechanism in WT and *fhy3 far1* mutant plants with Col-0 ecotype, and to create a basis for an analysis of the *CRK13*-Ox and *mc2* transcriptional changes upon biotic challenges, the transcriptional differences between No-0 and Col-0 ecotypes have to be discussed first.

Mock treatment results showed a substantial difference in the initial gene expression profiles of the *fhy3 far1* mutants in the two ecotypes. The double mutant with Col-0 ecotype showed a strong upregulation of the defence response-associated JA/ET- and SA-signalling marker genes, whereas in the No-0 ecotype, these genes were found to be downregulated. This difference is partly unexpected, especially considering the occurrence of leaf-lesion formation and dwarf phenotype in both ecotypes. However, the extent of these *fhy3 far1* mutant phenotypic characteristics also differed in the two ecotypes. *fhy3 far1* mutants with No-0 ecotype suffered from more severe dwarfing and developed leaf-lesions earlier than double mutants with Col-0 ecotype. At the time of treatment with biotic stressors (22 days), mutant plants in No-0 already displayed much more extensive leaf-lesions, when grown on soil. Agar-grown double mutant plants with both ecotypes, however, showed very similar phenotypes, where the difference in leaf-lesion formation was not that prevalent. H_2O_2 accumulation, demonstrated by DAB assay, was very similar in both ecotypes as well. In the previous chapter, it was proposed that the downregulation of defence gene expression seen in the No-0 ecotype could be the result of negative feedback. This suggests the non-existence of the proposed negative feedback on SA- and JA/ET-signalling dependent defence response in the Col ecotype, or alternatively a different threshold to trigger this mechanism. Indeed, previously published observations revealed a non-identical cross talk between SA- and JA/ET-defence response signalling pathways in both ecotypes (Korolev *et al.*, 2008; Zheng *et al.*, 2008). The upregulation of defence response marker gene expression in the Col-0 ecotype more conforms to Ma *et al.* (2016)'s finding of increased SA accumulation in *fhy3 far1* mutants.

4.3.2.4 Transcriptional changes upon biotic challenges in *fhy3 far1*, *CRK13*-Ox and *mc2* mutants

When challenged with *Pst* DC3000, *B. cinerea* and FB1, *fhy3 far1* mutants retained approximately WT responsiveness, displaying an upregulation of the tested marker genes. Again, this represents a difference in the *fhy3 far1* phenotype between the two ecotypes. In the No-0 ecotype, biotic challenge of *fhy3 far1* mutants led to increased downregulation of defence gene expression, presumably through negative feedback. *fhy3 far1* mutants with Col-0 ecotype showed no evidence of negative feedback on defence response gene expression. This could be attributed to Zheng *et al.* (2008)'s findings of less SA accumulation in *A. thaliana* plants with Col-0 ecotype compared to plants with No-0 ecotype. This could lead to less enhanced endogenous SA levels in *fhy3 far1* (Col-0) mutant plants upon pathogen challenge. Comparison

of the ecotypes after biotic challenges points to stronger physical symptoms / defence response in both, WT and *fhy3 far1* plants with the No-0 ecotype (though, H_2O_2 accumulation demonstrated by DAB staining is not conclusive). This either implies the absence of a ROS-mediated negative feedback on defence response gene expression in the Col-0 ecotype or, more likely, a higher threshold for its activation. In response to chitin treatment, *fhy3 far1* mutants showed a downregulation of SA-inducing genes, which is suggestive of a negative feedback. However, this was in contrast to the No-0 ecotype results. Also, WTs in both ecotypes showed opposite marker gene expression. It is possible that the responses to various triggers, and thereby activation of the assigned signalling pathways, have different thresholds for induction and repression, attuned to the specific environmental conditions to which the two ecotypes adjusted (the Col-0 ecotype originated from USA and the No-0 ecotype from Germany (The Arabidopsis Information Resource. (2001) Ecotype/Species: Columbia. [online] Available from: www.arabidopsis.org [28.12.2016]; The Arabidopsis Information Resource. (2001) Ecotype/Species: Nossen. [online] Available from: www.arabidopsis.org [28.12.2016])). These complexities could result in quite different gene expression patterns.

Mock treatment, and therefore the initial state of *CRK13*-Ox mutants, showed increased expression of SA-inducing and JA/ET-responsive defence response marker genes, consistent with previous findings of CRK13-mediated induction of *SID2*, *PR1* and *PR5* by Acharya *et al.* (2007). *SID2, PR1* and *PR5* have been described to be associated to SA-mediated defence response (Ukens *et al.,* 1992). Significantly, Acharya *et al.* (2007) proposed that overexpression of *CR13* caused PCD due to upregulated SA and ROS pathways. The enhanced PCD in that study was confirmed in this study by DAB staining, which showed strong H_2O_2 accumulation in *CRK13*-Ox mutant plants.

In response to *Pst* DC3000 and *B. cinerea*, *CRK13*-Ox mutants showed a loss of induction, in fact, a downregulation of SA-inducing genes. It is conceivable that here the reported stimulation of SA pathways, due to a challenge with *Pst* DC3000, in combination with the already accelerated ROS accumulation, leads to activation of the proposed negative feedback. This conforms to the lack of further enhanced H_2O_2 accumulation and chlorosis upon *Pst* DC3000 infection. Since *B. cinerea* challenge induced SA marker genes in WT, it could be possible that the *B. cinerea*-mediated activation of SA-signalling in *CRK13*-Ox triggered the proposed negative feedback similar to the *Pst* DC3000 challenge. Chlorosis in response to *B. cinerea* treatment was similar to mock treatment, and DAB staining was slightly reduced compared to mock treatment. DAB staining upon *B. cinerea* treatment was still stronger than in response to *Pst* DC3000 challenge,

possibly attributed to the necrotrophic nature of *B. cinerea*. Interestingly, *B. cinerea* did not trigger SA-inducing genes in WT with No-0 ecotype, again pointing to a different cross-talk between signalling pathways between the two ecotypes.

Challenge of *CRK13*-Ox plants with FB1 further induced PCD, seen by additionally enhanced chlorosis. However, no feedback effects on SA marker genes were observed, suggesting that the associated SA pathways are not triggered by FB1 to the same extent as the pathogens. This is consistent with the findings by Asai *et al.* (2000), who concluded that FB1 can only induce little SA accumulation in *A. thaliana*.

CRK13-Ox mutants also showed a loss of JA/ET-responsive marker gene expression relative to WT upon infection with *Pst* DC3000, and to some extent upon infection with *B. cinerea*, which could also possibly be part of the proposed negative feedback on defence response genes as a whole.

Chitin treatment induced the expression of all marker genes in *CRK13*-Ox mutants, activating all defence signalling pathways, yet seemingly not to a sufficient extent to activate the proposed negative feedback. This further adds to the complexity in the organisation of *A. thaliana* defence responses. During the three days of inoculation, chitin treatment resulted in the strongest chlorosis amongst all treatments.

Overall, the responses of *CRK13*-Ox mutants showed only little similarity with those of *fhy3 far1* mutants, making it unlikely that the upregulation of *CRK13* in *fhy3 far1* mutant plants is a primary cause for the increased leaf-lesion formation in the double mutant.

The initial situation in terms of defence response for *mc2* mutants, shown by mock treatment, displays an upregulation of JA/ET-responsive and SA-inducing gene expression, even stronger than that observed in *CRK13*-Ox mutants. This was less expected, since the mock-treated *mc2* mutant shows an otherwise phenotype similar to WT and the *mc2* mutation has been shown mainly to enhance PCD following initiation of a defence response (Coll *et al.* 2010). Loss-of-function of *mc2* possibly leads to a subtle phenotype that previously was not realised by Coll *et al.* (2010), as the group looked at phenotypical lesion formation and not gene expression. PCD occurs continuously to a certain degree within leaves, potentially impacting the mutant's defence response gene expression without actually causing visible leaf-lesion formation. In the present investigation of this thesis, mutant plants did not display leaf-lesions but DAB staining showed slightly increased H_2O_2 accumulation, compared to WT.

Increased H_2O_2 accumulation upon infection with *Pst* DC3000 and *B. cinerea* was observed in *mc2* mutants, most likely attributed to the reduced inhibition of the pro-PCD activity of *MC1*.

Coll *et al.* (2010) showed strongly increased occurrence of dead cells by trypan blue staining, when *mc2* mutant plants were treated with avirulent *Pst* DC3000 (avrRpm1).

Interestingly, *mc2* mutants also showed a loss of activation of SA-inducing genes in response to *Pst* DC3000, *B. cinerea* and FB1. This also suggests a possible negative regulation of SA-signalling. MC1 was described as part of NB-LRR-mediated ETI in *A. thaliana* (Coll *et al.*, 2010 and 2011), and thus is expected to be responsive to *Pst* DC3000 infection. MC1 was also reported to be induced in tomato by infection with *B. cinerea* (Kwon *et al.,* 2013), implicating MC1, and thereby probably its inhibitor MC2, in defence signalling pathways triggered by both pathogens. Pathogen infection activates MC1, leading to enhanced PCD in consequence of *MC2* loss-of-function. This enhancement was seen by enhanced chlorosis and H_2O_2 accumulation in response to both, biotrophic and necrotrophic pathogens, as well as to FB1. This possibly activates a negative feedback on defence response signalling, leading to repression of SA-inducing genes upon *Pst* DC3000, *B. cinerea* and FB1 treatment. This feedback seems to be directed in some extent to the nature of the pathogen, as SA-inducing marker genes were more affected in response to the biotrophic pathogen.

Results of the treatment with the MAMP chitin, on the other hand, rather resemble WT results, which points to ETI-specificity of *MC2* (and possibly *MC1*), and less involvement of PTI.

These responses, similar to the *CRK13*-ox results, show little similarities of *mc2* with *fhy3 far1* mutants. It is unlikely that the downregulation of *MC2* in *fhy3 far1* mutant plants is part of the primary cause responsible for increased leaf-lesion formation in the double mutant.

4.4 Conclusion

Global transcriptional investigations of the *fhy3 far1* microarray in search for potential disrupted key elements that are misregulated in the double mutant and could contribute to the formation of the observed leaf-lesions pointed to two defence response associated genes, *CRK13* and *MC2*, in particular. The upregulation of the PCD-inducing *CRK13* and downregulation of the PCD-inhibiting *MC2* was confirmed in *fhy3 far1* mutants by RT-qPCR. Biotic challenge assays, however, showed only little similarity in defence marker gene responses of *CRK13*-Ox and *mc2* mutants with the responses of *fhy3 far1* mutants. This suggests that both misregulated genes are unlikely to be part of the primary reasons of enhanced leaf-lesion formation in *fhy3 far1* mutants. As a result, neither component was pursued further.
In addition, ecotype-specific differences upon biotic challenges were found in WT and *fhy3 far1* mutants with Col-0 and No-0 ecotype, indeed, suggesting the presence of a proposed negative feedback on defence response gene expression, whose thresholds for activation, however, seem to differ between ecotypes (Figure 4.15).

As mentioned at the end of chapter 3, during the course of this study, Ma *et al.* (2016) demonstrated increased SA accumulation in *fhy3 far1* mutant plants as the cause for the leaf-lesion formation. They demonstrated a FHY3- and FAR1-dependent misregulation of two key components of the *myo*-inositol biosynthesis (*MIPS1* and *2*), which normally acts to suppress SA accumulation and SA-mediated PCD response. This is consistent with the enhanced SA-associated responses observed in *fhy3 far1* mutants in the investigations of this chapter. However, the data in the present investigations additionally suggest increased activation of JA/ET-associated pathways in the double mutant and, thereby, a yet wider influence of *FHY3* and *FAR1* on the plant defence response.

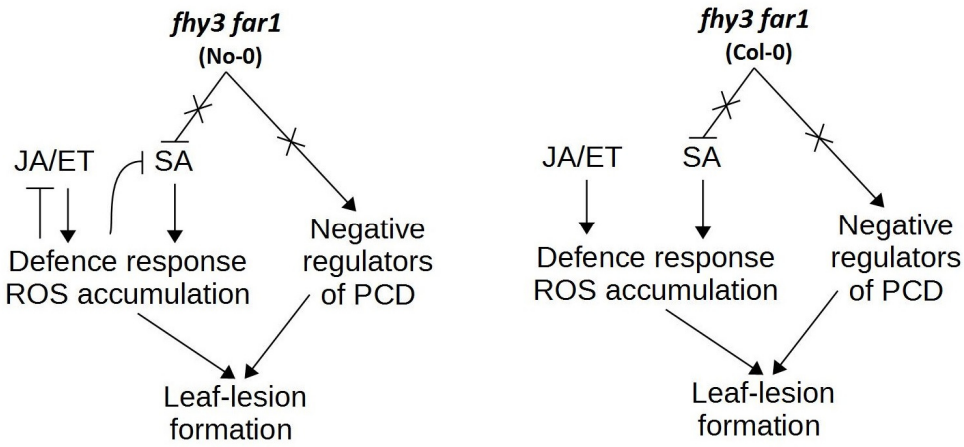

Figure 4.15: Ecotype differences in the hypothesised negative feedback on defence response gene expression in *fhy3 far1* mutants with No-0 and Col-0 background. *fhy3 far1* mutants with both backgrounds seem to have an impaired SA biosynthesis and expression of negative regulators of PCD, leading to misregulated defence response and ROS accumulation, and a development of leaf-lesions. *fhy3 far1* mutants with Col-0 background, additionally, show defence response and ROS accumulation mediated negative regulation of JA/ET signalling.

5 ANALYSIS OF FHY3 FAR1 MUTANT PHYLLOSPHERIC MICROBIOTA

5.1 Introduction

5.1.1 Commensal, non-pathogenic microbes

The above ground growing parts of a plant are called phyllosphere, with leaves (phylloplane) as the major surface. They are colonised by microorganisms that are categorised into either surface-dwelling epiphytes or internal tissue-inhabiting endophytes (mainly in the apoplast and dying / dead cells). Their majority is commensal / mutualistic and only a minority falls into the category of pathogens (commensalism and mutualism describe the relationship of two organisms during which one organism, here microbes, benefits from the other, here host plant, without harming or affecting it, or both benefit from each other's activity) (Sattelmacher, 2001; Lindow and Brandl, 2003; Turner *et al.*, 2013).

The phyllospheric microbial community (microbiota) is comprised mainly of bacteria, ranging from 10^6 to 10^7 cells per cm^2, filamentous fungi, yeasts, algae and even protozoa and nematodes; in descending quantity as listed. Population size and composition differs between plant species. Population size and composition also varies during a plant's life cycle, and may depend on environmental conditions as determined by location and season, and nutrient availability (Lindow and Brandl, 2003; Whipps *et al.*, 2008; Vorholt, 2012).

Generally, the phyllosphere is regarded as a less favourable environment for microbes than the rhizosphere. Fluctuations in water availability are particularly problematic. Water evaporation through stomata, formation of a thin layer of surface moisture, and retention of water in troughs of the leaf topography, for example, reduces the water stress for microbes. However, bacteria were found to aggregate, even in combination with fungi, in structures similar to biofilms, to form a slime (due to their extracellular polysaccharides) and, thereby, compensate for water fluctuations, amongst other things. Carbon and nitrogen are accessed in the form of simple sugars, organic acids and amino acids that diffuse from inside the plant on a scale to sustain the microbial community (in the range of single digit µg sugar per leaf). They are also accessed as methanol from pectin metabolism. Nitrogen-fixing commensal microbes were also reported in the phyllosphere. However, carbon and nitrogen availability, as well as their fluctuation during micro- and macro-cycles (day / night cycles and plant life cycle), is a major limiting factor for microbial growth. UV-radiation is also a limiting factor, which is believed to be the reason why many epiphytes were found to produce pigments to create UV-tolerance. The rhizosphere, in comparison, is a much more favourable habitat and shows higher and more stable water and

nutrient availability, as well as less fluctuating temperatures and the absence of UV-radiation. Nevertheless, the phyllosphere is a prevalent habitat for microbes and represents an extensive surface area. The phyllosphere is actually proposed to show a higher microbial diversity than the rhizosphere; this diversity being promoted by environmental variability (Lindow and Brandl, 2003; Whipps *et al.*, 2008; Delmotte *et al.*, 2009; Innerebner *et al.*, 2011; Vorholt, 2012; Bringel and Ivan Couée 2015) , since it is exposed to more altering condition in which air and water are the main carrier to distribute bacteria and fungi, in contrast to the more stable environment of the rhizosphere that is more protected against environmental alterations due to its dense and solid characteristic.

Certain commensal / mutualistic bacteria are beneficial for plants by occupying space and antagonising / inhibiting colonisation by pathogens. *Sphingomonas* spp. inhibited colonisation of *A. thaliana* by the pathogen, *Pst* DC3000, by 340-fold, when a *Sphingomonas* spp. inoculation was performed one day after *Pst* DC3000 inoculation. *Sphingomonas* spp. even inhibited colonisation of *A. thaliana* by *Pst* DC3000 by 10-fold when performed 26 days after *Pst* DC3000 inoculation. Also, severe disease symptoms were prevented from occurring in those investigations. These data even surpassed the results from resistant plants that showed a 10- to 200-fold-reduction of *Pst* DC3000 cfu, compared to susceptible host plants. The exact mechanisms of protection are elusive, but could be linked to competition for space and nutrients, as well as possible utilisation of antimicrobial agents by *Sphingomonas*. The induction of plant defence responses by *Sphingomonas*, which would then also be effective against the pathogen, was also proposed (Lindow and Brandl, 2003; Innerebner *et al.*, 2011; Vogel *et al.*, 2016).

5.1.3 Life history theory and constitutively activated defence response

Plants and organisms in general have limited resources of energy, nutrients and of course time, which all need to be allocated to competing processes, such as growth, defence response and reproduction.

Investing resources into one process reduces the resources that could have been invested into other processes. In the worst case, the allocation-choice can have a direct influence on survival and reproduction of the individual. Life history theory studies factors, aspects and correlation of the concerned processes to gain understanding of the various life cycle strategies (Rauw, 2012; Denancé *et al.*, 2013).

In general, defence responses are energetically expensive. As a result, many defence responses are inducible; therefore, mitigating the "cost". Consequentially, plants tolerate the majority of colonising microbes, both of commensal and partly pathogenic nature. Defence response and tolerance are not to be understood as separate states but rather a blend that creates an intermediate state of resistance and tolerance. However, defence- and tolerance-mechanisms are associated to different genes and processes, suggesting that net costs will change in response to altered microbial community compositions (Fornoni *et al.*, 2004; Rauw, 2012).

Constitutively activated defence responses, such as the constitutively activated SA-dependent defences in the *CONSTITUTIVE EXPRESSOR OF PATHOGENESIS RELATED GENES 1* (*cpr1*) loss-of-function mutant, result in enhanced resistance to pathogens. However, these alterations are often accompanied by reduced plant fitness in the form of dwarf phenotypes, lesion formation, accelerated senescence and impaired flowering and seed production, amongst other things (Heidel *et al*., 2004; Denancé *et al.*, 2013). Even priming crop plants with the SA-analogue BTH was shown to reduce plant fitness (reduced lateral shoot and inflorescence production) alongside increased resistance to powdery mildew (Heil *et al.*, 2000; Huot *et al.*, 2014). Conversely, allocation of extra reserves to growth reduces defence responses. Shade-avoidance triggers rapid elongation growth and depends on resource allocation to associated processes. Shade-grown plants were shown to be more susceptible to the hemibiotroph *P. syringae* and the necrotroph *B. cinerea*. In this case, growth is prioritized over defence response (Huot *et al.*, 2014).

In the preceding chapters, global transcript analysis of *fhy3 far1* mutant plants (3.2.3.4 Misregulation of PCD and defence response signalling), as well as investigations of defence responses upon biotic challenges (3.2.4.5 Transcriptional changes upon biotic challenges), suggested an inappropriately activated SA-dependent defence response in *fhy3 far1*. This chapter set out to study the effect of these constitutively activated SA-mediated defence responses on the microbial community in the *fhy3 far1* mutant plants. In this respect, the double mutant plant provides a unique opportunity to discover the wider effects of plant defence responses on the potentially-beneficial microbial community without the confounding collateral effects of a plant pathogen infection assay. It is hypothesised here that immune responses will be detrimental to both pathogenic and beneficial microbiota, alike. This investigation will, therefore, address another potentially negative aspect of the plant defence response in addition to the energetic cost. It may be that the balance between tolerance and defence is also

important in maintaining a habitat for beneficial microbes which may, in turn, provide a degree of defence at no cost to the plant. Such an analysis has not been previously performed and could be of tremendous interest. A high-throughput sequencing approach was taken in order to characterise both the bacterial and fungal communities. It was hoped that information about the composition or structure of these communities, particularly with respect to known beneficial microbes, might give an indication of whether the microbial community is altered in a way that is detrimental for the plant.

It was observed that the microbial community structure showed major alterations in *fhy3 far1* mutant plants. It showed greatly increased bacterial species richness and a more even spectrum of species abundances, compared to a stronger dominance by fewer species in WT plants. Notably, those bacterial taxa becoming dominant in WT plants were associated with the production of antimicrobials. In addition, while the fungal community structure showed little change in *fhy3 far1*, the mutant was found to host a number of fungal taxa associated with pathogenesis, compared to a predominance of more saprophytic taxa in WT. Based on these findings a model is discussed which proposes that the plant-protective characteristic of beneficial microbes in the phyllosphere of a healthy plant may be a community feature linked to microbial competition. Given that this community structure is impaired by a constitutively activated plant defence response, it is proposed that this adds greater weight in favour of tolerance mechanisms as opposed to defence mechanisms in the balance that creates the intermediate state of resistance and tolerance.

5.2 Results

5.2.1 Trial run

In preparation for the culture-independent 16S high-throughput sequencing-based taxonomic identification of the phyllospheric microbial community of WT and *fhy3 far1* plants, primers and the targeting of the bacterial and fungal rRNA genes were tested. The trial run represents a quality control of this procedure for the culture-independent high-throughput sequencing (5.2.2 Culture-independent taxonomic identification of phyllospheric microbiota in short days). The phyllospheric microbes of WT and *fhy3 far1* mutant plants were extracted (utilising Tetrasodium pyrophosphate ($Na_4P_2O_7$) and Sodium Chloride (NaCl) solutions, 2.7.1 Extraction of phyllospheric microbes for trial run), plated and grown on sterile medium. Since this was the pivotal step in

this culture-dependent approach, six different kinds of media were selected to provide diverse nutrient content and therefore maximise the recovery of microbes. Morphologically distinct colonies were subcultured on separate plates with the same six different kinds of media. Based on a visual inspection of this small-scale analysis, the bacterial flora appeared more diverse on the *fhy3 far1* double mutant while fungal diversity appeared similar to WT. However, it is well documented that culture-based approaches have the limitation that only a low single digit percentage (0.1 to 5 %) of the microbial community is cultivable and therefore cannot give a precise representation of the vast majority of microorganisms (Wagner *et al*. 1993; Müller and Ruppel, 2014). The taxonomic identification results of the trial run remain a very preliminary observation at this stage.

Subsequent to subsampling, individual colonies of five bacterial and eight fungal samples for WT and *fhy3 far1* mutant, for each BR, were subjected to PCR amplification targeting the bacterial 16S rRNA gene or the fungal ITS-region. Samples were selected based on their distinct colony morphology (form, surface characteristic, and pigmentation), evaluated by eye. Representative bacterial and fungal colony morphologies are shown in Figure 5.3.

Bacterial 16S rDNA occurs at least in one genomic copy and contains hypervariable regions (V1-V9), flanked by highly conserved regions. It allows for PCR amplification and subsequent sequencing of the resulting amplicons that can allow identification of the bacterium. This approach is the well-established standard for bacterial classification and based on comprehensive reference databases (Chakravorty *et al.*, 2007). To prevent false-positive PCR amplifications of chloroplast and mitochondrial DNA with universal bacterial primers, due to the homology of bacterial 16S, chloroplast 16S and mitochondrial 18S rRNA genes (Müller and Ruppel, 2014), PCR amplification consisted of two steps, as described by Sakai *et al.* (2004). The first PCR with the primer pair 63f (CAGGCCTAACACATGCAAGTC) and 1492r (GGCTACCTTGTTACGACTT) resulted in mitochondria-specific amplicons of approximately 1850 bp, bacteria-specific amplicons of approximately 1470 bp, and chloroplast-specific amplicons of approximately 1420 bp (Figure 5.1), which allowed a size fractionated recovery of bacterial 16S rDNA and chloroplast amplicons. These were used as a template to PCR-amplify the bacterial sequence, and simultaneously minimise chloroplast sequence amplification with the primer pair 63f/783r (783r: CTACCVGGGTATCTAATCCBG), due to primer mismatches and reduced annealing of the degenerative reverse primer to chloroplast 16S rDNA. This resulted in PCR amplicons of approximately 760 bp (Figure 5.1).

For sequencing-based taxonomic identification of the fungal community, the highly conserved internal transcribed spacer 1 (ITS1) region of the multi-copy nuclear ribosomal DNA (rDNA) was targeted. This region separates the small subunit (SSU: 18S) and the large subunit (LSU: 5.8S) of the rRNA gene. The combination of highly conserved regions linked to highly variable regions allows for universal fungal PCR amplification and distinction between genera. Reference databases for ITS regions are well-established and widely available, making this approach the standard for fungal identification (Turner *et al.*, 2013; Lindahl *et al.*, 2013).

To amplify the fungal sequence, one PCR with the universal primer pair ITS1-F (CTTGGTCATTTAGAGGAAGTAA) and ITS2 (GCTGCGTTCTTCATCGATGC) (White *et al.*, 1990) (Figure 5.2) was conducted, resulting in amplicons of approximately 280 bp (Figure 5.1).

In order to minimise the production of inhibitory compounds such as pyrophosphates that are released from dNTPs during the elongation step and that could inhibit polymerases, thermal inactivation of polymerases, and formation of primer mismatches during PCR (Müller and Ruppel, 2014), amplification steps for both, bacterial- and fungal-specific PCRs, were reduced to 20 thermocycles (Sakai *et al.*, 2004).

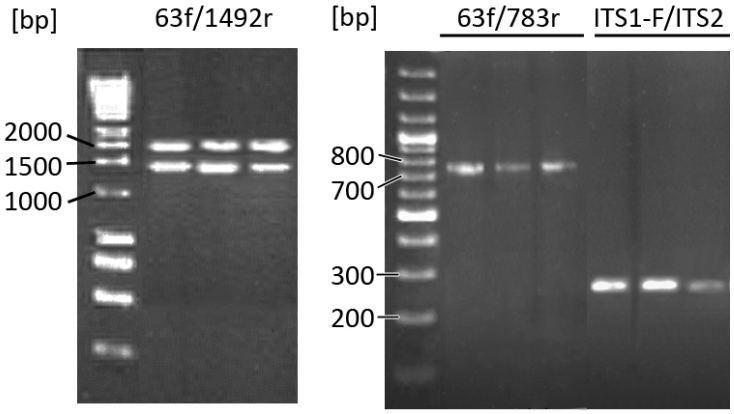

Figure 5.1: PCR amplicons of rDNA produced with the primer pair 63f/1492r and 63f/783r for bacterial samples, and ITS1-F/ITS2 for fungal samples, separated by gel electrophoresis, 1.5 % agarose.

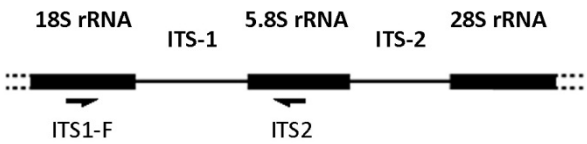

Figure 5.2: Scheme of the fungi specific universal primer pair ITS1-F and ITS2 annealing sites in the fungal rDNA that were used in the PCR-amplification step.

The individual bacteria- and fungi-specific PCR amplicons were sequenced (Sanger sequencing) and the results were subject to a DNA database alignment search using BLAST, showing an occurrence of the bacterial genera *Bacillus* and *Paenibacilus* on both WT and *fhy3 far1* mutant plants. Additionally to these, the genera *Sphingobium* and *Microbacterium* were found only on *fhy3 far1* mutant plant. These molecular identifications consistently corresponded to morphologically distinct colonies, adding confidence to these data (Figure 5.3 a). A similar variety of fungal taxa were found in both genotypes that consisted of the genera *Acremonium, Sarocladium, Penicillium* and *Cladosporium*. The WT phyllosphere was furthermore inhabited by species of the genus *Pseudogymnoascus*. Again, these molecular identifications consistently corresponded to morphologically distinct cultures (Figure 5.3 b).

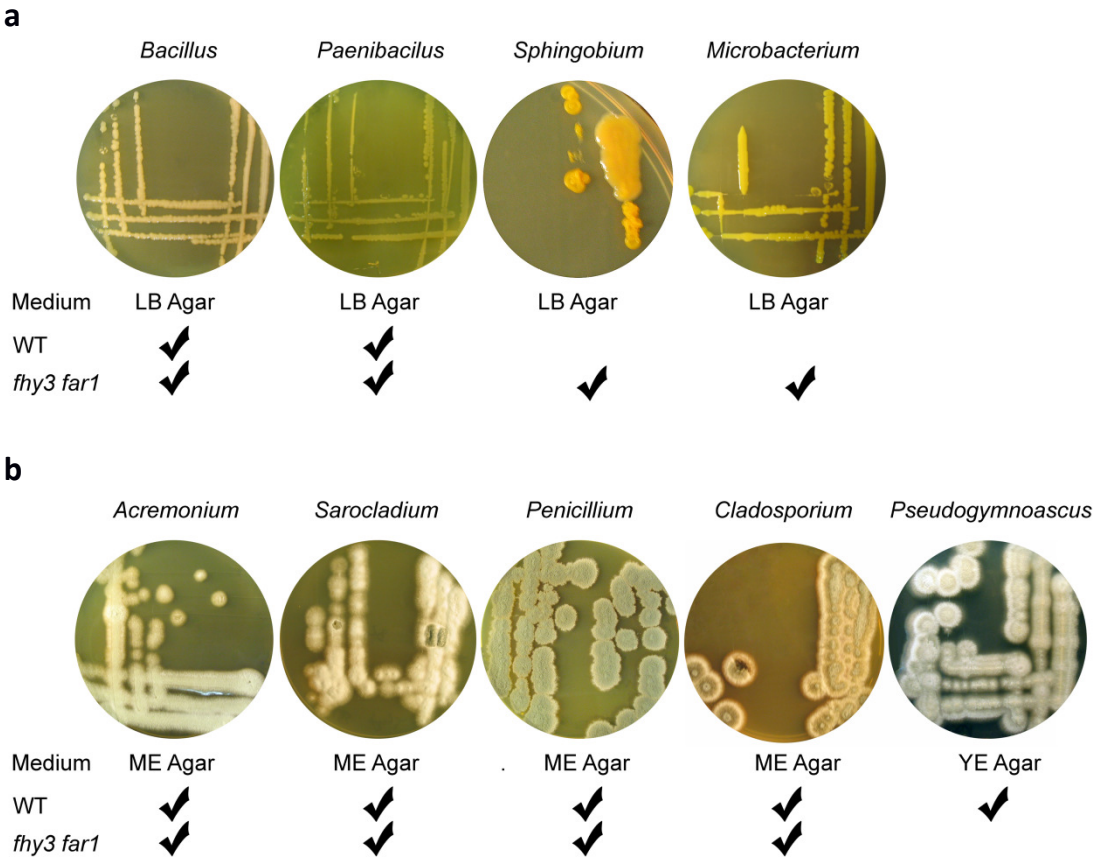

Figure 5.3: Monoculture plates of bacteria and fungi extracted from the phyllosphere of WT and *fhy3 far1* mutant plants, with examples of a) bacterial and b) filamentous fungal colonies of the respective identified genera. Ticks indicate the plant genotype from which the identified microbes were isolated from. LB Agar: Lysogen Broth Agar, ME Agar: Malt Extract Agar, YE Agar: Yeast Extract Agar.

5.2.2 Culture-independent taxonomic identification of phyllospheric microbiota in short days

Culture-independent high-throughput sequencing-based taxonomic identification has the advantage of acquiring a much wider range of microbes, giving a more precise representation of the microbiota than a culture-dependent approach.

The phyllospheric microbial community was extracted from 35 days old WT (No-0) and *fhy3 far1* (No-0) mutant plants, grown on soil in SD, in two temporal independent BRs, one replicate each (according to the protocol of Zhou *et al.,* 1996), and their rRNA genes utilised for identification. 35 days old plants were selected for this investigation. These were, therefore, older than the 25 days old plants that were used for the investigations with biotic challenges (3.2.4.2 Symptoms upon biotic challenges and histochemical staining, 3.2.4.5 Transcriptional changes upon biotic challenges, 4.2.5.1 Phenotypic changes and histochemical staining upon biotic challenge, 4.2.5.2 Transcriptional changes upon biotic challenges). SD grown WT (No-0) plants were at seven to eight rosette leaves development stage and *fhy3 far1* (No-0) mutant plants at six to seven rosette leaves development stage. The intent was to use older plants, since the microbial community would have more time to establish a steady state. In addition, the plants had to have a bigger size in order to present more space for microbes and, therefore, to yield sufficient microbial DNA after extraction. For PCR amplification, the primer pairs 63f/1492r, 63f783r, ITS1-F/ITS2, and PCR conditions as stated in the trial run were used.

Bacterial and fungal amplicons were combined in equal proportion by mass for each BR, reducing the required number of high-throughput sequencing reactions (bacterial and fungal sequences can easily be distinguished during subsequent analysis). High-throughput sequencing of the PCR-amplicons was carried out using the Illumina MiSeq single read platform, resulting in 63,968 and 118,250 sequences for the *fhy3 far1* sample BR1 and BR2, respectively, as well as 322,242 and 174,001 sequences for WT BR1 and BR2, respectively. The quality of the sequences was reviewed with the program FastQC (Andrews, 2010). FastQC is a quality control tool for high throughput sequence data (Babraham Bioinformatics, 2007). The analysis showed good sequence quality (mean Phred score of >30, corresponding to greater than 99.9 % base call accuracy) across the first 210 and 190 bp for WT samples (BR1 and BR2, respectively), as well as across the first 190 and 170 bp for *fhy3 far1* samples (BR1 and BR2, respectively) (see appendix). The mean sequence quality (Phred Score) for all samples showed a relatively tight distribution with high quality for the vast majority of sequences. (For all samples, a peak of mean Phred score per sequence at 33 / 34 was observed, corresponding to greater than 99.9 % base call accuracy).

Subsequent to this initial quality control (QC), the sequencing data were submitted to SILVAngs - high quality ribosomal RNA database web interface (Quast *et al.* 2013) for quality control and initial analysis of the bacterial community sequence data. SILVAngs provides a web-based pipeline for the analysis of microbial community 16S and 18S rDNA next generation sequence data. It is, therefore, ideal for the rapid analysis of 16S bacterial rDNA in these samples. However, the ITS fungal sequences contained only approximately 65 bp of 18S rDNA sequence (Fig 5.2). This will not provide accurate identification of fungal sequences beyond domain level (i. e. eukaryote / prokaryote). But, based on this classification, the eukaryotic sequences could then be weeded out and used for alternative analysis of the fungal community. Approximately one-third of the submitted sequences were rejected based on their alignment score and identity to an rRNA gene seed database (an alignment over a 50 bp stretch was required for further processing of each sequence by SILVAngs), as well as based on quality in terms of content of ambiguous bases and homopolymers (Table 5.1). All sequences had a mean GC content of approximately 50 %.

In order to justifiably compare the bacterial and fungal communities between WT and *fhy3 far1* mutant plants, it is important that a similar number of sequences are compared in each case for each sample. For each sample, 64,000 randomly-selected sequences were initially uploaded to SILVAngs corresponding to the approximately 64,000 sequences of the *fhy3 far1* BR1 sample, which was the smallest sample.

For both WT and *fhy3 far1* BR1 samples, approximately two thirds of the sequences were accepted for further analysis after initial quality control by SILVAngs. Sequences were grouped via a dereplication step involving clustering of essentially-identical sequences into operational taxonomic units (OTUs). OTUs are the most commonly utilised microbial diversity units and are an operational definition to classify closely related individual based on a 97 % similarity in identity. This classification is used to describe taxonomic groups on genus level in this thesis (Maignien *et al.*, 2014; Schlaberg *et al.*, 2012). This grouping yielded approximately 20,000 OTUs in each case (Table 5.1). For both WT and *fhy3 far1* BR2 samples, approximately half of the sequences were accepted for further analysis after initial quality control, and dereplication yielded approximately 7,000 OTUs in each case (Table 5.1). OTUs were then subjected to sequence alignment searches in order to classify each to the maximal possible taxonomic level. The analysis resulted in comparable numbers of eukaryotic (fungal) sequences for each sample (Table 5.1), but, since the proportion of bacterial to eukaryotic sequences varied in each sample, additional sets of randomly-selected sequences were uploaded in order to ensure balanced

bacterial numbers for bacterial analysis. For WT BR1, 128,000 sequences produced a similar number of bacterial sequences as were found for *fhy3 far1* BR1 in the initial upload (22,765 and 18,794 sequences, respectively), making the phyllospheric bacterial communities of both genotypes of BR1 comparable in terms of sequences numbers, thus, their diversity and evenness could be compared. However, uploading close to the maximum sequences for WT BR2 (150,000) only yielded approximately 8,000 bacterial sequences. Since a similar number of bacterial sequences for *fhy3 far1* BR2 had to be returned by SILVAngs, and therefore also make both genotypes of BR2 comparable in terms of bacterial sequences numbers, the initial upload for *fhy3 far1* BR2 with 64,000 sequences was used here, as it already yielded ~7,000 bacterial sequences (Table 5.2).

At the stage in the above analysis, the accepted sequences for bacterial analysis were clustered by SILVAngs into 38,700 and 17,059 OTUs (in total) respectively for BR1 (with 128,000 uploaded sequences) and BR2 (with 150,000 uploaded sequences) (Table 5.2). For *fhy3 far1* samples, the accepted sequences were clustered into 22,172 and 7,878 OTUs (in total) respectively for BR1 (with 63,968 uploaded sequences) and BR2 (with 64,000 uploaded sequences) (Table 5.2).

Sequence alignment also identified a significant number of chloroplast and mitochondrial sequences in each sample. Chloroplast and mitochondrial sequences represented approximately 20 % and 30 % of the total WT sequences, respectively, and approximately 2 % and 10 % of the *fhy3 far1* sequences (Tables 5.1 and 5.2). It was shown by Gao *et al.* (2013) that *FHY3* (and possibly *FAR1*) is a positive regulator of chloroplast division and that *fhy3* mutants showed reduced chloroplast numbers per cell, albeit, chloroplast sizes were increased. In their investigation, Gao *et al.* (2013) did not determine the different amounts of chloroplast DNA between WT and *fhy3* mutant plants. It, therefore, cannot be concluded with certainty that the *FHY3 and FAR1* loss-of-function is the cause for the reduced occurrence of chloroplast sequences in the above analysis, but this seems a likely explanation. The reduced mitochondrial sequences in *fhy3 far1* mutant plants could point to a not yet investigated involvement of both TF in mitochondria division. Likewise, the lower "health status" of the double mutant (leaf-lesion formation, dwarf phenotype) could be the cause for both results.

As mentioned earlier in this subheading, SILVAngs aligned eukaryotic sequences to an 18S rDNA-based reference database. Since the 18S region only accounted for a short part of the PCR amplicons used for sequencing (Figure 5.10), OTUs were often classified as simply eukaryotic. Hence, a SILVAngs-independent BLAST analysis for all eukaryotic OTUs was performed.

Table 5.1: Number of sequences from high-throughput 16S rRNA amplicon sequencing of WT's and *fhy3 far1*'s microbial community across two BRs submitted to the web interface SILVAngs and the resulting number of sequences and OTUs assigned to eukaryote, seq.= sequences.

Fungi		Submitted total number sequences		Total number of OTUs	Eu-karyote OTUs	Fungal seq.	Pro-karyote OTUs	
		Before QC	After QC					
BR1	**WT**	**64,000**	40,913	19,825	11,340	**17,855**	8.485	
	fhy3 far1	**63,968**	44,385	22,172	4,996	**21,466**	17,083	
BR2	**WT**	**64.000**	31,965	6,660	3,490	**24,832**	3,170	
	fhy3 far1	**64,000**	34,130	7,878	1,645	**26,372**	6,180	

Table 5.2: Number of sequences from high-throughput 16S rRNA amplicon sequencing of WT's and *fhy3 far1*'s microbial community across two BRs submitted to the web interface SILVAngs and the resulting number of sequences and OTUs assigned to bacteria, seq.= sequences.

Bacteria		Submitted total number sequences		Total number of OTUs	Pro-karyote OTUs	Total pro-karyote seq.	Bacterial seq.	Chloro.seq.	Mito. Seq.
		Before QC	After QC						
BR1	**WT**	**128,000**	82,146	38,700	22,274	46,298	**22,765**	8,945	14,588
	fhy3 far1	**63,968**	44,385	22,172	17,083	22,246	**18,794**	547	2,905
BR2	**WT**	**150,000**	76,532	17,059	8,160	18,914	**8,451**	3,762	6,701
	fhy3 far1	**64,000**	34,130	7,878	6,180	7,751	**6,793**	32	926

4,996 and 1,645 eukaryotic WT OTUs (BR1 and BR2, respectively) and 11,340 and 3,490 eukaryotic *fhy3 far1* OTUs (BR1 and BR2, respectively), representing the fungal community (Table 5.1, based on the initial 64,000 sequence uploads) were subjected to a DNA database alignment search using BLAST. The alignment results were evaluated according to the bit-score (S). Alignment results were selected when $S \geq 200$, which indicated a good alignment. A maximum of 10 alignments was selected per sequence. The alignment results with their NCBI accession IDs were uploaded to the web interface Batch Entrez (www.ncbi.nlm.nih.gov/sites/batchentrez) to retrieve a taxonomic identification on a genus / species level. The alignment results were further sorted by identity. For each sequence, the best alignment, among those alignments which gave a defined genus / species, were kept. Where a genus was not identified, the alignment result giving the most detailed taxonomic level was selected. A minimum cut-off that required an identity of at least 97 % was also applied. 97 % are generally applied for taxonomic identification on genus level (Stackebrandt and Goebel, 1994; Maignien *et al*., 2014; Schlaberg *et al*., 2012).

The identified genera together with their respective abundance data were subsequently used for visualisation in pie charts, for rarefaction curve analysis, for comparison of community diversity and evenness, as well as for hierarchical clustering, PCA and heatmap analysis, to compare the four samples.

5.2.2.1 Species richness of the bacterial and fungal communities of the WT and *fhy3 far1* phyllospheres

Bacterial and fungal rarefaction curves, representing the mean species richness as a function of the number of sequences sampled over multiple random resamplings, demonstrated a good depth of sampling in general. Rarefaction curves for the bacterial samples of WT and *fhy3 far1* BR1 indicated that the sequencing effort was approaching asymptote for both genotypes and therefore well-represented the bacterial community. The curves indicated that after 18,000 sequences, only a few additional species are likely to be found in each case. Curves of the second BR closely followed the curves of the first BR, suggesting a verification of BR1 data. Crucially, the rarefaction curves indicated a higher bacterial species richness in the *fhy3 far1* mutant phyllosphere than in the WT phyllosphere (Figure 5.4 a), which was confirmed by the Shannon's diversity index (Table 5.3).

Fungal rarefaction curves of both genotypes in the two BRs also indicated that the number of fungi truly represented this community and that after 18,000 sequences only a few additional species are likely to be found. The curve for the first fungal WT BR suggested that more intensive sampling is likely to yield further species; although, there is considerable overlap of the error bars meaning it could be considered similar to the other curves. Nevertheless, the rarefaction curves indicated similar fungal species richness in the phyllosphere for both genotypes (Figure 5.4 b). The fact that rarefaction curves generally approached asymptote indicates that species diversity comparisons between samples are appropriate and will be comparing a similar sampling depth in each case. In the case of the bacterial data for BR2, the rarefaction curves do not yet approach asymptote and, therefore, diversity indices for these samples will not be directly comparable on a quantitative level with those of the bacterial samples of BR1. However, the two BR2 bacterial samples (WT and *fhy3 far1*) will be directly comparable with each other, since the quantitative level of sampling depth is similar in each case. As a result, these BRs of bacterial samples can be considered as genuine replicates for the purposes of qualitative comparisons between WT and *fhy3 far1* samples.

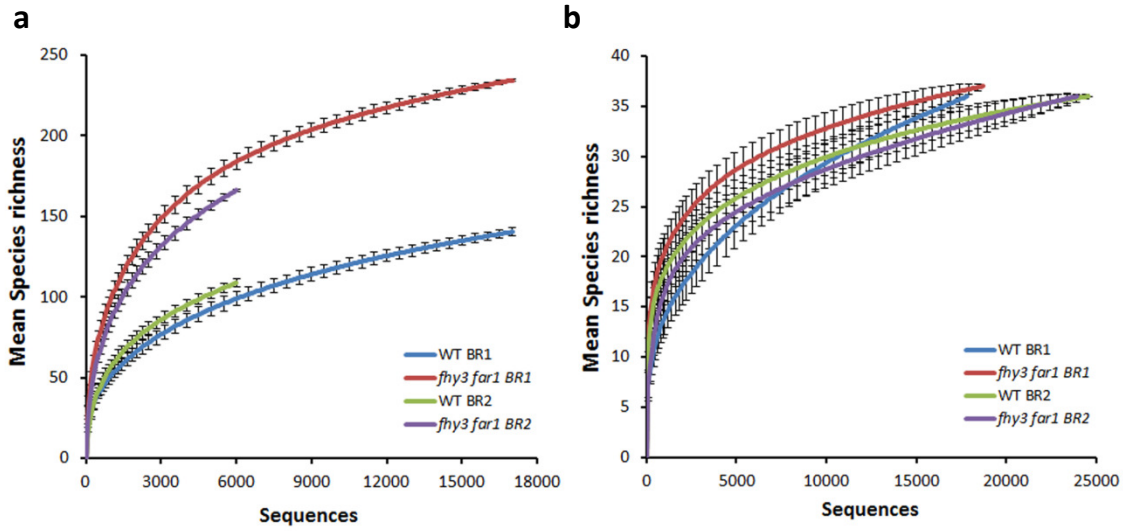

Figure 5.4: Rarefaction curves for a) bacterial and b) fungal mean species richness of the phyllospheric microbiota of WT and *fhy3 far1* mutant plants for both BRs. Rarefaction curves for the bacterial microbiota indicate a higher bacterial species richness in *fhy3 far1* than in WT. Rarefaction curves for the fungal microbiota indicate a similar species richness in *fhy3 far1* and WT.

5.2.2.2 Diversity and evenness of the bacterial and fungal communities of the WT and *fhy3 far1* phyllospheres

Shannon's diversity index is a commonly utilised mathematical model in ecology to calculate diversity, and it accounts for the abundance and evenness of the present microbial species (Begon *et al.*, 1996). Shannon's diversity index showed extensive phyllospheric bacterial diversity on both genotypes, although to a much higher degree on *fhy3 far1* mutant plants in both BRs (Table 5.3). Conversely, the evenness measure Buzas and Gibson's evenness index, which is also a commonly utilised model in ecology and it integrates Shannon's diversity index (Buzas and Hayek, 1996), showed much more even bacterial communities on *fhy3 far1* mutants than on WT plants (Table 5.3). This implied that the *FHY3* and *FAR1* loss-of-function led to a richer phyllospheric bacterial community.

In contrast, fungal diversity and evenness were fairly similar on WT and *fhy3 far1* mutant plants in both BRs. This suggested that the *fhy3 far1* mutation rather did not affect fungal taxa richness or evenness, and thereby diversity (Table 5.3).

Interestingly, many more eukaryotic OTUs of WT BR1 represented similar numbers of fungal sequences as far fewer eukaryotic OTUs for the *fhy3 far1* BR1 and BR2 samples (Table 5.1), without a change in diversity (Table 5.3). An explanation for this could be that sometimes

multiple OTUs represent the same fungal species. Small sequence differences within the population of a species could result in them being clustered in different OTUs, but the sequences would still map to the same species at the alignment step.

Table 5.3: Numbers of taxa, Shannon's diversity and Buzas and Gibson's evenness indices of bacterial and fungal genera across WT and *fhy3 far1* in two BRs. Shannon's diversity of the bacterial community was increased in *fhy3 far1* mutants in both BRs, which indicates higher diversity. Diversity of the fungal community was fairly similar on WT and *fhy3 far1*. Buzas and Gibson's evenness indices of the bacterial community shows more evenness on *fhy3 far1* compared to WT (higher value indicates more evenness). Evenness of the fungal community was fairly similar on WT and *fhy3 far1.*

	Bacterial genera				**Fungal genera**			
Genotype	**WT BR1**	***fhy3 far1* BR1**	**WT BR2**	***fhy3 far1* BR2**	**WT BR1**	***fhy3 far1* BR1**	**WT BR2**	***fhy3 far1* BR2**
Taxa (S)	147	235	115	167	36	37	36	36
Shannon-H	2.686	3.585	2.008	3.248	1.24	1.986	1.738	1.368
Evenness (e^H/S)	0.0998	0.1535	0.0648	0.1542	0.096	0.1968	0.1579	0.1091

5.2.2.3 Constitution of the bacterial and fungal communities of the WT and *fhy3 far1* phyllospheres

In the first BR, the majority of the bacterial community on WT plants is comprised of a few dominant taxa, consisting of Alphaproteobacteria with the genera *Brevundimonas* (19 %), *Martellela* (10 %) and *Sphingomonas* (10 %), as well as Gammaproteobacteria with the genera *Pseudomonas* (23 %) and *Lysobacter* (7 %). The bacterial abundance was much more evenly distributed on *fhy3 far1*, with the Alphaproteobacterium *Devosia* among the most abundant genera (11 %), along with the Gammaproteobacterium *Pseudomonas* (14 %) (Figure 5.5 a). Genera present in the second BR deviated from the first BR but showed a similar trend of fewer dominant taxa on WT and more even distribution on *fhy3 far1*. Here, the WT bacterial community was dominated by Firmicutes with the genus *Bacillus* (55 %), Actinobacteria with the genus *Brevibacterium* (11 %), and Alphaproteobacteria with the genus *Sphingomonas* (8 %), whereas for *fhy3 far1* mutant plants the highest abundances were seen for Alphaproteobacteria with the genus *Brevundimonas* (16 %), Betaproteobacteria with the genus *Advenella* (14 %), and Alphaproteobacteria with the genus *Devosia* (10 %) (Figure 5.5 b).

Overall, the phyllospheric bacterial community seemed to be altered toward more diversity due

to the *fhy3 far1* mutation.

The fungal community on WT plants in BR1 mainly consisted of a few Ascomycota genera, *Penicillium* (62 %), *Verticillium* (20 %) and *Fusarium* (17 %), together accounting for 99 % of the taxa. BR1 of *fhy3 far1* mutant plants also displayed few dominant Ascomycota genera, *Fusarium* (52 %), *Penicillium* (26 %), *Cladisporium* (7 %), *Verticillium* (5 %) and *Acremonium* (5 %) but also a more abundant presence of Basidiomycota, mainly represented by *Trichosporon* (4 %), together accounting for 99 % of the taxa (Figure 5.6 a). Even though both genotypes were also inhabited by just a few taxa, the composition of the second BR fungal community deviated to some degree from the first BR. On WT, the genera *Engyodontium* (36 %), *Acremonium* (28 %), *Penicillium* (26 %), *Fusarium* (3 %), *Villosiclava* (2 %) and *Cladosporium* (2 %), which are all Ascomycota, were the most abundant and accounted for 97 % of the taxa, whereas *fhy3 far1* mutant plants were the habitat for mainly *Villosiclava* (46 %), *Acremonium* (32 %) and *Penicillium* (19 %), also all Ascomycota, and accounted for 97 % of the taxa (Figure 5.6 b).
FHY3 FAR1 loss-of-function did not seem to influence fungal community diversity but perhaps altered the taxonomic composition (though, this also varied considerably between WT BRs, suggesting possible stochastic effects that could, likewise, be responsible).

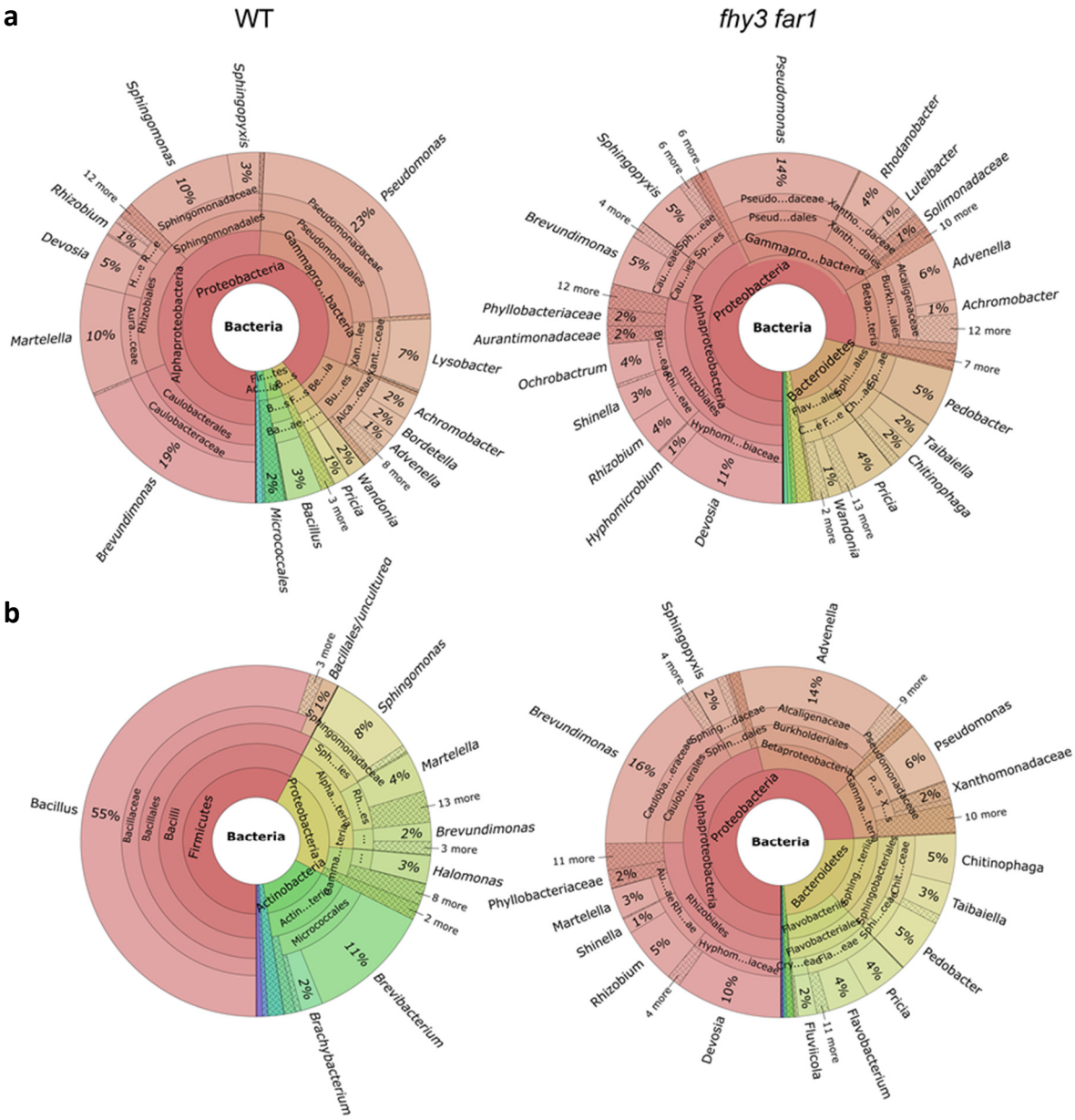

Figure 5.5: Taxonomic breakdown of bacterial genera identified in a) BR1 and b) BR2 on the phyllo-sphere of WT and *fhy3 far1* mutant plants. Bacterial diversity on WT is smaller than on *fhy3 far1* mutant, and the bacterial community on WT is rather dominated by fewer microbes with higher abundance, whereas on *fhy3 far1* the microbial abundance between the genera is rather even. *Pseudomonas*, *Brevundimonas*, *Martelella* and *Sphingomonas* have the highest abundance on WT in BR1, and *Bacillus* and *Brevibacterium* in BR2. *Pseudomonas* and *Devosia* are the most abundant bacteria on *fhy3 far1* mutants in BR1, and *Brevundimonas*, *Advenella* and *Devosia* in BR2.

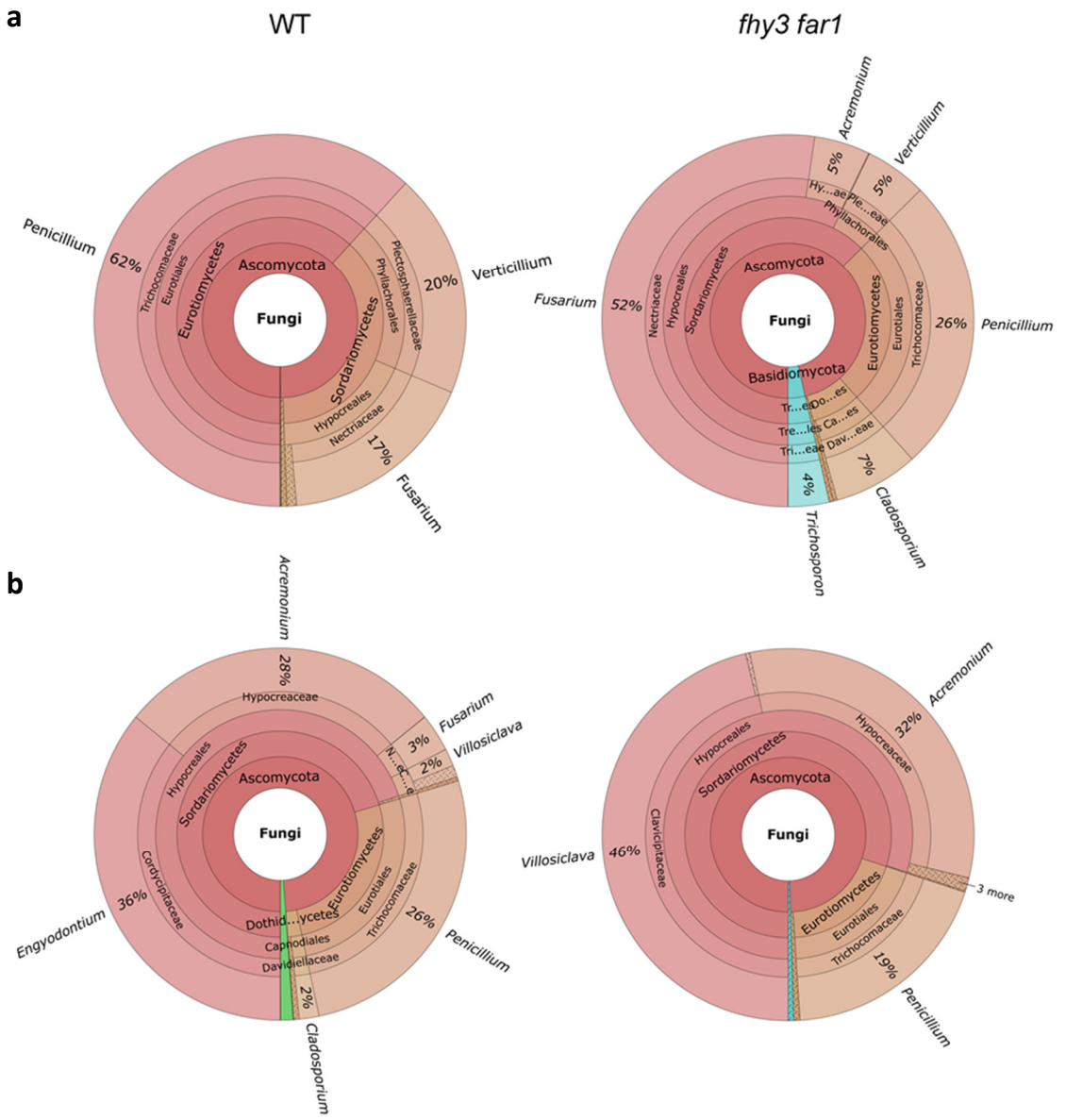

Figure 5.6: Taxonomic breakdown of fungal genera identified in a) BR1 and b) BR2 on the phyllosphere of WT and *fhy3 far1* mutant plants. Fungal diversity and evenness are fairly similar on WT and *fhy3 far1* mutant plants in both BRs. *Penicillium, Verticillium* and *Fusarium* have the highest abundance on WT in BR1, and *Engyodontium*, *Acremonium* and *Penicillium* in BR2. *Fusarium* and *Penicillium* are the most abundant fungi on *fhy3 far1* mutants in BR1, and *Villosiclava*, *Acremonium* and *Penicillium* in BR2.

5.2.2.4 Multivariate comparisons of the bacterial and fungal communities of the WT and *fhy3 far1* phyllospheres

The bacterial and fungal communities of the WT and *fhy3 far1* phyllospheres were compared using the multivariate analysis methods of principal component analysis (PCA) and hierarchical clustering, in order to explore the relationship between the complex data that represent the microbial communities of WT and *fhy3 far1* mutants. The abundance data for both analyses was log transformed ($Log_{10}(y+1)$) in order to prevent a displacement of the results by high abundant genera. This also allowed the differences in abundance of lower abundance genera to be considered when the samples were compared. Hierarchical clustering and PCA of both BRs demonstrated a clear grouping by plant genotype in the case of bacterial genera, showing reproducible differences in the bacterial community composition on WT and *fhy3 far1* mutants (Figures 5.7 and 5.8).

PCA also suggested a grouping by genotype for fungal genera with WT and *fhy3 far1* samples being grouped together in each case in a distinct quadrant of the PCA plot. However, hierarchical clustering suggested that the grouping between the two *fhy3 far1* BRs and the second WT BR was closer than the grouping between the two WT BRs. This does not disagree with the PCA result, which also shows that, despite being in separate quadrants, the second WT BR is closer to the two *fhy3 far1* BRs than it is to the first WT BR.

Overall, for both, bacterial and fungal analysis, the tighter grouping of the *fhy3 far1* BRs in the PCA projections indicated less variation in relative abundance of the most influential genera; hence, a higher degree of overall conservation of bacterial and fungal community structures, while WT samples showed a more divergent spread (Figure 5.8). This suggested that, while the community structure in WT was conserved, the formation of this structure may be a stochastic process in part. The *fhy3 far1* double mutation, however, could influence the phyllospheric microbiota composition to such a degree that environmental influences, such as soil batch-dependent factors, are superseded and have less influence.

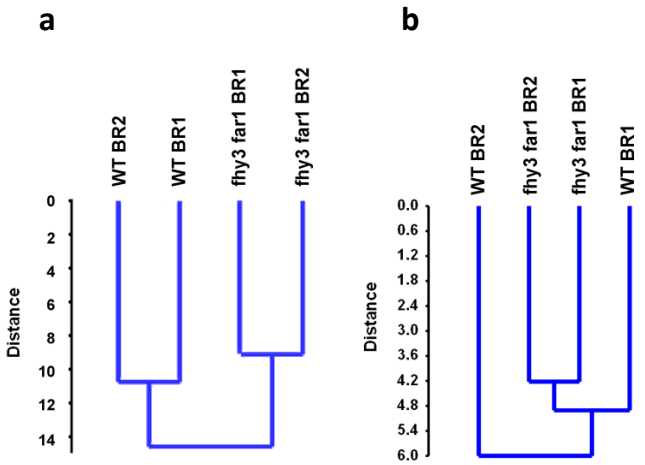

Figure 5.7.: Hierarchical clustering based on genera and their abundance (unweighted pair-group average for $log_{10}(y+1)$ transformed data) for a) bacterial and b) fungal community on WT and *fhy3 far1* mutant plants in two BRs, the Y axis shows Euclidean distance. Bacterial communities of both BRs show higher similarity within the genotypes. Fungal communities of both *fhy3 far1* BRs shows high similarity, fungal community of WT BR1 shows more similarity to the *fhy3 far1* communities than to the WT BR2 fungal community.

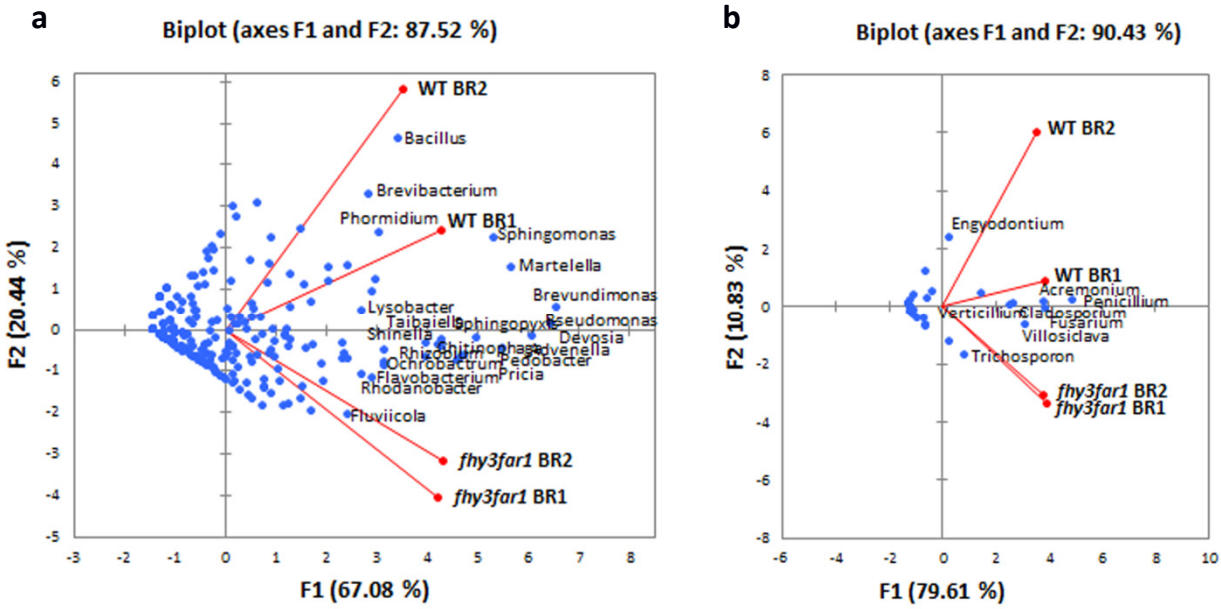

Figure 5.8: PCA of $Log_{10}(y+1)$ transformed abundance data from a) bacterial and b) fungal community genera of WT and *fhy3 far1* mutant plant phyllosphere in two BRs, most influential genera are labelled.

5.2.2.5 Analysis of the most abundant genera among the bacterial and fungal communities of the WT and *fhy3 far1* phyllospheres

A relative abundance-based heatmap analysis was done to propose certain genera as valid classifiers of the genotypes. The 20 most abundant bacterial genera across all samples, which account for 86 % and 83 % of the total bacterial species richness for WT BR1 and BR2, respectively, and 74 % and 85 % for *fhy3 far1* BR1 and BR2, respectively, showed agreement

with the PCA projections, proposing 17 of these 20 genera as valid classifiers of the two genotypes (Figure 5.8 a). Bacterial genera classifying the *fhy3 far1* mutant phyllospheric microbiota were *Devosia, Pricia, Pedobacter, Taibaiella, Rhizobium, Chitinophaga, Fluviicola, Advenella, Flavobacterium, Rhodanobacter, Ochrobactrum, Shinell* and *Sphingopyxis,* whereas WT classifiers were *Bacillus* and *Brevibacterium*, *Sphingomonas* and *Martelella* (Figure 5.9 a). Relative abundance-based heatmap analysis of the eight most abundant fungal genera (accounting for 99 % of species richness) suggested that more than half of these genera also showed genotype preference (Figure 5.9 b). Two genera, *Penicillium* and *Engyodontium,* were generally more abundant on WT plants than on *fhy3 far1* mutant plants in both BRs. *Verticillium* was more abundant on WT than on *fhy3 far1* if each BR is looked at separately. The two genera *Trichosporon* and *Villosiclava* were generally more abundant on mutant plants in both BRs. Again, this is in general agreement with the PCA analysis that suggests the WT and *fhy3 far1* phyllospheres favour distinct, specific microbes.

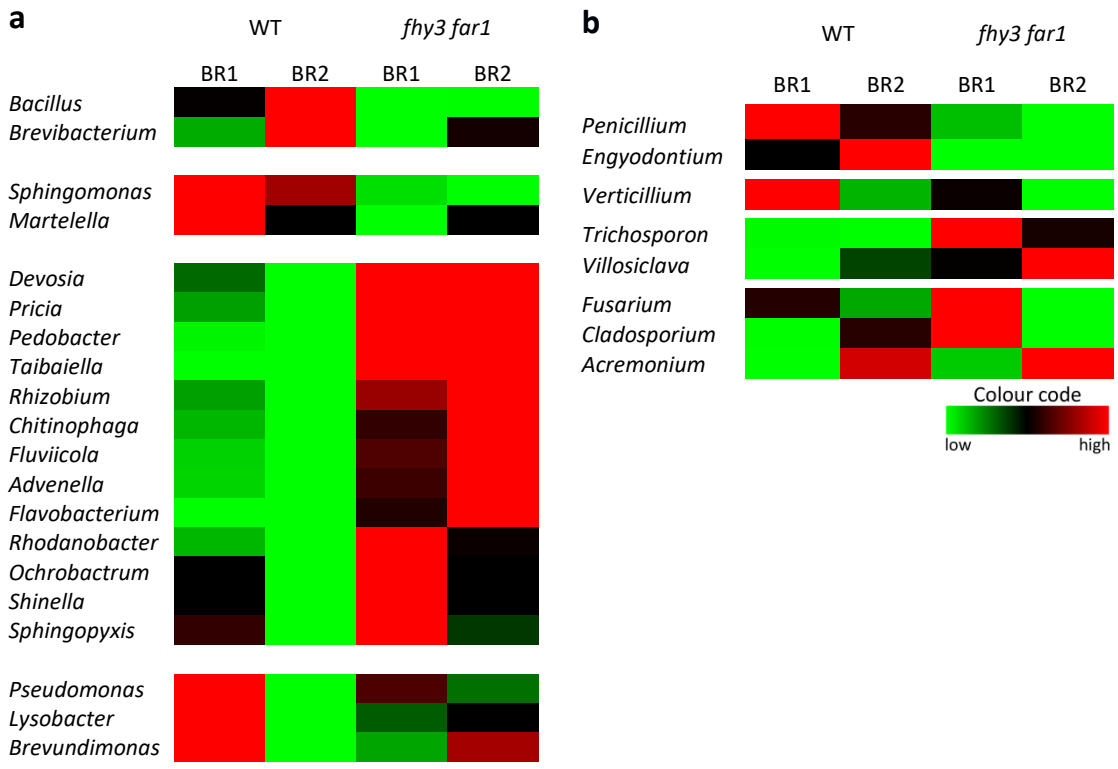

Figure 5.9: Heatmap analysis by relative abundance across two replicates for the 20 most abundant bacterial genera overall on WT and *fhy3 far1*. Highest abundance for each is labelled red, lowest green, 50th percentile black. *Bacillus*, *Brevibacterium*, *Sphingomonas* and *Martelella* show high abundance in WT bacterial community, whereas the genera starting from *Devosia* down to *Sphingopyxis* show high abundance in the *fhy3 far1* bacterial community. *Pseudomonas*, *Lysobacter* and *Brevundimonas* show high abundance in WT BR1. *Penicillium* and *Engyodontium* are more abundant in WT fungal community of both BRs, and *Trichosporon* and *Villosiclava* are more abundant in *fhy3 far1* fungal community of both BRs.

5.3 Discussion

5.3.1 Phyllospheric microbiota in short days

FHY3 FAR1 loss-of-function mutant plants were suggested in the previous investigations of this thesis (4.2.5.2 Transcriptional changes upon biotic challenges), and by Ma *et al.* (2016), to have a constitutively activated SA-dependent defence response in SD that is most likely linked to its enhanced leaf-lesion formation. The *fhy3 far1* (Col-0) mutant showed upregulation of the SA-mediated defence response marker genes *SID2*, *PAD4* and *EDS1*, and Ma *et al*. (2016) confirmed the increased *SID2* expression. Additionally, the group found increased expression of the SA-responsive genes *PR1* and *PR2* in the double mutant. The transformation of *fhy3 far1* mutants with a construct leading to a constitutively overexpression of SALICYLIC ACID 3-HYDROXYLASE (S3H), resulting in a block of SA accumulation, prevented the extensive leaf-lesion formation in SD (Ma *et al*., 2016).

The culture-independent high-throughput amplicon sequencing experiment in this chapter is the first large scale investigation of the impact of constitutively activated SA-mediated defence responses on the phyllospheric microbiota of *A. thaliana* plants.

5.3.1.1 *fhy3 far1* shows an altered bacterial but not fungal community structure

The resulting alterations of the bacterial community included higher bacterial diversity and more evenness relative to WT (Table 5.3, Figure 5.4 a). However, the most abundant bacterial genera were generally found on both WT and *fhy3 far1* mutant plants, but seemed unable to establish a significant abundance and dominance on the latter (Figure 5.5). This demonstrates that it is not simply the higher diversity of genera on the double mutant or absence of specific genera on WT that accounts for their phenotypical distinction. The constitutively activated SA-dependent defence response in *fhy3 far1* mutant plants could disrupt the bacterial community structure and prevent the establishment of dominant taxa, thereby making niche space available for the establishment of more opportunistic or generalist taxa.

The fungal community structure on the other hand was less affected by the constitutively activated SA-dependent defence response in terms of diversity (Table 5.3, Figure 5.4 b). On both plant genotypes in both BRs, a few dominant genera were found (Figure 5.6). However, the *fhy3 far1* BRs grouped in the PCA analysis, while WT BRs diverged (Figure 5.8 b). More than half of the top eight fungal genera, which accounted for 99 % of the richness, showed genotype

preference (Figure 5.9 b), indicating that a genotype-specific effect is exerted on the make-up of the fungal community.

Generally, an increase in diversity is associated with a continuing environmental disruption (Hutchinson, 1961; Chesson *et al.*, 1981; Mao-jones *et al*., 2010), which is most likely the case in *fhy3 far1* mutant plants with respect to their bacterial community, due to their constitutively activated SA-mediated defence response. Thus, a wider influence of the plant defence response on the commensal/mutualistic and non-pathogenic microbial community, which mainly consists of bacteria (Rauw, 2012), is proposed. It is likely that a stable, undisrupted environment would be inhabited by fewer but dominant species, and would ensure the occupation of the majority of niche-space, leaving less niche-space vacant for opportunists to establish themselves. This may even act as a protection against opportunistic pathogens, preventing them from gaining sufficient quorum for an infection of the host plant. Since the establishment of microbial dominance is associated with high competitiveness, often mediated by the ability to produce antimicrobials, a stable environment for the microbes could actually benefit the plant by provision of microbe-produced chemical defence against pathogens at no cost to the plant. Conversely, a disrupted environment could give rise to growth of less competitive taxa, in turn possibly leading to a proliferation of pathogenic species.

5.3.1.2 *fhy3 far1* shows an altered bacterial community composition

Bacterial genera with higher relative abundance hosted by WT plants, within both BRs, are *Sphingomonas, Martelella, Bacillus* and *Brevibacterium*. *Sphingomonas* and *Martelella* abundance contributed most to the PCA projection of WT BR1, while *Bacillus* and *Brevibacterium* contributed most to the WT BR2. The genera *Bacillus* is generally associated with roots but has been isolated from the phyllosphere of a wide range of plants, including *A. thaliana*, maize and rice (Kim *et al.*, 2015; Sartori *et al.*, 2015; Ritpitakphong *et al.*, 2016; Venkatachalam *et al.*, 2016). Bacillus species play well-established protective functions against pests and pathogens in plants and are commercially available as such. For instance, *B. subtilis* is used as biofungicide and *B. thuringiensis* as a bioinsecticide (CEASE® by BioWorks Inc. and Dipel Dust Biological Insecticide by Voluntary Purchasing Groups, Inc.). Phyllospheric *Bacillus* isolates have been demonstrated to act antagonistically against a wide range of fungal plant pathogens (Kim *et al.*, 2015; Sartori *et al.*, 2015) and in *A. thaliana*, *B. subtilis* has been shown to protect against *P. syringae* infection by a combination of Surfactin production, an antibacterial compound, and extensive biofilm

formation (Bais *et al.*, 2004). Additionally, antagonising effects of *B. subtilis* to the powdery mildew fungus *Podosphaera fusca* on melon leaves were shown to be mediated by the antifungal compounds Iturins and Fengycin (Ongena and Jacques, 2007).

Sphingomonas species are ubiquitously found on and isolated form the *A. thaliana* phyllosphere (Bodenhausen *et al.*, 2013; Vogel *et al.* 2016). The genus contains organo-heterotrophic and specialised commensal bacteria on the episphere (Ryffel *et al.*, 2016), found to confer protection against *P. syringae* and considered to act protectively on *A. thaliana* (Innerebner *et al.*, 2011).

Bacillus and *Sphingomonas* are two of a few genera that are transmitted via seeds in WT *A. thaliana* (Truyens *et al.*, 2013), implying a perpetual association and potential attraction or selection by *A. thaliana*. Specific bacterial recruitment by plants was suggested to structure the overall community composition via microorganism interactions (Whipps *et al.*, 2008; Vorholt, 2012) that is certainly dependent on the presence of specific microbial taxa (stochastic process), which could explain the difference between both BRs.

Similar to *Bacillus*, *Martelella* and *Brevibacterium* are generally associated with the rhizosphere, where they promote growth in plants, including *A. thaliana,* but isolation from the phyllosphere of several plant species has also been reported (Izhaki*et al.*, 2011; Martins *et al.*, 2013; Passari *et al.*, 2015; Faisal, 2013; Khan *et al.*, 2016). *Martelella* displayed antagonistic effects on pathogenic fungi and oomycetes (Bibi *et al.*, 2012 and 2013), but the role of the airborne *Brevibacterium* genera (Vokou *et al.*, 2012) in plant defence response has not been investigated yet, other than the production and exudation of 2-butanone (also exudated in large amounts by *Bacillus* species), which attracts ladybird beetles as natural predators of aphids on cucumber seedlings (Song and Ryu, 2013).

Overall, the abundant taxa of phyllospheric bacterial community of WT plants seem to exhibit anti-pathogenic and plant-protective properties.

Bacterial genera with high relative abundance inhabiting the phyllosphere of *fhy3 far1* mutant plants are *Devosia*, *Pedobacter*, *Pricia*, *Taibaiella*, *Rhizobium*, *Chitinophaga*, *Fluviicola*, *Advenella*, *Flavobacterium*, *Rhodanobacter*, *Ochrobactrum*, *Shinella* and *Sphingopyxis*. Many of these taxa were recently shown in sequencing based analyses to inhabit the WT *A. thaliana* phyllosphere (Bodenhausen *et al.*, 2013; Reisberg *et al.*, 2013; Ritpitakphong *et al.*, 2016), but also on the phyllosphere of soybean, clover and rice (Ceuppens *et al*., 2015, which suggests they generally form associations Some of these genera are connected to plant growth promoting and nitrogen cycling rhizobacterial effects in legumes (*Rhizobium*, *Devosia, Ochrobactrum and Shinella*) (Vanparys *et al.*, 2005; Lin *et al.*, 2008 b). Only *Ochrobactrum* was described as being

beneficial to a non-legume. *Ochrobactrum* isolated from the phyllosphere of tea plants inhibits the growth of various fungal plant pathogens (Sowndhararajan *et al.*, 2013). Thus, unlike those abundant genera associated with WT plants, these *fhy3 far1* associated genera appear to be less beneficial in terms of pathogen-protection. This overall absence of evidence of pathogen-protecting effects agrees with the proposal that these genera, which are not highly competitive on WT but abundant on *fhy3 far1* mutant plants, may not produce antimicrobial compounds.

Finally, the remaining of the 20 most-abundant bacterial genera, *Pseudomonas*, *Lysobacter* and *Brevundimonas* were found in the first BR of WT, but without a significant presence in the second WT BR. The possible abundance of these genera on WT, however, could only be confirmed by additional replicates. Similarly, they are all present at low abundance in the *fhy3 far1* BRs. Again, these three genera are described as being associated with significant anti-pathogenic effects in plants and are generally found in the *A. thaliana* phyllosphere (Delmotte *et al.*, 2009; Bodenhausen *et al.*, 2013; Reisberg *et al.*, 2013; Ritpitakphong *et al.*, 2016). The wide-ranging genus *Pseudomonas* does contain phyllospheric pathogens such as *P. syringae* but also unspecified beneficial species protecting against necrotrophic infection with *B. cinerea* (Ritpitakphong *et al.*, 2016). Conversely, though, other environmental *Pseudomonas* species were found to increase herbivory by leaf mining insect (*Scaptomyza nigrita*) in *Cardamine* (bittercress) (Humphrey *et al.*, 2014). This highlights the different ecological roles the species of this genus play, which makes it difficult to speculate on the significance of the *Pseudomonas* findings (without details on the species-level taxonomy of the identified bacteria).

The genus *Lysobacter* contains several species that produce anti-microbial exoenzymes and metabolites (Reichenbach, 2006). *Brevundimonas* species have also shown antifungal activity against *Fusarium oxysporum* on tomato plants (Al attar *et al.*, 2015) and suppression of bacterial blight on ornamental *Anthurium* (tailflower). Interestingly, the isolated species exhibited this protective effect specifically only when it was part of a bacterial community that included *Pseudomonas* and *Sphingomonas* (Fukui *et al.*, 1999).

This latter evidence that certain combinations of bacteria have effects not observed for individual taxa may be of great significance. It has been proposed that it is the competition between bacterial species that leads to the production of the antimicrobial compounds that then affect fungal pathogens (De Boer *et al.*, 2007). This ability to produce antimicrobial compounds is a significant competitive advantage and could explain the presence of the dominant species in WT, whose taxa are all, without exception, associated with protection against pathogens. Bacterial species that lack this genetic prerequisite are outcompeted quickly

in the highly variable and often short-lived habitat represented by the phyllosphere (Vorholt, 2012), resulting in the dominance of a small range of bacterial phyla, seen in various investigated plant species, *A. thaliana* amongst them (Stark *et al.*, 2010).

The observed difference in the bacterial community composition between BRs, whereby plants were grown in the same spatial conditions, but temporally separated, could be attributed to the stochastic presence of primary colonisers at this time that rapidly occupy the niche space. Secondary colonisers need to fit in the remaining niche space (according to stochastic niche theory) and/or represent taxa that favour the habitat that was altered by the primary colonisers. Hence the stochastic process of colonisation shaped the dominance of specific taxa in each BR (Maignien *et al.,* 2014). The most abundant genera on both WT BRs are either *Bacillus* or *Pseudomonas* / *Brevundimonas*. Species within all three genera have plant protective properties, containing high numbers of ribosomal operons, nine to ten (Jarvis *et al.*, 1988; Klappenbach *et al.*, 2000) and four to six (Klappenbach *et al.*, 2000) for the two first mentioned, associated with rapid growth in case of nutrient availability (Klappenbach *et al.*, 2000). This could suggest that functional equivalent taxa occupy WT niche space that is by itself neutral in its dynamics (in agreement with the neutral theory by Hubble, 2001). For *fhy3 far1*, in contrast, the BRs are very similar in composition, perhaps consistent with a continuous habitat disruption due to the constitutively-active defence responses. Secondary colonisers are likely to find niche space and so the structure is less dependent on which species happen to be the primary colonisers. Instead secondary colonisers could represent a wider proportion of the microbes present in the environment.

The bacterial genera identified in the trial run (using a culture-dependent approach) are consistent with those identified by the culture-independent approach, albeit, the number of samples in the trial run was too small to be considered a valid investigation.

The culturable bacterial genera *Bacillus* and *Paenibacillus* were found on both, WT and *fhy3 far1* mutant plants. *Bacillus*, as described before, is known to contain plant pathogens but at the same time species that antagonise pathogens. The same is true for the genus *Paenibacillus* (Niu *et al.,* 2013). The genera *Sphingobium* and *Microbacterium* were specifically found on the *fhy3 far1* mutant plant phyllosphere in the culture-dependent approach. Members of the genus *Sphingobium* are known to be rhizosphere bacteria that cause root disease (van Bruggen *et al.,* 2014, Francis *et al.*, 2014); *Microbacterium* species were reported as pathogens of leaves, and

as pathogens of roots, although they have been shown to have some root protective properties, too (Kaku *et al.* 2000; Rakhashiya *et al.*, 2015; Perera *et al.*, 2007).

5.3.1.3 *fhy3 far1* shows an altered fungal community composition

The fungal community on WT and *fhy3 far1* mutant plants is dominated by Ascomycota, in accordance with previous reports (reviewed by Vacher *et al.*, 2016). Fungal genera with higher relative abundance inhabiting WT plants are *Penicillium*, *Verticillium* and *Engyodontium*, all contributing to the PCA projection of WT BRs. The genus *Penicillium* is as a wide-ranging genus, occurring in both the rhizo- and phyllosphere (Yang *et al.*, 2013), containing plant-protecting species against *Pseudomonas syringae, Verticillium dahlia* and *Fusarium oxysporum* (Hossain *et al.*, 2007; Garcia *et al.*, 2011; De Cal *et al.*, 2000) However, the genus also contains saprophytic species (Raper and Thom, 1949), as well as plant pathogenic species, such as apple mould for instance (Moslem *et al.*, 2010). Its diverse ecological roles make it difficult to conjecture on this finding without taxonomic identification on species-level.

The genus *Verticillium* consists of ten species, of which seven species cause wilt and rot on lettuce and potato for example (Inderbitzin *et al.*, 2013; Barbara and Clewes, 2003). However, plant protecting species, such as *V. dahlia*-2379 against its pathogenic relative *V. dahlia* were observed on tomato (Garcia *et al.*, 2011). Thus, as with *Penicillium*, *Verticillium's* diverse ecological roles make it difficult to conjecture on this finding without taxonomic identification on species level.

The genus *Engyodontium* consists of four entomopathogenic fungi (Bisby *et al.*, 2011; Wu *et al.*, 2016) and the saprophytic, opportunistic *E. album*, found in soil and on plant debris (Augustinsky, 1990), but also in the endosphere of Ginseng plants (Wu *et al.*, 2013). However, it was not described to cause plant disease, rather only mycosis in humans (Macêdo *et al.*, 2007). The marine *E. album* strain LF069 was found to produces antibiotic compounds (Wu *et al.*, 2016). Overall, the genus in association with plants is poorly described and speculations about its high abundance on WT plants are difficult to make.

Fungal genera with higher relative abundance inhabiting the *fhy3 far1* mutant plant phyllosphere are *Villosiclava* and *Trichosporon*. *Villosiclava* is a monotypic genus with *V. virens* as pathogenic species that infects flowers of rice (Fan *et al.*, 2015) and roots, leaves and flowers of *A. thaliana,* causing false smut disease and chlorotic lesions (Andargie and Li, 2016),

respectively. Li *et al.* (2015) tested several biocontrol agents and suggested that *Penicillium oxalcium* antagonises *V. virens*, leading to decreased infection symptoms in rice. The reduced abundance of *Penicillium* in double mutant plants could possibly reduce biocontrol of *V. virens,* but without taxonomic identification of *Penicillium* on species-level, causation cannot be conjectured.

The *Trichosporon* genus contains saprophytic and opportunistic yeasts (*T. asahii* for example) and is mostly described in connection with pathogenicity of humans (Sugita, 2011). Yet, *Trichosporon* spp. were isolated from leaf mould, decayed wood and soil (Sugita *et al.*, 2000). They are not associated with production of antimicrobial compounds (Sugita, 2011). However, on maize kernels, *T. cutaneum* outcompeted other maize-associated yeast, such as *Candida maltose* and *S. cerevisiae* (Nout *et al.*, 1997). Since the genus *Trichosporon* contains cellulose decomposing species that were abundant in senescent oak leaves and leave litter (Voříšková and Baldrian, 2013), it is conceivable that through leaf-lesions on *fhy3 far1* mutant plants, the access to cellulose is facilitated for these saprophytes, creating a more favourable environment than on WT plants.

The remaining highly abundant genera *Fusarium*, *Acremonium* and *Cladosporium* did not show a reproducible pattern and occurred in similar abundance on both genotypes which points to a stochastic pattern. *Fusarium* species are abundant in soil and the plant rhizosphere, but are also found in the phyllosphere of various plants (Nelson *et al.*, 1994), *A. thaliana* amongst them (Horton *et al.*, 2014). They are mostly saprophytic but also pathogenic (Nelson *et al.*, 1994), and were shown to infect aerial parts of cereals and maize (Nelson *et al.*, 1994), as well to cause necrotic leaf-lesions in *A. thaliana* (*F. graminearum*) (Makandar *et al.*, 2010). Nevertheless, endophytic beneficial species and isolates of the otherwise pathogenic *F. oxysporum* were shown to reduce pathogen infection and induce the host plants defence response (Ting, 2013; Porras-Alfaro and Bayman, 2001). Both, *Acremonium* and *Cladosporium* genera mainly consist of saprophytes of plant debris and soil (Guarro *et al.*, 1997; Ogorek *et al.*, 2012), but also plant pathogens, such as *A. strictum* that infects crop plants (Tagne *et al.*, 2002) and *C. fulvum* and *C. cucumerinum*, causing lesions on leaves of tomato and cucumber, respectively (Ogorek *et al.*, 2012). *A. alternatum* on the other hand was reported to antagonise clubroot formation in *A. thaliana,* caused by infection with *Plasmodiophora brassicae* (Jäschke *et al.*, 2010).

Cladosporium spp. and *Fusarium* spp. were described as “opportunistic” endophytes that could easily infiltrate the endosphere of stressed plants, where they are potentially pathogenic (Currie *et al.,* 2013), but are also commonly found as beneficial fungi in the endosphere (Ting, 2013), as

are *Acremonium* species (Liarzi and Ezra, 2013). The utilised extraction method collected epiphytic microbes and plant cells, including their endophytes, which means that the phyllospheric microbe taxa described could consist of epiphytes and endophytes, as well as endophytes that were in the process of entering the plant.

The less abundant genus Candida was also found specifically on *fhy3 far1* and, therefore, also contributed to the distinction from WT. It is more-commonly associated with human disease but has also been found in the phyllosphere of the crop plants potato and cabbage for instance (Kvasnikov *et al.*, 1975), as well as in the phyllosphere wild plants, such as birch trees (*Betula*) (Glushakova *et al.*, 2007). Diverse *Candida* species are utilised as post-harvest biocontrol agents against *Botrytis cinerea and Penicillium* infection of apples and nectarines (Sharma *et al.*, 2009).

The genus *Simplicillium*, another low abundance genus, contributed somewhat to the clustering of WT (through, not specifically labelled in figure 5.9). It contains mostly non-plant pathogenic species, as well as protective species against pathogenic fungi, bacteria and insects on various plant species (Ward *et al.*, 2012; Le Dang *et al.*, 2014; Fernandes and Bittencourt, 2008).

The fungal genera identified in the trial run are also consistent with those identified by the culture-independent method. On both genotypes, *Penicillium, Acremonium, Cladosporium* and *Sarocladium* were found. Furthermore, *Pseudogymnoascus* was found in WT but not *fhy3 far1* mutant plants.

The genus *Penicillium*, as described before, can be saprophytic, pathogenic or plant-protecting, dependent on the species, whereas *Acremonium* and *Cladosporium* are mainly saprophytic on plant debris and soil; *Sarocladium* is known for saprophytic and phyto-pathogenic species (Helfer, 1991; Ayyadurai *et al.*, 2005). *Pseudogymnoascus* species are found as saprophytes in soil, plant debris, roots and as bat (*Microchiroptera*)-infecting pathogens (Sigler *et al.*, 2000; Rice and Currah, 2006), but have not been described as either plant pathogenic or plant protective.

Amongst the phyllospheric community, microbial taxa were found that are rather associated with opportunistic human pathogens, such as *Engyodontium* (*E. album*), *Trichosporon* (*T. asahii*) and *Candida* (*C. albicans*). Parke and Gurian-Sherman (2001) commented that some very effective biocontrol agents are also opportunistic pathogens for humans. Rhizospheric *Stenotrophomonas maltophilia* for example is a biocontrol agent against brown rot causing

Ralstonia solanacearum in eggplant, and causes secondary disease in immune-compromised patients (Hayward *et al*., 2010). The production of antimicrobial components and high competitiveness for nutrients was suggested to be the basis for the wide-ranging occurrence of these taxa. However, an identification of the found phyllospheric taxa on species-level is necessary to conjecture on the findings.

Overall, the fungal results do imply a shift of the fungal phyllospheric community. The *fhy3 far1* mutant was found to host a number of fungal taxa associated with pathogenesis, compared to a predominance of more saprophytic taxa in WT.

Overall, these conclusions on benefit and pathogenicity, however, are made with the reservation that taxonomic identification on genus level makes it difficult to speculations on the significance of these findings. For more substantial speculations, identifications on species and even strain level would be necessary. Different species within one genus and even different strains within one species have been shown to vary in their characteristics. For instance, certain strains of *P. syringae* are well known pathogens on Arabidopsis, whereas certain strains of *P. fluorescens* and *P. aeruginosa* are known to mediate disease resistance in plants (Mercado-Blanco and Bakker, 2007). The saprophytic *Verticillium dahlia* strain 2379 exhibits plant protecting properties against its pathogenic relative *V. dahlia* in tomato (Garcia *et al*., 2011).
Taxonomic identifications on species and strain level, however, would still not suffice to make a clear statement, since taxonomic identifications are based on databases and the different species and strains have only been identified partially thus far. Different strains and even (undiscovered) species could have identical sequences in the regions that are utilised for identification (mainly 16S rRNA gene for bacteria and ITS regions for fungi).

It is also conceivable that the *FHY3 FAR1* loss-of-function affects the endophytic community of the Arabidopsis phyllosphere by mechanisms that are not mediated by increased SA/ROS accumulation. Arnold *et al*. (2003) showed that asymptotic fungal endophytes decrease necrosis on leaves of cocoa tree (*Theobroma cacao*) and death of cocoa tree seedlings when challenged with pathogenic *Phytophthora* species (oomycete). This effect was, however, limited to endophyte-infected tissues and not observed on endophyte free tissue, suggesting the protective effect is not mediated by systemic defence but rather mediated by direct interactions of endophytes with pathogens. Significantly, the antagonising effect of endophytic fungi isolated from cocoa tree leaves on the cocoa tree pathogens *Phytophthora* sp., *Moniliophthora roreri*

and *Crinipellis perniciosa* differed in quality and quantity when the investigations were done on MEA and medium containing leaf extracts of cocoa trees. A sensitivity of the endophytes to the host-specific leaf chemistry for protective effects was concluded. Accordingly, an altered leaf chemistry in *fhy3 far1* plants could result in an alteration of the endophyte community and/or the endophytes effect on interactions between microbes.

5.3 Conclusion

The original hypothesis examined in this chapter proposed that the constitutive SA-mediated defence responses exhibited by the *fhy3 far1* double mutant will be detrimental to both pathogenic and beneficial microbes, alike. It was proposed that the balance between tolerance and defence in the plant immune response may be important in maintaining a habitat for beneficial microbes which may, in turn, provide a degree of defence at no cost to the plant. The investigation in this chapter reveals that the phyllospheric microbial community composition and structure shows major alterations in *fhy3 far1* mutant plants. Double mutant plants had greatly increased bacterial species richness and a more even spectrum of species abundances, compared to a stronger dominance by fewer species in WT plants (altered community structure). Notably, those bacterial taxa becoming dominant in WT plants are associated with the production of antimicrobials.

The bacterial data in particular suggest that microbe-mediated plant protection from pathogens could be viewed as a system property, resulting from the competition between microbes. Those which compete most strongly will be those that produce antimicrobial compounds that act against their competitors. These competitors will, undeniably, include some potential plant pathogens and, thus, the plant will also receive protection from pathogens by tolerating these dominant, antimicrobial-producing taxa. Conversely, in the continually disturbed phyllospheric environment of *fhy3 far1* mutant plants, all microbes are subject to antimicrobial compounds originating from the mutant plant that affect the whole community. This leads to an alteration of the community in favour of non-protective taxa. It is proposed that the same will be true with respect to a normally-activated defence response in WT plants. The activation of defence responses, when a plant is challenged by potential pathogens, will protect the plant, but it will do so at far higher energetic cost than simply allowing the commensal / mutualistic and non-pathogenic microbes to perform this function on the phyllosphere. It is proposed that this will, evolutionary, add greater weight in favour of tolerance as opposed to defence in the balance

between potential responses to a pathogen challenge. Ultimately, of course, the plant must survive and so an immune response will still be required as a defence against a particularly virulent pathogen.

While the phyllospheric fungal community structure showed little change in *fhy3 far1*, the double mutant plant was found to host a number of fungal taxa associated with pathogenesis, compared to a predominance of more saprophytic taxa in the WT plant. It would seem that this is more likely to be detrimental than favourable to the plant. Since bacteria represents the bulk of the microbial community, the abundant presence of bacterial genera that do not produce antimicrobial compounds in *fhy3 far1* mutant plants could possibly have facilitated this shift in the fungal community (de Boer *et al.*, 2007). However, an additional possibility is that the extended leaf-lesions in *fhy3 far1* mutant plants would additionally create a favourable environment for certain fungi.

There does not appear to be a major change in the fungal community structure as there is for the bacterial community. This may be due to the fact that the constitutive SA-mediated defence pathway in *fhy3 far1* is more likely to affect bacteria rather than fungi, which are more often targeted by the JA/ET-mediated defence response. The largest group of pathogenic fungi is of necrotrophic nature (Wang *et al*., 2014). It would be very interesting to investigate the effects of a constitutively activated JA/ET-mediated defence responses on the microbiota in order to determine whether this would have a similar effect on the fungal community structure, as alteration of the SA pathway has on the bacterial community. It could equally be proposed that there may be a shift in balance in favour of tolerance for this pathway too in order to allow establishment of a small number of dominant, non-pathogenic fungi that could benefit the plant by providing a degree of protection from less-competitive, invasive pathogenic fungi.

5.4 Future Work

The SILVAngs QC rejected approximately 30 to 50 % of the total number of uploaded sequences, mostly due to failure to align to the Silva "SEED" ssu rRNA Ref dataset, but it is unknown to what extent prokaryotic and eukaryotic sequences contribute to the rejected group, as this information was not returned by the SILVAngs analysis. FastQC analysis suggested that quality was generally very good, meaning that sequence quality seemed unlikely to be the issue. One exclusion criterion applied by SILVAngs during the initial processing, which checks against the Silva "SEED" ssu rRNA Ref dataset, is an insufficient recognisable length of 16S or 18S sequence

included within the read. Here, an alignment over a region greater than 50 bp is required for further processing by SILVAngs. The Silva "SEED" ssu rRNA Ref dataset is based on a collection of 16S and 18S rRNA gene sequences, but is not publicly known, due to contractual agreements. The commonly used primers for sequencing of the full fungal 18s rRNA gene are NS1 and NS8 (Figure 5.10 a), judging from the 18s rRNA gene sequences found in NCBI GenBank (Sayers *et al.*, 2008), and so it is likely that these SEED 18s rRNA gene sequences are based on these primers. The NS8 primer binding site is situated almost at the end of the 18S gene and a comparison to the binding site of the utilised ITS1F primer (Figure 5.10 a), which is positioned upstream, shows an overlap of 58 bp in the randomly-chosen example of *Peridermium harknessii* (Figure 5.10 b), thereby providing sufficient sequence length to meet the requirement of 50 bp of alignment with a recognised 18S sequence. The 18S rRNA gene seems to be conserved in this region and an alignment of the submitted sequences to the kingdom fungi can reasonably be trusted. However, not all data returned from this sequencing assay may contain the full 58 bp of 18S rDNA and such samples may therefore be rejected.

Future work could involve a repetition of analysis with another analysing software package, such as those offered by the web-based “Galaxy“ suite (Afgan *et al.*, 2016) or “MG-RAST metagenomics analysis server“ (Meyer *et al.*, 2008), which would not necessitate this pre-alignment quality check.

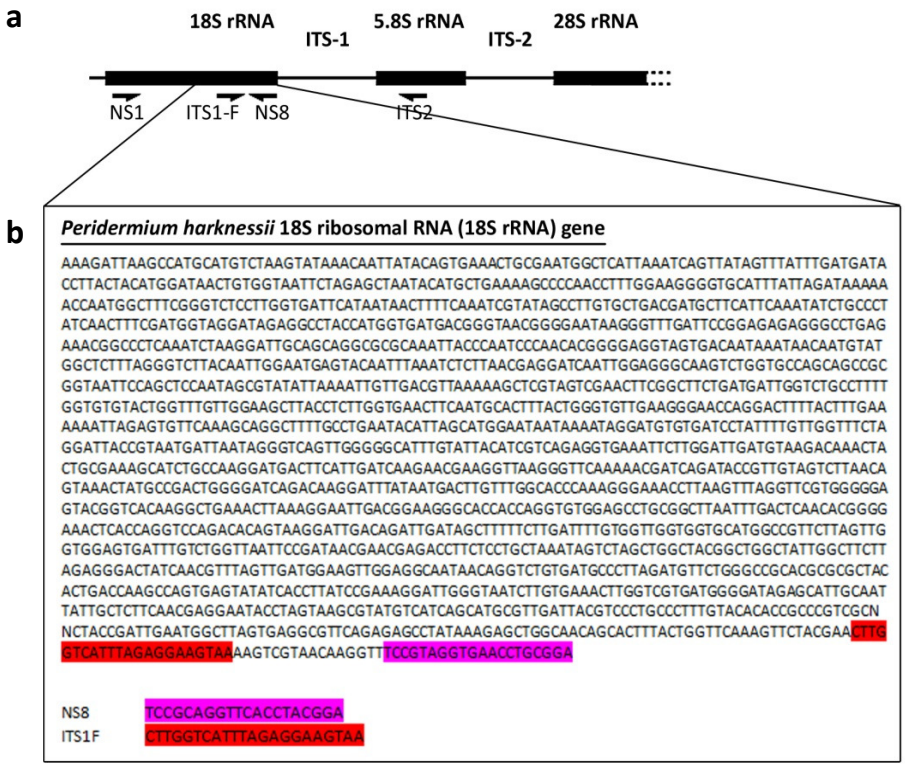

Figure 5.10: Primer binding sites for NS1, ITS1-F, ITS2 and NS8 primers in the fungal rRNA gene a) in principle and b) in *P. harknessii* (GenBank: M94339.1), according to White *et al.* (1990).

Future investigations could also be aimed at investigating how constitutively activated SA-mediated defence responses influences the root microbial community. It would be especially interesting to investigate the root endosphere and its plant growth promoting microbes. Since the phyllospheric microbiota showed substantial alterations, the rhizospheric microbiota (including the beneficial growth promoting taxa) could also be affected.

6 GENERAL DISCUSSION

In *A. thaliana*, the transcription factors *FHY3* and *FAR1* were shown to function in several mechanisms, such as resetting the circadian clock (1.1.4.4 *FHY3* and *FAR1* in integration of red light to the circadian rhythm), flowering (1.1.5 *FHY3* and *FAR1* in flowering), chloroplast division and chlorophyll biosynthesis (1.1.6 *FHY3* and *FAR1* in chloroplast division and chlorophyll biosynthesis), shoot branching and plant architecture (1.1.7 *FHY3* and *FAR1* in shoot branching and plant architecture), as well as ABA-signalling (1.1.8 *FHY3* and *FAR1* in Abscisic Acid signalling). Loss-of-function of both genes leads to phenotypic alterations; double mutant plants exhibit extensive leaf-lesion formation and dwarfing, which is more pronounced when they are grown in SD (3.2.1 Lesion formation phenotype of *fhy3 far1* mutants with Nossen ecotype). Additionally, FHY3 and FAR1 were suggested to act in SA-mediated defence response in Arabidopsis (Ma *et al*., 2016). The work carried out during this PhD advanced the knowledge on the effects of FHY3 and FAR1 in Arabidopsis, and suggests that the observed downregulation of SA- and JA/ET-associated defence response marker gene expression in *fhy3 far1* mutant plants could be the result of negative regulatory feedback (6.4 Future outlook and impact of the work carried out) (Figure 6.1).

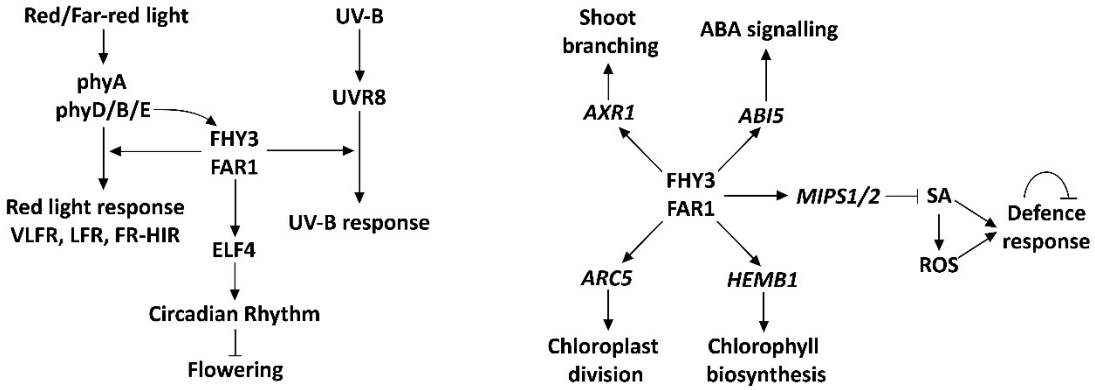

Figure 6.1: Schematic diagram summarizing the state of research on the involvement of FHY3 and FAR1 in a) red, far-red and UV-B light responses, light signal integration to the circadian clock and flowering, and in b) shoot branching, chloroplast division, chlorophyll biosynthesis, abscisic acid (ABA) and salicylic acid (SA) signalling (in reference to Li *et al*., 2011; Stirnberg *et al*., 2012; Gao *et al*., 2013; Tang *et al*., 2013; Wang and Wang, 2015; Ma *et al*., 2016), and defence response.

6.1 *FHY3* and *FAR1* in defence response signalling

Global transcript analysis based on an Affymetrix chip in this thesis revealed a downregulation of negative regulators of PCD. This finding agrees with the result of Ma *et al.* (2016)'s investigations. The researchers found that *MIPS1* and *MIPS2,* the encoding genes of two essential enzymes in the *myo*-inositol (MI) biosynthesis pathway, are direct targets of FHY3 and FAR1, and that their expression is reduced in *FHY3* and *FAR1* loss-of-function mutants. The increased PCD in *fhy3 far1* mutants was proposed to occur due to an impaired SA homeostasis, caused by the cessation of MI- and/or inositol derivate-mediated prevention of SA accumulation.

The link between MI and SA biosynthesis was investigated by Chaouch and Noctor (2010) in *cat2* mutant plants. These mutant plants experience high oxidative stress (accumulation of H_2O_2 due to reduced scavenging), display leaf-lesion formation and have reduced levels of MI. Chaouch and Noctor (2010) were able to rescue the mutant's phenotype by application of MI that was shown to supresses *SID2* transcript accumulation, or by introducing a *SID2* loss-of-function mutation. In both cases (*cat2 sid2* double mutant and *cat2* single mutant treated with MI), however, the oxidative stress (H_2O_2-levels) was not found to be decreased; the SA content on the other hand was decreased below WT levels. The group suggested that the oxidative stress / H_2O_2 in *cat2* mutants triggers SA accumulation by inducing ICS1/*SID2, and* MI would dampen this SA accumulation. Since *SID2* expression and SA levels were not affected by MI treatment in WT (Col-0) plants, which do not experience increased oxidative stress, it was proposed that a prevention of SA accumulation below the level in WT requires simultaneous oxidative stress. The group proposed a regulatory mechanism, in which MI acts as a checkpoint that regulates SA production (MI up- or downregulates SA biosynthesis) in response to oxidative stress. The resulting SA levels would then regulate PCD and lesion formation (*cat2* mutants, when concurrently treated with MI and SA, restored leaf-lesion formation) (Figure 6.2).

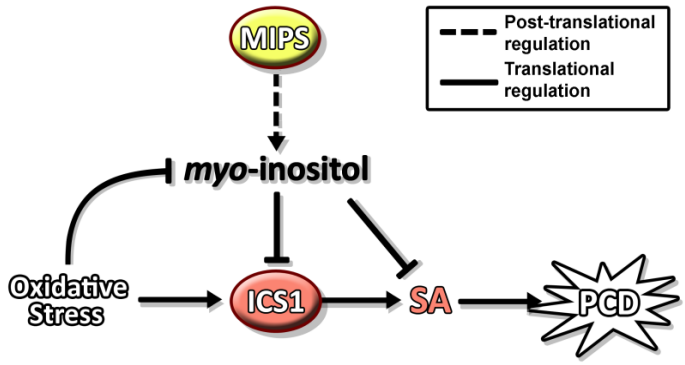

Figure 6.2: Schematic of interactions between oxidative stress, MI and SA to regulate PCD. MIPS = *myo*-inositol phosphate synthase, ICS1 = isochorismate synthase 1, SA = Salicylic Acid, PCD = programmed cell death (in reference to Chaouch and Noctor, 2010).

An impaired MI biosynthesis in *fhy3 far1* mutants would suggest a reduced functionality of this MI-checkpoint. Therefore, SA accumulation could be inappropriately induced by oxidative stress. The impaired MI biosynthesis in *fhy3 far1* mutants would not be the cause for the leaf-lesion formation, but rather lead to an amplification of oxidative stress-mediated SA accumulation. The cause for the oxidative stress, however, remains elusive.

The increased severity of leaf-lesion formation in SD could suggest that possible impaired mechanisms that cause oxidative stress depend on the night length, since mutant plants grown in LD and constant light showed less leaf-lesion formation (Ma *et al*., 2016). *fhy3 far1* mutant plants were found to transcriptionally downregulate SA- and JA/ET-signalling associated genes during the night time in SD, as shown in the *fhy3 far1* microarray analysis in this thesis. Ma *et al*. (2016)'s microarray analysis, which was based on *fhy3 far1* mutant plants sampled during the day, conversely showed increased SA- and JA/ET-signalling associated gene expression. Increased oxidative stress during the long night in SD could lead to SA accumulation during this time, which in turn might activate feedback mechanisms, leading to the downregulation of SA-, as well as JA/ET-signalling associated genes specifically in the night time.

An effect of the *fhy3 far1* double mutation on other mechanisms was also suggested by Ma *et al.* (2016). They found that a constitutively overexpression of *MIPS1* in *fhy3 far1* background was not sufficient to completely rescue the mutant phenotype. This was especially obvious in SD. The remaining (but reduced) leaf-lesion formation could be caused by MI-independent mechanisms, as suggested by Ma *et al.* (2016), or represent the oxidative stress that actually triggers the SA accumulation that is mediated by the impaired MI biosynthesis in *fhy3 far1* mutants. A source of oxidative stress could be the increased accumulation of ROS in SD grown plants that is needed to change the cells' redox state and thereby regulate the starch

metabolism (Lepistö and Rintamäki, 2012; Gibon *et al*., 2004; 1.2.8 Circadian rhythm and pathogen defence response).

Investigations are needed to unveil further causes for the leaf-lesion formation in *fhy3 far1* mutants. Impaired mechanisms could possibly be found in chloroplasts, mitochondria or peroxisomes, which are cell compartments that produce high levels of ROS, and are responsible for oxidative stress (Foyer and Noctor, 2003).

In this thesis, the response of *fhy3 far1* mutant plants to a range of biotic challenges, represented by the hemibiotroph *P. syringae*, the necrotroph *B. cinerea*, the PCD-inducing mycotoxin FB1 and the MAMP chitin, was also accessed. These challenges often resulted in a negative regulation of the defence response-associated marker gene expression in *fhy3 far1* mutants contrary to WT. Here, the threshold of the proposed feedback mechanism could have been reached, leading to negative feedback on the plant defence in order to prevent potentially very-damaging excessive responses.

Negative feedback on defence response-associated gene expression has been suggested before. For instance, upon pathogen attack and subsequent ROS accumulation, MAPK cascades were shown to be activated by ROS. In a MAPK cascade downstream of ROS accumulation, consisting of *MAPK/ERK KINASE KINASE1 - MAPKK KINASE2 - MAP KINASE4/6* (*MEKK1 - MKK2 - MPK4/6*), *MPK4* was found to be a negative regulator of SAR in *A. thaliana* (Gao *et al.*, 2008; Kong *et al*., 2012) (FHY3 and FAR1 are negative regulators of SA). Pitzschke *et al*. (2009) investigated *MPK4* loss-of-function mutant plants and found that these plants displayed a dwarf phenotype, constitutive expression of PR genes, increased production of SA and ROS, as well as extensive PCD that is similar to the one seen in *fhy3 far1* mutant plants. The group also found that *mpk4* mutants showed altered expression of SA- and ROS-regulated genes, contrary to WT. They suggested that increased accumulation of proteins from the constitutively activated SA-mediated gene expression could, after reaching a threshold, act as negative regulators of SA-mediated gene expression. It was proposed that this mechanism was in place to prevent interference of excessive stress gene products with developmental processes of the plant. In JA/ET-mediated defence response, *MPK4* has been described as a positive regulator. *mpk4* mutants do not induce JA/ET-associated defence response marker genes such as PDF1.2a in response to JA or ET. Contrary to the proposed negative feedback on JA/ET-mediated defence response in *fhy3 far1* mutants (3.2.3.4 Misregulation of PCD and defence response signalling, 3.2.4.5 Transcriptional changes upon biotic challenges), the non-activation of JA/ET-associated

defence response was suggested to be caused by the absence of MPK4's inhibitory activity on *EDS1/PAD4* that, in turn, antagonise JA/ET signalling (Brodersen *et al*., 2006)

The suggested feedback regulatory mechanism in *fhy3 far1* mutants could be associated to accumulation of SA and could involve *NON-EXPRESSOR OF PR1* (*NPR1*) and *SALICYLIC ACID BINDING PROTEIN 3* (*SABP3*) for instance. *NPR1* encodes a very important regulator of defence response downstream of SA (*NPR1* loss-of-function mutants have an impaired PR-gene expression and are susceptible to pathogens) that is present as a homopolymer in the cytoplasm. SA accumulation changes the redox state of cells, leading to monomerisation of NPR1. NPR1 monomers then translocate to the nucleus, where they activate the expression of defence response genes. These defence response genes, however, positively and negatively regulate SA-mediated defence response; *WRKY18*/*53*/*54*/*70* positively and *WRKY38*/*62* negatively regulate SA-mediated defence (Vlot *et al.*, 2009). In addition, nitrogen species, the signalling molecules generated upon pathogen challenge, are utilised for S-nitrosylation (addition of a nitric oxide (NO) moiety) of NPR1. S-nitrosylation was found to facilitate oligomerisation of NPR1 and thereby supresses SA-mediated defence response (Tada *et al.*, 2008). Cytosolic *NPR1* has been suggested to be crucial for the cross-talk between SA and JA signalling by inhibiting JA signalling. *npr1* mutants do not show a SA-mediated suppression of JA-associated genes (Koorneef and Pieterse, 2008). It could be argued that the increased SA levels in *fhy3 far1* mutants would lead to a removal of NPR1 from the cytosol and facilitate its accumulation into the nucleus, and, thereby, reducing NPR1's inhibitor activity on JA signalling. However, *NPR1* expression has been shown to increase upon SA treatment (Dong, 2004), resulting in higher levels of cytosolic NPR1 and subsequently a possible inhibition of JA signalling. This could point to a possible negative feedback on JA-associated genes in *fhy3 far1* mutants (3.2.3.4 Misregulation of PCD and defence response signalling, 3.2.4.5 Transcriptional changes upon biotic challenges) mediated by cytosolic NPR1.

The chloroplast located *SABP3*, encoding a carbonic anhydrase, was found to be linked to defence response in *A. thaliana* and tobacco. Its carbonic anhydrase (CA) activity is required for resistance against *P. syringae*. S-nitrosylation of SABP3 causes the reduction of the protein's SA-binding capacity and carbonic anhydrase (CA) activity. The reduced CA activity was suggested to decrease fatty acid biosynthesis in the chloroplast and thereby lipid based defence response signals (such as 12-oxophytodienoic acid that is also further converted to JA in the peroxisome (Stintzi *et al.*, 2001)). S-nitrosylation could, thereby, represent a negative feedback loop on defence response (Slaymaker *et al*., 2002; Wang *et al*., 2009).

The proposed feedback regulatory mechanism on plant defence response could differ in threshold setting during day and night. A lower setting during the night could be in place to prevent resource allocation to defence mechanisms and instead channel them to growth mechanisms, since plant growth mainly takes place at night (Smith and Stitt, 2007),

The search for misregulated genes that could contribute to the leaf-lesion formation in *fhy3 far1* mutants found an upregulation of the defence response-related, PCD-inducing *CRK13*, and a downregulation of the PCD-inhibiting *MC2* in *fhy3 far1* mutant plants during the *fhy3 far1* microarray analysis. This suggested a possible contribution of both genes to the phenotypic alteration in the double mutant. However, *CRK13* overexpression and *MC2* loss-of-function mutant plants were found to show only little similarity of defence response gene transcripts with *fhy3 far1* mutant plants upon challenge with the biotic stressors *P. syringae*, *B. cinerea*, FB1 and chitin. This suggested that both misregulated genes are unlikely to be part of the primary reasons for the observed increased leaf-lesion formation in *fhy3 far1* mutants. Future investigations could concentrate on the other nine found misregulated candidate genes in *fhy3 far1* that are associated with defence response and control of ROS/PCD: *UVR2, ARD1*, Unnamed-disease resistance protein At4g11340, *SUV2, ATCSA-1, ERF6, RbohD, GIM1* and *ERF4* (4.2.1 *fhy3 far1* microarray analysis for disrupted FHY3 and FAR1 target genes involved in defence response). *ADR1* and Unnamed-disease resistance protein At4g11340 encode NB-LRR disease resistance proteins and were upregulated in *fhy3 far1* mutants. If the upregulation of these genes is part of the primary cause for leaf-lesion formation in *fhy3 far1* mutants, overexpressor mutants of these two genes are predicted to exhibit leaf-lesions, and defence response marker gene expression would be expected to be similar to that found in *fhy3 far1* mutants. *UVR2, SUV2* and *ATCSA-1* are associated with DNA damage response/maintaining genome integrity and were also upregulated in in *fhy3 far1* mutants. *UVR2, SUV2* and *ATCSA-1* could be upregulated to counteract increased DNA damage and PCD. Investigations could aim to localise the proteins by fusion to a marker such as fluorescent protein and see if they localise in areas of lesions or increased ROS accumulation in *fhy3 far1* mutant leaves.

ERF6 and *RbohD* are involved in ROS response and ROS production and were downregulated in *fhy3 far1* mutants. If the downregulation of *ERF6* is part of the primary cause for leaf-lesion formation in *fhy3 far1* mutants, the loss-of-function mutant is predicted to exhibit leaf-lesions, and defence response marker gene expression is predicted to be similar to that found in *fhy3 far1* mutants. Peroxidases have been suggested to initiate ROS accumulation/the oxidative burst upon pathogen recognition. NADPH oxidases such as RbohD have been suggested to amplify the

ROS accumulation, since RBOHD (and RBOHF) was only activated in the presence of H_2O_2 that is produced by peroxidases (Doehlemann and Hemetsberger, 2013). The downregulation of *RbohD* in *fhy3 far1* mutants could be part of negative feedback to prevent further ROS accumulation and ROS-mediated defence response signalling. Ma *et al*. (2016) (partially) rescued the H_2O_2 accumulation phenotype of *fhy3 far1* mutants in SD and LD by introducing *MIPS1* overexpression and S3H overexpression. In this mutant, *RbohD* expression would be expected to be at WT level. *GMI1* is involved in DNA damage response and was downregulated in *fhy3 far1* mutants. If the downregulation of *GMI1* is part of the primary cause for leaf-lesion formation in *fhy3 far1* mutants, the loss-of-function mutant is expected to exhibit leaf-lesions. *GMI1* expression is expected to be downregulated at the site of lesion formation and ROS accumulation, which could be investigated by fusion of a fluorescent marker protein to the GMI1 protein and DAB staining.

ERF4 negatively regulates JA-mediated defence response and was downregulated in *fhy3 far1* mutants. This could indicate negative feedback on JA/ET-mediated defence response. Similar to *RbohD,* the *fhy3 far1 MIPS1* overexpression or *fhy3 far1* SH3 overexpression mutant is expected to have WT levels of *ERF4* expression.

Future experiments to investigate the proposed negative feedback on SA- and JA/ET-signalling-dependent defence response in *A. thaliana* could aim at measuring the defence response associated signalling molecules SA and JA/ET throughout the day and night in SD conditions, as well as upon treatment with the utilised biotic stressors *Pst* DC3000, *B. cinerea*, FB1 and chitin. Other defence response inducing stressors such as victorin, a PCD inducing agent, *Xanthomonas campestris*, a biotrophic bacterium, and *Peronospora parasitica*, a biotrophic oomycete could be utilised to further determine *fhy3 far1* mutants' reaction to biotic stressors.

For this purpose, defence response associated marker gene investigation could be expanded on and include the SA-dependent *NONEXPRESSOR OF PR GENES 1* (*NPR1*) that was found to regulate PR gene expression and is a regulator of SAR (Koornneef and Pieterse, 2008; Maier *et al*., 2011), the JA-associated *JASMONATE RESISTANT 1* (*JAR1*) that is involved in JA biosynthesis (Kazan and Manners, 2008), and the JA and ET-responsive *ETHYLENE RESPONSE FACTOR1* (*ERF1*) that was shown to be involved in resistance to necrotrophic pathogens (Lorenzo *et al*., 2003).

By measuring defence response expression and SA levels throughout the day, it could be determined if the proposed negative feedback on defence response-associated gene expression is associated with decreased SA-levels or if the negative feedback acts downstream of SA signalling. Total and free SA levels (free SA and glucoside conjugate SA (SAG)) could be measured

by HPLC (Verberne *et al*., 2002).

Additionally, defence associated mechanisms could be studied, such as callose deposition by histochemical staining (aniline-blue) and fluorescence microscopy (Nguyen *et al.*, 2010), and camalexin (a phytoalexin) production by fluorospectrometry (Ren *et al*., 2008; Beets and Dubery, 2011).In the course of the investigations, ecotype-specific differences in WT and *fhy3 far1* mutants with Col-0 and No-0 ecotype were observed. Phenotypic comparisons of SD-grown plants found a more extensive leaf-lesion formation in *fhy3 far1* mutant plants with No-0 ecotype. Leaf-lesions also started to form earlier here than in *fhy3 far1* mutants with Col-0 ecotype. Similar differences in the severity of the dwarf phenotype were observed; dwarfing was more pronounced in No-0 background. Overall, WT, as well as *fhy3 far1* mutant plants with No-0 ecotype seemed to be smaller than with Col-0 ecotype. The biotic stressor assay also showed ecotype-specific differences in WT and *fhy3 far1* mutants with Col-0 and No-0 ecotype. Similar differences were reported by Gao *et al.* (2008). *MPK4* loss-of-function in Landsberg (Ler-0) background resulted in SA accumulation and a constitutively expression of *PR* genes, but no lesion formation. The loss-of-function mutation in Col-0 background, on the other hand, resulted in additionally occurring PCD, which lead to death at seedling stage.

Overall, the biotic stressor assays demonstrated the extreme complexity of the plant defence response and that it is not merely based on simple upregulation of defence-associated genes. Defence involves interconnected regulatory mechanisms so that the plant can adjust its response to specific pathogens.

6.2 Effect of *FHY3 FAR1* loss-of-function on phyllospheric microbiota

Investigations of detrimental effects of a constitutively activated defence response in *fhy3 far1* mutant plants on their phyllospheric microbial community showed greatly increased bacterial species richness and a more even spectrum of species abundances. WT, in contrast, displayed a stronger dominance by fewer species that, interestingly, were associated with the production of antimicrobial compounds. This was not the case for those in *fhy3 far1* mutants. The fungal community in *fhy3 far1* mutants contained taxa that are rather associated to pathogens, whereas the taxa in WT are rather associated to saprophytes (and plant protective fungi). Based on these findings it was proposed that the plant protection from pathogens by beneficial microbes could be viewed as a community feature, resulting from the competition between microbes. This feature is impaired in the continually disturbed phyllospheric environment of

fhy3 far1 mutant plants, where all microbes are subject to antimicrobial compounds of the constitutively activated plant defence response. A community alteration to non-protective taxa is the consequence. For the *fhy3 far1* mutant it means that the inferred production of plant-antimicrobial compounds do indeed protect the plant, but at far higher energetic cost than simply having commensal / mutualistic and non-pathogenic microbes conduct the protection against pathogens.

Examples of reported plant-protecting bacteria that could be affected by a constitutively activated defence response in crop plants are the bacteria *Pseudomonas fluorescens* and *Curtobacterium flaccumfaciens*.
P. fluorescens was reported to be a biocontrol agent against several rice disease causing pathogens. This beneficial bacterium reduced the *Sarocladium oryzae*-caused sheath rot by up to 40 % when applied before pathogen infection, the *Rizoctonia solani*-caused sheat blight by up to 50 %, *Pyricularia grisea*-caused leaf blast by almost up to 80 %, as well as the *Sarocladium oryzae*-caused sheath rot and *Sclerotium oryzae*-caused stem rot. *P. fluorescens*-mediated disease suppression was suggested to be caused by induction of systemic plants resistance and the production of antimicrobial compounds (Vasudevan *et al.*, 2002).
The endophytic *C. flaccumfaciens* was suggested to protect citrus plants from the bacterial pathogen *Xylella fastidiosa* that infects, besides citrus plants, a wide range of crop plants, such as grapevines and olive trees. *C. flaccumfaciens* was frequently isolated from *X. fastidiosa*-infected but asymptomatic *Citrus reticulate* and *C. sinensis* and was reported as biocontrol agent. The bacterium acts via induction of the plant resistance and production of antibiotics (Araujo *et al.*, 2002).

The impact of a constitutively activated defence response on the phyllospheric microbial community is very sparsely investigated. Kniskern *et al.* (2007) were the first to investigate the effect of elevated SA-mediated defence response on the phyllospheric bacterial community of *A. thaliana* plants in a natural population in Michigan, USA. WT (Col-0) plants were treated with SA and the phyllospheric bacterial community of the endo- and the episphere investigated in a limited culture-dependent approach, utilising 16S rRNA sequencing-based taxonomic identification. The group found a lower bacterial diversity of the endophytic bacterial community, but no effect on the diversity of the epiphytic community, after induction of SA-mediated defence response. This finding is contrary to the culture-independent approach of this

thesis that showed increased phyllospheric bacterial diversity. Here, no distinction between endo- and episphere was made, but it seems likely that this difference is due to the difference between culture-dependent and culture-independent approaches. Culture-based approaches are limited in that they are estimated to capture only a low single digit percentage (0.1 to 5 %) of the microbial community due to the dependency on a cultivation step. Even if several different growth media are used for cultivation, metabolic/nutritional and physiological/environmental requirements for microbes can be very specific and are often unknown. Additionally, fast growing species would out-compete slower growing ones, most likely leading to a further loss of microbial species (Wagner *et al*. 1993; Müller and Ruppel, 2014). Nevertheless, Kniskern *et al.* (2007) identified pathogenic species (*Xanthomonas campestris*, *Pseudomonas viridiflava and P. syringae,* and *Agrobacterium tumefaciens*), as well as *Bacillus cereus* that is known for beneficial strains, to dominate overall in the endosphere of SA-treated and untreated plants. The more diverse WT epiphytic community was, overall, dominated by saprophytes (*Nocardia corynebacteroides*, *Curtobacterium* spp. and *Flavobacterium* spp.) and pathogens (X. *campestris and A. tumefaciens*).

The group did not analyse the community ecology but according to the stated bacterial abundances in SA-treated and untreated plants, only one dominant species, the pathogenic *X. campestris*, was less abundant in the endosphere after SA treatment. This suggests that the induction of SA-mediated defence response only had little effect on the dominant bacterial taxa of the phyllospheric endosphere, at least on the cultivable fraction. More interesting alterations took place amongst the less abundant species. Here, two plant-protective species were only present in the endosphere of untreated plants, and not found in plants after induction of SA-mediated defence response: 1) *Rhodococcus erythropolis*, which produces antibiotics (Kitagawa and Tamura, 2008) and was shown to disrupt communication of Gram-negative soft-rot bacteria (by interfering with quorum sensing), thereby preventing plant disease (Latour *et al.*, 2013), and 2) *Pseudomonas fluorescens*, which suppresses plant pathogens via antibiotic productions (Paulsen *et al.*, 2005).

Less abundant species in the episphere that were only present in untreated plants and not after induction of SA-mediated defence response, were also mostly species that produce antimicrobial compounds: *B. megaterium* (Malanicheva *et al.,* 2012), *Sphingomonas* sp. (Fukui *et al*., 1999), *P. fluorescens*, *R. erythropolis*, *B. cereus* (Silo-Suh *et al*., 1994) and *Pantoea ananatis* (Smith *et al.*, 2013).

These results, therefore, conform to the findings of the culture-independent approach of this thesis, which suggest that a constitutively activated SA-mediated defence response continually

disturbs the phyllospheric environment and the whole microbial community is subject to inferred antimicrobial compounds originating from the mutant plant. This leads to a community shift to rather non-protective taxa.

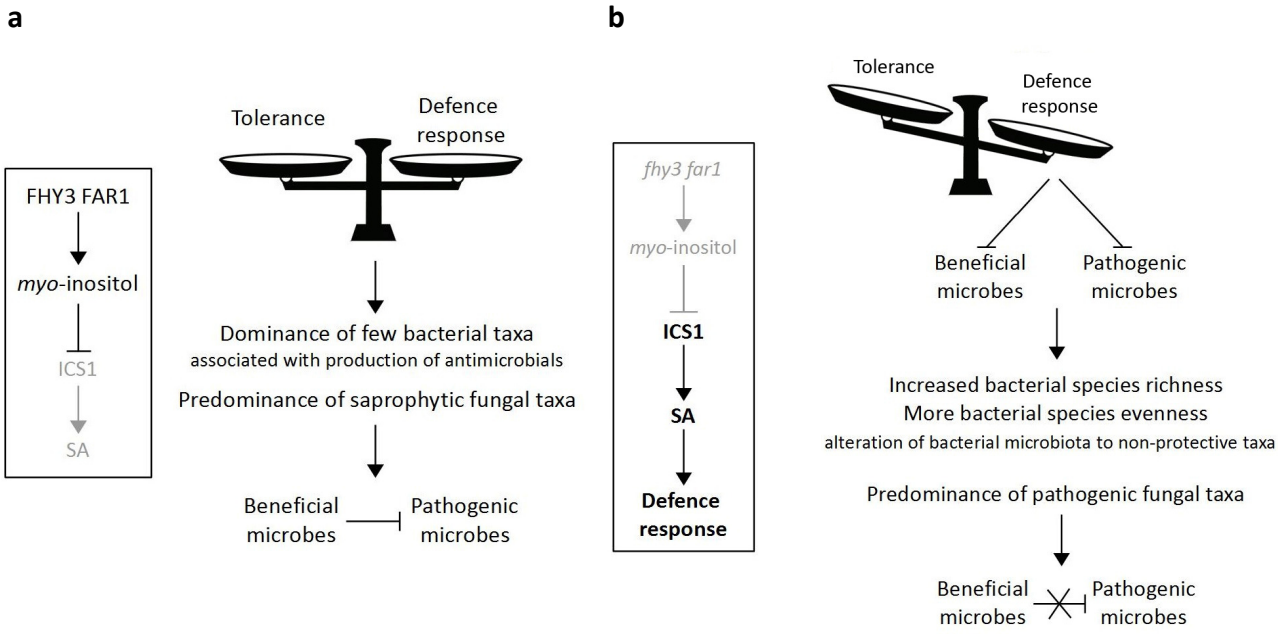

Figure 6.3: Schematic depiction of the hypothesised mechanism of *FHY3 FAR1* (a) and *fhy3 far1* mutation (b) on the phyllospheric microbiota of the phyllosphere in SD grown *A. thaliana* plants.

6.3 Effects of disease treatments on phyllospheric microbiota

Interesting questions are how plant disease treatments (fungicides and bactericides) used by farmers might disrupt the beneficial microbial community of crop plants and if there are similarities to the observed alterations of the microbiota on *fhy3 far1* mutant plants.

Reported effects differed between specific crop plants and applied agents. Karlsson *et al*. (2014) investigated the effect of several fungicides and reported an alteration of the fungal community composition on the phyllosphere of wheat. Fungicide treatment led to decreased fungal species richness and evenness. The fungicide treatment-altered community structure showed reduced abundance of saprobes, and, interestingly, a trend of increased abundance of certain wheat pathogens. However, another pathogen, *Puccinia striiformis,* that dominated the fungal community of untreated wheat, showed a strongly decreased abundance after fungicide treatment (taxonomic identification was based on culture-independent 18S high throughput sequencing). Fungicide resistance by some fungal taxa was attributed to the latter finding.

Fungicide treatment was also shown to affect the bacterial community. Application of the fungicide Enostroburin (used against powdery mildew) on wheat altered the phyllospheric bacterial community structure and increased bacterial diversity (investigation was based on culture-independent 16S rDNA restriction fragment length polymorphism (RFLP) analysis and PCR with denaturing gradient gel electrophoresis (PCR-DGGE) analysis). It was speculated that the resources previously occupied by fungi (carbon and nitrogen source) were available for bacteria after fungicide treatment, leading to growth and establishment of certain bacteria (Gu *et al.*, 2010).

Even though the community ecology in terms of microbial competition was not discussed in these studies, it is possible that the altered abundances of pathogen-inhibiting fungi after fungicide treatments could have contributed to the increased abundance of certain wheat pathogens found by Karlsson *et al.* (2014).

Contrary to these studies, Yashiro and McManus (2012) reported no alterations of the phyllospheric bacterial community of apple tree leaves after long term treatment with streptomycin (streptomycin is used against the fire blight-causing *Erwinia amylovora*). This agent did not disrupt the phyllospheric microbial community upon application (investigation was based on taxonomic identification by culture-independent 16S rDNA high-throughput sequencing). However, the percentage of cultured phyllospheric bacteria that were resistant to streptomycin was lower on streptomycin-treated plants than on untreated plants. This finding, however, could not be explained (cultured bacteria were not taxonomically identified in this latter case).

Similar to these findings, Ottesen *et al.* (2015) reported only little alteration of the phyllospheric microbial community of tomato plants after treatment with commercially available copper oxychloride based (Kocide) and acibenzolar-S-methyl (Actigard) agents. Copper oxychloride inhibits fungal and bacterial growth, and acibenzolar-S-methyl, a BTH, potentially induces SAR in plants. The group found reduced abundance of some Gammaproteobacteria, including a trend of reduced abundance of the pathogenic *Salmonella,* after treatment with both agents. The fungal community, however, was not affected (taxonomic identification was based on culture-independent 16S and 18S high throughput sequencing). The most significant effect on the bacterial community found in this investigation was independent of treatments and depended on the time of sampling (September to October).

Overall, the farming treatments seem to have little effect on the phyllospheric microbial community (Table 6.1). Even when some effect was shown after fungicide treatment, it could be argued that combatting one fungal pathogen leads to the establishment of other fungal

pathogens. However, investigations are rare and those executed did not examine the ecology of the phyllospheric microbial community. It would be important to look more at this, using culture independent approaches.

Table 6.1: Effects of fungicide and bactericide treatments on phyllospheric microbiota of different plant species observed in several investigations, seq. = sequencing

Plant	Treatment	Effect on phyllospheric microbiota	Reference
Wheat	Fungicide	Decreased fungal species richness and evenness, reduced abundance of saprobes, trend of increased abundance of certain wheat pathogens, decreased abundance of pathogenic *Puccinia striiformis* that dominated the fungal community of untreated wheat	Karlsson *et al*., 2014
Wheat	Fungicide	Increased bacterial diversity	Gu *et al.*, 2010
Wheat	Fungicide	Increased abundance of certain wheat pathogens due to possible altered abundances of pathogen-inhibiting fungi	Karlsson *et al.*, 2014
Apple	Bactericide	No disruption of the phyllospheric microbial community, specifically no alterations of phyllospheric bacterial community,	Yashiro and McManus, 2012
Tomato	Fungicide/ Bactericide	Little alteration of the phyllospheric bacterial community, no alteration of fungal community, reduced abundance of some *Gammaproteobacteria*, trend of reduced abundance of pathogenic *Salmonella,* most significant effect on bacterial community was depended on the time of sampling	Ottesen *et al.*, 2015

Future investigations could aim to identify whether *fhy3 far1* plants are more susceptible to necrotrophic pathogens, since SA-mediated defence response, and the associated increased PCD, would rather support necrotrophic pathogen infection (Glazebrook, 2005). Infection with the necrotroph *B. cinerea*, in the course of the biotic stressor assay of this thesis, after all, resulted in increased DAB staining and therefore H_2O_2 production, and in a more severe and comprehensive leaf chlorosis in *fhy3 far1* mutant than in WT plants (Figures 3.9, 3.8 and 4.8).
Future experiments could also utilise lower-than-quorum infections of *fhy3 far1* mutant plants with biotrophs and necrotrophs to investigate the pathogens' establishment on the phyllosphere and possibly associated alteration of the microbiota. The decreasing prices for culture-independent high-throughput sequencing could allow for larger pathogen infection experiments with different concentrations that would correspond more closely to field conditions of pathogens, or over a time course. This could possibly reveal new plant-protecting phyllospheric microbes or microbial interactions that contribute to plant protection.

Studies of a similar direction could aim to investigate the effects of a constitutively activated JA/ET-mediated defence responses on the phyllospheric microbiota in order to determine whether this would have a similar effect on the microbial community structure, as alteration of the SA-mediated defence response showed.

6.4 Future outlook and impact of the work carried out

Due to the world's exponentially growing population (Roser and Ortiz-Ospina, 2017) food production including crops needs to increase. It was estimated that worldwide crop production has to increase two-fold in order to cover the demand in 2050 (Tilman *et al*., 2011). A key factor in meeting this goal would be improving disease resistance of crop plants. This has been done by selective breeding for disease resistance and application of disease treatments (fungicides and bactericides). This, however, could be accompanied by detrimental effects. Increasing plant defence response could lead to resource allocation to defence response mechanisms (5.1.3 Life history theory and constitutively activated defence response), potentially resulting in decreased yield. Application of disease treatments could quickly result in resistance of the pathogen to the treatment, and is overall deemed to be cost ineffective. For instance, approximately 16 billion US dollars are invested annually into fungicides that prevent an estimated loss of 20 % of global crop production. Application of disease treatments additionally poses risks for environment and consumers in long-term, especially due to the combination of residues of different disease treatments in food products (Jørgensen *et al*., 2017).

An alternative for these two strategies has been found in biological plant protective agents also termed biological control agents (BCA). BCAs mainly consist of bacteria such as *Bacillus* spp., *Pseudomonas* spp., and *Streptomyces* spp. that have been utilised for disease control of bacterial wilt caused by *Ralstonia solanacearum* on several crops (Yuliar *et al*., 2015), *Exserohilum turcicum* on maize (Sartori *et al*., 2015), and *Podosphaera fusca* on melon (Ongena and Jacques, 2007) for instance. It was suggested that the beneficial properties of BCAs are mediated by competition for nutrients and space, production of antimicrobial compounds, induction of plant defence response, as well as parasitism on potentially harming microbes (Bais *et al*., 2004; Vorholt, 2012; Yuliar *et al*., 2015). This indicates that beneficial microbes in high abundance form a dynamic of plant protection against pathogens. The WT phyllosphere was found to be dominated by few bacterial taxa, and members of these taxa have been found to be beneficial for plants and even to produce antimicrobial compounds (5.3.1.2 *fhy3 far1* shows an altered

bacterial community composition). This dynamic, however, seems to be disrupted when SA-mediated plant defence response is activated, as proposed in the *fhy3 far1* mutant (1.3 Aim and objectives). Here, plant defence effectors, which probably affect all phyllospheric microbes, could have disrupted the microbiota and allowed an establishment of microbial taxa that have been associated with pathogenicity. Thereby, the pathogen resistance mediated by the beneficial microbes could be removed (5.3.1.2 *fhy3 far1* shows an altered bacterial community composition).

The hypothesised negative feedback on defence response potentially mediated by increased ROS and SA accumulation could add to our understanding of plant defence response and be integrated in the invasion model of plant defence (1.2.3 Inducible plant defence responses). SA and ROS themselves could represent invasion patterns (IPs - 1.2.3.1 Overview) that, however, could induce a negative feedback on the plant defence when a certain threshold is reached in order to prevent potentially very-damaging excessive responses.

7 REFERENCES

Acharya, B. R., Raina, S., Maqbool, S. B., Jagadeeswaran, G., Mosher, S. L., Appel, H. M., Schultz, J. C., Klessig D. F., Raina R. (2007) Overexpression of CRK13, an Arabidopsis cysteine-rich receptor-like kinase, results in enhanced resistance to Pseudomonas syringae. The Plant Journal, 50, v488-99.

Afgan, E., Baker, D., van den Beek, M., Blankenberg, D., Bouvier, D., Čech, M., Chilton, J., Clements, D., Coraor, N., Eberhard, C., Grüning, B., Guerler, A., Hillman-Jackson, J., Von Kuster, G., Rasche, E., Soranzo, N., Turaga, N., Taylor, J., Nekrutenko, A., Goecks, J. (2016) The Galaxy platform for accessible, reproducible and collaborative biomedical analyses: 2016 update. Nucleic Acids Research, 44 (Web Server issue), W3-W10.

Al attar, N.S., Aldeen, S.B., Al Shahwany, A.W. (2015) Antifungal Activity of Brevundimonas diminuta Against Fusarium oxysporum on Tomato Plants under Greenhouse Condition. Iraqi Journal of Science, 56, 3346-56.

Alfano, J. R., Collmer, A. (2004) TYPE III SECRETION SYSTEM EFFECTOR PROTEINS: Double Agents in Bacterial Disease and Plant Defence. Annual Review of Phytopathology, 42, 385-414.

Allen, T., Koustenis, A., Theodorou, G., Somers, D.E., Kay, S.A., Whitelam, G.C., Devlin, P.F. (2006) Arabidopsis FHY3 Specifically Gates Phytochrome Signaling to the Circadian Clock. Plant Cell, 18(10), 2506-16.

Ambrose, K.V., Tian, Z., Wang, Y., Smith, J., Zylstra, G., Huang, B., Belanger, F.C. (2015) Functional characterization of salicylate hydroxylase from the fungal endophyte Epichloë festucae. Scientific Reports, 5, 10939.

Andargie, M. and Li, J. (2016) Arabidopsis thaliana: A Model Host Plant to Study Plant–Pathogen Interaction Using Rice False Smut Isolates of Ustilaginoidea virens. Frontiers in Plant Science, 7, 192.

Andrés, F. and Coupland, G. (2012) The genetic basis of flowering responses to seasonal cues. Nature Reviews Genetics, 13, 627-39.

Andrews, S. (2010) FastQC: a quality control tool for high throughput sequence data. [online] Available from: http://www.bioinformatics.babraham.ac.uk/projects/fastqc [06.01.2016].

Aoyama, T. and Chua, N.H. (1997) A glucocorticoid-mediated transcriptional induction system in transgenic plants. The Plant Journal, 11(3), 605-12.

Araújo, W. L., Marcon, J., Maccheroni, W., van Elsas, J. D., van Vuurde, J. W. L., & Azevedo, J. L. (2002) Diversity of Endophytic Bacterial Populations and Their Interaction with Xylella fastidiosa in Citrus Plants. Applied and Environmental Microbiology, 68(10), 4906-14.

Arnold, A. E., Mejía, L. C., Kyllo, D., Rojas, E. I., Maynard, Z., Robbins, N., & Herre, E. A. (2003) Fungal endophytes limit pathogen damage in a tropical tree. Proceedings of the National Academy of Sciences of the United States of America, 100(26), 15649-54.

Aryal, S. (2015) Potato Dextrose Agar (PDA)- Principle, Uses, Composition, Procedure and Colony Characteristics. [online] Available from: http://www.microbiologyinfo.com [01.08.2015].

Asai, T., Stone, J.M., Heard, J.E., Kovtun, Y., Yorgey, P., Sheen, J. and Ausubel, F.M. (2000) Fumonisin B1–Induced Cell Death in Arabidopsis Protoplasts Requires Jasmonate-, Ethylene-, and Salicylate-Dependent Signaling Pathways. Plant Cell, 12(10), 1823-36.

Augustinsky, J., Kammeyer, P., Husain, A., de Hoog, G.S., Libert, C.R. (1990) Engyodontium album endocarditis. J. Clin. Microbiol., 28, 1479-81.

Ayyadurai, N., Kirubakaran, S.I., Srisha, S., Sakthivel, N. (2005) Biological and molecular variability of Sarocladium oryzae, the sheath rot pathogen of rice (Oryza sativa L.). Curr Microbiol., 50(6), 319-23.

Barbara, D.J. and Clewes, E. (2003) Plant pathogenic Verticillium species: how many of them are there? Molecular Plant Pathology, 4(4), 297-305.

Babraham Bioinformatics. (2007) FastQC v0.11.5. [online] Available from: www.bioinformatics.babraham.ac.uk/projects/fastqc [06.01.2016].

Bais, H. P., Fall, R., & Vivanco, J. M. (2004) Biocontrol of Bacillus subtilis against Infection of Arabidopsis Roots by Pseudomonas syringae Is Facilitated by Biofilm Formation and Surfactin Production. Plant Physiology, 134(1), 307-19.

Balbi, V. and Devoto, A. (2008) Jasmonate signalling network in Arabidopsis thaliana: crucial regulatory nodes and new physiological scenarios. New Phytol., 177, 301-18.

Barnes, S. A., Nishizawa, N. K., Quaggio, R. B., Whitelam, G. C., & Chua, N. H. (1996). Far-red light blocks greening of Arabidopsis seedlings via a phytochrome A-mediated change in plastid development. The Plant Cell, 8(4), 601-15.

Becker, B., Holtgrefe, S., Jung, S., Wunrau, C., Kandlbinder, A., Baier, M., Dietz, K.J., Backhausen, J.E., Scheibe, R. (2006) Influence of the photoperiod on redox regulation and stress responses in Arabidopsis thaliana L. (Heynh.) plants under long- and short-day conditions. Planta. 224, 380-93.

Beets, C., Dubery, I. (2011) Quantification of camalexin, a phytoalexin from Arabidopsis thaliana: a comparison of five analytical methods. Anal Biochem. 419(2), 260-5.

Begon, M., J. L. Harper, and C. R. Townsend (1996) Ecology: Individuals, Populations, and Communities, 3rd edition. Blackwell Science Ltd., Cambridge, MA.

Berardini, T.Z., Mundodi, S., Reiser, R., Huala, E., Garcia-Hernandez, M., Zhang, P., Mueller, L.M., Yoon, J., Doyle, A., Lander, G., Moseyko, N., Yoo, D., Xu, I., Zoeckler, B., Montoya, M., Miller, N., Weems, D., Rhee, S.Y. (2004) Functional annotation of the Arabidopsis genome using controlled vocabularies. Plant Physiol., 135(2), 1-11.

Berkey, R., Bendigeri, D., Xiao, S. (2012) Sphingolipids and plant defense/disease: the “death” connection and beyond. Frontiers in plant science, 3, 68.

Bertani, G. (1951) STUDIES ON LYSOGENESIS I. : The Mode of Phage Liberation by Lysogenic Escherichia coli. Journal of Bacteriology, 62(3), 293-300.

Bhardwaj, V., Meier, S., Petersen, L.N., Ingle, R.A., Roden, L.C. (2011) Defence Responses of Arabidopsis thaliana to Infection by Pseudomonas syringae Are Regulated by the Circadian Clock. PLoS ONE, 6(10), e26968.

Bibi, F., Yasir, M., Song, G., Lee, S., Chung, Y.R. (2012) Diversity and characterization of endophytic bacteria associated with tidal flat plants and their antagonistic effects on oomycetous plant pathogens. Plant Pathol J., 28, 20-31.

Bibi, F., Chung, E.J., Khan, A., Jeon, C.O., Chung, Y.R. (2013) Martelella endophytica sp. nov., an antifungal bacterium associated with a halophyte. Int J Syst Evol Microbiol., 63, 2914-19.

Biedermann, S., Hellmann, H. (2010) The DDB1a interacting proteins ATCSA-1 and DDB2 are critical factors for UV-B tolerance and genomic integrity in Arabidopsis thaliana. Plant J., 62(3), 404-15.

Birkenbihl, R.P., Diezel, C., Somssich, I.E. (2012) Arabidopsis WRKY33 Is a Key Transcriptional Regulator of Hormonal and Metabolic Responses toward Botrytis cinerea Infection. Plant Physiology, 159(1), 266-85.

Bisby, F.A., Roskov, Y.R., Orrell, T.M., Nicolson, D., Paglinawan, L.E., Bailly, N., Kirk, P.M., Bourgoin, T., Baillargeon, G., Ouvrard, D. (2011) Species 2000 & ITIS Catalogue of Life: 2011 Annual Checklist. [online] Available from: www.catalogueoflife.org/annual-checklist/2011/browse/tree/id/2392393 [17.09.2016].

Bodenhausen, N., Horton, M.W., Bergelson, J. (2013) Bacterial Communities Associated with the Leaves and the Roots of Arabidopsis thaliana. PLoS ONE, 8(2), e56329.

Böhmdorfer, G., Schleiffer, A., Brunmeir, R., Ferscha, S., Nizhynska, V., Kozák, J., Angelis, K.J., Kreil, D.P., Schweizer, D. (2011) GMI1, a structural-maintenance-of-chromosomes-hinge domain-containing protein, is involved in somatic homologous recombination in Arabidopsis. Plant J., 67(3), 420-33.

Bonardi, V., Tang, S., Stallmann, A., Roberts, M., Cherkis, K., Dangl, J.L. (2011) Expanded functions for a family of plant intracellular immune receptors beyond specific recognition of pathogen effectors. Proceedings of the National Academy of Sciences of the United States of America, 108(39), 16463-68.

Bringel, F. and Couée, I. (2015) Pivotal roles of phyllosphere microorganisms at the interface between plant functioning and atmospheric trace gas dynamics. Front Microbiol., 6, 486.

Brodersen, P., Petersen, M., Bjørn Nielsen, H., Zhu, S., Newman, M.A., Shokat, K.M., Rietz, S., Parker, J., Mundy, J. (2006) Arabidopsis MAP kinase 4 regulates salicylic acid- and jasmonic acid/ethylene-dependent responses via EDS1 and PAD4. Plant J. 47(4), 532-46.

Brooks, D.M., Hernández-Guzmán, G., Kloek, A.P., Alarcón-Chaidez, F., Sreedharan, A., Rangaswamy, V., Peñaloza-Vázquez, A., Bender, C.L., Kunkel, B.N. (2004) Identification and characterization of a well-defined series of coronatine biosynthetic mutants of Pseudomonas syringae pv. tomato DC3000. Mol Plant Microbe Interact., 17(2), 162-74.

Büttner, D. and He, S.Y. (2009) Type III Protein Secretion in Plant Pathogenic Bacteria. Plant Physiol., 150(4), 1656-64.

Buzas, M. A. and Hayek, L.-A. C. (1996) Biodiversity Resolution: An Integrated Approach. Biodiversity Letters, 3(2), 40-3.

Carding, S., Verbeke, K., Vipond, D.T., Corfe, B.M., Owen, L.J. (2015) Dysbiosis of the gut microbiota in disease. Microbial Ecology in Health and Disease, 26, 10.3402/mehd.v26.26191.

Casal, J.L. (2000) Phytochromes, Cryptochromes, Phototropin: Photoreceptor Interactionsin Plants. Photochemistry and Photobiology, 71(1), 1-11.

Ceuppens, S., Delbeke, S., De Coninck, D., Boussemaere, J., Boon, N., & Uyttendaele, M. (2015) Characterization of the Bacterial Community Naturally Present on Commercially Grown Basil Leaves: Evaluation of Sample Preparation Prior to Culture-Independent Techniques. International Journal of Environmental Research and Public Health, 12(8), 10171-97.

Chai, T., Zhou, J., Liu, J., Xing, D. (2015) LSD1 and HY5 antagonistically regulate red light induced-programmed cell death in Arabidopsis. Front. Plant Sci., 6, 292.

Chakravorty, S., Helb, D., Burday, M., Connell, N., Alland, D. (2007) A detailed analysis of 16S ribosomal RNA gene segments for the diagnosis of pathogenic bacteria. Journal of Microbiological Methods, 69(2), 330-39.

Chaouch, S., Noctor, G. (2010) Myo-inositol abolishes salicylic acid-dependent cell death and pathogen defence responses triggered by peroxisomal hydrogen peroxide. New Phytol., 188(3), 711-8.

Chen, M., Han, G., Dietrich, C.R., Dunn, T.M., Cahoonc, E.B. (2006) The Essential Nature of Sphingolipids in Plants as Revealed by the Functional Identification and Characterization of the Arabidopsis LCB1 Subunit of Serine Palmitoyltransferase. The Plant Cell, 18, 3576-93.

Chen, H., Zhang, J., Neff, M.M., Hong, S.W., Zhang, H., Deng, X.W., Xiong, L. (2008) Integration of light and abscisic acid signaling during seed germination and early seedling development. Proc Natl Acad Sci USA, 105, 4495-500.

Chen, C.W., Panzeri, D., Yeh, Y.H., Kadota, Y., Huang, P.Y., Tao, C.N., Roux, M., Chien, S.C., Chin, T.C., Chu, P.W., Zipfel, C., Zimmerli, L. (2014) RETRACTED: The Arabidopsis Malectin-Like Leucine-Rich Repeat Receptor-Like Kinase IOS1 Associates with the Pattern Recognition Receptors FLS2 and EFR and Is Critical for Priming of Pattern-Triggered Immunity. The Plant Cell, 26(7), 3201-19.

Chesson, P.L., Warner, R.R. (1981) Environmental variability promotes coexistence in lottery competitive-systems. American Naturalist, 117, 923-43.

Cipollini, D., Walters, D., Voelckel, C. (2014) Costs of resistance in plants: from theory to evidence. In *Annual Plant Reviews 47: Insect-Plant Interactions* (ed. by Voelckel, C. and Jander, G.), pp 263-307. John Wiley & Sons, Ltd., Chichester.

Coll, N.S., Vercammen, D., Smidler, A., Clover, C., Van Breusegem, F., Dangl, J.L., Epple, P. (2010) Arabidopsis Type I Metacaspases Control Cell Death. Science, 330, 1393-97.

Coll, N.S., Epple, P., Dangl, J.L. (2011): Programmed cell death in the plant immune system. Cell Death and Differentiation, 18, 1247-56.

Cook, D.E., Mesarich, C.H., Thomma, B.P. (2015) Understanding plant immunity as a surveillance system to detect invasion. Annu Rev Phytopathol. 53, 541-63.

Covington, M.F., Maloof, J.N., Straume, M., Kay, S.A., Harmer, S.L. (2008) Global transcriptome analysis reveals circadian regulation of key pathways in plant growth and development. Genome Biol., 9(8), R130.

Cox, P. (2011) Characterization of the metacaspase gene family in Arabidopsis thaliana. (Master thesis in Biology at the dept of Forest Genetics and Plant Physiology. Swedish University of Agricultural Sciences. Faculty of Forest Sciences. Department of Forest Genetics and Plant Physiology).

Craigon, D.J., James, N., Okyere, J., Higgins, J., Jotham, J., May, S. (2004) NASCArrays: a repository for microarray data generated by NASC's transcriptomics service. Nucl Acids Res., 32 (suppl 1), D575-7.

Currie, A.F., Wearn, J., Hodgson, S., Wendt, H., Broughton, S., Jin, L. (2013) Foliar fungal endophytes in herbaceous plants: a marriage of convenience?. In *Advances in Endophytic Research* (ed. by Verma, V.C., Gange, A.C.), 61-81. Springer, New Delhi, Heidelberg, New York, Dordrecht, London.

Dangl, J.L., Horvath, D.M., Staskawicz, B.J. (2013) Pivoting the Plant Immune System from Dissection to Deployment. Science, 341, 746-51.

Daniels, M.J., Barber, C.E., Turner, P.C., Cleary, W.G., Sawczyc, M.K. (1984) Isolation of mutants of Xanthomonas campestris pathovar campestris showing altered pathogenicity. J Gen Microbiol., 130, 2447-55.

De Boer, W., Wagenaar, A.M., Klein Gunnewiek, P.J., van Veen, J.A. (2007) In vitro suppression of fungi caused by combinations of apparently non-antagonistic soil bacteria. FEMS Microbiol Ecol., 59, 177-85.

De Cal, A., García-Lepe, R., Melgarejo, P. (2000) Induced resistance by Penicillium oxalicum against Fusarium oxysporum f. sp. lycopersici: histological studies of infected and induced tomato stems. Phytopathology, 90, 260-68.

De Montaigu, A., Tóth, R., Coupland, G. (2010) Plant development goes like clockwork. Trends Genet., 26(7), 296-306.

Delmotte, N., Knief, C., Chaffron, S., Innerebner, G., Roschitzki, B., Schlapbach, R., *et al*. (2009) Community proteogenomics reveals insights into the physiology of phyllosphere bacteria. Proc Natl Acad Sci USA, 106, 16428-33.

Denancé, N., Sánchez-Vallet, A., Goffner, D., Molina, A. (2013) Disease resistance or growth: the role of plant hormones in balancing immune responses and fitness costs. Front Plant Sci., 4, 155.

Dewdney, J., Reuber, T.L., Wildermuth, M.C., Devoto, A., Cui, J., Stutius, L.M., Drummond, E.P., Ausubel, F.M. (2000) Three unique mutants of Arabidopsis identify eds loci required for limiting growth of a biotrophic fungal pathogen. Plant J., 24(2), 205-18.

Dinan, T.G., Stilling, R.M., Stanton, C., Cryan, J.F. (2015) Collective unconscious: How gut microbes shape human behaviour. Journal of Psychiatric Research, 63, 1e9.

Doehlemann, G. and Hemetsberger C. (2013) Apoplastic immunity and its suppression by filamentous plant pathogens. New Phytologist, 198, 1001-16.

Dong, X. (2004) NPR1, All Things Considered. Curr Opin Plant Biol. 7(5), 547-52.

Van Doorn, W.G., Beers, E.P., Dangl, J.L., Franklin-Tong, V.E., Gallois, P., Hara-Nishimura, I., Jones, A.M., Kawai-Yamada, M., Lam, E., Mundy, J., Mur, L.A., Petersen, M., Smertenko, A., Taliansky, M., Van Breusegem, F., Wolpert, T., Woltering, E., Zhivotovsky, B., Bozhkov, P.V. (2011) Morphological classification of plant cell deaths. Cell Death Differ., 18(8), 1241-6.

Dos Santos, C.V., Letousey, P., Delavault, P., Thalouarn, P. (2003) Defense Gene Expression Analysis of Arabidopsis thaliana Parasitized by Orobanche ramose. Phytopathology, 93(4), 451-57.

Durrant, W.E. and Dong, X. (2004) Systemic Acquired Resistance. Annu. Rev. Phytopathol., 42, 185-209.

Ebrahim, S., Usha, K., Singh, B. (2011) Pathogenesis Related (PR) Proteins in Plant Defense Mechanism. In *Science against microbial pathogens: communicating current research and technological advances* (ed. by Méndez-Vilas, A.), pp 1043-54. Formatex, Badajoz, E.

Ederli, L., Madeo, L., Calderini, O., Gehring, C., Moretti, C., Buonaurio, R., Paolocci F., Pasqualini, S. (2011) The Arabidopsis thaliana cysteine-rich receptor-like kinase CRK20 modulates host responses to Pseudomonas syringae pv. tomato DC3000 infection. Journal of Plant Physiology, 168(15), 1784-94.

Faisal, M. (2013) Inoculation of Plant Growth Promoting Bacteria Ochrobactrum intermedium, Brevibacterium Sp. and Bacillus cereus Induce Plant Growth Parameters. Journal of Applied Biotechnology, 1, 45-53.

Falcón-Rodríguez, A.B., Wégria, G., Cabrera J.C. (2012) Exploiting Plant Innate Immunity to Protect Crops Against Biotic Stress: Chitosaccharides as Natural and Suitable Candidates for this Purpose. In *New Perspectives in Plant Protection* (ed. by Bandani, A.R.), pp 139-166. Available from: DOI: 10.5772/36777.

Fan, J., Yang, J., Wang, Y.Q., Li, G.B., Li, Y., Huang, F., Wang, W.M. (2015) Current understanding on Villosiclava virens, a unique flower-infecting fungus causing rice false smut disease. Mol Plant Pathol., 17(9), 1321-30.

Farre, E.M., Liu, T. (2013) The PRR family of transcriptional regulators reflects the complexity and evolution of plant circadian clocks. Current Opinion in Plant Biology, 16(5), 621-9.

Favory, J.J., Stec, A., Gruber, H., Rizzini, L., Oravecz, A., Funk, M., Albert, A., Cloix, C., Jenkins, G.I., Oakeley, E.J., Seidlitz, H.K., Nagy, F., Ulm, R. (2009) Interaction of COP1 and UVR8 regulates UV-B-induced photomorphogenesis and stress acclimation in Arabidopsis. EMBO J., 28(5), 591-601.

Fernandes, E.K. and Bittencourt, V.R. (2008) Entomopathogenic fungi against South American tick species. Exp Appl Acarol., 46(1-4), 71-93.

Ferrari, S., Savatin, D.V., Sicilia, F., Gramegna, G., Cervone, F., De Lorenzo, G. (2013) Oligogalacturonides: plant damage-associated molecular patterns and regulators of growth and development. Front. Plant Sci. 4(49), 1-9.

Feys, B.J., Moisan, L.J., Newman, M.A., Parker, J.E. (2001) Direct interaction between the Arabidopsis disease resistance signaling proteins, EDS1 and PAD4. EMBO J., 20(19), 5400-11.

Fornoni, J., Núñez-Farfán, J., Valverde, P.L., Rausher, M.D. (2004) Evolution of mixed strategies of plant defense allocation against natural enemies. Evolution, 58, 1685-95.

Foyer, C.H. and Noctor, G. (2003) Redox sensing and signalling associated with reactive oxygen in chloroplasts, peroxisomes and mitochondria. Physiologia Plantarum, 119, 355-64.

Francis, I.M., Jochimsen, K.N., De Vos, P., van Bruggen A.H. (2014) Reclassification of rhizosphere bacteria including strains causing corky root of lettuce and proposal of Rhizorhapis suberifaciens gen. nov., comb. nov., Sphingobium mellinum sp. nov., Sphingobium xanthum sp. nov. and Rhizorhabdus argentea gen. nov., sp. nov. Int J Syst Evol Microbiol., 64, 1340-50.

Franklin, K.A. and Quail, P.H. (2010) Phytochrome functions in Arabidopsis development. J Exp Bot., 61(1), 11-24.

Freeman, B. C. and Beattie, G.A. (2008) An Overview of Plant Defenses against Pathogens and Herbivores. The Plant Health Instructor. Available from: DOI: 10.1094/PHI-I-2008-0226-01

Fu, Z.Q. and Dong X. (2013) Systemic Acquired Resistance: Turning Local Infection into Global Defence. Annu Rev Plant Biol., 64, 839-63.

Fukui, R., Fukui, H., Alvarez, A.M. (1999) Suppression of bacterial blight by a bacterial community isolated from the guttation fluids of anthuriums. Appl Environ Microbiol., 65, 1020-28.

Furukawa, T., Curtis, M.J., Tominey, C.M., Duong, Y.H., Wilcox, B.W., Aggoune, D., Hays, J.B., Britt, A.B. (2010) A shared DNA-damage-response pathway for induction of stem-cell death by UVB and by gamma irradiation. DNA Repair (Amst), 9(9), 940-8.

GABI-Kat. (2014) Frequently asked questions (FAQ). [online] Available from: www.gabi-kat.de/faq.htm [28.06.2014].

Galloway, L.D. and Burgess, R. (1952) Applied Mycology and Bacteriology. Leonard Hill, London, UK, 54-57.

Gao, M., Liu, J., Bi, D., Zhang, Z., Cheng, F., Chen, S., Zhang, Y. (2008) MEKK1, MKK1/MKK2 and MPK4 function together in a mitogen-activated protein kinase cascade to regulate innate immunity in plants. Cell Res., 18(12), 1190-8.

Gao, Y., Liu, H., An, C., Shi, Y., Liu, X., Yuan, W., Zhang, B., Yang, J., Yu, C., Gao, H. (2013) Arabidopsis FRS4/CPD25 and FHY3/CPD45 work cooperatively to promote the expression of the chloroplast division gene ARC5 and chloroplast division. Plant J., 75, 795–807.

García, M., Arriagada, C., García-Romer, I., Ocampo, J.A. (2011) Are plant cell wall hydrolysing enzymes of saprobe fungi implicated in the biological control of the Verticillium dahliae pathogenesis? Crop Protection, 30(1), 85-7.

Gibon, Y., Blasing, O:E:, Palacios-Rojas, N., Pankovic, D., Hendriks, J.H., Fisahn, J., Hohne, M., Gunther, M., Stitt, M. (2004) Adjustment of diurnal starch turnover to short days: depletion of sugar during the night leads to a temporary inhibition of carbohydrate utilization, accumulation of sugars and post-translational activation of ADP-glucose pyrophosphorylase in the following light period. Plant J. 39, 847-62.

Glazebrook, J. (2005) Contrasting mechanisms of defense against biotrophic and necrotrophic pathogens. Annu Rev Phytopathol., 43, 205-27.

Glushakova, A.M., Iurkov, A.M., Chernov, I. (2007) Massive isolation of anamorphous ascomycete yeasts Candida oleophila from plant phyllosphere. Mikrobiologiia, 76(6), 896-901.

Goff, K. E. and Ramonell, K. M. (2007) The Role and Regulation of Receptor-Like Kinases in Plant Defense. Gene Regulation and Systems Biology, 1, 167-75.

GONUTS. (2016) Category:GO:0043069 ! negative regulation of programmed cell death. [online] Available from: http://gowiki.tamu.edu/wiki/index.php/Category:GO:0043069_ !_negative_regulation_of_programmed_cell_death [16.04.2016].

Graf, A., Schlereth, A., Stitt, M., Smith, A.M. (2010) Circadian control of carbohydrate availability for growth in Arabidopsis plants at night. Proc Natl Acad Sci USA, 107(20), 9458-63.

Gu, L., Bai, Z., Jin, B., Hu, Q., Wang, H., Zhuang, G., Zhang, H. (2010) Assessing the impact of fungicide enostroburin application on bacterial community in wheat phyllosphere. J Environ Sci (China), 22(1), 134-41.

Guarro, J., Gams, W., Puhhol, I., Gene, J. (1997) Acremonium species: new emerging fungal opportunists—in vitro antifungal susceptibilities and review. Clinical Infectious Diseases, 25, 5, 1222-29.

Hammer, Ø., Harper, D.A.T., Ryan, P.D. (2001) PAST: Paleontological statistics software package for education and data analysis. Palaeontologia Electronica, 4(1), 9.

Harmer, S.L., Hogenesch, J.B., Straume, M., Chang, H.S., Han, B., Zhu, T., Wang, X., Kreps, J.A., Kay, S.A. (2000) Orchestrated transcription of key pathways in Arabidopsis by the circadian clock. Science, 290(5499), 2110-3.

Harmer, S.L., Panda, S., Kay, S.A. (2001) Molecular bases of circadian rhythms. Annu Rev Cell Dev Biol., 17, 215-53.

Hayward, A.C., Fegan, N., Fegan, M., Stirling, G.R. (2010) Stenotrophomonas and Lysobacter: ubiquitous plant-associated gamma-proteobacteria of developing significance in applied microbiology. J Appl Microbiol., 108(3), 756-70.

Hazen, S. P., Schultz, T. F., Pruneda-Paz, J. L., Borevitz, J. O., Ecker J. R., Kay S. A. (2005) LUX ARRHYTHMO encodes a Myb domain protein essential for circadian rhythms. PNAS, 102(29), 10387-92.

Heidel, A.J., Clarke, J.D., Antonovics, J., Dong, X.N. (2004) Fitness costs of mutations affecting the systemic acquired resistance pathway in Arabidopsis thaliana. Genetics, 168, 2197-206.

Heil, M., Hilpert, A., Kaiser, W., and Linsenmair, K.E. (2000). Reduced growth and seed set following chemical induction of pathogen defence: does systemic acquired resistance (SAR) incur allocation costs? J Ecol., 88, 645-54.

Helfer, W. (1991) Pilze auf Pilzfruchtkörpern. Untersuchungen zur Ökologie, Systematik und Chemie. Libri Botanici, 1, 1-157.

Heyndrickx, K.S. and Vandepoele, K. (2012) Systematic identification of functional plant modules through the integration of complementary data sources. Plant Physiol., 159, 884-901.

Hiltbrunner, A., Viczian, A., Bury, E., Tscheuschler, A., Kircher, S., Toth, R., Honsberger, A., Nagy, F., Fankhauser C., Schäfer E. (2005) Nuclear accumulation of the phytochrome A photoreceptor requires FHY1. Curr. Biol., 15, 2125-30.

Honys, D., Dupľáková, N., Reňák D. (2008) Online Tools foR Presentation and Analysis of Plant Microarray Data. In *Oligonucleotide Array Sequence Analysis*. (ed. by Moretti, M.K. and Rizzo, L.J.), 265-95. Nova Science Publishers, Inc., Hauppauge NY, USA.

Horton, M.W., Bodenhausen, N., Beilsmith, K., Meng, D., Muegge, B.D., Subramanian, S., Vetter, M.M., Vilhjálmsson, B.J., Nordborg, M., Gordon, J.I., Bergelson, J. (2014) Genome-wide association study of Arabidopsis thaliana leaf microbial community. Nature Communications, 5, 5320.

Hossain, M., Sultana, F., Kubota, M., Koyama, H., Hyakumachi, M. (2007) The Plant Growth-Promoting Fungus Penicillium simplicissimum GP17-2 Induces Resistance in Arabidopsis thaliana by Activation of Multiple Defense Signals. Plant Cell Physiol., 48(12), 1724-36.

Hsu, P.Y. and Harmer, S.L. (2013) Wheels within wheels: the plant circadian system. Trends in Plant Science, 19(4), 240-9.

Huang, J., Gu, M., Lai, Z., Fan, B., Shi, K., Zhou, Y.H., Yu, J.Q., Chen, Z. (2010 a) Functional Analysis of the Arabidopsis PAL Gene Family in Plant Growth, Development, and Response to Environmental Stress. Plant Physiol., 153(4), 1526-38.

Huang, X., Li, Y., Zhang, X., Zuo, J., Yang, S. (2010 b)The Arabidopsis LSD1 gene plays an important role in the regulation of low temperature-dependent cell death. New Phytol. 187(2),301-12.

Huang, X., Ouyang, X., Yang, P., Lau, O.S., Li, G., Li, J., Chen, H., Deng, X.W. (2012) Arabidopsis FHY3 and HY5 positively mediate induction of COP1 transcription in response to photomorphogenic UV-B light. Plant Cell, 24(11), 4590-606.

Hubbell, S.P. (2001) The unified neutral theory of biodiversity and biogeography. Princeton University Press, Woodstock, UK.

Hudson, M., Ringli, C., Boylan, M.T., Quail, P.H. (1999) The FAR1 locus encodes a novel nuclear protein specific to phytochrome A signaling. Genes Dev., 13(15), 2017-27.

Hudson, M.E. and Quail, P.H. (2003) Identification of Promoter Motifs Involved in the Network of Phytochrome A-Regulated Gene Expression by Combined Analysis of Genomic Sequence and Microarray Data. Plant Physiology, 133, 1605-16.

Hudson, M.E., Lisch, D.R., Quail, P.H. (2003) The FHY3 and FAR1 genes encode transposase-related proteins involved in regulation of gene expression by the phytochrome A-signaling pathway. The Plant Journal, 34, 453-71.

Humphrey, P.T., Nguyen, T.T., Villalobos, M.M., Whiteman, N.K. (2014) Diversity and abundance of phyllosphere bacteria are linked to insect herbivory. Mol Ecol., 23, 1497-515.

Huot, B., Yao, J., Montgomery, B.L., He, S.Y. (2014) Growth–Defense Tradeoffs in Plants: A Balancing Act to Optimize Fitness. Molecular Plant, 7, 1267-87.

Hutchinson, G.E. (1961) The paradox of the plankton. American Naturalist 95, 137-45.

Igarashi, D., Bethke, G., Xu, Y., Tsuda, K., Glazebrook, J., Katagiri F. (2013) Pattern-Triggered Immunity Suppresses Programmed Cell Death Triggered by Fumonisin B1. PLoS ONE, 8(4), e60769.

Inderbitzin, P., Davis, R.M., Bostock, R.M., Subbarao, K.V. (2013) Identification and Differentiation of Verticillium Species and V. longisporum Lineages by Simplex and Multiplex PCR Assays. PLoS ONE, 8(6), e65990.

Ingle, R.A. and Roden, L.C. (2014) Circadian Regulation of Plant Immunity to Pathogens. Methods in Molecular Biology, 1158, 273-83.

Innerebner, G., Knief, C., Vorholt, J.A. (2011) Protection of Arabidopsis thaliana against Leaf-Pathogenic Pseudomonas syringae by Sphingomonas Strains in a Controlled Model System. Appl. Environ. Microbiol., 77, 3202-10.

Ishiga, Y., Ishiga, T., Uppalapati, S. R., & Mysore, K. S. (2011) Arabidopsis seedling flood-inoculation technique: a rapid and reliable assay for studying plant-bacterial interactions. Plant Methods, 7, 32.

Izhaki, I., Fridman, S., Gerchman, Y., Halpern, M. (2011) Variability of bacterial community composition on leaves between and within plant species. Curr Microbiol., 66, 227-35.

Jacobs, J. (2011) Individual Based Rarefaction using R-package. [online] Available from: www.jennajacobs.org/R/rarefaction.html [01.09.2016].

Jarvis, E.D., Widom, R.L., LaFauci, G., Setoguchi, Y., Richter, I.R., Rudner, R. (1988) Chromosomal Organization of rRNA Operons in Bacillus subtilis. Genetics, 120, 625-635.

Jäschke, D., Dugassa-Gobena, D., Karlovsky, P., Vidal, S., Ludwig-Müller, J. (2010) Suppression of clubroot (Plasmodiophora brassicae) development in Arabidopsis thaliana by the endophytic fungus Acremonium alternatum. Plant Pathology, 59, 100-111.

Jones, J.D. and Dangl, J.L. (2006) The plant immune system. Nature, 444, 323-9.

Jørgensen, L.N, van den Bosch, F., Oliver, R.P., Heick, T.M., Paveley, N. (2017) Targeting Fungicide Inputs According to Need. Annu. Rev. Phytopathol. 55, 8.1-8.23.

Josse, E.M., and Halliday, K.J. (2008) Skotomorphogenesis: The Dark Side of Light Signalling. Curr Biol. 18(24), R1144-6.

Kaiser, G., Kleiner, O., Beisswenger, C., Batschauer, A. (2009) Increased DNA repair in Arabidopsis plants overexpressing CPD photolyase. Planta, 230(3), 505-15.

Kaku, H., Subandiyah, S., Ochiai, H. (2000) Red stripe of rice is caused by bacterium Microbacterium sp. J. Gen. Plant Pathol., 66, 149-52.

Karlsson, I., Friberg, H., Steinberg, C., Persson, P. (2014) Fungicide Effects on Fungal Community Composition in the Wheat Phyllosphere. PLOS ONE, 9(11), e111786.

Kazan, K., and Manners, J. M. (2008) Jasmonate Signaling: Toward an Integrated View. Plant Physiology, 146(4), 1459-68.

Kersey, P.J., Allen, J.E., Armean, I., Boddu, S., Bolt, B.J., Carvalho-Silva, *et al.* (2015) Ensembl Genomes 2016: more genomes, more complexity. Nucleic Acids Research, Available from: doi:10.1093/nar/gkv1209.

Khan, A., Mohammad, M.T., Park, H.C., Yun, D.-J., Shim, S.H., Chung, Y.R. (2016) Development of root system architecture of Arabidopsis thaliana in response to colonization by Martelella endophytica YC6887 depends on auxin signalling. Plant and Soil, 405(1), 81-96.

Khanna, R., Kikis, E. A., Quail P. H. (2003) EARLY FLOWERING 4 Functions in Phytochrome B-Regulated Seedling De-Etiolation. Plant Physiol., 133(4), 1530-38.

Kim, M.G., da Cunha, L., McFall, A.J., Belkhadir, Y., DebRoy, S., Dangl, J.L., Mackey, D. (2005) Two Pseudomonas syringae Type III Effectors Inhibit RIN4-Regulated Basal Defense in Arabidopsis. Cell, 121(5), 749-59.

Kim, B.Y., Lee, S.Y., Ahn, J.H., Song, J., Kim, W.G., Weon, H.Y. (2015) Complete Genome Sequence of Bacillus amyloliquefaciens subsp. plantarum CC178, a Phyllosphere Bacterium Antagonistic to Plant Pathogenic Fungi. Genome Announc., 3, e01368-14.

Kitagawa, W. and Tamura, T. (2008) Three Types of Antibiotics Produced from Rhodococcus erythropolis Strains. Microbes Environ., 23(2), 167-71.

Klappenbach, J.A., Dunbar, J.M., Schmidt, T.M. (2000) rRNA Operon Copy Number Reflects Ecological Strategies of Bacteria. Applied and Environmental Microbiology, 66(4), 1328-33.

Kniskern, J.M., Traw, M.B., Bergelson, J. (2007) Salicylic acid and jasmonic acid signaling defense pathways reduce natural bacterial diversity on Arabidopsis thaliana. Mol Plant Microbe Interact., 20(12), 1512-22.

Kolesnikov, N., Hastings, E., Keays, M., Melnichuk, O., Tang, Y.A., Williams, *et al.* (2015) ArrayExpress update--simplifying data submissions. Nucleic Acids Res., 43(Database issue), D1113-6. Available from: DOI: 10.1093/nar/gku1057.

Kong, Q., Qu, N., Gao, M., Zhang, Z., Ding, X., Yang, F., Li, Y., Dong, O.X., Chen, S., Li, X., Zhang, Y. (2012) The MEKK1-MKK1/MKK2-MPK4 Kinase Cascade Negatively Regulates Immunity Mediated by a Mitogen-Activated Protein Kinase Kinase Kinase in Arabidopsis. The Plant Cell, 24(5), 2225-36.

Koornneef, A. and Pieterse, C.M.J. (2008) Cross Talk in Defence Signaling. Plant Physiology, 146,839-44.

Korolev, N., David, D.R., Elad, Y. (2008) The role of phytohormones in basal resistance and Trichoderma-induced systemic resistance to Botrytis cinerea in Arabidopsis thaliana. BioControl., 53(4), 667-83.

Kraepiel, Y. and Barny, M.A. (2016) Gram-negative phytopathogenic bacteria, all hemibiotrophs after all? Molecular Plant Pathology, 17(3), 313-16.

Kuroyanagi, M., Yamada, K., Hatsugai, N., Kondo, M., Nishimura, M., Hara-Nishimura, I. (2005) Vacuolar processing enzyme is essential for mycotoxin-induced cell death in Arabidopsis thaliana. J Biol Chem., 280(38), 32914-20.

Kvasnikov, E.I., Nagornaia, S.S., Shchelokova, I.F. (1975) Yeast flora of plant rhizosphere and phyllosphere. Mikrobiologiia, 44(2), 339-46.

Kwon, S. and Hwang, D.J. (2013) Expression Analysis of the Metacaspase Gene Family in Arabidopsis. J. Plant Biol., 56, 391-98.

Lai, A.G., Doherty, C.J., Mueller-Roeber, B., Kay, S.A., Schippers, J.H.M., Dijkwela, P.P. (2012) CIRADIAN CLOCK-ASSOCIATED 1 regulates ROS homeostasis and oxidative stress responses. PNAS, 109(42), 17129-34.

Lam, E. and Zhang, Y. (2012) Regulating the reapers: activating metacaspases for programmed cell death. Trends Plant Sci., 17(8), 487-94.

Latour, X., Barbey, C., Chane, A., Groboillot, A., Burini, J.F. (2013) Rhodococcus erythropolis and Its γ-Lactone Catabolic Pathway: An Unusual Biocontrol System That Disrupts Pathogen Quorum Sensing Communication. Agronomy, 3, 816-38.

Le Dang, Q., Shin, T.S., Park, M.S., Choi, Y.H., Choi, G.J., Jang, K.S,. Kim, I.S., Kim, J.C. (2014) Antimicrobial activities of novel mannosyl lipids isolated from the biocontrol fungus Simplicillium lamellicola BCP against phytopathogenic bacteria. J Agric Food Chem., 62(15), 3363-70.

Le, M.H., Cao, Y., Zhang, X.C., Stacey, G. (2014) LIK1, A CERK1-Interacting Kinase, Regulates Plant Immune Responses in Arabidopsis. PLoS ONE, 9(7), e102245.

Lee, J., Nam J., Park, H.C., Na, G., Miura, K. Jin, J.B., *et al*. (2006) Salicylic acid-mediated innate immunity in Arabidopsis is regulated by SIZ1 SUMO E3 ligase. The Plant Journal, 49, 79–90.

Leelasuphakul, W., Hemmanee, P., Chuenchitt, S. (2008) Growth inhibitory properties of Bacillus subtilis strains and their metabolites against the green mold pathogen (Penicillium digitatum Sacc.) of citrus fruit. Postharvest Biology and Technology. 48, 113-21.

Lepistö, A., and Rintamäki, E. (2012) Coordination of Plastid and Light Signaling Pathways upon Development of Arabidopsis Leaves under Various Photoperiods. Molecular Plant. 5(4), 799-816.

Li, G., Siddiqui, H., Teng, H., Lin, R., Wan, X, Li, J., Lau, O., Ouyang, X., Dai, M., Wan, J., Devlin, P.F., Deng, X.W., Wang, H. (2011) Coordinated transcriptional regulation underlying the circadian clock in Arabidopsis. Nature Cell Biology, 13, 616-41.

Li, Y., Chen, L., Mu, J., & Zuo, J. (2013) LESION SIMULATING DISEASE1 Interacts with Catalases to Regulate Hypersensitive Cell Death in Arabidopsis. Plant Physiology, 163(2), 1059-70.

Li, D., Deng, Q., Yong, M., Wang, H., Lai, C., Chen, H., He, W., Hu, D. (2015) Screening of Biocontrol Fungi against Sclerotia of Villosiclava virens and Their Mechanisms. journal1, 32(2), 258-64.

Liarzi, O. and Ezra, D. (2013) Endophyte-Mediated Biocontrol of Herbaceous and Non-herbaceous Plants. In *Advances in Endophytic Research*. (ed. by Verma, V.C., Gange, A.C.), pp 335-69. Springer, New Delhi, Heidelberg, New York, Dordrecht, London.

Lin, R. and Wang, H. (2004) Arabidopsis FHY3/FAR1 gene family and distinct roles of its members in light control of Arabidopsis development. Plant Physiol., 136, 4010-22.

Lin, R., Ding, L., Casola, C., Ripol, D.R., Feschotte, C., Wang, H. (2007) Transposase-derived transcription factors regulate light signaling in Arabidopsis. Science, 318(5854), 1302-5.

Lin, R., Teng, Y., Park, H.-J., Ding, L., Black, C., Fang, P., & Wang, H. (2008 a) Discrete and Essential Roles of the Multiple Domains of Arabidopsis FHY3 in Mediating Phytochrome A Signal Transduction. Plant Physiol., 148(2), 981-92.

Lin, D.X., Wang, E.T., Tang, H., Han, T.X., He, Y.R., Guan, S.H., Chen, W.X. (2008 b) Shinella kummerowiae sp. nov., a symbiotic bacterium isolated from root nodules of the herbal legume Kummerowia stipulacea. Int J Syst Evol Microbiol., 58, 1409-13.

Lindahl, B.D., Nilsson, R.H., Tedersoo, L., Abarenkov, K., Carlsen, T., Kjøller, R., Koljalg, U., Pennanen, T., Rosendahl, S., Stenlid, J., Kauserud, H. (2013) Fungal community analysis by high-throughput sequencing of amplified markers - a user's guide. New Phytologist, 199, 288-99.

Lindow, S.E. and Brandl, M.T. (2003) Microbiology of the Phyllosphere. Appl. Environ. Microbiol., 69(4), 1875-83.

Lisch, D. R., Freeling, M., Langham R.J., Choy, M.Y. (2001) Mutator Transposase Is widespread in the Grasses. Plant Physiol. 125(3), 1293-303.

Lisch D. (2015) Mutator and MULE Transposons.Microbiol Spectr. 3(2), MDNA3-0032-2014.

Liu, W.X., Zhang, F.C., Zhang, W.Z., Song, L.F., Wu, W.H., Chen, Y.F. (2013 a) Arabidopsis Di19 Functions as a Transcription Factor and Modulates PR1, PR2, and PR5 Expression in Response to Drought Stress. Molecular Plant, 6(5), 1487-02.

Liu, Y., Wang, L., Cai, G., Jiang, S., Sun, L., Li, D. (2013 b) Response of tobacco to the Pseudomonas syringae pv. Tomato DC3000 is mainly dependent on salicylic acid signaling pathway. FEMS Microbiol Lett., 344(1), 77-85.

Liu, X., Sun, Y., Kørner, C.J., Du, X., Vollmer, M.E., Pajerowska-Mukhtar, K.M. (2015) Bacterial Leaf Infiltration Assay for Fine Characterization of Plant Defense Responses using the Arabidopsis thaliana-Pseudomonas syringae Pathosystem. J Vis Exp., (104), e53364.

Lorenzo, O., Piqueras, R., Sánchez-Serrano, J. J., & Solano, R. (2003) ETHYLENE RESPONSE FACTOR1 Integrates Signals from Ethylene and Jasmonate Pathways in Plant Defense. The Plant Cell. 15(1), 165-78.

Lorrain, S., Vailleau, F., Balagué, C., Roby, D. (2003) Lesion mimic mutants: keys for deciphering cell death and defense pathways in plants. Trends in Plant Science, 8(6), 263-71.

Lu, S.X., Knowles, S.M., Andronis, C., Ong, M.S., Tobin, E.M. (2009) CIRCADIAN CLOCK ASSOCIATED1 and LATE ELONGATED HYPOCOTYL Function Synergistically in the Circadian Clock of Arabidopsis. Plant Physiology, 150(2), 834-43.

Ma, L., Tian, T., Lin, R., Deng, X.W., Wang, H., Li, G. (2016) Arabidopsis FHY3 and FAR1 Regulate Light-Induced myo-Inositol Biosynthesis and Oxidative Stress Responses by Transcriptional Activation of MIPS1. Mol Plant, 9(4), 541-57.

Macêdo, D.P.C., Neves, R.P., de Souza-Motta, C.M., Correia Magalhães, O.M. (2007) Engyodontium Album Fungaemia: The First Reported Case. Braz J Microbiol., 38(1),110-12.

Mahalingam, R., Gomez- Buitrago, A., Eckardt, N., Shah, N., Guevara- Garcia, A., Day, P., Raina R., Fedoroff, N.V. (2003) Characterizing the stress/ defense transcriptome of Arabidopsis. Genome Biology, 4, R20.

Maier, F., Zwicker, S., Hückelhoven, A., Meissner, M., Funk, J., Pfitzner, A.J., Pfitzner, U.M. (2011) NONEXPRESSOR OF PATHOGENESIS-RELATED PROTEINS1 (NPR1) and some NPR1-related proteins are sensitive to salicylic acid. Mol Plant Pathol. 12(1), 73-91.

Maignien, L., DeForce, E.A., Chafee, M.E., Eren, A.M., Simmons, S.L. (2014) Ecological Succession and Stochastic Variation in the Assembly of Arabidopsis thaliana Phyllosphere Communities. mBio, 5(1), e00682-13.

Makandar, R., Nalam, V., Chaturvedi, R., Jeannotte, R., Sparks, A.A., Shah, J. (2010) Involvement of Salicylate and Jasmonate Signaling Pathways in Arabidopsis Interaction with Fusarium graminearum. MPMI, 23(7), 861-70.

Malanicheva, I.A., Kozlov, D.G., Sumarukova, I.G. *et al.* (2012) Antimicrobial activity of Bacillus megaterium strains. Microbiology, 81, 178.

Mancinelli, A.L. (1994) The physiology of phytochrome action. In *Photomorphogenesis in Plants*. (ed. by Kendrick, R.E. and Kronenberg, G.H.M.), pp 21211-269. Kluwer Academic Publishers, Dordrecht, NL.

Manter, D.K., Vivanco, J.M. (2007) Use of the ITS primers, ITS1F and ITS4, to characterize fungal abundance and diversity in mixed-template samples by qPCR and length heterogeneity analysis. J Microbiol Methods, 71(1), 7-14.

Mao-Jones, J., Ritchie, K. B., Jones, L. E., & Ellner, S. P. (2010) How Microbial Community Composition Regulates Coral Disease Development. PLoS Biology, 8(3), e1000345.

Martins, G., Lauga, B., Miot-Sertier, C., Mercier, A., Lonvaud, A., Soulas, M.L., Soulas, G., Masneuf-Pomarède, I. (2013) Characterization of epiphytic bacterial communities from grapes, leaves, bark and soil of grapevine plants grown, and their relations. PLoS One, 8, e73013.

McGrath, K.C., Dombrecht, B., Manners, J.M., Schenk, P.M., Edgar, C.I., Maclean, D.J., Scheible, W.R., Udvardi, M.K., Kazan, K. (2005) Repressor- and Activator-Type Ethylene Response Factors Functioning in Jasmonate Signaling and Disease Resistance Identified via a Genome-Wide Screen of Arabidopsis Transcription Factor Gene Expression. Plant Physiology, 139(2), 949-59.

McWatters, H.G. and Devlin P.F. (2011) Timing in plants – A rhythmic arrangement. FEBS Letters, 585(10), 1474-84.

Mercado-Blanco, J. and Bakker, P.A. (2007) Interactions between plants and beneficial Pseudomonas spp.: exploiting bacterial traits for crop protection. Antonie Van Leeuwenhoek. 92(4), 367-89.

Meyer, F., Paarmann, D., D'Souza, M., Olson, R., Glass, E.M., Kubal, M., Paczian, T., Rodriguez, A., Stevens, R., Wilke, A., Wilkening, J., Edwards, R.A. (2008) The Metagenomics RAST server - A public resource for the automatic phylogenetic and functional analysis of metagenomes. BMC Bioinformatics, 9, 386.

Mi, H., Muruganujan, A., Casagrande, J.T., Thomas, P.D. (2013) Nature Protocols, 8, 1551-66.

Millar, A.J. (2004) Input signals to the plant circadian clock. J Exp Bot., 55, 277-83.

Minibayeva, F. and Beckett, R.P. (2015) RNS Binding by Heme Proteins. In *Reactive Oxygen and Nitrogen Species Signaling and Communication in Plants 23* (ed. by Gupta, K.J., Igamberdiev, A.U.), p 49. Springer, Cham, Heidelberg, New York, Dordrent, London.

Miya, A., Albert, P., Shinya, T., Desaki, Y., Ichimura, K., Shirasu, K., Narusaka, Y., Kawakami, N., Kaku, H., Shibuya, N. (2007) CERK1, a LysM receptor kinase, is essential for chitin elicitor signaling in Arabidopsis. Proc. Natl Acad. Sci. USA, 104, 19613-18.

Mockler, T.C., Michael, T.P., Priest, H.D., Shen, R., Sullivan, C.M., Givan, S.A., McEntee, C., Kay, S., Chory, J. (2007) THE DIURNAL PROJECT: Diurnal and circadian expression profiling, model-based pattern matching and promoter analysis. Cold Spring Harb Symp Quant Biol., 72, 353-63.

Moore, L.W. (1988) Pseudomonas syringae: disease and ice nucleation activity. Ornamentals Northwest Newsletter. 12, 4-16.

Moslem, M., Abd-Elsalam, K., Yassin, M., Bahkali, A. (2010) First morphomolecular identification of Penicillium griseofulvum and Penicillium aurantiogriseum toxicogenic isolates associated with blue mold on apple. Foodborne Pathog Dis., 7(7), 857-61.

Müller, T. and Ruppel, S. (2014) Progress in cultivation-independent phyllosphere microbiology. FEMS Microbiol Ecol., 87(1), 2-17.

Nagano, M., Ihara-Ohori, Y., Imai, H., Inada, N., Fujimoto, M., Tsutsumi, N., Uchimiya, H., Kawai-Yamada, M. (2009) Functional association of cell death suppressor, Arabidopsis Bax inhibitor-1, with fatty acid 2-hydroxylation through cytochrome b_5. Plant J., 58(1), 122-34.

Neff, M.M. and Chory, J. (1998) Genetic Interactions between Phytochrome A, Phytochrome B, and Cryptochrome 1 during Arabidopsis Development. Plant Physiol., 118, 27-36.

Neff, M.M., Neff, J.D., Chory, J., Peppe, A.E. (1998) dCAPS, a simple technique for the genetic analysis of singlenucleotide polymorphisms: experimental applications in Arabidopsis thaliana genetics. The Plant Journal, 14(3), 387-92.

Nelson, P.E., Dignani, M.C., Anaissie, E.J. (1994) Taxonomy, biology, and clinical aspects of Fusarium species. Clin Microbiol Rev., 7(4), 479-504.

Newman, M.A, Sundelin, T., Nielsen, J.T., Erbs, G. (2013) MAMP (microbe-associated molecular pattern) triggered immunity in plants. Frontiers in Plant Science, 6(4), 139.

Nguyen, H.P., Chakravarthy, S., Velásquez, A.C., McLane, H.L., Zeng, L., Nakayashiki, H., Park, D.-H., Collmer, A., Martin, G.B. (2010) Methods to Study PAMP-Triggered Immunity Using Tomato and Nicotiana benthamiana. MPMI. 23(8), 991-9.

Nishimura, M.T. and Dangl, J.L. (2010) Arabidopis and the plant immune system. The Plant Journal. 61, 1053-1066.

Nitschke, S., Cortleven, A., Iven, T., Feussner, I., Havaux, M., Riefler, M., Schmülling, T. (2016) Circadian Stress Regimes Affect the Circadian Clock and Cause Jasmonic Acid- Dependent Cell Death in Cytokinin-Deficient Arabidopsis Plants. Plant Cell, 28(7), 1616-39.

Niu, B., Vater, J., Rueckert, C., Blom, J., Lehmann, M., Ru, J.J., Chen, X.H., Wang, Q., Borriss, R. (2013) Polymyxin P is the active principle in suppressing phytopathogenic Erwinia spp. by the biocontrol rhizobacterium Paenibacillus polymyxa M-1. BMC Microbiol., 13, 137.

Nout, M.J.R., Platis, C.E., Wicklow, D.T. (1997) Biodiversity of yeasts from Illinois maize. Can. J. Microbial., 43, 362-67.

Nusinow, D.A., Helfer, A., Hamilton, E.E., King, J.J., Imaizumi, T., Schultz, T.F., Farré, E.M., Kay, S.A. (2011) The ELF4-ELF3-LUX complex links the circadian clock to diurnal control of hypocotyl growth. Nature, 475(7356), 398-402.

Ogórek, R., Lejman, A., Pusz, W., Miłuch, A., Miodyńska, P. (2012) Characteristics and taxonomy of Cladosporium fungi. Mikologia Lekarska, 19(2), 80-85.

Ohtake, Y., Takahashi, T., Komeda Y. (2000) Salicylic Acid Induces the Expression of a Number of Receptor-Like Kinase Genes in Arabidopsis thaliana. Plant Cell Physiol., 41(9), 1038-44.

Ó'Maoiléidigh, D.S., Graciet, E., Wellmer, F. (2013) Gene networks controlling Arabidopsis thaliana flower development. New Phytologist, 201(1), 16-30.

Ondov, B.D., Bergman, N.H., Phillippy, A.M. (2011) Interactive metagenomic visualization in a Web browser. BMC Bioinformatics, 12(1), 385.

Ongena, M. and Jacques, P. (2007) Bacillus lipopeptides: versatile weapons for plant disease biocontrol. Trends in Microbiology, 16(3), 115-25.

Oome, S., Raaymakers, T.M., Cabral, A., Samwel, S., Böhm, H., Albert, I., Nürnberger, T., Van den Ackerveken, G. (2014) Nep1-like proteins from three kingdoms of life act as a microbe-associated molecular pattern in Arabidopsis. Proc Natl Acad Sci U S A. 111(47), 16955-60.

Oravecz, A., Baumann, A., Máté, Z., Brzezinska, A., Molinier, J., Oakeley, E.J., Ádám, E., Schäfer, E., Nagy, F., Ulm, R. (2006) CONSTITUTIVELY PHOTOMORPHOGENIC1 Is Required for the UV-B Response in Arabidopsis. The Plant Cell, 18(8), 1975-90.

Ottesen, A.R., Gorham, S., Pettengill, J.B., Rideout, S., Evans, P., Brown, E. (2015) The impact of systemic and copper pesticide applications on the phyllosphere microflora of tomatoes. Journal of the Science of Food and Agriculture, 95(5), 1116-25.

Ouyang, X., Li, J., Li, G., Li, B., Chen, B., Shen, H., *et al.* (2011) Genome-wide binding site analysis of FAR-RED ELONGATED HYPOCOTYL3 reveals its novel function in Arabidopsis development. Plant Cell, 23, 2514-35.

Ovadia, A., Tabibian-Keissar, H., Cohen, Y., Kenigsbuch, D. (2010) The 5'UTR of CCA1 includes an autoregulatory cis element that segregates between light and circadian regulation of CCA1 and LHY. Plant Mol Biol, 72, 659.

Parke, J.L. and Gurian-Sherman, D. (2001) Diversity of the Burkholderia cepacia complex and implications for risk assessment of biological control strains. Annu. Rev. Phytopathol., 39, 225-58.

Passari, A.K., Mishra, V.K., Gupta, V.K., Yadav, M.K., Saikia, R., Singh, B.P. (2015) In Vitro and In Vivo Plant Growth Promoting Activities and DNA Fingerprinting of Antagonistic Endophytic Actinomycetes Associates with Medicinal Plants. PLoS ONE, 10(9), e0139468.

Pastor, V., Luna, E., Ton, J., Cerezo, M., García-Agustín, P., Flors, V. (2013) Fine tuning of reactive oxygen species homeostasis regulates primed immune responses in Arabidopsis. Mol Plant Microbe Interact. 26(11), 1334-44.

Paulsen, I.T., Press, C.M., Ravel, J. (2005) Complete genome sequence of the plant commensal Pseudomonas fluorescens Pf-5. Nature Biotechnology, 23, 873-78.

Pel, M.J.C. and Pieterse, C.M.J. (2013) Microbial recognition and evasion of host immunity. Journal of Experimental Botany, 64(5), 1237-48.

Pereira, P., Nesci, A., Etcheverry, M. (2007) Effects of biocontrol agents on Fusarium verticillioides count and fumonisin content in the maize agroecosystem: Impact on rhizospheric bacterial and fungal groups. Biological Control, 42(3), 281-7.

Petutschnig, E.K., Jones, A.M.E., Serazetdinova, L., Lipka, U., Lipka, V. (2010) The Lysin Motif Receptor-like Kinase (LysM-RLK) CERK1 Is a Major Chitin-binding Protein in Arabidopsis thaliana and Subject to Chitin-induced Phosphorylation. Journal of Biological Chemistry, 285(37), 28902-11.

Pitzschke, A., Djamei, A., Bitton, F., Hirt, H. (2009) A Major Role of the MEKK1–MKK1/2–MPK4 Pathway in ROS Signalling. Molecular Plant, 2(1), 120-37.

Pokhilko, A., Fernández, A.P., Edwards, K.D., Southern, M.M., Halliday, K.J., Millar, A.J. (2012) The clock gene circuit in Arabidopsis includes a repressilator with additional feedback loops. Mol Syst Biol., 8, 574.

Pokhilko, A., Mas, P., Millar, A.J. (2013) Modelling the widespread effects of TOC1 signalling on the plant circadian clock and its outputs. BMC Syst Biol., 7, 23.

Porras-Alfaro, A. and Bayman, P. (2011) Hidden Fungi, Emergent Properties: Endophytes and Microbiomes. Annu Rev Phytopathol., 49, 291-315.

Pritchard, L. and Birch, P. R. J. (2014) The zigzag model of plant–microbe interactions: is it time to move on? Mol Plant Pathol. 15(9), 865-70.

Provart, N.J., Gil, P., Chen, W., Han, B., Chang, H.S., Wang, X., Zhu, T. (2003) Gene Expression Phenotypes of Arabidopsis Associated with Sensitivity to Low Temperatures. Plant Physiol., 132, 893-906.

Pryce-Williams, R. (2009) An analysis of microbial niche communities within the rhizosphere of Arabidopsis thaliana. (Bachelor thesis. Course Unit: BS3010. School of Biological Sciences, RHUL, UK).

Quast, C., Pruesse, E., Yilmaz, P., Gerken, J., Schweer, T., Yarza, P., Peplies, J., Glöckner, F.O. (2013) The SILVA ribosomal RNA gene database project: improved data processing and web-based tools. Nucl. Acids Res., 41(D1), D590-6.

Quirino, B. F. and Brent, A. F. (2003) Deciphering host resistance and pathogen virulence: the Arabidopsis/ Pseudomonas interaction as a model. Molecular plant pathology, 4(6), 517-30.

Rabe, F., Ajami-Rashidi, Z., Doehlemann, G., Kahmann, R., Djamei, A. (2013) Degradation of the plant defence hormone salicylic acid by the biotrophic fungus Ustilago maydis. Mol Microbiol., 89(1), 179-88.

Raizada, M.N., Benito, M.I., Walbot, V. (2001) The MuDR transposon terminal inverted repeat contains a complex plant promoter directing distinct somatic and germinal programs. Plant J. 25(1), 79-91.

Rakhashiya, P.M., Patel, P.P., Thaker, V.S. (2015) High-quality complete genome sequence of Microbacterium sp. SUBG005, a plant pathogen. Genomics Data, 5, 316-17.

Ramonell, K.M., Zhang, B., Ewing, R.M., Chen, Y., Xu, D., Stacey, G., Sommerville, S. (2002) Microarray analysis of chitin elicitation in Arabidopsis thaliana. Molecular Plant Pathology, 3, 301-11.

Raper, K.B. and Thom, C. (1949) A Manual of the Penicillia. pp 359-64. Williams and Wilkins Co., Baltimore, USA.

Rausenberger, J., Tscheuschler, A., Nordmeier, W., Wüst, F., Timmer, J., Schäfer, E., Fleck, C., Hiltbrunner, A. (2011) Photoconversion and nuclear trafficking cycles determine phytochrome A's response profile to far-red light. Cell, 146(5), 813-25.

Rauw, W.M. (2012) Immune response from a resource allocation perspective. Frontiers in Genetics, 3(267), 1-14.

Reasoner, D.J., Blannon, J.C., Geldreich, E.E. (August 1979) Rapid seven-hour fecal coliform test. Appl. Environ. Microbiol., 38(2), 229-36.

Reichenbach, H. (2006) The Genus Lysobacter. In *The Prokaryotes* (ed. by Dworkin, M., Falkow, S., Rosenberg, E., Schleifer, K.H., Stackebrandt, E.), pp 939-57. Springer, New York, USA.

Reisberg, E.E., Hildebrandt, U., Riederer, M., Hentschel, U. (2013) Distinct phyllosphere bacterial communities on Arabidopsis wax mutant leaves. Plos ONE, 8, e78613.

Ren, D., Liu, Y., Yang, K.-Y., Han, L., Mao, G., Glazebrook, J., Zhang, S. (2008) A fungal-responsive MAPK cascade regulates phytoalexin biosynthesis in Arabidopsis. PNAS. 105(14), 5638-43.

Rice, A.V. and Currah, R.S. (2006) Two new species of Pseudogymnoascus with Geomyces anamorphs and their phylogenetic relationship with Gymnostellatospora. Mycologia, 98(2), 307-18.

Ritpitakphong, U., Falquet, L., Vimoltust, A., Berger, A., Métraux, J.P., L'Haridon, F. (2016) The microbiome of the leaf surface of Arabidopsis protects against a fungal pathogen. New Phytol., 210, 1033-43.

Rocher, F., Chollet, J.F., Jousse, C., Bonnemain, J.L. (2006) Salicylic Acid, an Ambimobile Molecule Exhibiting a High Ability to Accumulate in the Phloem. Plant Physiology, 141(4), 1684-93.

Roser, M. and Ortiz-Ospina, E. (2017) World Population Growth. Published online at OurWorldInData.org. Retrieved from: https://ourworldindata.org/world-population-growth/ [Online Resource]

Rustérucci, C., Aviv, D.H., Holt, III B.F., Dangl, J.L., Parker, J.E. (2001) The Disease Resistance Signaling Components EDS1 and PAD4 Are Essential Regulators of the Cell Death Pathway Controlled by LSD1 in Arabidopsis. The Plant Cell, 13, 2211-24.

Ryffel, F., Helfrich, E.J., Kiefer, P., Peyriga, L., Portais, J.C., Piel, J., Vorholt, J.A. (2016) Metabolic footprint of epiphytic bacteria on Arabidopsis thaliana leaves. ISME J., 10, 632-43.

Sakai, M., Matsuka, A., Komura, T., Kanazawa, S. (2004) Application of a new PCR primer for terminal restriction fragment length polymorphism analysis of the bacterial communities in plant roots. Journal of Microbiological Methods, 59(1), 81-9.

Sakamoto, A.N., Lan, V.T., Puripunyavanich, V., Hase, Y., Yokota, Y., Shikazono, N., Nakagawa, M., Narumi, I., Tanaka, A. (2009) A UVB-hypersensitive mutant in Arabidopsis thaliana is defective in the DNA damage response. Plant J., 60(3), 509-17.

Salk Institute Genomic Analysis Laboratory. (2003) T-DNA Primer Design. [online] Available from: http://signal.salk.edu/tdnaprimers.2.html [27.06.2014]

Sanchez-Casas, P., & Klessig, D. F. (1994). A Salicylic Acid-Binding Activity and a Salicylic Acid-Inhibitable Catalase Activity Are Present in a Variety of Plant Species. Plant Physiology, 106(4), 1675–1679.

Sartori, M., Nesci, A., Formento, Á., Etcheverry, M. (2015) Selection of potential biological control of Exserohilum turcicum with epiphytic microorganisms from maize. Rev Argent Microbiol., 47, 62-71.

Sattelmacher, B. (2001) The apoplast and its significance for plant mineral nutrition. New Phytologist, 149, 167-92.

Schenk, P.M., Kazan, K., Wilson, I., Anderson, J.P., Richmond, T. (2000) Coordinated plant defense responses in Arabidopsis revealed by microarray analysis. PNAS, 97(21), 11655-60.

Schlaberg, R., Simmon, K. E., Fisher, M. A. (2012) A Systematic Approach for Discovering Novel, Clinically Relevant Bacteria. Emerging Infectious Diseases, 18(3), 422-30.

Schwacke, R., Schneider, A., Van Der Graaff, E., Fischer, K., Catoni, E., Desimone, M., Frommer, W.B., Flügge, U.I., Kunze, R. (2003) ARAMEMNON, a Novel Database for Arabidopsis Integral Membrane Proteins. Plant Physiol., 131(1), 16-26.

Shapiguzov, A., Vainonen, J.P., Wrzaczek, M., Kangasjärvi, J. (2012) ROS-talk – how the apoplast, the chloroplast, and the nucleus get the message through. Front Plant Sci., 3, 292.

Sharma, R.R., Singh, D., Singh, R. (2009) Biological control of postharvest diseases of fruits and vegetables by microbial antagonists: A review. Biol Control, 50, 205-21.

Shim, J.S. and Imaizumi, T. (2015) Circadian Clock and Photoperiodic Response in Arabidopsis: From Seasonal Flowering to Redox Homeostasis. Biochemistry 54(2), 157-70.

Siddiqui, H., Khan, S., Rhodes, B.M., Devlin, P.F. (2016) FHY3 and FAR1 Act Downstream of Light Stable Phytochromes. Front Plant Sci., 7, 175.

Sigler, L., Lumley, T.C., Currah, R.S. (2000) New species and records of saprophytic ascomyces (Myxotrichaceae) from decaying logs in the boreal forest. Mycoscience, 41, 495-502.

Silo-Suh, L., Lethbridge, B., Raffel, S.J., He, H., Clardy, J., Handelsman, J. (1994) Biological activities of two fungistatic antibiotics produced by Bacillus cereus UW85. Applied Environmental Microbiology, 60(6), 2023-30.

SIGnAL Salk Institute Genomic Analysis Laboratory. (2005) T-DNA Primer Design. [online] Available from: http://signal.salk.edu/tdnaprimers.2.html [27.06.2014].

Slaymaker, D.H., Navarre, D.A., Clark, D., del Pozo, O., Martin, G.B., Klessig, D.F. (2002) The tobacco salicylic acid-binding protein 3 (SABP3) is the chloroplast carbonic anhydrase, which exhibits antioxidant activity and plays a role in the hypersensitive defense response. Proceedings of the National Academy of Sciences, 99, 11640-45.

Smith, G. (1960) An introduction to industrial mycology. Edward Arnold Ltd., London, UK.

Smith, H. (1995) Physiological and ecological function within the phytochrome family. Annual Review of Plant Physiology and Plant Molecular Biology, 46, 289-315.

Smith, A.M. and Stitt, M. (2007) Coordination of carbon supply and plant growth. Plant, Cell & Environment, 30, 1126-49.

Smith, D.D.N., Kirzinger, M.W.B., Stavrinides, J. (2013) Draft Genome Sequence of the Antibiotic-Producing Epiphytic Isolate Pantoea ananatis BRT175. Genome Announcements, 1(6), e00902-13.

Social Science Statistics. (2016) P Value from Z Score Calculator. [online] Available from: www.socscistatistics.com/pvalues/normaldistribution.aspx [01.10.2016].

Song, G.C. and Ryu, C.M. (2013) Two Volatile Organic Compounds Trigger Plant Self-Defense against a Bacterial Pathogen and a Sucking Insect in Cucumber under Open Field Conditions. International Journal of Molecular Sciences, 14(5), 9803-19.

Sowndhararajan, K., Marimuthu, S., Manian, S. (2013) Biocontrol potential of phylloplane bacterium Ochrobactrum anthropi BMO-111 against blister blight disease of tea. J Appl Microbiol., 114, 209-18.

Stackebrandt, E., and B. M. Goebel. (1994) Taxonomic note: a place for DNA-DNA reassociation and 16S rRNA sequence analysis in the present species definition in bacteriology. Int J Syst Bacteriol., 44, 846-49.

Stark, M., Berger, S.A., Stamatakis, A., von Mering, C. (2010) MLTreeMap - accurate Maximum Likelihood placement of environmental DNA sequences into taxonomic and functional reference phylogenies. BMC Genomics, 11, 461.

Stintzi, A., Weber, H., Reymond, P., Browse, J., Farmer, E.E. (2001) Plant defense in the absence of jasmonic acid: the role of cyclopentenones. Proc Natl Acad Sci USA, 98(22), 12837-42.

Stirnberg, P., Zhao, S., Williamson, L., Ward, S., Leyser, O. (2012) FHY3 promotes shoot branching and stress tolerance in Arabidopsis in an AXR1-dependent manner. The Plant Journal, 71, 907-20.

Stone, J.M., Heard J.E., Asa T., Ausubel, F.M. (2000) Simulation of Fungal-Mediated Cell Death by Fumonisin B1 and Selection of Fumonisin B1–Resistant (fbr) Arabidopsis Mutants. Plant Cell, 12(10), 1811-22.

Sugita, T., Nishikawa, A., Ichikawa, T., Ikeda, R., Shinoda, T. (2000) Isolation of Trichosporon asahii from environmental materials. Med Mycol., 38(1), 27-30.

Sugita, T. (2011) Trichosporon Behrend (1890). In *The Yeasts: A Taxonomic Study*. (ed. by Kurtzman, C., Fell, C.W., Boekhout, T.), p 61. Elsevier Science Publish, Amsterdam, NL.

Sutton, J.C. (1998) Botrytis Fruit Rot (Gray Mold) and Blossom Blight. In *Compendium of Strawberry Diseases*. (ed. by Maas, J.L.), pp. 28-31. APS Press, St. Paul, MN.

Tada, Y., Spoel, S.H., Pajerowska-Mukhtar, K., Mou, Z., Song, J., Wang, C., Zuo, J., Dong, X. (2008) Plant Immunity Requires Conformational Charges of NPR1 via S-Nitrosylation and Thioredoxins. Science, 321(5891), 952-56.

Tagne, A., Neergaard, E., Hansen, H.J., The, C. (2002) Studies of Host—pathogen Interaction Between Maize and Acremonium strictum From Cameroon. European Journal of Plant Pathology, 108(2), 93-102.

Tanaka, R., Kobayashi, K., Masuda, T. (2011) Tetrapyrrole Metabolism in Arabidopsis thaliana. The Arabidopsis Book / American Society of Plant Biologists, 9, e0145.

Tang, W., Wang, W., Chen, D., Ji, Q., Jing, Y., Wang, H., Lin, R. (2012) Transposase-derived proteins FHY3/FAR1 interact with PHYTOCHROME-INTERACTING FACTOR 1 to regulate chlorophyll biosynthesisby modulating HEMB1 during deetiolation in Arabidopsis. Plant Cell, 24, 1984-2000.

Tang, W., Ji, Q., Huang, Y., Jiang, Z., Bao, M., Wang, H., Lin, R. (2013) FAR-RED ELONGATED HYPOCOTYL3 and FAR-RED IMPAIRED RESPONSE1 transcription factors integrate light and abscisic acid signaling in Arabidopsis. Plant Physiol., 163(2), 857-66.

Taoka, K., Ohki, I., Tsuji, H., Kojima, C., Shimamoto, K. (2013) Structure and function of florigen and the receptor complex. Trends in Plant Science, 18(5), 287-94.

Taylor, W.E. (1958) *The Examination of Waters and Water Supplies*. Churchill Ltd., London, UK.

Ternes, P., Feussner, K., Werner, S., Lerche, J., Iven, T., Heilmann, I., Riezman, H., Feussner, I. (2011) Disruption of the ceramide synthase LOH1 causes spontaneous cell death in Arabidopsis thaliana. New Phytol., 192(4), 841-54.

The Arabidopsis Information Resource. (2016) Download – Gene Ontology Annotations. [online] Available from: https://www.arabidopsis.org [10.4.2016].

The UniProt Consortium. (2015) UniProt: a hub for protein information. Nucleic Acids Res., 43, D204-12.

Thom, C. (1930) *The Penicillia.* Williams and Wilkins Co., Baltimore, USA.

Thomma, B.P.H.J., Eggermont, K., Penninckx, I.A.M.A., Mauch-Mani, B., Vogelsang, R., Cammue, B.P.A., Broekaert, W.F. (1998) Separate jasmonate-dependent and salicylate-dependent defense-response pathways in Arabidopsis are essential for resistance to distinct microbial pathogens. Proceedings of the National Academy of Sciences of the United States of America, 95(25), 15107-11.

Thomma, B.P.H.J., Eggermont, K., Tierens, K.F.M.J., Broekaert, W.F. (1999) Requirement of Functional Ethylene-Insensitive 2 Gene for Efficient Resistance of Arabidopsis to Infection by Botrytis cinerea. Plant Physiology, 121(4), 1093-101.

Tierens, K.F., Thomma, B.P., Bari, R.P., Garmier, M., Eggermont, K., Brouwer, M., Penninckx, I.A., Broekaert, W.F., Cammue, B.P. (2002) Esa1, an Arabidopsis mutant with enhanced susceptibility to a range of necrotrophic fungal pathogens, shows a distorted induction of defense responses by reactive oxygen generating compounds. Plant J., 29(2), 131-40.

Tilman, D., Balzer, C., Hill, J., Befort, B.L. (2011) Global food demand and the sustainable intensification of agriculture. Proc. Natl. Acad. Sci. USA. 108, 20260-64.

Ting, A.S.Y. (2013) Biosourcing endophytes as biocontrol agents of wilt disease. In *Advances in Endophytic Research*. (ed. by Verma, V.C., Gange, A.C.), pp 283-300. Springer, New Delhi, Heidelberg, New York, Dordrecht, London.

Torres, M.A., Jones, J.D., Dangl, J.L. (2005) Pathogen indiced, NADPH oxidase-derived reactive oxygen intermediates suppress spread of cell death in Arabidopsis thaliana. Nature Genetics, 37(10), 1130-4.

Torres, M.A., Jones, J.D., Dangl, J.L. (2005) Pathogen-induced, NADPH oxidase-derived reactive oxygen intermediates suppress spread of cell death in Arabidopsis thaliana. Nat Genet. 37(10), 1130-4.

Torres, M.A., Jones, J.D.G., Dangl, J.L. (2006) Reactive Oxygen Species Signaling in Response to Pathogens. Plant Physiol., 141(2), 373-8.

Truyens, S., Weyens, N., Cuypers, A., Vangronsveld, J. (2013) Changes in the population of seed bacteria of transgenerationally Cd-exposed Arabidopsis thaliana. Plant Biology, 15, 971-81.

Tsuda, K., Mine, A., Bethke, G., Igarashi, D., Botanga, C. J., Tsuda, Y., *et al.* (2013) Dual regulation of gene expression mediated by extended MAPK activation and salicylic acid contributes to robust innate immunity in Arabidopsis thaliana. PLoS Genet., 9, e1004015.

Turner, T.R., James, E.K., Poole, P.S. (2013) The plant microbiome. Genome Biology, 14, 209.

Uknes, S., Mauch-Mani, B., Moyer, M., Potter, S., Williams, S., Dincher, S., Chandler, D., Slusarenko, A., Ward, E., Ryals, J. (1992) Acquired resistance in Arabidopsis. The Plant Cell, 4(6), 645-56.

Ulm, R. and Jenkins, G.I. (2015) Q&A: How do plants sense and respond to UV-B radiation? BMC Biol, 13, 45.

Vacher, C., Hampe, A., Porté, A.J., Sauer, U., Compant, S., Morris, C.E. (2016) The Phyllosphere: Microbial Jungle at the Plant–Climate Interface. Annu Rev Ecol Evol Syst., 47, 1-24.

Van Bruggen, A.H.C., Francis, I.M., Jochimsen, K.N. (2014) Non-pathogenic rhizosphere bacteria belonging to the genera Rhizorhapis and Sphingobium provide specific control of lettuce corky root disease caused by species of the same bacterial genera. Plant Pathology, 63, 1384-94.

Vanparys, B., Heylen, K., Lebbe, L., De Vos, P. (2005) Devosia limi sp. nov., isolated from a nitrifying inoculum. Int J Syst Evol Microbiol, 55, 1997-2000.

Vasudevan, P., Kavitha, S., Priyadarisini, V.B., Babujee, L., Gnanamanickam, S.S. (2002) Biological control of rice diseases. In *Biological Control of Crop Diseases* (ed. by Gnanamanickam SS), pp. 11-32. Marcel Dekker Inc. New York.

Venkatachalam, S., Ranjan, K., Prasanna, R., Ramakrishnan, B., Thapa, S., Kanchan, A. (2016) Diversity and functional traits of culturable microbiome members, including cyanobacteria in the rice phyllosphere. Plant Biol., 18(4), 627-37.

Verberne, M.C., Brouwer, N., Delbianco, F., Linthorst, H.J., Bol, J.F., Verpoorte, R. (2002) Method for the extraction of the volatile compound salicylic acid from tobacco leaf material. Phytochem Anal. 13, 45–50.

Veronese, P., Nakagami, H., Bluhm, B., AbuQamar, S., Chen, X., Salmeron, J., Dietrich, R.A., Hirt, H., Mengistea, T. (2006) The Membrane-Anchored BOTRYTIS-INDUCED KINASE1 Plays Distinct Roles in Arabidopsis Resistance to Necrotrophic and Biotrophic Pathogens. The Plant Cell, 18, 257-73.

Vlot, A.C., Dempsey, D.A., Klessig, D.F. (2009) Salicylic Acid, a Multifaceted Hormone to Combat Disease. Annual Review of Phytopathology, 47, 177-206.

Vogel, C., Bodenhausen, N., Gruissem, W., Vorholt, J.A. (2016) The Arabidopsis leaf transcriptome reveals distinct but also overlapping responses to colonization by phyllosphere commensals and pathogen infection with impact on plant health. New Phytologist, 212(1), 192-207.

Vokou, D., Vareli, K., Zarali, E., Karamanoli, K., Constantinidou, H.I., Monokrousos, N., Sainis, J. (2012) Exploring Biodiversity in the Bacterial Community of the Mediterranean Phyllosphere and its Relationship with Airborne Bacter. Microbial Ecology, 64(3), 714-24.

Vorholt, J.A. (2012) Microbial life in the phyllosphere. Nat Rev Microbiol., 10, 828-40.

Voříšková, J. and Baldrian, P. (2013) Fungal community on decomposing leaf litter undergoes rapid successional changes. The ISME Journal, 7(3), 477-86.

Vriens, K., Cammue, B.P.A., Theevissen, K. (2014) Antifungal Plant Defensins: Mechanisms of Action and Production. Molecules, 19, 12280-303.

Wagner, M., Amann, R., Lemmer, H., Schleifer, K. H. (1993) Probing activated sludge with oligonucleotides specific for proteobacteria: inadequacy of culture-dependent methods for describing microbial community structure. Appl Environ Microbiol, 59, 1520-25.

Wakesman, S.A. (1931) Principles of soil microbiology. Baillière Tindall and Cox, London, UK.

Wan, J., Zhang, X.C., Neece, D., Ramonell, K.M., Clough, S., Kim, S.Y., Stacey, M.G., Stacey, G. (2008) A LysM receptor-like kinase plays a critical role in chitin signaling and fungal resistance in Arabidopsis. Plant Cell, 20(2), 471-81.

Wang, H. and Deng, X.W. (2002) Arabidopsis FHY3 defines a key phytochrome A signaling component directly interacting with its homologous partner FAR1. EMBO J., 21(6), 1339-49.

Wang, Y.Q., Feechan, A., Yun, B.W., Shafiei, R., Hofmann, A., Taylor, P., Xue, P., Yang, F.Q., Xie, Z.S., Pallas, J.A., Chu, C.C., Loake, G.J. (2009) S-nitrosylation of AtSABP3 antagonizes the expression of plant immunity. J Biol Chem., 284(4), 2131-7.

Wang, P., Du, Y., Zhao, X., Miao, Y., Song, C.P .(2013) The MPK6-ERF6-ROS-responsive cis-acting Element7/GCC box complex modulates oxidative gene transcription and the oxidative response in Arabidopsis. Plant Physiol., 161(3), 1392-408.

Wang, X., Jiang, N., Liu, J., Liu, W., Wang, G.L. (2014) The role of effectors and host immunity in plant–necrotrophic fungal interactions. Virulence 5(7), 722-32; together with http://website.nbm-mnb.ca/mycologywebpages/NaturalHistoryOfFungi/PlantParasites.html.

Wang, H. and Wang, H. (2015) Multifaceted roles of FHY3 and FAR1 in light signaling and beyond. Trends Plant Sci. 20(7), 453-61.

Wang, W., Tang, W., Ma, T., Niu, D., Jin, J.B., Wang, H., Lin, R. (2015) A pair of light signaling factors FHY3 and FAR1 regulates plant immunity by modulating chlorophyll biosynthesis. J Integr Plant Biol. 58(1), 91-103.

Ward, N.A., Robertson, C.L., Chanda, A.K., Schneider, R.W. (2012) Effects of Simplicillium lanosoniveum on Phakopsora pachyrhizi, the soybean rust pathogen, and its use as a biological control agent. Phytopathology, 102(8), 749-60.

Whalen, M.C., Innes, R.W., Bent, A.F., Staskawicz, B.J. (1991) Identification of Pseudomonas syringae pathogens of Arabidopsis and a bacterial locus determining avirulence on both Arabidopsis and soybean. The Plant Cell, 3(1), 49-59.

Whipps, J.M., Hand, P., Pink, D., Bending, G.D. (2008) Phyllosphere microbiology with special reference to diversity and plant genotype. Journal of Applied Microbiology, 105(2008), 1744-55.

White, T.J., Bruns, T., Lee, S., Taylor, J.W. (1990) Amplification and direct sequencing of fungal ribosomal RNA genes for phylogenetics. In *PCR Protocols: A Guide to Methods and Applications* (ed. by Innis, M.A., Gelfand, D.H., Sninsky, J.J., White, T.J.), pp 315-22. Academic Press, Inc., New York, USA.

Whitelam, G.C., Johnson, E., Peng, J., Carol, P., Anderson, M.L., Cowl, J.S., Harberd, N.P. (1993) Phytochrome A null mutants of Arabidopsis display a wild-type phenotype in white light. Plant Cell, 5, 757-68.

Wildermuth, M.C., Dewdney, J., Wu, G., Ausubel, F.M. (2001) Isochorismate synthase is required to synthesize salicylic acid for plant defence. Nature, 414(6863), 562-5.

Williamson, B., Tudzynski, B., Tudzynski, P., van Kan, J.A. (2007) Botrytis cinerea: the cause of grey mould disease. Mol Plant Pathol, 8(5) 561-80.

Windram, O., Madhou, P., McHattie, S., Hill, C., Hickman, R., Cooke, E., *et al.* (2012) Arabidopsis Defense against Botrytis cinerea: Chronology and Regulation Deciphered by High-Resolution Temporal Transcriptomic Analysis. Plant Cell, 24(9), 3530-57.

Winter, D., Vinegar, B., Nahal, H., Ammar, R., Wilson, G.V., Provart, N.J. (2007) An "Electronic Fluorescent Pictograph" Browser for Exploring and Analyzing Large-Scale Biological Data Sets. PLoS ONE, 2(8), e718.

Wrzaczek, M., Brosché, M., Salojärvi, J., Kangasjärvi, S., Idänheimo, N., Mersmann, S., *et al.* (2010) Transcrtriptional regulation of the CRK/DUF26 group of Receptor-like protein kinases by ozone and plant hormones in Arabidopsis. BMC Plant Biology, 10, 95.

Wu, H., Yang, H.Y., You, X.L., Li, Y.H. (2013) Diversity of endophytic fungi from roots of Panax ginseng and their saponin yield capacities. Springerplus, 2(1), 107.

Wu, B., Wiese, J., Wenzel-Storjohann, A., Malien, S., Schmaljohann, R., Imhoff, J.F. (2016) Engyodontochones, Antibiotic Polyketides from the Marine Fungus Engyodontium album Strain LF069. Chemistry, 22(22), 7452-62.

Xiao, S., Brown, S., Patrick, E., Brearley, C., Turner, J.G. (2013) Enhanced Transcription of the Arabidopsis Disease Resistance Genes RPW8.1 and RPW8.2 via a Salicylic Acid–Dependent Amplification Circuit Is Required for Hypersensitive Cell Death. The Plant Cell, 15(1), 33-45.

Yakir, E., Hilman, D., Harir, Y., Green, R.M. (2007) Regulation of output from the plant circadian clock. FEBS J., 274(2), 335-45.

Yang, T., Du, W., Zhou, J., Wang, X.X., Dai, C.C. (2013) Effects of the symbiosis between fungal endophytes and Atractylodes lancea on rhizosphere and phyllosphere microbial communities. Symbiosis, 61(1), 23-36.

Yashiro, E. and McManus, P.S. (2012) Effect of Streptomycin Treatment on Bacterial Community Structure in the Apple Phyllosphere. PLoS ONE, 7(5), e37131.

Ye, J., Coulouris, G., Zaretskaya, I., Cutcutache, I., Rozen, S., Madden, T. (2012) Primer-BLAST: A tool to design target-specific primers for polymerase chain reaction. BMC Bioinformatics, 13, 134.

Yeh, Y.H., Chang, Y.H., Huang, P.Y., Huang, J.B., Zimmerli, L. (2015) Enhanced Arabidopsis pattern-triggered immunity by overexpression of cysteine-rich receptor-like kinases. Front. Plant Sci., 6, 322.

Yu, J., Gao, J., Wang, X.Y., Wei, Q., Yang, L.F., Qiu, K., Kuai, B.K. (2010) The Pathway and Regulation of Salicylic Acid Biosynthesis in Probenazole-Treated Arabidopsis. Journal of Plant Biology 53(6), 417–24.

Yuliar, Nion, Y. A., & Toyota, K. (2015) Recent Trends in Control Methods for Bacterial Wilt Diseases Caused by Ralstonia solanacearum. Microbes and Environments, 30(1), 1–11.

Xiao, S., Brown, S., Patrick, E., Brearley, C., Turner, J.G. (2013) Enhanced Transcription of the Arabidopsis Disease Resistance Genes RPW8.1 and RPW8.2 via a Salicylic Acid–Dependent Amplification Circuit Is Required for Hypersensitive Cell Death. The Plant Cell, 15(1), 33-45.

Zhang, B., Ramonell, K., Somerville, S., Stacey, G. (2002) Characterization of Early, Chitin-Induced Gene Expression in Arabidopsis. MPMI, 15(9), 963-70.

Zhang, C., Xie, Q., Anderson, R.G., Ng, G., Seitz, N.C., Peterson, T., *et al.* (2013) Crosstalk between the Circadian Clock and Innate Immunity in Arabidopsis. PLoS Pathogens, 9(6), e1003370.

Zhang, X., Wu, Q., Cui, S., Ren, J., Qian, W., Yang, Y., et al. (2015) Hijacking of the jasmonate pathway by the mycotoxin fumonisin B1 (FB1) to initiate programmed cell death in Arabidopsis is modulated by RGLG3 and RGLG4. Journal of Experimental Botany, 66(9), 2709-21.

Zhanga, X., Yanga, G., Shia, R., Hana, X., Qib, L., Wanga, R., Xiongc L., Lia, G. (2013): Arabidopsis cysteine-rich receptor-like kinase 45 functions in the responses to abscisic acid and abiotic stresses. Plant Physiology and Biochemistry, 67, 189-98.

Zheng, Z., Qualley, A., Fan, B., Dudareva, N., Chen, Z. (2008) An important role of a BAHD acyl transferase-like protein in plant innate immunity. Plant Journal. 57(6), 1040-53.

Zhou, J., Bruns, M.A., Tiedje, J.M. (1996) DNA Recovery from Soils of Diverse Composition. Applied and Environmental Microbiology, 62(2), 316-22.

Zhou, M., Wang, W., Karapetyan, S., Mwimba, M., Marqués, J., Buchler, N.E., Dong, X. (2015) Redox rhythm reinforces the circadian clock to gate immune response. Nature, 523(7561), 472-6.

Zimmerli, L., Métraux, J.P., Mauch-Mani, B. (2001) β-Aminobutyric Acid-Induced Protection of Arabidopsis against the Necrotrophic Fungus Botrytis cinerea. Plant Physiol., 126(2), 517-23.

Zipfel, C. and Robatzek, S. (2010) Pathogen-Associated Molecular Pattern-Triggered Immunity: Veni, Vidi…? Plant Physiol. 154, 551-54.

Zipfel, C., Robatzek, S., Navarro, L., Oakeley, E.J., Jones, J.D., Felix, G., Boller, T. (2004) Bacterial disease resistance in Arabidopsis through flagellin perception. Nature, 428(6984), 764-7.